

Microfluidic manufacturing and development of a liposomal vaccine for *Clostridium difficile*

Author

Neil Forbes

Supervisors

Prof. Yvonne Perrie

Prof. Nicolas Szita

**PhD in Pharmaceutical Sciences (Drug Delivery) at Strathclyde
Institute of Pharmacy and Biomedical Sciences**

DECLARATION OF AUTHENTICITY

'This thesis is the result of the author's original research. It has been composed by the author and has not been previously submitted for examination which has led to the award of a degree.' 'The copyright of this thesis belongs to the author under the terms of the United Kingdom Copyright Acts as qualified by University of Strathclyde Regulation 3.50. Due acknowledgement must always be made of the use of any material contained in, or derived from, this thesis.'

Signed: Neil Forbes

Date: 19/08/2020

Acknowledgements

I would like to thank my supervisor Professor Yvonne Perrie for her mentorship throughout my PhD. Yvonne's vast network of connections has made the PhD an incredible experience, visiting both national and international conferences, collaborating with teams across Europe and working on projects that would not have been possible without her. I would also like to thank my supervisor at University College London, Professor Nicolas Szita for his input and guidance. For the team down at NIBSC (Dr Fatme Mawas, Dr Donna Bryan and the rest of the team) – I am very grateful for your teachings and support during my time down south, the techniques I learnt during this time were invaluable for my scientific career. For everyone working in RW317 (Swapnil, Maryam, Gustavo, Giulia, Rob, Despo, Rachel, Cameron and Gillian) – thanks for the help throughout the last four years and most of all – thanks for all the times (good and bad) we shared together!

To all my friends, (wizards, knights and peasants), your distractions from reality were crucial in keeping me level-headed, muchas gracias.

I would like to thank all my family that helped me through the whole process, in particular my mother Susan, my father Iain, my sister Lyndsay and my brother Colm. Without your support and advice, none of this would have been possible. Finally, I would like to thank Carla – in 2016 we embarked on this journey in Glasgow as individuals, but 4 years later we are finishing it together. You have been with me at every step, here's to many more!

Abstract

Oral vaccines offer significant social and economic advantages over vaccines delivered by parenteral routes including higher patient compliance and ease of administration, allowing vaccines to be given by health workers without medical training. Furthermore, oral immunisation can generate both systemic and localised immune responses, making it ideal for generating effective protection against many enteric pathogens such as the gram-positive spore forming bacterium *Clostridium difficile* (*C. difficile*). However, design of an effective vaccine for oral administration remains a significant challenge. In order to reach the relevant sites for the induction of immunological responses, the vaccine must first traverse the hostile environment of the gastrointestinal tract (GIT). For subunit antigens, the acidic pH, degradative enzymes and bile salts present in the GIT can adversely impact their structural stability. This can limit the effectiveness of the immune response. In addition, the mucosal surface within the gut can impair the transport of the vaccine antigen and limit the accessibility to the underlying antigen presenting cells. In order to circumvent these barriers, delivery systems can be employed. Lipid-based delivery systems are commonly used to deliver therapeutics via the oral route of administration. Of the lipid based systems, liposomes have been widely investigated but tend to be used for parenteral delivery. Therefore, the aim of the work in this thesis was to explore the use of liposomes for the oral delivery of a *C. difficile* vaccine. Liposomes generally exhibit low toxicity, enhance interactions with biological membranes and can be incredibly versatile in regards to what compounds they can incorporate (whether they are encapsulated within the aqueous core, within the lipid bilayer or surface associated). However, the manufacture of liposomes has been limited to batch scale production which has inherent risk associated. By employing microfluidics as a manufacturing platform, in conjunction with tangential flow filtration for purification, scalable production can be achieved. Therefore, this method was employed for the formulation and manufacture of the liposomal vaccine systems. Key production parameters were identified and formulations were selected based upon their physicochemical characteristics and protein loading efficiency. Selected formulations were screened for immunological effectiveness on THP-1 macrophage-like cells regarding antigen processing ability and activation marker expression. Finally, a range of formulations were then administered orally to mice to determine *in vivo* efficacy. Enhanced antibody responses (IgG) could be observed when antigen was administered encapsulated within liposomal formulation DSPC:Chol (alongside the potent adjuvant cholera toxin) when compared to free antigen alone; however, poor localised IgA responses were observed for all liposomal formulations tested. The work within this thesis presents a platform for the rapid and scalable manufacture, purification and at-line analysis of liposomal formulations incorporating protein, de-risking the translation of liposomal based protein products from bench to large scale production.

List of Publications

***Forbes, N.**, M. T. *Hussain, M. L. Briuglia, D. P. Edwards, J. H. ter Horst, N. Szita and Y. Perrie (2019). "Rapid and scale-independent microfluidic manufacture of liposomes entrapping protein incorporating in-line purification and at-line size monitoring." International journal of pharmaceutics 556: 68-81.

*Hussain, M. T., **N. *Forbes** and Y. Perrie (2019). "Comparative Analysis of Protein Quantification Methods for the Rapid Determination of Protein Loading in Liposomal Formulations." Pharmaceutics 11(1): 39.

Webb, C., S. Khadke, S. Tandrup Schmidt, C. B. Roces, **N. Forbes**, G. Berrie and Y. Perrie (2019). "The impact of solvent selection: strategies to guide the manufacturing of liposomes using microfluidics." Pharmaceutics 11(12): 653.

Hussain, M. T., **N. Forbes**, Y. Perrie, K. P. Malik, C. Duru and P. Matejtschuk (2020). "Freeze-drying cycle optimization for the rapid preservation of protein-loaded liposomal formulations." International journal of pharmaceutics 573: 118722.

Webb, C., **N. Forbes**, C. B. Roces, G. Anderluzzi, G. Lou, S. Abraham, L. Ingalls, K. Marshall, T. J. Leaver and J. A. Watts (2020). "Using microfluidics for scalable manufacturing of nanomedicines from bench to GMP: A case study using protein-loaded liposomes." International Journal of Pharmaceutics: 119266.

*Denotes shared first authorship

List of Posters and Oral Presentations

Forbes N, Szita N, Perrie Y (2017) Manufacturing of liposomal formulations using microfluidics: Determining criticality-process parameters that impact on physicochemical attributes. Controlled Release Society (CRS) 2017, Hynes Convention Centre, Boston Massachusetts, U.S.A (Poster).

Forbes N, Szita N, Perrie Y (2017) Microfluidics manufacture of liposomes: The impact of lipid concentration and continuous on-line particle sizing. APS International PharmSci 2017, University of Hertfordshire, Hatfield (UK). (Poster).

Forbes N, Szita N, Perrie Y (2017) Microfluidic production of an oral liposomal delivery system: Effect of phosphatidylserine on liposomal formulation. International Liposome Society (ILS) 2017, Royal Olympic Hotel, Athens (Greece). (Poster).

Forbes N, Szita N, Perrie Y (2017) Microfluidic production of liposomal delivery systems: Continuous on-line particle sizing and key process parameters for an anionic liposomal formulation. United Kingdom and Ireland controlled release society (UKICRS) 2017, University of Strathclyde, Scotland (UK). (Poster).

Forbes N, Szita N, Perrie Y (2017) Continuous microfluidic production of liposomes: The effect of lipid concentration on liposomal physicochemical properties. Centre for Doctoral Training (CDT), University College London (UCL), London (UK). (Poster).

Forbes N, Szita N, Perrie Y (2018). Microfluidic Protein Loading into Liposomal Delivery Systems for Oral Vaccination: Optimization of Key Production Parameters. Controlled Release Society (CRS) 2018, New York Hilton Midtown Manhattan Hotel, New York, New York (U.S.A). (Poster).

Forbes N, Szita N, Perrie Y (2018). Thermoanalytical based design of a freeze drying recipe for liposomal formulations incorporating protein. APS@FIP International PharmSci 2018, Hilton Hotel, Glasgow (UK). (Poster).

Forbes N, Szita N, Perrie Y (2018). High-Throughput Microfluidic Protein Loading of Nano-Scale Delivery Systems for Oral Vaccination. United Kingdom and Ireland controlled release society (UKICRS) 2018, Queen's University, Belfast (UK). (Poster).

Forbes N, Perrie Y (2019). Rapid Manufacture of Lipid-based Nanoscale Systems for Oral Antigen Delivery. Vaccine Workshop 21st of March, 2019, Leiden, The Netherlands. (Oral Talk)

Forbes N, Szita N, Bryan D, Mawas F, Perrie Y (2019). Microfluidic Manufacture of Antigen Loaded Nanoparticles in a Scale-Independent Process for use as Oral Vaccine Delivery Vehicles. Controlled Release Society (CRS) 21st-24th of July 2019, Valencia, Spain. (Poster)

Forbes N, Szita N, Bryan D, Mawas F, Perrie Y (2019). Protein Delivery to the G.I Tract: Microfluidics as a scale-independent production platform for protein loaded nanoparticles. Liposome Research Days (LRD) 15-18th of September 2019, Sapporo, Japan. (Poster)

Forbes N, Szita N, Bryan D, Mawas F, Perrie Y (2019). Antigen Delivery to the G.I Tract: Microfluidics as a scale-independent production platform for protein loaded nanoparticles. Pha-St-Train-Vac Meeting 8th of November 2019, Glasgow, Scotland. (Oral Talk)

Forbes N, Perrie Y (2020). Protein Delivery to the G.I Tract: Microfluidics as a scale-independent production platform for protein loaded nanoparticles. Doctoral School Multidisciplinary Symposium 26th of May, 2020, Glasgow, UK. (Oral Talk)

Forbes N, Szita N, Bryan D, Mawas F, Perrie Y (2020). Antigen Delivery to THP-1 Derived Human Macrophages using Liposomal Delivery Systems Manufactured by Microfluidics. Controlled Release Society (CRS) 29th of June to the 2nd of July 2020, Virtual Annual Meeting. (Poster)

Forbes N, Szita N, Bryan D, Mawas F, Perrie Y (2020). Microfluidics as an oral vaccine production platform: The use of liposomes as adjuvants. Controlled Release Society (CRS) 29th of June to the 2nd of July 2020, Virtual Annual Meeting. (On-demand Oral Talk)

List of Figures

Figure 1.1 Schematic diagram of the pH differences found throughout the human gastrointestinal tract. Initially the gastric environment (stomach) contains highly acidic pH, dependent upon the fed / fasted state of the individual. As you traverse through, the small intestine (duodenum, jejunum and ileum) becomes less acidic, where pH can range between approximately pH 3-8. Finally, the large intestine (caecum, colon and rectum) pH can be between 5-8 dependent on fed / fasted state. Adapted from (Ndibewu and Ngoben, 2013).

Figure 1.2 Schematic diagram of the physiology of a Peyer's patch. Antigen from the lumen can transcytose across the epithelial layer via specialised M cells (lacking a mucosal layer). The antigen is passed to the subepithelial dome (SED) where they can interact with underlying APCs (DCs / macrophages). T cell ($CD4^+$) priming can then occur in the thymus dependent area via interactions with DCs before migration towards lymph nodes for subsequent GC formation. Adapted from (Kang et al., 2018).

Figure 1.3 Schematic diagram of the generation of IgA producing plasma B cells. Antigen within the lumen can traverse the epithelial barrier via M cell transcytosis or directly sampled by APCs from the lumen. The antigen is passed onto underlying DCs / macrophages within the lamina propria where they uptake, process and present the antigen fragments on MHC II molecules. $CD4^+$ T cells are primed and the formation of a germinal centre (GC) occurs within the PPs or mesenteric lymph nodes (MLNs). The primed T cells, in the presence of DCs presenting the antigen, can then activate B cells, which initiates somatic hypermutation (SHM) for Fab region variations, followed by class switching (CSR) if antigen affinity is maintained. These IgA^+ B cells then leave the PPs / MLNs via the thoracic duct, entering the circulatory system. Due to the imprinting of homing receptors, these B cells then enter the lamina propria, mature and become IgA producing plasma B cells. Adapted from (Ramirez et al., 2017).

Figure 1.4 Graphical representation of a liposome, composed of a bilayer of lipids with the hydrophilic head facing the aqueous environment and the hydrophobic tail imbedding within the bilayer.

Figure 1.5 Overview of liposome-based products currently on the market, adapted from Bulbake et al. (Bulbake et al., 2017)

Figure 1.6 A graphical illustration of liposome formation. Initially, lipids form into a planar lipid disc when exposed to a threshold concentration of aqueous. The planar layer then begins to bend as a result of more favourable energy confirmation, eventually closing into a spherical bilayer (liposome).

Figure 2.1 Down-sizing using hand-held extrusion: Evaluating particle size (columns) and polydispersity index (circle) through a series of decreasing pore sized membranes during hand-held extrusion for liposomal formulation DSPC:Chol 10.5 (w/w) at a total lipid concentration of 1 mg/mL. Results represent mean \pm SD, n =3 of independent batches.

Figure 2.2 Particle size (columns) and polydispersity index (circles) during probe sonication for liposomal formulation DSPC:Chol 10:5 (w/w) at a total lipid concentration of 1 mg/mL. Samples were DLS analysis were removed every minute during sonication exposure. Results represent mean \pm SD, n =3 of independent batches.

Figure 2.3 Liposome manufacturing comparison. Particle size (columns) and polydispersity index (circles) for hand-held extrusion (100 nm membrane), probe sonication (subjected to sonication for 5 minutes) and microfluidics (3:1 flow rate ratio, 10 mL/min total flow rate) for liposomal formulation DSPC:Chol 10:5 (w/w) at a final total lipid concentration of 1 mg/mL. Results represent mean \pm SD, n =3 of independent batches.

Figure 2.4. The effect of cholesterol content and heating block temperature during microfluidic manufacture for the high transition temperature lipid DSPC were investigated in regards to (A) z-average (particle size) and B) PDI. Results represent mean \pm SD, n = 3 independent batches.

Figure 2.5. Liposomal formulation DSPC:Chol (10:5 w/w) in methanol, investigating the effect of initial total lipid concentration on physicochemical attributes: size (columns) and PDI (circle) (A) and zeta potential (B). Microfluidic parameters selected were flow rate ratio 3:1 and a total flow rate of 10 mL/min. Solvent purification was conducted by dialysis. Results represent mean \pm SD, n = 3 of independent batches.

Figure 2.6 Liposomal formulation DSPC:Chol (10:5 w/w) in methanol, effect of initial total lipid concentration and flow rate ratio on physicochemical attributes: size (columns) and PDI (circles). Microfluidic parameters selected were flow rate ratio 1:1, 3:1 and 5:1 and a total flow rate of 10 mL/min. Solvent purification was conducted by dialysis. Results represent mean \pm SD, n = 3 of independent batches.

Figure 2.7. Liposomal formulation DSPC:Chol (10:5 w/w) in methanol, effect of total flow rate on physicochemical attributes: size (columns) and PDI (circles) (A) and Intensity (%) (B). Microfluidic parameters selected were flow rate ratio 3:1 and total flow rates between 5 – 20 mL/min. Solvent purification was conducted by dialysis. Results represent mean \pm SD, n = 3 of independent batches.

Figure 2.8. The effect of solvent during microfluidic manufacture of liposomal formulation DSPC:Chol (10:5 w/w) (3:1 FRR, 15 mL/min) in methanol (MeOH), ethanol (EtOH) and isopropyl alcohol (IPA): size (columns) and PDI (circles). Solvent purification was conducted by tangential flow filtration. Results represent mean \pm SD, n = 3 of independent batches.

Figure 2.9. The effect of adding PS incrementally to the liposomal formulation DSPC:Chol, liposome size (bar) and PDI (circles) (A) and Zeta Potential (mV) (B) across three distinct flow rate ratios (1,3 and 5:1). Initial total lipid concentration as fixed at 4 mg/mL. Results represent mean \pm SD, n =3 of independent batches.

Figure 2.10. Liposomal formulation DSPC:Chol:PS (10:5:4 w/w) in methanol, effect of initial total lipid concentration on physicochemical attributes: size (columns) and PDI (circles). Microfluidic parameters selected were flow rate ratio 3:1 and a total flow rate of 10 mL/min. Solvent purification was conducted by dialysis. Results represent mean \pm SD, n = 3 of independent batches.

Figure 2.11. Liposomal bridging study for phosphatidylserine. Formulation DSPC:Chol:PS (10:5:4 w/w) and DSPC:Chol:DOPS (10:5:4 w/w) in methanol at a range of initial total lipid concentrations were compared for physicochemical attributes: size (columns) and PDI (circles) (A) and Zeta Potential (mV) (B). Microfluidic parameters selected were flow rate ratio 3:1 and a total flow rate of 10 mL/min. Solvent purification was conducted by dialysis. Results represent mean \pm SD, n = 3 of independent batches.

Figure 2.12. The effect of adding DOTAP incrementally to the liposomal formulation DSPC:Chol, liposome size (bar) and PDI (circles) (A) and Zeta Potential (mV) (B) for flow rate ratio 1:1. Initial total lipid concentration was fixed at 4 mg/mL. Results represent mean \pm SD, n =3 of independent batches.

Figure 2.13. The effect of initial lipid concentration on cationic liposomal formulation DSPC:Chol:DOTAP (10:5:4 w/w) liposome size (bar) and PDI (circles) for flow rate ratio 1:1, total flow rate 10 mL/min. Results represent mean \pm SD, n =3 of independent batches.

Figure 2.14. (A) The effect of the choice of purification method applied to liposomal formulations manufactured by microfluidics. The liposome size (bar) and PDI (circles) are shown for liposomal formulations DSPC:Chol (10:5 w/w), DSPC:Chol:PS (10:5:4 w/w) and DSPC:Chol:DOTAP (10:5:4 w/w) after microfluidics, dialysis, Sephadex column and tangential flow filtration. (B) Recovery rate (%)

measured by Dil of liposomal formulations DSPC:Chol (10:5 w/w) and DSPC:Chol:PS (10:5:4 w/w) manufactured by microfluidics and subsequently purified by dialysis, sephadex column or tangential flow filtration. Results represent mean \pm SD, n = 3 of independent batches.

Fig 2.15. Concentration of liposomal formulation DSPC:Chol:PS (10:5:4 w/w) using tangential flow filtration. The liposomes were prepared at 4 mg/mL initial lipid concentration, 3:1 FRR, 10 mL/min TFR following microfluidics, followed by 1,2 and 4-fold concentration steps. Particle Size (Z-Avg; represented by bars) and PDI (represented by discrete points). Results represent mean \pm SD, n = 3 of independent batches.

Figure 2.16. Residual solvent post TFF or dialysis for liposomal formulation DSPC:Chol (10:5 w/w) initial lipid concentration 4 mg/mL, prepared at a flow rate ratio of 3:1 and 10 mL/min TFR, compared to the ICH guideline benchmark for residual methanol. Results in collaboration with Pierce Lyons, at the University of Strathclyde. Results represent mean \pm SD, n = 3 of independent batches.

Figure 2.17. Size (bars) and PDI (circles) comparison for formulation DSPC:Chol (10:5 w/w) measured by two (At-line and Off-line) before and after purification by TFF. Results represent mean \pm SD, n = 3.

Figure 3.1 The calibration curves for micro BCA with ovalbumin in water: Intra-day curves (A), Inter-day curves (generated over 5 separate days) (B). Intra-day (C) and inter-day (D) precision were calculated across three different concentrations with %RSD shown. Finally, using the average curve (E), accuracy, LOD and LOQ values were determined (F). Results represent mean \pm SD, of at least n = 3 of independent batches.

Figure 3.2 The calibration curves for RP-HPLC with ovalbumin in water: Intra-day curves (A), Inter-day curves (generated over 5 separate days) (B). Intra-day (C) and inter-day (D) precision were calculated across three different concentrations with %RSD shown. Finally, using the average curve (E), accuracy, LOD and LOQ values were determined (F). Results represent mean \pm SD, of at least n = 3 of independent batches.

Figure 3.3 The calibration curves for micro BCA with ovalbumin and liposomes: Intra-day curves (A), Inter-day curves (generated over 5 separate days) (B). Intra-day (C) and inter-day (D) precision were calculated across three different concentrations with %RSD shown. Finally, using the average curve (E), accuracy, LOD and LOQ values were determined (F). Results represent mean \pm SD, of at least n = 3 of independent batches.

Figure 3.4 The effect of increasing liposome concentration on micro BCA absorbance with no ovalbumin added. Three liposomal formulations were produced using microfluidics (FRR 3:1 and 1:1, TFR 10 mL/min), DSPC:Chol, DSPC:Chol:PS and DSPC:Chol:DOTAP and assessed for BCA absorbance interference. Results represent mean \pm SD, of at least n = 3 of independent batches.

Figure 3.5 The calibration curves for micro BCA with ovalbumin in the presence of solubilisation mixture (IPA/Buffer 50/50 v/v): Intra-day curves (A), Inter-day curves (generated over 5 separate days) (B). Intra-day (C) and inter-day (D) precision were calculated across three different concentrations with %RSD shown. Finally, using the average curve (E), accuracy, LOD and LOQ values were determined (F). Results represent mean \pm SD, of at least n = 3 of independent batches.

Figure 3.6 The calibration curves for RP-HPLC with ovalbumin in the presence of solubilisation mixture (IPA/Buffer 50/50 v/v): Intra-day curves (A), Inter-day curves (generated over 5 separate days) (B). Intra-day (C) and inter-day (D) precision were calculated across three different concentrations with %RSD shown. Finally, using the average curve (E), accuracy, LOD and LOQ values were determined (F). Results represent mean \pm SD, of at least n = 3 of independent batches.

Figure 3.7 The calibration curves for micro BCA with ovalbumin in the presence of both liposomes (DSPC:Chol) and solubilisation mixture (IPA/Buffer 50/50 v/v): Intra-day curves (A), Inter-day curves (generated over 5 separate days) (B). Intra-day (C) and inter-day (D) precision were calculated across three different concentrations with %RSD shown. Finally, using the average curve (E), accuracy, LOD and LOQ values were determined (F). Results represent mean \pm SD, of at least $n = 3$ of independent batches.

Figure 4.1 Removal of unentrapped ovalbumin using tangential flow filtration. Preformed “empty” liposomes DSPC:Chol (10:5 w/w) prepared by microfluidics (4 mg/mL initial total lipid, 3:1 FRR and 15 mL/min TFR) were mixed with ovalbumin at final protein concentrations of 500, 1000 and 2000 μ g/mL. Ovalbumin concentrations at each wash cycle was measured in the permeate using micro BCA. Results represent mean \pm SD, $n = 3$ of independent batches.

Figure 4.2 Manufacturing technique comparison for the production of protein loaded liposomal formulations entrapping protein. Neutral formulation DSPC:Chol (10:5 w/w) and anionic formulation DSPC:Chol:PS (10:5:4 w/w) were manufactured by microfluidics or lipid-film hydration followed by hand held extrusion. A final liposome and ovalbumin concentration of 1 mg/mL and 0.18 mg/mL respectively were maintained across both techniques. A) Entrapment efficiency of the formulations, B) physicochemical attributes of the same formulations. Results represent mean \pm SD, $n = 3$ of independent batches.

Figure 4.3 The structural integrity of ovalbumin loaded into the liposomes measured by circular dichroism. DSPC:Chol (10:5 w/w) liposomes were prepared with ovalbumin (8 mg/mL initial total lipid and ovalbumin, 3:1 FRR, 15 mL/min TFR) and purified via TFF. Spectra was measured across 180 – 260 nm.

Figure 4.4 The effect of protein concentration in aqueous phase on entrapment efficiency and liposomal physicochemical characteristics for a neutral liposomal formulation (DSPC:Chol 10:5 w/w) using initial total lipid concentration of 4 mg/mL, 3:1 flow rate ratio and 15 mL/min TFR. (A) Entrapment efficiency and protein loading across initial ovalbumin concentrations for neutral liposomal formulation. (B) Average particle size and PDI, and (C) Zeta Potential for the same formulation. Results represent mean \pm SD, $n = 3$ of independent batches.

Figure 4.5 The effect of protein concentration in aqueous phase on entrapment efficiency and liposomal physicochemical characteristics for the anionic liposomal formulation (DSPC:Chol:PS 10:5:4 w/w) using an initial total lipid concentration of 4 mg/mL, 3:1 flow rate ratio and 15 mL/min TFR. (A) Entrapment efficiency and protein loading across initial ovalbumin concentrations for anionic liposomal formulation. (B) Average particle size and PDI, and (C) Zeta Potential for the same formulation. Results represent mean \pm SD, $n = 3$ of independent batches.

Figure 4.6 The effect of microfluidic process parameter flow rate ratio on entrapment efficiency and liposomal physicochemical characteristics for the liposomal formulation (DSPC:Chol 10:5 w/w) (A and B respectively). Total final lipid concentration was fixed at 1 mg/mL, with a final ovalbumin concentration of 0.525 mg/mL and a total flow rate of 15 mL/min. Results represent mean \pm SD, $n = 3$ of independent batches.

Figure 4.7 The effect of microfluidic process parameter flow rate ratio on entrapment efficiency and liposomal physicochemical characteristics for the liposomal formulation (DSPC:Chol:PS 10:5:4 w/w) (A and B respectively). Total final lipid concentration was fixed at 1 mg/mL, with a final ovalbumin concentration of 0.525 mg/mL and a total flow rate of 15 mL/min. Results represent mean \pm SD, $n = 3$ of independent batches.

Figure 4.8 The effect of microfluidic process parameter total flow rate on entrapment efficiency and liposomal physicochemical characteristics for the liposomal formulation DSPC:Chol 10:5 w/w (A and B) and DSPC:Chol:PS 10:5:4 w/w (C and D). Total final lipid concentration was fixed at 1 mg/mL, with a

final ovalbumin concentration of 0.525 mg/mL (initial concentrations of 4 mg/mL and 0.7 mg/mL respectively) and a flow rate ratio of 3:1. Results represent mean \pm SD, n = 3 of independent batches.

Figure 4.9 Scale-independent production study. Liposomal formulation DSPC:Chol (10:5 w/w) was manufactured at a 3:1 FRR, 15 mL/min TFR at a concentration of 4 mg/mL (initial 0.25 mg/mL ovalbumin) using both NanoAssemblr (2 mL) and Blaze (20 mL). (A) Particle size, PDI and loading efficiency for both batches, (B) overlay of the intensity plots derived from dynamic light scattering.

Figure 4.10 The effect of flow rate ratio on empty cationic liposomal formulations produced by microfluidics. Particles were prepared at at 3.6 mg/mL (DDA:TDB 5:1 w/w, IPA) and 4 mg/mL (DSPC:Chol:DOTAP/DDA 10:5:4 w/w, methanol) initial total lipid, with TRIS buffer 10 mM, pH 7,4 as aqueous phase. A total flow rate of 15 mL/min was selected, while flow rate ratios were increased through 1,3 and 5:1. For solvent purification, dialysis was conducted using TRIS buffer Average particle size (columns), polydispersity Index (PDI) (circles) and Zeta Potential (mV) (values) are shown. Results represent mean \pm SD from three independent batches.

Figure 4.11 The effect of total flow rate on cationic liposomal formulations during complexation. Empty DSPC:Chol:DDA 10:5:4 w/w was prepared in TRIS buffer 10 mM, pH 7.4 at a flow rate ratio of 1:1 and purified by dialysis. The purified particles were then passed back through the NanoAssemblr in one inlet, with ovalbumin in TRIS passed through the second inlet using a fixed flow rate ratio of 1:1. Total flow rates of 5,10,15 and 20 mL/min were assessed and a final liposome: ovalbumin ratio of 10:1 w/w was chosen. Average particle size (columns) and polydispersity Index (PDI) (circles) are shown with zeta potential in text above. Results represent mean \pm SD from three independent batches.

Figure 4.12 The effect of flow rate ratio on cationic liposomal formulations during complexation. Empty DSPC:Chol:DOTAP/DDA 10:5:4 w/w were prepared in TRIS buffer 10 mM, pH 7.4 at a flow rate ratio of 1:1 and purified by dialysis. The purified particles were then passed back through the NanoAssemblr in one inlet, with ovalbumin in TRIS passed through the second inlet at three flow rate ratios (1, 3 and 5:1) using a fixed total flow rate of 15 mL/min. Both final lipid and ovalbumin concentrations were fixed at 1 mg/mL and 0.1 mg/mL respectively. Average particle size (columns) and polydispersity Index (PDI) (circles) are shown with zeta potential in text above. Results represent mean \pm SD from three independent batches.

Figure 4.13 The effect of liposome to protein ratio following complexation. DSPC:Chol:DDA (10:5:4 w/w) was produced at an initial total lipid concentration of 4 mg/mL in methanol, with TRIS 10 mM pH 7.4 as aqueous phase. Following purification, complexation was conducted by passing the liposomes back through the NanoAssemblr alongside ovalbumin in TRIS at a flow rate ratio of 1:1. Final ovalbumin concentrations were scaled from 10:1 to 1:3. (A) Average particle size (columns) and polydispersity Index (PDI) (circles) are shown (B) Average Zeta Potential (mV). Results represent mean \pm SD from three independent batches.

Figure 5.1 Gating strategy for the identification of differentiated THP-1 cells, with example DQ-OVA and DiIC gating (selected at 2% for auto fluorescence). The example shown is the negative control (RPMI) THP-1 cells with no liposomal formulation added.

Figure 5.2 Differentiated THP-1 macrophage-like cells were co-cultured with four liposomal formulations containing DiIC within the membrane. Time points were removed across 24 h incubation, with unstained controls receiving just serum-free RPMI (A). Time points 1 h (B) and 24 h (C) comparison for DiIC %positive cells, with unstained controls receiving just serum-free RPMI. Results represent mean \pm SD, n = 3.

Figure 5.3 Differentiated THP-1 macrophage-like cells were co-cultured with four liposomal formulations containing DQ-OVA adsorbed to the surface or entrapped within. Time points were

removed across 24 h incubation, with unstained controls receiving just serum-free RPMI or free ovalbumin without a liposomal formulation (A). Time points 1 h (B) and 24 h (C) comparison for DQ-OVA % positive cells, with unstained controls receiving just serum-free RPMI. Results represent mean \pm SD, n = 3.

Figure 5.4 DQ-OVA processing (%) vs association (%) for the four liposomal formulations DSPC:Chol, DSPC:Chol:DOPS, DSPC:Chol:DDA and DDA:TDB at time points 1 h (closed symbol) and 24 h (open symbols). Results represent mean \pm SD, n = 3

Figure 5.5 Differentiated THP-1 macrophage-like cells were co-cultured with four liposomal formulations for 24 h incubation, with negative controls receiving serum-free RPMI or just free ovalbumin. % Positive cells with surface co-stimulatory molecules CD14, CD40, CD80 and MHC II were analysed with FACs using specified antibodies. Results represent mean \pm SD, n = 3.

Figure 5.6 Differentiated THP-1 macrophage-like cells were co-cultured with four liposomal formulations for 24 h incubation, with negative controls receiving serum-free RPMI. MFI (median) of cell surface co-stimulatory molecules CD14, CD40, CD80 and MHC II (A, B, C and D respectively) were analysed with FACs using specified antibodies. Results represent mean \pm SD, n = 3.

Figure 6.1 Immunisation schedule used for in vivo experimentation. Five mice per group were orally administered liposomal formulations (or s/c injection for positive control) weekly over a period of five weeks in order to evaluate systemic IgG and mucosal IgA.

Figure 6.2 Average size (d.nm), PDI and zeta potential (mV) of three empty liposomal formulations A) DSPC:Chol (10:5 w/w) B) DSPC:Chol:PS (10:5:4 w/w) and C) DSPC:Chol:DOTAP (10:5:4 w/w) prepared by microfluidics and subjected to an increasing acidic environment using the MPT-2 Auto Titrator from Malvern Panalytical. The isoelectric point (pI) is indicated by the red dotted line. Results represent mean \pm SD, n=3 of independent batches.

Figure 6.3 Formulations DSPC:Chol (10:5 w/w), MPG:Chol:PS (10:5:4 w/w), DSPC:Chol:PS (10:5:4 w/w) with ovalbumin encapsulated inside and DSPC:Chol:DOTAP (10:5:4 w/w) with surface adsorbed ovalbumin were subjected to acidic conditions (pH 1.2) for up to 120 minutes at 37 °C. Samples were removed, neutralised and washed to remove untrapped antigen using tangential flow filtration (DSPC:Chol, MPG:Chol:PS and DSPC:Chol:PS) or dialysis (DSPC:Chol:DOTAP). The final time point was further subjected to a neutralisation of pH (7.4) (indicated by the red-dotted line) and retained for an additional 120 minutes before sample removal and washing. Antigen retention within the vesicles was then determined using RP-HPLC. Results represent mean \pm SD, n=3 of independent batches.

Figure 6.4 Average size (d.nm) (bars), PDI (circles) and zeta potential (mV) (values) of the four formulations prior to oral administration. Microfluidic manufacture of DSPC:Chol (10:5 w/w), DSPC:Chol:PS (10:5:4 w/w) and MPG:Chol:PS (10:5:5 w/w) (3:1 FRR, 15 mL/min TFR) with a final ovalbumin concentration of 1 mg/mL entrapped. Cationic formulation DSPC:Chol:DOTAP (10:5:2 w/w) (1:1 FRR, 15 mL/min TFR) with a final ovalbumin concentration of 1 mg/mL adsorbed on the surface. Results represent mean \pm SD, n = 5 of independent batches.

Figure 6.5 Anti-OVA antibody systemic immune responses following oral administration of liposomal formulations in mice (BALB/c mice 6–8 weeks old). Mice were terminally bled on day 35 and serum antibody analysis was conducted using ELISA. (A) Serum IgG response and (B) Serum IgA response. Each sample/dilution was tested in duplicate and data are presented as mean optical density (OD 450) with each individual sample (circle) and Geo-mean (black line) shown. Results represent geo-mean \pm SD, n=5 of independent batches.

Figure 6.6 Anti-OVA antibody mucosal immune responses following oral administration of liposomal formulations in mice (BALB/c mice 6–8 weeks old). (A) Intestinal wash (B) caecum (C) colon and (D) faecal samples were analysed for IgA antibody response using ELISA. Each sample/dilution was tested

in duplicate and data are presented as mean optical density (OD 450) with each individual sample (circle) and Geo-mean (black bar) shown. Results represent geo-mean \pm SD, n = 5 of independent batches.

Figure 6.7 Average size (d.nm) (bars), PDI (circles) and zeta potential (mV) (values) of the four formulations prior to oral administration. Microfluidic manufacture of empty DSPC:Chol (10:5 w/w), DSPC:Chol (10:5 w/w) encapsulating ovalbumin with co-mixed CTX, DSPC:Chol (10:5 w/w) encapsulating ovalbumin with surface conjugated CTX, DSPC:Chol:DDA (10:5:4 w/w) in-line loaded with ovalbumin and DDA:TDB (5:1 w/w) with surface complexed ovalbumin. All formulations had a final antigen concentration of 1 mg/mL. Results represent mean \pm SD, n=5 of independent batches.

Figure 6.8 Anti-OVA antibody systemic immune responses following oral administration of liposomal formulations in mice (C57BL/6 mice 20g, 6-12 weeks old). Mice were terminally bled on day 35 and serum IgG antibody analysis was conducted using ELISA. Each sample/dilution was tested in duplicate and data are presented as mean optical density (OD 450) with each individual sample (circle) and Geo-mean (black bar) shown. Results represent geo-mean \pm SD, n=5 of independent batches

Figure 6.9 Anti-OVA antibody mucosal immune responses following oral administration of liposomal formulations in mice (C57BL/6 mice 20g, 6-12 weeks old). (A-B) Intestinal wash IgA and IgG respectively, (C) caecum IgA (D-E) colon IgA and IgG respectively were analysed for antibody responses using ELISA. Each sample/dilution was tested in duplicate and data are presented as the endpoint titre with each individual sample (circle) and Geo-mean (black bar) shown. Results represent geo-mean \pm SD, n=5 of independent batches.

List of Tables

Table 1.1 Current *C. difficile* vaccine candidates in clinical trials (adapted from (Riley et al., 2019)).

Table 1.2 Examples of commonly used adjuvants, the corresponding components and how the adjuvant exerts its immunostimulatory effects

Table 1.3 Examples of commonly used lipids (name in abbreviation) with the molecular weight, chemical structure, transition temperature and common applications in liposomal form.

Table 1.4 Examples of commonly used methods for the manufacturing of liposomes entrapping protein within. The protein entrapped is listed, along with the liposomal formulation used, the manufacturing technique employed and the subsequent entrapment efficiency (loading efficiency).

Table 3.1 Comparative protein loading for liposomal formulations DSPC:Chol (10:5 w/w), DSPC:Chol:PS (10:5:4 w/w) and DSPC:Chol:DOTAP (10:5:4 w/w) between two protein quantification techniques, RP-HPLC and micro BCA assay.

Table 4.1 The effect of product concentration using Tangential flow filtration. Liposomal sample DSPC:Chol:PS (10:5:4 w/w) initial total lipid of 4 mg/mL, FRR 3:1 and TFR 10 mL/min was loaded with initial ovalbumin concentration of 15 mg/mL. The product was purified and then concentrated from 2 mL to 1 mL and assessed for protein concentration and vesicle physicochemical attributes.

Table 5.1 Physicochemical attributes (size, PDI and zeta potential) of the four formulations DSPC:Chol (10:5 w/w) DSPC:Chol:DOPS (10:5:4 w/w), DSPC:Chol:DDA (10:5:4 w/w) and DDA:TDB (5:1 w/w). Neutral and anionic formulations were dialyzed over night to remove untrapped DQ-OVA, while cationics were dialyzed for 1 h to remove solvent before the addition of fluorescent protein. Results represent mean \pm SD, n = 3.

Table 6.1 Liposomal formulations physicochemical characteristics prior to subjection to acidic autotitration. Results show neutral (DSPC:Chol), anionic (DSPC:Chol:PS) and cationic (DSPC:Chol:DOTAP) formulations with average size (d.nm), PDI and zeta potential (mV) indicated. Results represent mean \pm SD, n=3 of independent batches.

Table 6.2 Conjugation efficiency of fluorescent ovalbumin (Alexa Fluor) to liposome surface (DSPC:Chol) containing 5% PE:MCC. The effect of DMSO for SPDP solubilisation and buffer pH during SPDP and protein incubation is shown, with % conjugation efficiency measured by fluorescence.

Table of Contents

Abstract	4
List of Publications.....	5
List of Posters and Oral Presentations.....	6
List of Figures	8
List of Tables	15
Chapter 1	21
General Introduction	21
1.1 <i>Clostridium Difficile</i> infection	22
1.2 <i>Clostridium difficile</i> diagnosis and current treatments.....	23
1.3 Vaccine development: An overview	25
1.4 The challenge of developing an oral vaccine	26
1.4.1 The degradative environment of the gastrointestinal tract.....	26
1.4.2 Mucosal immune system overview	28
1.4.2.1 Intestinal epithelial barrier	28
1.4.2.2 Mucosal immune system.....	29
1.4.2.3 Mucosal B cells: Somatic hypermutation, class switching and IgA production	34
1.5 Developing an oral vaccine against <i>C. difficile</i>	36
1.5.1 Adjuvants.....	37
1.5.2 Liposomes as vaccine adjuvants	38
1.5.3 Liposome physicochemical attributes as oral vaccine adjuvants	40
1.5.3.1 Lipid composition	41
1.5.3.2 Vesicle size.....	43
1.5.3.3 Liposomal targeting for enhanced immunological responses	44
1.5.3.4 Adjuvanticity of liposomes	45
1.6 Traditional liposomal manufacturing techniques.....	47
1.6.1 Manufacturing of protein loaded liposomes.....	48
1.6.2 Microfluidics as a production method	49
1.6.3 Continuous manufacturing.....	50
1.7 General aim and thesis objectives.....	51
Chapter 2	52
Scale-up production of liposomal delivery systems	52
2.1 Introduction	53
2.2 Aim and objectives	54
2.3 Materials	54
2.4 Methods.....	54

2.4.1 Top-down liposome manufacture: Lipid-film hydration	54
2.4.1.1 Size reduction: Hand-held extrusion	55
2.4.1.2 Size reduction: Probe sonication	55
2.4.2 Bottom-up microfluidic manufacture of liposomes.....	55
2.4.3 Purification of microfluidic formulations	56
2.4.3.1 Dialysis.....	56
2.4.3.2 Gel filtration.....	56
2.4.3.3 Tangential flow filtration	56
2.4.4 Liposome recovery using fluorescence tracking.....	56
2.4.5 Dynamic light scattering: Physicochemical analysis (off-line and at-line)	57
2.4.6 Gas chromatography: Quantification of residual solvent	57
2.4.7 Statistics	57
2.5 Results and Discussion	58
2.5.1 Comparison of liposomal manufacture: Top-down and bottom-up approaches.....	58
2.5.2 Cholesterol content can be adjusted to control vesicle size	63
2.5.3 Establishing normal operating parameters for microfluidics	65
2.5.4 The choice of organic solvent impacts upon formulation size	70
2.5.5 The effect of the inclusion of charged lipids on microfluidic manufacture	71
2.5.5.1 The addition of phosphatidylserine (PS) within liposomal formulation DSPC:Chol.....	71
2.5.5.2 The effect of cationic lipid addition to DSPC:Chol formulation	76
2.5.6 Down-stream processing: Formulation purification.....	79
2.5.7 Continuous at-line particle sizing.....	83
2.6 Conclusions	85
Chapter 3	86
Method Validation for Protein Loading Quantification within liposomes	86
3.1 Introduction	87
3.2 Aim and Objectives	89
3.3 Materials	90
3.4 Methods	90
3.4.1 Protein quantification techniques	90
3.4.1.1 Micro BCA protein assay kit.....	90
3.4.1.2 Reversed-phase high performance chromatography (RP-HPLC).....	90
3.4.2 Liposome production	91
3.4.3. Liposome purification	91
3.4.4 Method validation	91
3.4.4.1 Linearity.....	91

3.4.4.2 Limit of Detection and Limit of Quantification	92
3.4.4.3 Accuracy, Repeatability and Precision	92
3.5 Results and Discussion	94
3.5.1 Quantification of ovalbumin to determine linearity.....	94
3.5.2 Effect of liposome inclusion on protein quantification.....	97
3.4.3 Effect of solubilisation agent on ovalbumin quantification	100
3.4.4 Effect of ovalbumin quantification in the presence of liposomes and solubilisation mixture for micro BCA protein quantification	103
3.4.5 Protein loading quantification within liposomal formulations: Comparative study between RP-HPLC and micro BCA.....	105
3.6 Conclusions	108
Chapter 4	109
Microfluidics as a manufacturing platform for protein loaded liposomal formulations.....	109
4.1 Introduction	110
4.2 Aim and objectives	111
4.3 Materials	111
4.3.1 Materials used for the preparation of liposomes.....	111
4.4 Methods.....	112
4.4.1 Traditional manufacture of protein loaded liposomes: Lipid-film hydration.....	112
4.4.1.1 Size reduction: Hand-held extrusion	112
4.4.2 Microfluidic manufacture of liposomes entrapping protein	112
4.4.2.1 Purification of liposomes entrapping protein.....	112
4.4.3 Microfluidic manufacture and complexation of cationic vesicles adsorbing protein.....	113
4.4.3.1 Manufacture of empty vesicles.....	113
4.4.3.2 Purification of empty formulations.....	113
4.4.3.3 Complexation of protein.....	113
4.4.4 Circular Dichroism.....	113
4.4.5 Dynamic light scattering (off-line)	114
4.4.6 Protein quantification	114
4.4.7 Statistics	114
4.5 Results and Discussion	115
4.5.1 Tangential flow filtration as a purification tool for liposomes entrapping protein	115
4.5.2 Microfluidic manufacture of vesicles entrapping protein.....	116
4.5.3 Identification of critical microfluidic process parameters.....	121
4.5.3.1 The effect of FRR on protein entrapment efficiency for neutral and anionic vesicles...	121
4.5.3.2 The effect of TFR on protein entrapment efficiency for neutral and anionic vesicles...	123

4.5.4 Tangential flow filtration as a tool for the concentration of protein loaded vesicles	124
4.5.5 Scale independent manufacture of protein loaded liposomes	125
4.5.6 Microfluidic complexation using cationic vesicles	126
4.5.6.1 Optimisation of empty vesicles: Microfluidic parameters	126
4.5.6.2 Microfluidic complexation: Identifying critical process parameters.....	128
4.6 Conclusions	134
Chapter 5	135
<i>In vitro</i> vaccine study: cellular association, antigen processing and surface marker expression ...	135
5.1 Introduction	136
5.2 Aim and Objectives	138
5.3 Materials	139
5.4 Methods	139
5.4.1 Liposome manufacture and purification	139
5.4.2 THP-1 culture and differentiation	140
5.4.3 Liposome association and DQ-OVA studies	140
5.4.4 Activation markers	141
5.4.5 Flow cytometry analysis	141
5.4.6 Statistical analysis	141
5.5 Results and Discussion	142
5.5.1 Determination of cellular association using a range of liposomal formulations.....	143
5.5.2 The effect of liposomal delivery systems on the rate of antigen processing using DQ-OVA	147
5.5.3 Cellular surface marker expression following liposomal delivery system incubation	151
5.6 Conclusions	156
Chapter 6	157
Oral administration of liposomes manufactured by microfluidics: Mucosal and systemic antibody responses.....	157
6.1 Introduction	158
6.2 Aim and objectives	159
6.3 Materials	159
6.3.1 Materials used for the preparation of liposomes.....	159
6.4 Methods	160
6.4.1 Liposome manufacture and purification	160
6.4.1.1 Anionic and neutral formulations entrapping protein	160
6.4.1.2 Cationic formulations	160
6.4.1.3 Cholera Toxin conjugation process	161
6.4.2 Dynamic light scattering: Physicochemical analysis and pH autotitration.....	161

6.4.3 Antigen retention following acidic exposure.....	162
6.4.4 <i>In Vivo</i> studies.....	162
6.4.4.1 Immunisation schedule	162
6.4.4.2 Quantification of antibodies using ELISA.....	163
6.4.5 Statistics	163
6.5 Results and discussion	164
6.5.1 Liposomal vesicle characteristics and antigen retention under acidic conditions	164
6.5.2 Mucosal and systemic antibody responses following oral administration of liposomal formulations.....	170
6.5.3 Inclusion of immunostimulatory components to liposomal formulations and the effect on mucosal and systemic antibody response	176
6.5.3.3 Systemic antibody response	179
6.5.3.4 Mucosal antibody response.....	180
6.6 Conclusions	186
Chapter 7	187
Overall Conclusions	187
7.1 Introduction.....	188
7.2 Microfluidics as a manufacturing platform for liposomal vaccines.....	189
7.3 Validation of protein quantification tools.....	190
7.4 Microfluidic manufacture of liposomal formulations incorporating protein.....	190
7.5 <i>In vitro</i> screening of liposomal formulations.....	191
7.6 <i>In vivo</i> vaccine efficacy: Antibody responses	192
7.7 Concluding Remarks and future work.....	193
References	195

Chapter 1

General Introduction

1.1 *Clostridium Difficile* infection

Within the global population, the gram-positive spore forming bacterium *Clostridium difficile* (*C. difficile*) can reside in as much as 5% of healthy adults, with some studies showing as up to 17.5% of individuals tested containing *C. difficile* spores within their stools (Schaeffler and Breitrueck, 2018, Czepiel et al., 2019), with the clinical implications exhibiting a wide range of severity, from asymptomatic carriers, to diarrhoea and in extreme cases, death, as a result of pseudomembranous colitis and toxic megacolon (Kelly and Kyne, 2011, Abt et al., 2016). Bacterial spores can be ingested from the environment where they can persist for up to 5 months on certain surfaces, having been previously shed by either asymptomatic or symptomatic carriers (Claro et al., 2014, Hong et al., 2017). The financial burden of *C. difficile* infection (CDI) within Europe alone was estimated to be approximately £2.5 billion annually (Foglia et al., 2012) and within the US the total CDI-attributed cost was \$6.3 billion over a ten year period (Zhang et al., 2016). The extent of *C. difficile* colonization and the subsequent severity of the downstream impact is primarily determined by the health status of the individual, and most importantly, the status of the individual's microbiome. Symbiotic relationships with microorganisms occur at the surfaces of our epithelia, with the majority of these being found within the gastrointestinal tract (GIT) (Tlaskalová-Hogenová et al., 2011). Within the lumen of the colon, resident microorganisms can actively produce free sialic acid and short-chain fatty acids from dietary sources which are then readily available as energy sources for commensal bacteria. These resources are normally under tight competition; however, when the individual's natural biome has been altered, through for instance the use of antibiotics (such as cephalosporins, penicillin and fluoroquinolones) or chemotherapeutics, an excess of these resources accumulates leading to uncontrolled growth of potential pathogens such as *C. difficile* (Abt et al., 2016, Schaeffler and Breitrueck, 2018). This makes *C. difficile* an important microbe for places such as hospitals and other healthcare settings where large groups of immunocompromised patients are in close proximity. Thus such environments can become reservoirs for the bacterial spores, with some hospitals and nursing homes registering *C. difficile* infection rates as high as 73% (Péchiné et al., 2007).

The primary virulence toxins associated with CDI are two large cytotoxic glucosyltransferases, toxin A (TcdA, 308 kDa) and toxin B (TcdB, 270 kDa) which bind to epithelial cells and inactivate GTPases by irreversible glycosylation, although there are a number of strain dependent secondary proteins involved in virulence including a number of proteolytic enzymes as well as a third toxin known as *C. difficile* binary toxin (Gerding et al., 2014, Péchiné et al., 2007). Rho (RhoA,-B,-C), Rac and Cdc42 are proteins within the cell which are essential for cytoskeletal development and therefore glycosylation of these proteins by TcdA and TcdB results in a wide range of cellular disruption mechanisms including actin condensation, loss of structural integrity, membrane blebbing and therefore inevitable cellular

apoptosis (Voth and Ballard, 2005). The downstream implications of these cellular mechanisms results in a strong pro-inflammatory reaction. Intestinal cells exposed to TcdA and TcdB have been shown to result in neutrophil infiltration, a wide range of chemokine and reactive oxygen species (ROS) production as well as tight junction damage (the damage to tight junctions further increases the rate of neutrophil leakage into the intestinal lumen). Epithelial cells that come in contact with TcdA and TcdB release pro-inflammatory cytokines such as interleukin-8 (IL-8) further increasing the inflammation. As the infection proliferates through the mucosa, macrophages, dendritic cells and monocytes further increase the pro-inflammatory cascade, producing a plethora of pro-inflammatory interleukins and tumour necrosis factors, driving the epithelial damage sustained during CDI (Spencer et al., 2014).

1.2 *Clostridium difficile* diagnosis and current treatments

There are a broad range of approaches for the treatment of CDI currently advised by the European Society of Clinical Microbiology and Infectious Disease (ESCMID), with the choice of treatment depending upon the degree of CDI severity, patient factors such as age and immune status, as well as geographical location. While most European countries have their own CDI treatment guidelines, those published by the ESCMID act as a structure and a set of guidelines that can be followed (Fitzpatrick et al., 2018). Following a CDI diagnosis (there remains some ambiguity about this between healthcare professionals as a number of factors can determine the extent of CDI, such as raised leukocyte counts, decreased albumin and a rise in serum creatinine levels and toxin A/B counts in patient's stool samples), the primary conventional therapeutic options rely on the use of antibiotics such as metronidazole and vancomycin to control the *C. difficile* proliferation. In these cases the relapse occurrence has been found to be as high as 29% with a subsequent disproportionate increase in mortality rates being found (Guo et al., 2015, Fitzpatrick et al., 2018). There are also an increasing number of reports documenting the emergence of antibiotic resistant hyper virulent strains of *C. difficile*, reducing the effectiveness of new antibiotic therapies approved by the FDA for more severe cases of CDI, such as fidaxomicin (Schaeffler and Breitrueck, 2018, Du et al., 2014). The use of therapies targeting the proliferation of microbiota to out-compete *C. difficile* within the gut has shown some signs of potential, including the use of faecal matter transplants or probiotic administration (e.g. *Lactobacillus* strains) in conjunction with antibiotic administration; yet, the long term efficacy and the potential for the development of other downstream complications remains largely unknown and requires further development (Schaeffler and Breitrueck, 2018, Czepiel et al., 2019). Furthermore, prophylactic therapies such as Ribaxamase (an oral formulation designed to limit the damage to the gut microflora through degradation of unmetabolised antibiotic) and DAV132 (a charcoal capsule,

which binds and inactivates excess antibiotic within the colon) are currently undergoing clinical development and could be potential tools used to limit *C. difficile* proliferation (de Gunzburg et al., 2018, Kaleko et al., 2016).

Alternative treatments to CDI, such as long term protection through vaccination has been explored in both animal models and human subjects with varying levels of success. A correlation between CDI protection and prevention of relapse has been found with both the presence of systemic and localised production of anti-toxin immunoglobulins (Spencer et al., 2014, Solomon, 2013). When comparing asymptomatic patients to more severe cases of CDI, strong systemic anti-toxin A and B IgG as well as high serum levels of IgM and IgA was shown to reduce both infection severity and relapse recurrence rates, highlighting the potential of a vaccine as a promising option in the battle against CDI (Kyne et al., 2001, Kyne et al., 2000, Kelly and Kyne, 2011).

Currently, the majority of vaccine development (Table 1) focuses on the use of chemically/genetically modified toxoid formulations, with the exception being VP20621, where an oral suspension of non-toxigenic spores of an *C. difficile* strain is used (Villano et al., 2012, Riley et al., 2019). A formalin inactivated toxoid vaccine for toxins A and B containing aluminium hydroxide as an adjuvant produced by Sanofi Pasteur showed the greatest potential out of all the current vaccine candidates following numerous clinical Phase I and II trials, although poor results from Phase III data in terms of efficacy against primary CDI resulted in the decision by Sanofi Pasteur to discontinue development (de Bruyn et al., 2016, Riley et al., 2019). Similarly, Pfizer are currently undergoing Phase III trials for their vaccine candidate PF-06425090, again using modified toxoids TcdA and TcdB, while toxicity in this formulation is further reduced by genetic modification of amino acid sequences, Phase III data is expected within 2020 (Donald et al., 2013, Riley et al., 2019). Finally, Valneva's CDI vaccine candidate focuses on a slightly different mechanism than traditional inactivated toxoid vaccines, by combining epitopes of both toxins (A and B) into a single chimeric protein antigen. While current human Phase II data shows effective levels of neutralising antibodies being generated against both toxins, there remains some unanswered questions in regards to efficacy across strains of *C. difficile*, in part due to the highly specific epitopes chosen for the chimera (Bézay et al., 2016, Riley et al., 2019). A summary of these vaccine candidates is shown in Table 1, including the possible mechanisms of action and their current stage of development.

Table 1.1 Current *C. difficile* vaccine candidates in clinical trials (adapted from (Riley et al., 2019)).

Vaccine Candidate	Manufacturer	Development Status	Mechanism of action
C diffense	Sanofi/Pasteur	Terminated at Phase III	Formalin inactivated TcdA and TcdB toxoid vaccine with aluminium hydroxide for injection
PF-06425090	Pfizer	Phase III	Genetically/chemically detoxified TcdA and TcdB toxoid vaccine
VLA84	Valneva	Phase II	Recombinant chimeric protein incorporating both binding domains of TcdA and TcdB
VP20621	Shire	Phase II	Live non-toxigenic <i>C. difficile</i> strain for oral delivery

1.3 Vaccine development: An overview

Conventional vaccines traditionally focused on the use of live-attenuated whole cells or killed/inactivated, which have had their toxicity mitigated or removed through the use of chemical, radioactive or heat-based methods to induce active immunity against their pathogen (Vartak and Sucheck, 2016). Historically, these types of vaccines have proven time and time again to be valuable tools within our healthcare systems, with diseases such as measles and polio largely eradicated throughout the western world as a result (Minor, 2015). However, a number of recurrent issues arise when using live-attenuated and killed/inactivated vaccines, such as the potential for causing harm and even disease, particularly amongst immuno-compromised individuals, as well as broad ranges of vaccine efficacy being exhibited (Minor, 2015, Angsantikul et al., 2017). These issues have largely resulted in a shift in vaccine development and regulation, with attention now being focused on safer, more controllable vaccine methods. Subunit vaccines are more well-defined antigens, derived from parts of the pathogen but not incorporating the entire cell as a whole, thus removing reactogenic components such as lipopolysaccharides, DNA and RNA (Foged, 2011, Petrovsky, 2015). These subunit antigens could be composed of toxoids, cellular membrane fragments from the pathogen or specific surface molecules, and in the case of chimeric and recombinant subunit vaccines, a combination of these components (Vartak and Sucheck, 2016). With an improved safety profile, subunit antigen based vaccines offer great potential; however, this move away from whole cell microorganisms comes at a cost in regard to vaccine efficacy due to a loss of inherent immunogenicity. To overcome this,

adjuvants can be incorporated within the vaccine to boost and or direct the subsequent immune response and these will be discussed in greater detail in section 1.5.1. In addition to conventional vaccine approaches, nucleic acid based therapies are emerging as a promising technology. In the 1990s, injection of nucleic acid in mice models resulted in the expression of their coded proteins, opening the door to RNA based vaccinology. Advancements in mRNA immunogenicity and the use of delivery systems has now pushed the field into a range of successful clinical and preclinical trials. Currently, self-amplifying RNA can result in potent immune responses, a result of the inclusion of genes encoding for replication remaining intact (Zhang et al., 2019, Fuller and Berglund, 2020). This promise in regards to vaccine efficacy and safety has now led to self-amplifying RNA incorporating SARS-Cov-2 antigen, encapsulated within a lipid nanoparticle being tested in humans to help combat the SARS-Cov-2 pandemic (McKay et al., 2020).

1.4 The challenge of developing an oral vaccine

1.4.1 The degradative environment of the gastrointestinal tract

In order to further understand the challenges of developing an oral vaccine against enteric pathogens such as *C. difficile*, an overview of the gastrointestinal tract and mucosal immune system is first required. The gastrointestinal tract (GIT) serves primarily to digest and absorb nutrients, while excreting excess and unused waste. The GIT must also act to protect the body from enteric pathogens, and as a result, the GIT collectively forms the largest immunological organ within the body (Pasetti et al., 2011). The digestive processes within the GIT result in a highly degradative environment which poses challenges for the delivery of oral therapeutics, in particular the delivery of oral antigen for vaccination. The GIT can be separated into either upper and lower sections. The upper gastrointestinal tract involves the mouth (oral cavity), pharynx, oesophagus and the stomach, while the lower section includes the small intestine (duodenum, jejunum and ileum), the large intestine (cecum, colon and rectum) and finally the anus (Ramirez et al., 2017). Initially, materials entering the mouth are subjected to salivary enzymes such as lysozymes, followed by a highly acidic environment of the stomach, where degradation is undergone by the gastric juice which includes additional degradative enzymes and hydrochloric acid. For protein degradation, a number of protease enzymes are secreted by the pancreas and stomach including pepsin, trypsin and chymotrypsin which facilitate the breakdown of protein into smaller peptides for nutrient absorption, which presents obvious barriers for the oral route of administration for vaccine antigens. Fat digestion occurs throughout the GIT and is facilitated by lipases from the bile and pancreas where short chain diglycerides and monoglycerides are formed. The gastric environment has a pH range approximately between 1-3 (in a fasted state, while fed can have a broad range between approximately 3-7), and the rate at which materials are

retained within the stomach varies considerably as a result of individual variation, environmental factors such as smoking and drinking as well as stress levels and quantities of material ingested (Hellmig et al., 2006). The typical gastric emptying time following mastication and swallowing can be up to as long as 4 hours for total meal clearance (Vasavid et al., 2014). Once the material has left the gastric environment it enters the small intestine. The small intestine adsorbs necessary nutrients while simultaneously serving an important immunological aspect – being host to the concentration of Peyer’s patches (PPs) – crucial organised lymphatic follicles which will be discussed later within this chapter (Collins and Badireddy, 2019). The first section of the small intestine is known as the duodenum, where the pH is much closer to neutral than that of the stomach (approximately between 3 and 6, varying during fed and fasted states). Material will then pass into the jejunum, followed by the final section of the small intestine, the ileum. Both these sections have a near neutral pH environment (between 6 and 7). The estimated time of travel through the small intestine is between 3-5 hours; although this can vary greatly, depending on the person (including age and gender), environmental factors and the state of the *in vivo* system, i.e. whether it has just fed, or whether it is in a fasted-state (Robertson, 2013). Upon leaving the small intestine, material that is largely void of nutrients now enters the large intestine, composed of the cecum, colon and rectum, where the absorption of any remaining water, electrolytes and nutrients occurs prior to elimination (Azzouz and Sharma, 2019).

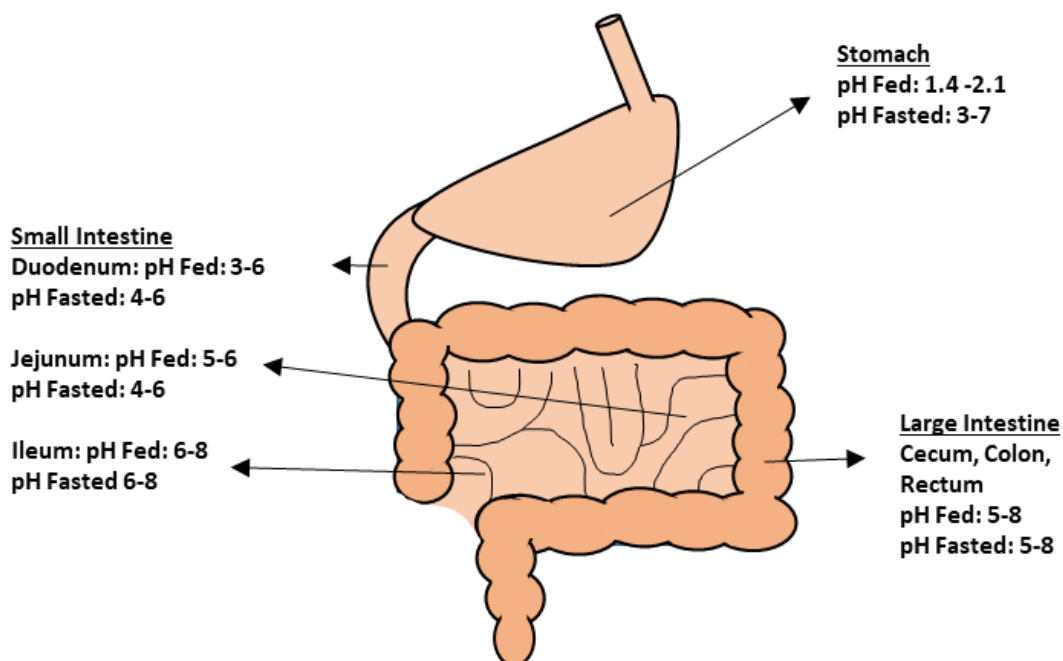


Figure 1.1 Schematic diagram of the pH differences found throughout the human gastrointestinal tract. Initially the gastric environment (stomach) contains highly acidic pH, dependent upon the fed fasted state of the individual. As you traverse through, the small intestine (duodenum, jejunum and ileum) becomes less acidic, where pH can range between approximately pH 3-8. Finally, the large intestine (caecum, colon and rectum) pH can be between 5-8 dependent on fed / fasted state. Adapted from (Ndibewu and Ngoben, 2013).

1.4.2 Mucosal immune system overview

1.4.2.1 Intestinal epithelial barrier

The human GIT is thought to be between 300 – 400 m² and is constantly exposed to the outside external environment, which poses a complex question of how the body retains homeostasis and repels foreign invaders such as pathogens looking to gain entry within. The large intestine alone is thought to contain as much as 1,000 individual species of bacteria (not including other microorganisms such as fungi, archaea, protozoans, viruses and so on) with population numbers around 10¹² bacterium/cm² and the complexity of the gut microbiome is only now gradually being understood (Lazar et al., 2018). The complicated relationship between the human body and our symbiotic microorganisms is now being viewed as essential for development, with the microbiome playing key roles in our immune system, host homeostasis and even communicating with our brain via the gut-brain axis impacting on our social behaviours such as stress response physiology (Foster et al., 2017). This ecosystem within our gut has meant our body requires a complex barrier and protective systems in place to regulate and remove pathogenic species, while simultaneously not disrupting commensal species that are key to our health (Yap and Mariño, 2018). The intestinal mucosal barrier allows for containment of potentially pathogenic and immunogenic entities from entering the body. A layer of intestinal epithelium forms a cellular barrier between the intestinal mucosa beneath, and the external gut lumen. The epithelial layer is composed of a range of cell types, with enterocytes forming tight junctions to control nutrient absorption and general barrier integrity, while goblet cells secrete mucus. Enteroendocrine cells, paneth cells (secrete antimicrobial molecules and growth factors) and microfold cells also reside within the intestinal epithelial layer, all of which are replenished from a source of pluripotent stem cells found within the crypts (Salim and Söderholm, 2011). The secreted mucus layer forms the first barrier of protection against the vast numbers of microorganisms that reside within the gut (Peled et al., 2016). The mucus layer contains gel-like proteins such as mucins, antimicrobial peptides (AMPs) and secretory immunoglobulins such as sIgA – produced by effector plasma cells. The density of the mucus layer varies throughout the GIT, with the small intestine consisting of a single mucus layer, while the colon contains two distinct layers, an outer loose area, where commensal bacteria can pass through, and an inner dense layer, restricting further microbial penetration to the underlying epithelia (Vancamelbeke and Vermeire, 2017). In addition to acting as a barrier for microbes, the mucus layer also inhibits interactions between the epithelial layer and the vaccine antigens administered orally. Following through the epithelial tissue layer, the lamina propria can be found, where a range of cell types reside. As well as structural cell types such as fibroblasts, endothelial cells and smooth muscle cells, a vast network of vascular and lymphatic vessels supplies the region with dense populations of effector immune cells such as macrophages, mast cells,

lymphocytes and plasma cells (Hunyady et al., 2000). These immune cells, and others, together form the mucosal branch of the innate and adaptive immune defence system. The final layer of the mucosa on the other side of the epithelium, flanking the lamina propria, is the *muscularis mucosae*, a thin layer of muscle tissue fibres that can be found throughout the GIT (Salim and Söderholm, 2011).

1.4.2.2 Mucosal immune system

The human body relies on the mucosal immune system to form a protective barrier against environmental pathogens, prevent the entry of un-degraded antigens (such as dietary, environmental or microbial sources) and to regulate the immunological responses appropriately, in order to not generate unnecessary pro-inflammatory damage (Holmgren and Czerkinsky, 2005). The mucosal immune system is composed of the lymphatics (or mucosal associated lymphoid tissue, MALT) and its associated localised mucosal tissue such as the gut-associated lymphoid tissue (GALT), bronchus-associated lymphoid tissue (BALT) and nasopharynx-associated lymphoid tissue (NALT) (Montilla et al., 2004). The mucosal immune system is a separate, distinguishable branch of the immune system from that of the systemic immune system. It comprises of lymphoid tissues such as Peyer's patches (lymphoid follicles found throughout the small intestine, predominately within the ileum, containing populations of B and T cells), lymph nodes such as the mesenteric lymph node, and other lymphoid follicles found throughout the GIT, acting as induction sites for immune responses (Holmgren and Czerkinsky, 2005). Peyer's patches are covered by a layer of epithelium known as the follicle associated epithelium (FAE), forming a dome like structure projecting into the lumen, visible by the human eye. The FAE also has many immune cell types such as macrophages, DCs, B and T cells intercalated throughout (Mowat, 2003). The FAE contains specialised epithelial cells known as M cells, which play a critical role in antigen sampling from the lumen. These cells are phenotypically different from their epithelial counterparts, with reduced microvilli and a minimal mucus layer for coverage, allowing them to sample antigen and transport from the lumen across to the lamina propria to waiting APCs (Bilsborough and Viney, 2004). The FAE expresses specific chemokines (CCL9 and CCL20) which act as homing receptors to accumulate APCs underneath the M cells for efficient antigen uptake. This area directly below the specialised M cells is known as the subepithelial dome (SED), an area that is highly populated with DCs and macrophages. Following M cell uptake, antigen is passed to the APCs of the SED for degradation, processing and subsequent presentation (Da Silva et al., 2017). The priming of naïve CD4⁺ T cells (generating the memory response of the immunological system) then occurs in the thymus-dependent area (TDA), or directly in lymph nodes (such as the mesenteric lymph node) by APCs that have migrated from the PPs, more information relating to memory response will be discussed further on (Figure 1.2) (Kang et al., 2018).

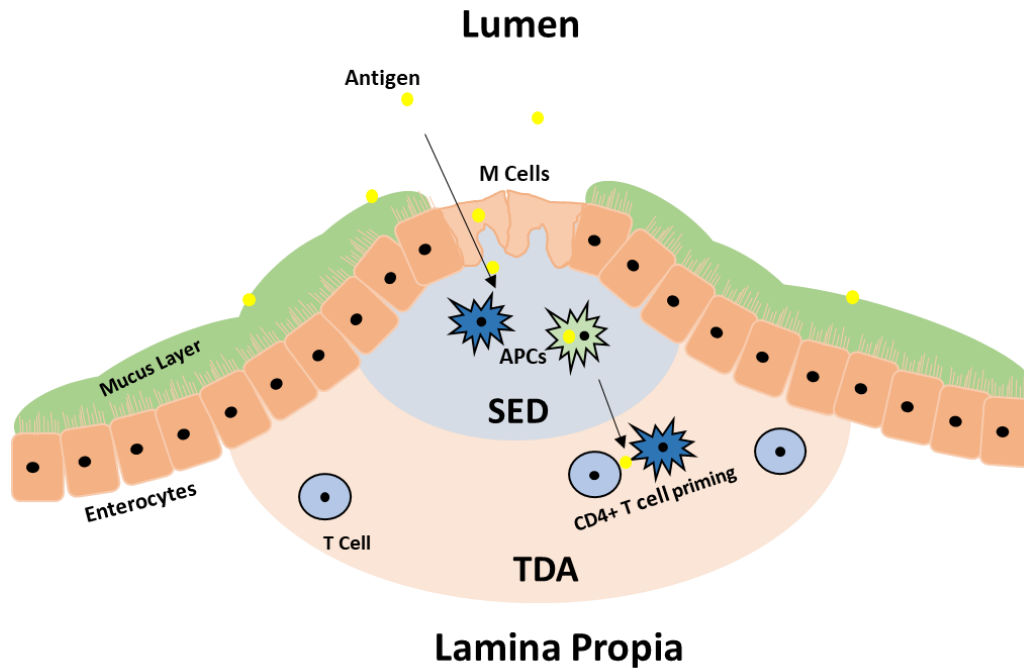


Figure 1.2 Schematic diagram of the physiology of a Peyer's patch. Antigen from the lumen can transcytose across the epithelial layer via specialised M cells (lacking a mucosal layer). The antigen is passed to the subepithelial dome (SED) where they can interact with underlying APCs (DCs / macrophages). T cell (CD4⁺) priming can then occur in the thymus dependent area via interactions with DCs before migration towards lymph nodes for subsequent GC formation. Adapted from (Kang et al., 2018).

The cells of the mucosal immune system charged with non-specific defence are known as the innate immune cells. These cells such as intestinal macrophages and DCs are derived from monocytes that constantly enter the intestine from the macrophage – DC bone marrow derived progenitor cells. The ultimate fate of differentiation of these cells is dictated by the microenvironment that they are exposed to. For example, intestinal macrophage development is directed by growth factors such as Csf1 (colony-stimulated factor 1), while different subsets of intestinal DCs are similarly controlled into different developmental pathways by cytokines and growth factors like Flt3 (FMS-like tyrosine kinase 3) (Flannigan et al., 2015). Typically, these resident antigen presenting cells (APCs) reside in a tolerant state, in order to not generate pro-inflammation in the presence of commensal microbiota and food antigens. Traditionally these cell types typically involve the binding of antigen through pathogen associated microbial patterns (PAMPs) to specific receptors known as pattern recognition receptors (PRRs), such as toll-like receptors (TLRs). Upon binding, the APCs internalize their antigenic target through phagocytosis, pinocytosis or clathrin-dependent endocytosis (Gaudino and Kumar, 2019). There are a number of factors which influence which pathway the antigen is internalised, and therefore the subsequent immune response is determined by the internalisation pathway. Following

internalisation, the PAMP is degraded and processed by the cell, with antigenic components being expressed on either major histocompatibility complex I or II (MHC I or II) for presentation to CD8⁺ or CD4⁺ T cells respectively to initiate the memory immune response (Gaudino and Kumar, 2019).

Immature DCs have a wide range of receptors capable stimulating pro-inflammatory responses such as TLRs, Mannose Receptors and DC-sign receptors and they act as the main link between antigen capture, presentation and subsequent adaptive immune response, often described as the interface between the innate and adaptive systems. Specialised mucosal DCs are found in MALT, found beneath the mucosal epithelium (Owen et al., 2013). Following antigen binding, the immature DCs undergo a phenotypic maturation change where they present the antigen on their cellular surface and start their migration towards the lymph nodes where activation of helper T-cells, killer T-cells and B-cells begins. Furthermore, DCs are capable of stimulating the activation of both naïve and memory T-cells, unlike any other professional antigen presenting cells (Apostolopoulos et al., 2013).

Intestinal macrophages have high affinity and microbicidal activity against potential pathogens that cross the epithelial barrier, although the classical pro-inflammatory response (e.g. IL-1, 6, 12, 23) observed in peripheral macrophages are heavily downregulated within the gut as a result of the tolerogenic environment within the GALT, largely a result of IL-10 produced by CD4⁺Foxp3⁺ regulatory T cells (Flannigan et al., 2015). Simultaneously, these intestinal macrophages influence the proliferation of CD4⁺ T cells into CD4⁺Foxp3⁺ regulatory T cells, thus furthering the immunotolerant environment within the gut. Intestinal DCs (CD103⁺) are also key factors in gut homeostasis through communication with the adaptive immune system. Like their macrophage counterparts, intestinal DCs can drive CD4⁺ T cell differentiation into Foxp3⁺Treg cells. Intestinal DCs also actively and continuously migrate to the mesenteric lymph nodes, driving immune tolerance for commensal antigen and dietary protein. During inflammation or injury, this tolerogenic state can quickly change to high levels of pro-inflammation. New migrating monocytes entering the intestinal environment no longer develop into tolerogenic macrophages and DCs, instead upregulate TLRs and other inflammatory markers, becoming highly aggressive against microbial entities, driving pro-inflammation through IL-1, IL-6, IL-12, IL-23 and tumour necrosis factor alpha (TNF-alpha). This pro-inflammation promotes further DC activation, and the DCs preferentially favour proliferation of Th1 and Th17 cells instead of the CD4⁺Foxp3⁺ regulatory T cells found during a healthy non-inflammatory state (Flannigan et al., 2015).

There are a number of ways in which antigen can be bound and presented to cells of the adaptive immune system within the GIT. DCs and macrophages within the lamina propria can intercalate within the epithelial layer and extend dendrites into the lumen to sample antigens, returning to lymphoid tissue for antigen presentation. The epithelial layer itself can also act as antigen sampling cells,

through specialised microvilli-lacking (M cells). M cells can be found in high levels within the FAE, actively binding some pathogens and particulate antigens for the generation of adaptive responses. These specialised epithelial cells lack MHC II molecules, thus rely on intermediate antigen presenting cells to migrate to T cell/B cell areas within lymphoid tissue where they can present the processed antigen to naive lymphocytes (Mowat, 2003). As well as M cells and traditional APCs, intestinal epithelial cells such as enterocytes also play an important immunological role. Plasma cells from the lamina propria and PPs secrete IgA which binds on to the polymeric immunoglobulin A receptor (pIgR) on the basolateral side of the epithelial layer. The IgA dimer is then transcytosed to the apical membrane surface where it is secreted into the lumen as sIgA. A strong indicator of a healthy mucosal immune response is the local secretion of sIgA as it is capable of effectively functioning within the degradative environment of the GI tract due to its relatively protease resistant nature (Owen et al., 2013).

Intestinal epithelial cells have been shown to produce both cytokines and chemokines in response to microbes within the lumen through a range of TLRs (e.g. TLR3, 4, 5, 9), communicating with the immune cells within the lamina propria (Goto, 2019). Furthermore, intestinal epithelial cells may play a role in the development of Th1, Th17, Tregs and CD8⁺ T cells. Within the lamina propria, it has been shown that these T cell types can proliferate and differentiate accordingly to the environmental stimulus, thus in the presence of particular bacterial species within the lumen, Th17 induction occurs. It is suspected that the association of these bacteria to the intestinal epithelial cells induces a signalling cascade which then in turn directs T cell differentiation within the lamina propria (Goto, 2019).

Following the innate immune system, the secondary line of immunological defence is the adaptive immune system. An adaptive immune response is the basis behind immunological memory, and functions through specific cell types (primarily T and B cells) in order to generate long lasting protection against previously encountered antigen. After an initial response to a pathogenic infection ends, the effector cells generated decline in number, leaving a small population of memory T and B cells which can then quickly proliferate upon re-exposure. In the case of T cells, a very general classification into two main subtypes results in either CD4⁺ helper T cells or CD8⁺ cytotoxic T cells. Helper T cells are capable of orchestrating other immune cells through cytokines and chemokines, while cytotoxic T cells generally produce cytokines for the elimination of infected cells (however this statement is not a rule, as there are cases where CD4⁺ / CD8⁺ cells function in the opposite sense) (Pennock et al., 2013). Naive T cells are activated following binding of the antigen peptide fragments associated to the APCs on the MHC I or II through their T cell receptor. Alongside co-stimulatory molecules, T cell activation occurs, allowing further differentiation to enable cytokine production (Schwendener, 2014). The cytokines and co-stimulatory molecules present during activation (as a

result of the specific pathogen exposed) then further dictates differentiation into subsets with specific effector functions. These include Th1, Th2, Th17, Th9, follicular helper T (Tfh), and regulatory T cells (Tregs). Th1 subsets of helper T cells are known for generation of high levels of interferon-gamma (IFN γ) and TNF-alpha, activating APCs and upregulating phagocytic capability. Th2 cells in general are found in IL-4 environments for the clearance of parasitic pathogens through eosinophil, mast cells and basophils. Th17 subsets can produce IL-17, which activates neutrophils for bacterial and fungal infections (Pennock et al., 2013). Conversely to these pro-inflammatory orchestrator subtypes, Tregs are present to balance out the negative effect of inflammation. The suppressive nature of this helper T cell subtype will be explained in further detail, in relation to their role in oral tolerance.

Helper T cells can then further orchestrate the immunological response by activating B cells, which have also encountered the specific antigen, through the B-cell receptor (BCR) (Janeway Jr et al., 2001). Naïve B cells express cell surface IgM and IgD; however, following activation, isotype switching (the process in which B cells change their immunoglobulin production from one type to another, i.e. from IgD to IgG) occurs, regulated by the presence helper T cells through specific cytokine production as well as CD40 and / or TLR binding, more of which will be discussed later. (Stavnezer et al., 2008).

These lymphocytes are originally derived from naive immune cells from the bone marrow and thymus, which have travelled through the lymphatics of the mucosal immune system via the bloodstream and are the key modulators of the adaptive mucosal immune response. Once within the lymphoid tissue associated with the gut (e.g. PPs), they encounter antigen, either directly or indirectly through antigen presentation cells and become primed. They drain from the intestinal lymphatics through the mesenteric lymph nodes (MLNs), undergoing differentiation, before re-entering the blood circulatory system (Habtezion et al., 2016). Once within the systemic circulatory system, the distinct mucosal lymphocytes are capable of homing back to the mucosal sites of induction through the upregulation of surface proteins such as alpha(4)beta(7) integrin – which binds with mucosal addressin cell adhesion molecule (MAdCAM) found throughout high endothelial venules of the mucosal lymphoid tissues (Petrovic et al., 2004). Furthermore, these high endothelial venules within the GALT produce cytokines such as CCL21, further driving chemotaxis of lymphocytes through CCR7. The upregulation of chemotactic factors allows for highly specific localisation of these lymphocytes within the GALT, and expression of various types can direct localisation to the lamina propria (CCR9) and intestinal epithelium to become intraepithelial lymphocytes and B cell localisation back to PPs to become plasma cells for sIgA secretion (Habtezion et al., 2016). The importance of this compartmentalisation between the mucosal and systemic immune system, in regards to oral vaccination will be discussed further.

1.4.2.3 Mucosal B cells: Somatic hypermutation, class switching and IgA production

As stated previously, the immune cells of the MALT (as well as the GALT) are distinctly separate from the systemic immune system. Within the GALT, mucosal B cells play a critical role due to their ability to produce highly specific antibodies that can effectively bind and neutralise toxins and pathogens. These antibodies are typically in the form of IgA and IgM, and represent a non-inflammatory defence mechanism at effector tissue and the gut lumen. Antibody secreting B cells are highly abundant throughout the MALT, so much so that approximately 80% of all human plasma cells can be found associated with the gut. These cells predominately produce sIgA (approximately 80%), where on average 3 g can be produced every day (Brandtzaeg and Johansen, 2005). In humans, IgA can be found in two isotypes, IgA1 and IgA2, differing in both structure and localisation (while mice only express one IgA isotype). Within serum, IgA1 largely predominates (at a ratio of 9:1), whereas mucosal tissue is much more of a balanced ratio between the two isotypes (Steffen et al., 2020). IgA1 has additional amino acid sequences within the hinge region compared to IgA2, resulting in enhanced antigen recognition, but simultaneously results in a reduced stability within the lumen due to vulnerability to proteolytic degradation (Woof and Kerr, 2004). Human immunoglobulins are proteins that can be found both soluble and membrane bound. The proteins comprise of two identical chains, each containing a heavy and a light section. The two chains and the heavy and light chain fragments are connected by disulphide bridges. Two distinct antigen binding domains (Fabs) are bound to the Fc (fragment crystallisable) via a hinge region, allowing for conformational flexibility (Chiu et al., 2019).

Antigen within the lumen can be screened and processed through a number of different routes – including dendritic cells extending appendages through epithelial tight junctions for direct sampling, or through M cell entry within the FAE. Antigen that is moved through the M cells via transcytosis interacts with APCs as well as directly with T and B cells within the SED. In addition to this, APCs (in particular DCs) can migrate to intrafollicular T cell areas in the Peyer's patches (or mesenteric lymph nodes) for CD4⁺ priming, resulting in the formation of germinal centres (GCs), along with activated B cells (now a mature B cell) (Kang et al., 2018). The GCs are a crucial component for induction of antibody responses against antigenic material. Upon antigen activation (directly or indirectly through APCs and T cells), GC formation occurs within the follicles, orchestrated by follicular helper T cell activation. The GC comprises of two distinct zones, a light and dark zone. The mature B cell upon entering the GC (following T cell activation) express predominantly IgM and IgD antibodies on the cellular surface, and undergoes a process known as proliferative colonial expansion (or somatic hypermutation). During this process, random mutations coding for the variable region (light and heavy chain) occur (through an enzyme called activation-induced cytidine deaminase (AID)), producing a large number of B cells with Fab diversity. These B cells then migrate within the GC to the

light zone – where interactions with both follicular helper T cells and DCs expressing the particular antigen occur, undergoing a process of selection and enhanced affinity. If the random mutations resulted in poor affinity binding between the antigen and newly expressed antibody on the B cell surface, the cell undergoes apoptosis. However, if successful binding occurs (through somatic hyper mutations (SHM) resulting in enhanced affinity), positive selection occurs and the B cell then undergoes a process known as class switching (Stebegg et al., 2018). This process again involves changes in the DNA coding for the antibody, however the variable region is now kept constant (in order to not detrimentally impact upon the affinity of the antibody – antigen interaction) and the constant region is altered. This genomic alteration is a result of recombinant deletions through AID, therefore the process of class switching is irreversible (Hoh and Boyd, 2018). Prior to class switching, antibodies are default IgM, but upon undergoing recombinant class switching (CSR) at specific points along the constant domain sequence for the heavy chain, deletions result in the production of IgD, IgG, IgE and IgA. Importantly, these antibodies have the same affinity (variable region) as the IgM; however, the alterations to the constant domain on the heavy chain results in different antibody isotypes with new effector functions (Stavnezer, 1996). Class switching can proceed down two paths, either T-cell dependent class switching or T-cell independent class switching. The former relies on the presence of CD4⁺ T cells expressing CD40 ligands within GCs of PPs binding to CD40 on the activated B cell. Follicular DCs with the specific antigen presented then can interact with the B cell receptor and initiate the B cell towards class switching and eventual differentiation into either long-lived memory B cells or plasma cells (secreting IgA). T-cell independent class switching to IgA can occur through TLR activation and CD40L activation through follicular DCs and a number of co-stimulatory molecules such as BAFF (B-cell activating factor) and APRIL (proliferation inducing ligand) (Cerutti, 2008). T cell-dependent IgA class switching results in high-affinity antibodies and occurs within GCs, while T-cell independent class switching results in poorer affinity antibodies as a result of interactions between DCs and B cells in the lamina propria. Following CSR, IgA secreting plasma cells then exit the PPs to the blood circulatory system via the thoracic duct and migrate back to effector sites such as the lamina propria (where they produce soluble IgA) (Figure 1.3) via homing receptors as described previously (1.4.2.2) (Cerutti, 2008).

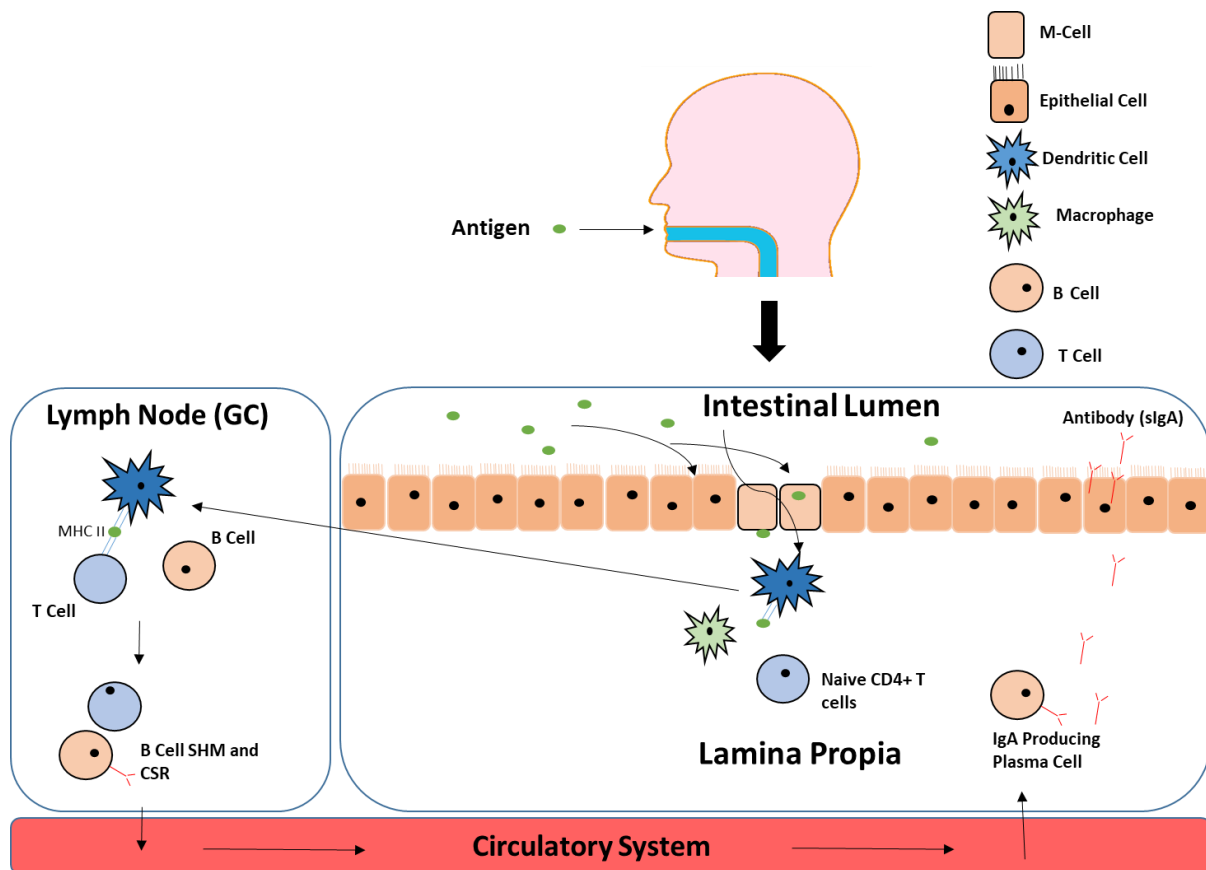


Figure 1.3 Schematic diagram of the generation of IgA producing plasma B cells. Antigen within the lumen can traverse the epithelial barrier via M cell transcytosis or directly sampled by APCs from the lumen. The antigen is passed onto underlying DCs / macrophages within the lamina propria where they uptake, process and present the antigen fragments on MHC II molecules. CD4⁺T cells are primed and the formation of a germinal centre (GC) occurs within the PPs or mesenteric lymph nodes (MLNs). The primed T cells, in the presence of DCs presenting the antigen, can then activate B cells, which initiates somatic hypermutation (SHM) for Fab region variations, followed by class switching (CSR) if antigen affinity is maintained. These IgA⁺ B cells then leave the PPs / MLNs via the thoracic duct, entering the circulatory system. Due to the imprinting of homing receptors, these B cells then enter the lamina propria, mature and become IgA producing plasma B cells. Adapted from (Ramirez et al., 2017).

1.5 Developing an oral vaccine against *C. difficile*

The development of a safe, efficacious vaccine against *C. difficile* which can provide long-term immunity to toxin damage remains a challenge, as evidenced by Sanofi Pasteur's decision to terminate their vaccine candidate in late stage clinical development. There are a number of potential reasons as to why vaccines cannot meet the expected criteria of protection against enteric toxins from *C. difficile*. For example, the compartmentalisation of the mucosal immune system. It is now understood that immunity, and adaptive immunity in particular, relies upon the homing of activated effector cells back to the site of induction. In addition to this, parenterally administered vaccines often fail to mount effective sIgA responses, therefore it is believed that in order to mount an effective immunological defence against enteric pathogens, oral administration of the vaccine must take place in order to induce localised vaccination at the mucosa within the GIT (Islam et al., 2019, Owen et al., 2013).

However, the oral route of administration of vaccination poses both opportunities and challenges. It remains the most patient friendly form of drug administration, due to its lack of invasiveness, reduced need for professional administration and minimal environmental implications by eliminating the use of needles as well as a reduction in needle-borne infections (Wilkhu and Perrie, 2015). The challenges of oral vaccination (section 1.4) is clearly exhibited in the disparity between the number of oral vaccines available on the market when compared to the vast number of enteric pathogens and resulting disease (Islam et al., 2019).

As stated previously (section 1.4.1), the oral route results in a low acidic environment as well as degradative enzymes found throughout the tract, which can compromise antigen integrity during transit. The mucosal immune system throughout the GIT has inherent associated tolerance mechanisms in order to prevent unnecessary pro-inflammation when faced with commensal microorganisms and dietary proteins, thus the addition of free antigen without an effective adjuvant may result in poor vaccine efficacy. It is therefore hypothesised that by employing a delivery system, such as a lipid-based nanoparticle, some of these challenges can be overcome.

1.5.1 Adjuvants

Typically, vaccines containing purified antigen subunits result in poor immunostimulatory efficacy, as a result of limited antibody responses and poor T cell activation therefore requiring multiple boost immunisations to maintain protective qualities. Through the use of delivery systems to improve protection and delivery of sub-unit antigens and/or inclusion of adjuvants, immunological responses can be enhanced and tailored, meaning required doses of antigen can be reduced while maintaining effective vaccination (Reed et al., 2013). A prime example of these dose limiting qualities of adjuvants is the addition of AS04 to a vaccine for hepatitis B by GSK, which resulted in approximately a 30% reduction in immunisation dose-regimen (Levie et al., 2002).

Adjuvants consist of a very broad spectrum of molecules which can be generally described as substances which boost the immunogenicity of an antigen (Apostólico et al., 2016). Due to their vast range of classification types, adjuvants act through a number of different mechanisms of action. Generally, adjuvants can be classified into either antigen delivery systems (such as microparticles, lipid-based nanoparticles, polymeric based nanoparticles, emulsions and mineral salts) or immunostimulatory compounds (such as poly(I:C), MPL and resiquimod) (Apostólico et al., 2016, Foged, 2011). While many of the mechanisms of action are still unclear, broadly speaking, antigen carriers can boost immunogenicity through the recruitment of innate immune cells such as dendritic cells (DCs) and macrophages and create pro-inflammation at the site of administration, while

immunostimulatory (or immunopotentiators) compounds, generally speaking, function through the activation of pattern-recognition receptors (PRRs) such as toll-like receptors (TLRs), to generate downstream inflammatory responses (Table 1.2) (Apostólico et al., 2016, Del Giudice et al., 2018, Petrovsky, 2015).

Table 1.2 Examples of commonly used adjuvants, the corresponding components and how the adjuvant exerts its immunostimulatory effects.

Adjuvant	Component	Possible mechanism of action	Immune response	References
Alum	Aluminium salts	NLRP3 Inflammasome	Enhanced antibody and Th2 type response	(Awate et al., 2013) (Ghimire, 2015)
MF59	Squalene in water emulsion	Immune cell recruitment, enhanced Ag uptake	Enhanced antibody and Th1 / Th2 type response	(Reed et al., 2013)
AS04	MPL and Alum	TLR4	Enhanced antibody and Th1 type response	(Reed et al., 2013)
Poly (I:C)	Synthetic dsRNA	TLR3	Enhanced antibody and Th1 type response, activation of CD8 ⁺ T cells	(Coffman et al., 2010)
CpG ODN	Synthetic ssDNA	TLR9	Enhanced Th1 response and CD8 ⁺ T cells	(Chatzikleantous, 2020)
AS01	Liposome based (MPL and QS-21)	TLR4	Enhanced antibody and promotion of antigen-specific CD4 ⁺ T cells	(Coccia et al., 2017)
CAF01	Cationic surfactant DDA and glycolipid immunomodulator TDB	TLR2,3,4 and 7	Strong TH1 and TH2 type response.	(Pedersen et al., 2018)

1.5.2 Liposomes as vaccine adjuvants

Liposomes form from lipids when hydrated in aqueous media. They form spherical vesicles as a result of the amphiphilic nature of the individual lipids – with a hydrophilic head group and lipophilic tail, thus orientating accordingly to reduce hydrophobic – water interactions, and can form with either a single lipid bilayer (known as unilamellar vesicles), as shown in Figure 1.1, or multiple lipid bilayers (multilamellar vesicles) (Gregoriadis, 2006). The physicochemical properties of the liposomes are primarily determined by the phospholipid composition used, the ratio between the specific phospholipids within the formulation and the method of production (Ahsan et al., 2002, Akbarzadeh et al., 2013). The use of liposomes as drug delivery systems can be highly advantageous, simply due to the liposomes physical attributes, their biocompatibility and low toxicity (Torchilin, 2005b). Liposomes can be loaded with a wide range of molecules, thus protecting them from degradative

environments within the body such as enzymes and bile salts in the GIT (Akbarzadeh et al., 2013). Due to the amphiphilic nature of the liposomes, lipophilic drugs can be trapped within the lipid bilayer of the liposome while water-soluble materials such as RNA and protein can be incorporated within the aqueous core (Torchilin, 2005b, Ramirez et al., 2017). The lipid composition used can determine the charge of the liposome, which can in turn determine cellular uptake mechanisms and mechanisms of action *in vivo* and thus it is possible to tailor liposomes for specific therapeutic needs. This malleability of the liposomes allows them to function as an effective delivery system as they can simultaneously provide protection to therapeutic payloads while increasing bioavailability of the drug at the target site while exhibiting low-toxicity as well as good biodegradability (Akbarzadeh et al., 2013).

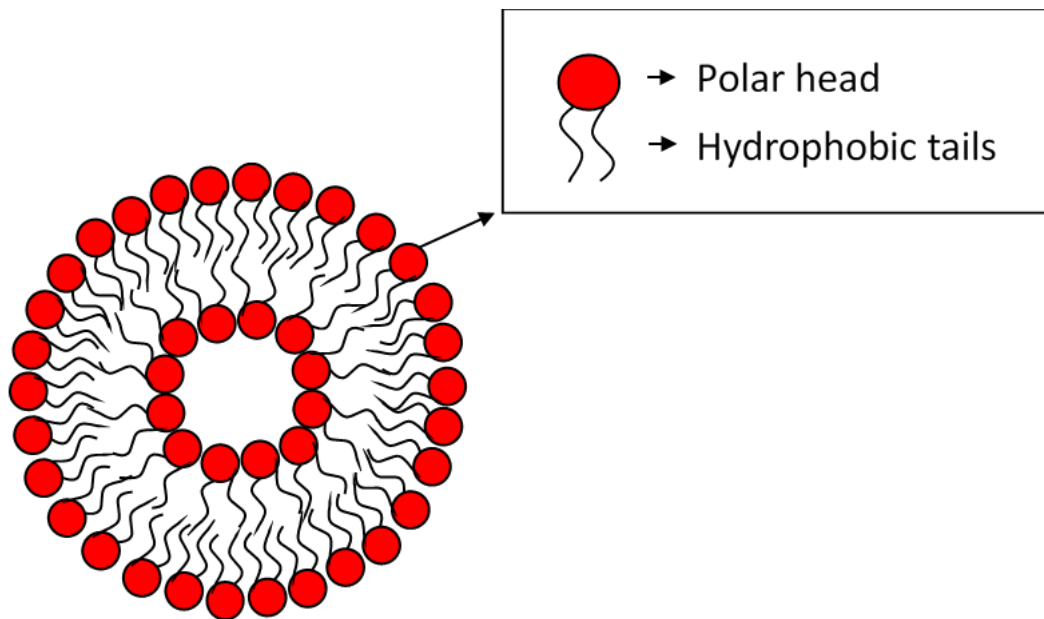


Figure 1.4 Graphical representation of a liposome, composed of a bilayer of lipids with the hydrophilic head facing the aqueous environment and the hydrophobic tail imbedding within the bilayer.

As a result of these favourable attributes, there are a number of liposomal formulations currently on the market (Figure 1.5). Products such as the anti-cancer formulation, Myocet, incorporates cyclophosphamide for the treatment of metastatic breast cancer, while Doxil (incorporating doxorubicin) can be used to treat a range of cancers including breast, ovarian and Kaposi's sarcoma. Anti-fungal products such as Ambisome, contain amphotericin B which can be used to fight a range of fungal infections. (Carugo et al., 2016, Akinc et al., 2019). Furthermore, the first product by the FDA for the delivery of siRNA (Patisiran) for the treatment of transthyretin-mediated amyloidosis using a lipid nanoparticle (DSPC, DLin-MC3-DMA and PEG₂₀₀₀-C-DMG) was approved in 2018 (Zhang et al., 2020). Physical parameters of the liposomal formulations such as liposome particle size, lipid composition and surface charge can influence how the liposomal delivery system interacts with the biological environment, such as the mucosal barrier, whether they are absorbed via M cells, between

enterocytes or through the tips of intestinal villi (Wilckhu and Perrie, 2015). This is of significant importance as the route of which the liposomal-vaccine system is taken up can greatly impact on the type of immune response that it is capable of eliciting, therefore when designing a liposomal delivery system for pharmaceutical use, it is crucial that these physicochemical parameters such as particle size and zeta potential are capable of being highly reproducible during liposome manufacture.

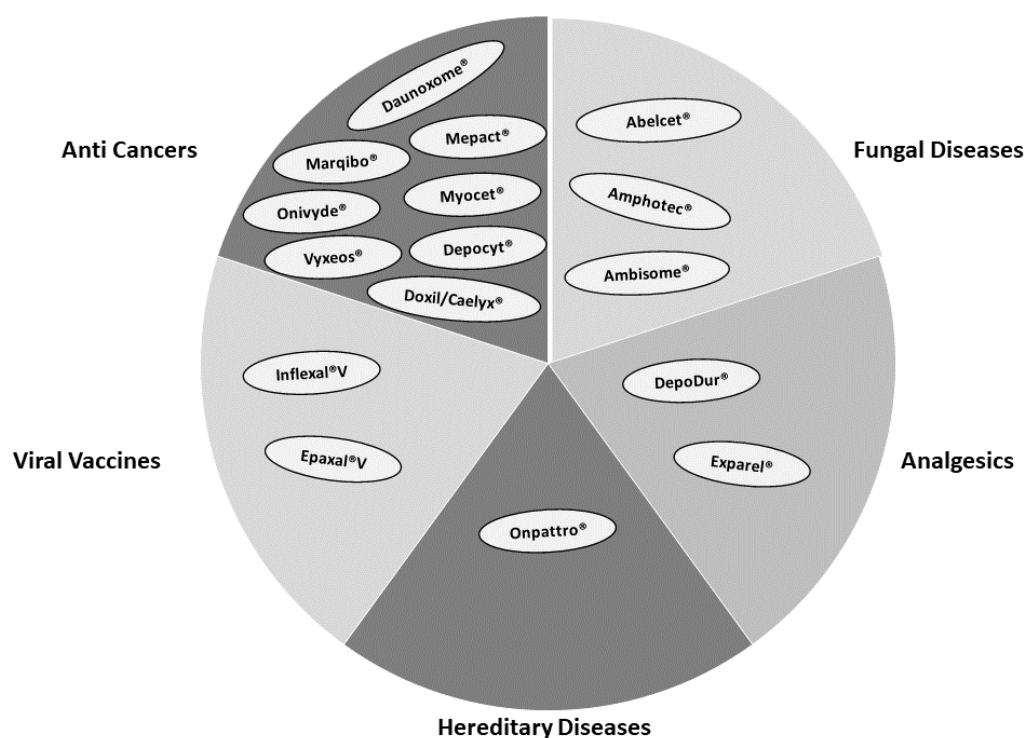


Figure 1.5 Overview of liposome-based products currently on the market, adapted from Bulbake et al. (Bulbake et al., 2017)

1.5.3 Liposome physicochemical attributes as oral vaccine adjuvants

The lipid components of the liposome vesicle are amphiphilic in composition, containing a hydrophilic head group composed of a phosphate group (with an organic molecule such as a choline attached to one side) and a glycerol molecule followed by the extension of two fatty acid chains (hydrophobic region, can be saturated or unsaturated) (Beltrán-Gracia et al., 2019). The assembly of individual lipids into liposomes can be generalised into two basic stages. The first is the formation of a symmetric bilayer within aqueous conditions – until the curvature energy favours bilayer bending, resulting in a stable vesicle forming (Figure 1.6). Lipid composition determines the critical packing parameter (CPP) – which relates the volume of the hydrophobic region, the effective chain length and the hydrophilic head group surface area, and thus can be used to predict the resulting structure of the aggregates. A calculated CPP value of less $\frac{1}{2}$ will likely result in micelle and cylindrical micelle formation while CPP values between $\frac{1}{2}$ and less than 1 form vesicles (Khalil and Al-hakam, 2014). Furthermore,

environmental conditions such as pH, temperature of the aqueous media and even the manufacturing method applied can also impact upon the final vesicle characteristics (Lombardo et al., 2016).

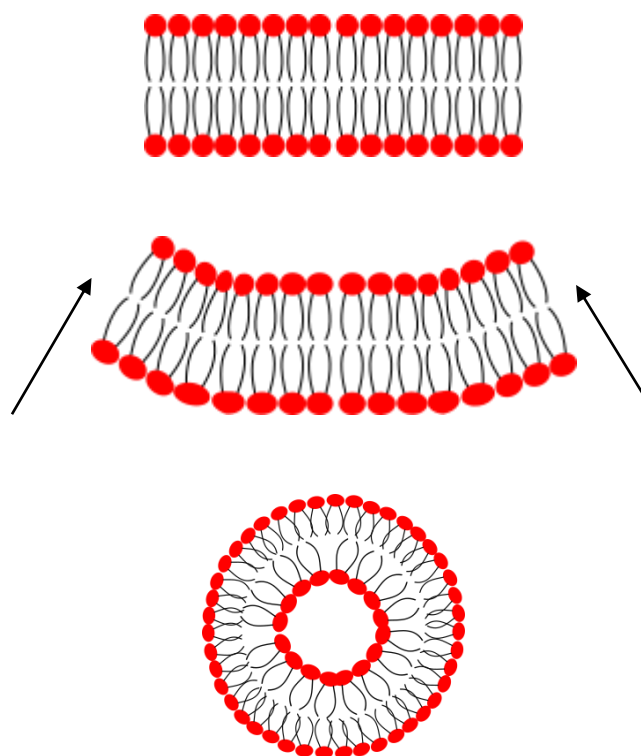


Figure 1.6 A graphical illustration of liposome formation. Initially, lipids form into a planar lipid disc when exposed to a threshold concentration of aqueous. The planar layer then begins to bend as a result of more favourable energy confirmation, eventually closing into a spherical bilayer (liposome).

1.5.3.1 Lipid composition

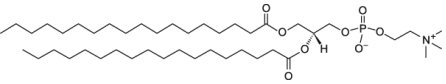
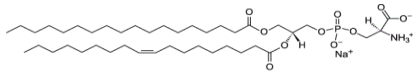
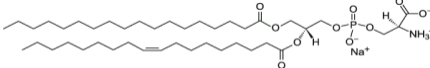
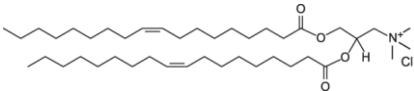
The combination of lipids employed in the formulation and any subsequent chemical attachments used to produce the liposomes will have a large impact on the resulting physicochemical properties exhibited, such as the overall surface charge of the liposomes being determined by the individual chemical properties of the lipids. Primarily positively charged liposomes have been shown to have increased adjuvant activity when compared to neutral and negatively charged particles. For example, the cationic adjuvant formulation 01 (CAF01), composed of a positively charged cationic surfactant dimethyldioctadecylammonium (DDA) and a glycolipid D-(+)- trehalose 6,6'-dibehenate (TDB), has been shown to increase immunogenicity of a number of antigens including Tuberculosis, HIV, Chlamydia and Malaria (Chadwick et al., 2009, van Dissel et al., 2014). Cationic liposomal formulations have been shown to have high mucoadhesive properties, due to the electrostatic interactions between the positively charged particles and the negatively charged mucosa (Sercombe et al., 2015). In a liposomal mucoadhesion study, positively charged surface modification (stearylamine (SA)) was

compared with anionic phosphatidylserine (PS) based liposomes. The cationic liposomes prepared with SA were shown to exhibit the highest levels of mucoadhesion when compared to the anionic (PS) (Ahn and Park, 2016). However, *in vivo* studies have also shown potential increased toxicity from cationic particles, though this will be dose dependent (Chadwick et al., 2009). Several studies have also considered the use of negatively charged liposomal formulations and studies have shown increased uptake rates by Peyer's patches (Wilkhu et al., 2013).

Alongside selecting the appropriate lipid composition to determine physicochemical properties such as surface charge, the liposomes can also provide adequate protection for the antigen. Liposome formulations can be prone to degradation in the presence of bile salts, lipases and low acidity pH (Chadwick et al., 2009). Indeed, a study aimed at determining the effects of bile salts and pancreatic lipases on a range of liposome formulations with encapsulated carboxyfluorescein found that lipids with low transition temperatures, such as phosphatidylcholine (PC) and 1,2-dimyristoyl-sn-glycero-3-phosphocholine (DMPC) resulted in the greatest leakage of loaded molecule. Lipids with higher transition temperatures such as 1,2-distearoyl-sn-glycero-3-phosphocholine (DSPC), 1,2-dipalmitoyl-sn-glycero-3-phosphocholine (DPPC) and *N*-palmitoyl-*D*-erythro-sphingosylphosphorylcholine (SM) along with cholesterol, yielded the highest retention rates of loaded fluorescent dye during bile salt exposure (Kokkona et al., 2000).

Bilayer modifications can be used to increase lipid composition stability throughout the GIT. The addition of cholesterol to the lipid bilayer is a well-known process to increase liposomal membrane stability. The addition of cholesterol to liposomal membranes reduces the required phase transition temperature by improving the packing dynamics of the lipids (Kaur et al., 2013). Addition of cholesterol at 50 mol% has been shown to improve membrane stability therefore reducing the permeability of the liposome bilayer (Kaur et al., 2013). The incorporation of bile salts within the lipid bilayer (known as bilosomes) has been shown to provide protection to loaded antigens in the presence of degradative enzymes from the GI tract while simultaneously providing an effective immune response. The bilosome formulation monopalmitoyl glycerol (MPG), cholesterol and dicetyl phosphate (DCP) 5:4:1 with 100 mM bile salts was assessed for stability within simulated gastric and intestinal fluid and showed high levels of antigen retention. When assessing the immune response *in vivo*, the bilosome carrier system provided greater antigen delivery when compared to free antigen alone and showed greater immune responses in ferret models (Wilkhu et al., 2013).

Table 1.3 Examples of commonly used lipids (name in abbreviation) with the molecular weight, chemical structure, transition temperature and common applications in liposomal form.

Lipid name abbreviation	Mw (g/mol)	Chemical structure	Transition Temperature (°C)	Application
DSPC	734		55°C	High T _c , increased rigidity and payload retention
PS	825	 Naturally occurring lipid mixture	~ 65°C (mix)	Anionic, naturally occurring (brain derived). Potent macrophage interactions
DOPS	810		-11°C	Synthetic brain PS substitute, similar properties yet enhanced stability
DOTAP	663		<5°C	Widely used, cheap cationic lipid. Enhanced cellular interactions, particularly for transfection

1.5.3.2 Vesicle size

During the oral route of administration, M cells represent an intriguing target to mount effective immunological responses for enteric pathogens. Some research has undergone to identify optimal physicochemical properties, including the effect of the delivery systems vesicle size on M cell uptake. However, the literature relating particle size to uptake has no definitive consensus on the most ideal vesicle size for the most efficient uptake rates, with most studies suggesting optimal uptake to arise from particles below 1 µm or below 10 µm (Islam et al., 2019). Interestingly, increased uptake of nanoparticles has been demonstrated when comparing sizes of polymers comprised of poly-(lactic:glycolic)-acid (PLGA), with vesicles within the 100 nm range resulting in improved uptake when comparing 100, 500, 1000 and 10,000 nm particles along the GIT of rats (along the duodenum and ileum). The results found improved Peyer's patch uptake was significantly higher for 100 nm sized

particles (30% and 27% respectively for duodenum and ileum), while all three of the other particle sizes tested resulted in under 10% uptake (Desai et al., 1996). This was true not only in terms of particle number, but also total mass up taken, thus indicating that for the greatest antigen uptake, particles within and around the 100 nm range could give the greatest potential for vaccine delivery systems. The disparity around a particle size consensus is likely attributed to the complexity involved around M cell and Peyer's patch uptake mechanisms, with a multitude of factors likely playing a role such as delivery system composition, surface charge and antigen loading.

As the human GI tract has such a large surface area, there are naturally differing levels of mucosal secretions associated with distinct areas within the tract. Polystyrene beads between the sizes of 0.5-2 μm have been shown to penetrate successfully through small intestinal mucus, while the inner colonic mucosal surface showed poor penetration (Chadwick et al., 2009). As well as small particles exhibiting an increased uptake rate at M cells, studies have shown that PLA (polylactic acid) microparticles were taken up by Peyer's Patches up to 10 μm in diameter. However, the ultimate fate of the particles following Peyer's patch uptake was found to differ according to vesicle size. Microparticles between the sizes of 5-10 μm were retained within the Peyer's patches, while smaller vesicles were found to travel through lymphatic vessels, stimulating a more systemic, circulatory immune response, as opposed to the desired mucosal immune response (Eldridge et al., 1990).

1.5.3.3 Liposomal targeting for enhanced immunological responses

In addition to providing protection from the degradative environment of the GIT and providing improved uptake of the vaccine formulation through delivery system physicochemical properties, liposomal delivery systems have the ability to attach a number of different targeting molecules, such as specific ligands or the incorporation of targeted moieties within the formulation. By selective binding to specific cell types, the rate of uptake of the contents of the liposome at the desired location can be greatly enhanced (Gupta and Vyas, 2011, Hua, 2014). It has been shown that DSPC based liposomes conjugated to a specific lectin, *Ulex europaeus agglutinin-1* (UEA-1) designed to target mice M cells resulted in greater M-cell uptake compared to the liposomes without lectin modification. The immune response was measured by looking at sIgA antibodies – as Peyer's patches are a main source for precursor IgA secreting B cells. UEA-1 coated liposomes were capable of eliciting increased IgA production, as well as eliciting significantly higher cytokine production rates (Interleukin-2 and interferon gamma) when compared to the uncoated liposomes (Clark et al., 2001). In addition, the adjuvant activity of liposomal formulation has been previously shown to be enhanced through the conjugation of recombinant subunit B of cholera toxin (rCTB) to the surface of small unilamellar

liposomes (DSPC, PC and cholesterol), increasing both sIgA and systemic IgG in mice following oral administration (Harokopakis et al., 1998). The incorporation of the anionic phospholipid phosphatidylserine (PS) into liposomal bilayers has also been used as a macrophage targeting systems (Shah et al., 2019). PS is heavily expressed on the inner leaflet of the mammalian cell membrane, however upon stress exposure or reduced membrane function, PS is disproportionately expressed on the outer leaflet, and is an important characteristic of apoptotic cells, thus acts as a macrophage targeting moiety (De et al., 2018). This ability to attach ligands for selective targeting in the GI tract, incorporation of targeting moieties, along with providing protection and providing adjuvant activity, make liposomes a very attractive oral vaccine delivery system.

1.5.3.4 Adjuvanticity of liposomes

As vaccine development shifts from live-attenuated to subunit vaccines, greater emphasis has been applied to the production of vaccine formulations capable of eliciting relevant immunogenic profiles. Subunit antigens suffer from a reduced ability to induce maturation of DCs, thus limiting the subsequent adaptive immunological response. The use of adjuvants and/or delivery systems in the vaccine formulation can circumvent the reduction of immunogenicity found when administering subunit antigens by improving antigen delivery and uptake to relevant antigen presenting cells, providing protection to the payload from enzymatic degradation and the formation of a depot resulting in sustained antigen release (Vartak and Sucheck, 2016, Silva et al., 2016, Henriksen-Lacey et al., 2010b). Since their inception as antigen carriers (Allison and Gregoriadis, 1974), liposomes have been broadly investigated as antigen delivery systems by adjusting lipid composition, membrane fluidity, particle size and charge as well as the localization of the antigen (surface adsorbed or encapsulated within) (Perrie et al., 2016). Owing to their versatility, liposomes therefore offer tremendous possibilities as vaccine adjuvants for next generation vaccine therapies. The addition of the antigen within the vesicle (encapsulation) offers payload protection to protease degradation, while simultaneously altering the release profile of the antigen as the liposomal vesicle degrades. Alternatively, chemical or electrostatic surface adsorption of antigen onto cationic vesicles could enhance the ability of the APCs to interact with the antigen through TLRs (Pati et al., 2018). The size of the delivery system can impact upon the draining kinetics, thus altering immunological responses, with smaller vesicles being shown to leave the site of injection faster than their larger vesicle counterparts (Carstens et al., 2011) (Tandrup Schmidt et al., 2016). The effect of charge similarly plays a major role in the determining the extent of immunological responses following vaccination, influencing the draining ability of the vaccine formulation. Parenterally administered cationic liposomal formulations have been shown to generate a depot effect, where there is increased APC

interactions with the delivered antigen (Henriksen-Lacey et al., 2010b). Furthermore, in regards to oral delivery, the encapsulation of antigen within liposomal vesicles as opposed to surface association via electrostatic interactions has been shown to provide improved localized IgA and systemic IgG when compared to admixed antigen and liposomes, although some potential questions arise in regards to how available the antigen can be to APCs (Fujii et al., 1993, Bernasconi et al., 2016). In regards to liposomal vaccines undergoing clinical trials, a number of successful cationic liposomal adjuvant systems are showing promise. Cationic liposomal adjuvant CAF01 is currently undergoing Phase 1 trials as a novel vaccine candidate for Chlamydia, using a recombinant antigen (CTH522) to generate cell-mediated immune responses (Abraham et al., 2019). In a similar Phase 1 trial, the safety and immunogenic efficacy of the CAF01 system in combination with a range of HIV peptides was assessed in Guinea-Bissau, West Africa, with 6/14 HIV-1 infected participants generating specific T-cell responses (Román et al., 2013). Wui et al have shown the effectiveness of their cationic liposomal vaccine formulation CIA09A, comprising a cationic liposome and TLR4 agonist de-O-acylated lipooligosaccharide to induce both humoral and cellular immunity in mouse models for Varicella zoster virus (VZV) (Wui et al., 2019).

While liposomes have been extensively studied as vaccine delivery systems and a great deal of success has emerged in respect to enhanced immunological activity, there remains limited research in regards to their ability as oral vaccine delivery systems. This is due to the challenges associated with oral delivery, and in particular the effect acidic pH, lipases and bile salts have on liposomal membranes (Davitt and Lavelle, 2015). As discussed, a major point of entry for any delivery system to the associated gut lymphoid tissue is access via M cells on PPs, where the mucus layer is limited allowing for easier points of entry. Previous studies have shown that liposomes can cluster around FAE and are readily taken up by M cells, however there remains limited understanding as to what the preferential characteristics of the vesicles are in relation to enhanced uptake rates (Zhou and Neutra, 2002). Despite this apparent advantage of liposomal vesicles to access the underlying lymphoid tissue, limited success in regards to effective immunological responses is often common (Harokopakis et al., 1998).

Recently, some promising research has emerged relating to liposomes as oral vaccine carriers. Using a cationic liposome transfection product known as lipofectamine (DOSPA: DOPE 3:1 w/w), the delivery of the M1 gene for Influenza was achieved orally. Employing the cationic liposomal formulation resulted in both enhanced humoral and cell mediated responses, as well as relevant protection against influenza following respiratory challenge (Liu et al., 2014). A more complicated liposomal construct was manufactured by Deng et al, where a mannose-PEG-cholesterol conjugate was surface bound to liposomal formulation (soy PC, monophosphoryl lipid A) containing encapsulated BSA. The liposome

– conjugate was found to be approximately 300 nm and following oral mucosal immunisation, enhanced systemic IgG was observed as well as mucosal IgA (throughout the saliva, intestine and vaginal secretions) (Wang et al., 2014).

As liposome manufacturing technology advances (as will be discussed further), as well as our understanding of how oral vaccination works, liposomes as adjuvant carriers offer a promising avenue of research. The versatility found across liposome formulations such as the use of cationic vesicles to enhance pro-inflammation, or the use of long-chain lipids with antigen encapsulated while simultaneously incorporating immunostimulatory components make this delivery system platform ideal for further mucosal vaccination research (Bernasconi et al., 2016).

1.6 Traditional liposomal manufacturing techniques

Currently, there are a number of ways of producing liposomes as delivery systems; however, they can be generally simplified into two main categories, a bottom-up approach or a top-down production approach. The top-down production approach incorporates a number of techniques which have been used to produce liposomes over a number of decades, and are very suitable for lab-scale use, yet these techniques often struggle in larger scale manufacturing systems. Batch production often falls short when manufacturing liposomal products in a rapid and cost effective manner in comparison to the more efficient continuous setups (Elhissi et al., 2015).

The lipid-film hydration technique (or Bangham method) was the first top-down production method to manufacture liposomes which involved the dissolution of lipids in organic solvent (such as chloroform, methanol mixtures), followed by solvent evaporation leaving a thin film of lipids covering the bottom of a flask. Upon hydration in aqueous media, multilamellar vesicles (MLV) can form, which are highly heterogeneous structures in terms of vesicle size, with concentric phospholipid spheres separated by aqueous phase (Nkanga et al., 2019, Akbarzadeh et al., 2013). The production of MLV requires further down-stream processing to produce a homogenous size distribution of vesicles. Such size reduction techniques to achieve small unilamellar vesicles (SUV) can include size extrusion, sonication or high-pressure homogenization (Kastner et al., 2014). Size reduction of vesicles by extrusion normally involves the use of a specific pore sized membrane, where MLV suspensions are passed through – either by hand held extrusion, or the use of a pump, in order to produce smaller and smaller vesicles. Vesicles that are too large to pass through the pores are blocked, and the pressure then ruptures the concentric vesicle layers and the process can be repeated until a homogenous population arises (Patty and Frisken, 2003, Frisken et al., 2000b). Sonication involves the use of

acoustic energy to break down the MLV into smaller more homogenous vesicles, while high-pressure homogenization uses kinetic energy to direct streams of vesicles at pressure to generate shear and impaction, reducing particle size and increasing population homogeneity (Anderluzzi et al., 2019). Each of these subsequent size reduction techniques required to achieve suitable size characteristics generates further complexity when attempting to scale-up production of these nanomedicines. Traditional manufacturing techniques such as lipid-film hydration and subsequent size reduction often generates inadequate volumes suitable for industrial scale manufacture, requiring the use of batch manufacturing (Kastner et al., 2014, Dimov et al., 2017, Worsham et al., 2019). Batch process manufacture operates through the production of material in bulk, the whole process is not designed to deal with fluctuations in product demand, and thus cannot readily scale down or up production when necessary. Furthermore, the bulk material is often tested off-line, meaning that if the product does not meet specific product specifications, large amounts material can be lost if the product does not meet quality criteria (Lee et al., 2015). This issue is highlighted by the liposomal formulation Doxil, an anti-cancer medication composing of doxorubicin encapsulated within a PEGylated liposomal formulation, where manufacturing issues involving standard violations resulted in a cease of production and a subsequent global Doxil shortage (Berger et al., 2014).

1.6.1 Manufacturing of protein loaded liposomes

The production of liposomal products incorporating protein (including sub-unit antigens) adds additional challenges to the manufacturing process. Processes that use high temperatures and pressure can induce denaturation of the protein. In addition to this, the presence of solvents, high ionic strength and fluctuations in pH can further alter physical and chemical stability of the protein. These denaturation events can result in irreversible association, hampering therapeutic effects (Forbes et al., 2019, Scharnagl et al., 2005). As a result of these complications, manufacturing of liposomal formulations containing protein must aim to limit the effect of these conditions. Table 1.4 indicates some common methods used to manufacture protein loaded formulations, including techniques such as thin-film hydration and freeze-thaw cycling. Limitations pertaining to some of these methods include poor vesicle homogeneity and reproducibility, and in the case of thin-film hydration, further down-stream processing techniques are required to produce homogenous samples.

Table 1.4 Examples of commonly used methods for the manufacturing of liposomes entrapping protein within. The protein entrapped is listed, along with the liposomal formulation used, the manufacturing technique employed and the subsequent entrapment efficiency (loading efficiency).

Protein Loaded	Formulation	Manufacturing Technique	Loading Efficiency (Reference)
Bovine Serum Albumin	PC:Chol	Dehydration – rehydration method	28% (Chan et al., 2004)
Bovine Serum Albumin	Soybean PC:Chol	Thin-film hydration method	22-32% (Vila-Caballer et al., 2016)
Ovalbumin	PC:Chol	Thin-film hydration method	10% (Habjanec et al., 2006)
Insulin	Hydrogenated PC:Cholesterol	Thin-film hydration method	28% (4°C), 30% (20°C), 50% (40 °C)(Huang and Wang, 2006)
Acetylcholinesterase	Egg PC	Thin-film hydration method	35% (Colletier et al., 2002)
Superoxide dismutase	DPPC:Chol, DSPC:Chol	Unilamellar vesicles mixed with freeze-thaw cycling	50% (Xu et al., 2012)

1.6.2 Microfluidics as a production method

A novel approach for liposome production involves the use of microfluidics, a bottom-up production method which can produce SUV in a microenvironment. Briefly, lipids dissolved in solvent are injected through nano-scale channels, where they are mixed with an aqueous stream. The two flows cross over each other, resulting in a nanoprecipitation reaction which is thought to produce the liposomes (Kastner et al., 2015). Microfluidic manufacture of liposomes offers the advantage of production of SUV in a one step process, thus circumventing the need for further size reduction, which enables the user to reproducibly manufacture liposomes through the control of specific production parameters during microfluidic operation. Controlling the particles physicochemical attributes such as size, membrane fluidity and surface charge is essential to the design of vaccine adjuvant formulations as these attributes greatly impact upon the pharmacokinetic profile and thus the immunogenic profile of the vaccine formulation (Roces et al., 2019). These processing parameters that can be controlled during microfluidic production including the speed at which the aqueous and solvent phases are passed through the microfluidic cartridge (total flow rate or TFR), the ratio between the two phases (Flow rate ratio or FRR), initial lipid concentration used and choice of solvent. Microfluidics as a manufacturing method for nanomedicines offers further advantages compared to more traditional

approaches in terms of scalability. The microfluidics platform can function across a range of process volumes, from bench scale screening of formulations, up to industrial scale production (Forbes et al., 2019).

1.6.3 Continuous manufacturing

Since the conceptualisation of Industry 4.0 in 2011, there has been an ever increasing demand on the pharmaceutical industry to innovate their core processes, such as manufacturing and data analysis protocols to push more towards digitization and automation. Currently, batch processing remains a staple for the pharmaceutical manufacturing industry, leading to potential inefficiencies throughout the supply chain (Ding, 2018). There is now more than ever a real need for innovative technologies to help push manufacturing in the pharmaceutical industry towards streamline production strategies. Technologies such as microfluidics, in combination with real-time data monitoring systems and efficient down-stream processing techniques could help shift the liposomal manufacturing industry towards digitization.

Within our laboratories, we are attempting to develop a continuous online assembly of liposomes with the use of several novel pieces of equipment, such as an on-line particle sizer for continuous monitoring of liposome population sizes in real time, and the development of a one-step production purification system incorporating tangential flow filtration (TFF). Tangential flow filtration is a process which employs specific pore-sized membranes to remove salts or solvents from solutions and separate particulate solutions based on size discrepancy principles. Unlike direct flow filtration, the solution stream is passed parallel to the membrane surface, where the permeate is filtered off, whilst the remainder of the solution is circulated back through the system. The advantage of TFF compared to direct flow filtration is the reduced chance of membrane fouling occurring- the parallel flow does not form a direct layer over the membrane surface – therefore as the volume passed through the membrane increases over time, the filtrate flux rate remains high (Schwartz and Seeley, 1999). This process of production, down-stream purification and monitoring of product quality can be operated across a range of scales.

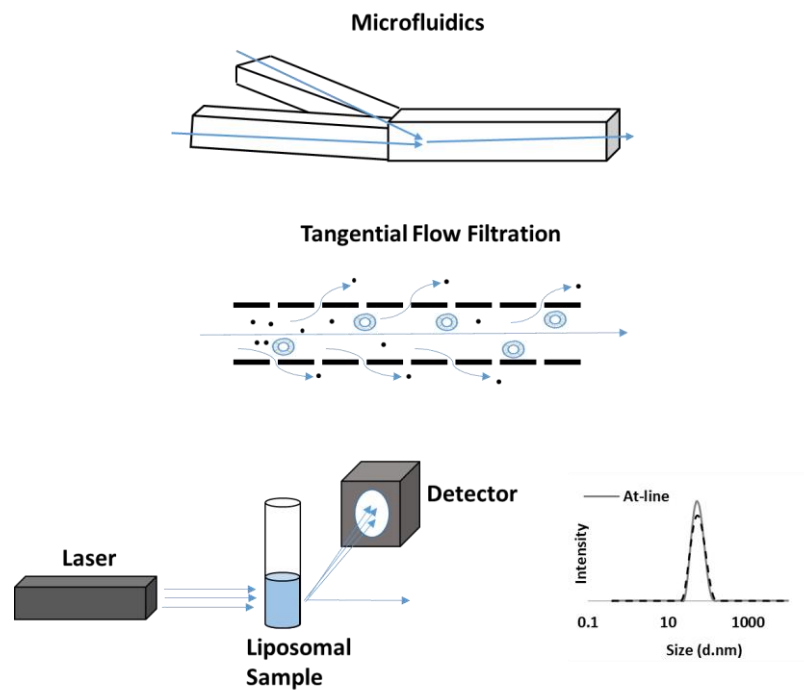
1.7 General aim and thesis objectives

As a result of the complexities involved when administering oral antigen, it is hypothesised that mucosal vaccination against enteric bacterium *C. difficile* can be enhanced through the use of liposomal delivery systems. To address this, microfluidic manufacture of antigen loaded liposomes was investigated through the following objectives:

- Determination of critical processing parameters during microfluidic manufacture of liposomal formulations.
- Identification of rapid quantification techniques for the determination of antigen loading within a range of liposomal vesicles.
- Optimise and validate the protein loading parameters for both entrapped and surface adsorbed antigen.
- Establish suitable down-stream analytical and purification techniques that can function within a continuous manufacturing platform.
- *In vitro* screening of liposomal formulations on THP-1 macrophage like cells.
- Evaluation of *in vivo* efficacy in regards to antibody responses following oral administration of a range of liposomal formulations.

Chapter 2

Scale-up production of liposomal delivery systems



The work presented in this chapter has been published in:

FORBES, N., HUSSAIN, M. T., BRIUGLIA, M. L., EDWARDS, D. P., TER HORST, J. H., SZITA, N. & PERRIE, Y. 2019. Rapid and scale-independent microfluidic manufacture of liposomes entrapping protein incorporating in-line purification and at-line size monitoring. *International journal of pharmaceutics*, 556, 68-81.

2.1 Introduction

Traditional manufacturing techniques such as lipid-film hydration have been used to prepare liposomes for a number of decades and are still commonly used within laboratory settings (Bangham et al., 1965). Despite this, challenges still remain in relation to the lack of control of vesicle size and effective drug loading using this approach. Adapted techniques such as ethanol injection (lipids dissolved in solvent are injected into an aqueous buffer stream) and supercritical fluid method (lipids are subjected to repeated cycles of carbon dioxide and ethanol, resulting in liposome suspension formation) can offer better vesicle size control (Perrie et al., 2017). Microfluidics as a liposome manufacturing method involves the manipulation of liquids in a constrained microchannel chip (Forbes et al., 2019). The technique was first described by Jahn et al where the hydrodynamic focusing of lipids dissolved in solvent using aqueous buffer streams on a microfluidic cartridge was shown (Jahn et al., 2004). The resultant mixing of water miscible solvents containing lipids and aqueous buffer streams results in a change of polarity, where lipids then form into liposomes through nanoprecipitation. The architectural design of the chip dictates how the fluid streams interact, producing flows such as laminar or turbulent. For example, by employing a staggered herringbone micromixer (SHM), chaotic advection can be encouraged (as a result of the protruding structures within the channel), resulting in efficient fluid mixing between both solvent and aqueous fractions, resulting in nanoprecipitation where homogeneous liposomal vesicles are formed (Jahn et al., 2007). By employing microfluidics as a manufacturing platform, there is potential to de-risk liposome production by moving away from traditional batch manufacture – wherein exists increased financial risk and inefficient production streams, and with the appropriate downstream purification and at-line analytics, a push towards continuous liposomal manufacture could be realised (Worsham et al., 2019).

The work within this chapter investigated microfluidics as a manufacturing platform for liposomes, while comparing this technique to more traditional manufacturing options, such as lipid film hydration followed by additional down-sizing steps including hand held extrusion and sonication. A range of lipids was investigated, including the addition of charged lipids (both cationic and anionic) and key microfluidic critical processing parameters were established. The functionality of microfluidics as a liposomal manufacturing platform within a continuous manufacturing stream was evaluated alongside a down stream purification technique that is capable of removing residual solvent. Finally the incorporation of real-time physicochemical analysis was tested in respect to achieving a continuous manufacturing platform for liposomal products.

2.2 Aim and objectives

The aim of the work outlined within this chapter was to develop a microfluidic manufacturing platform for liposomes. In order to achieve this, the objectives were:

1. Evaluate the applicability of microfluidics compared to traditional “top-down” techniques.
2. Identify the microfluidic critical operating parameters and determine how they impact on vesicle characteristics.
3. Determine a suitable purification method which can be applied within a continuous manufacturing setting.

2.3 Materials

The lipids 1,2-distearoyl-sn-glycero-3-phosphocholine (DSPC), 1,2-dioleoyl-3-trimethylammonium-propane (DOTAP) and L- α -phosphatidylserine (Brain PS, Porcine) were all purchased from Avanti Polar Lipids Inc., Alabaster, AL, US. Cholesterol (cholesterol), Sephadex® G-75 and 14,000 (MWCO) dialysis tubing cellulose, phosphate buffered saline (PBS; pH 7.4) in tablet form were purchased from Sigma Aldrich Company Ltd., Poole, UK. Dil Stain (1,1'-Dioctadecyl-3,3,3',3'-Tetramethylindocarbocyanine Perchlorate ('Dil'; DiIC18(3)) was purchased from Fisher Scientific, Loughborough, England, UK. Tris-base was obtained from IDN Biomedical Inc. (Aurora, OH, United States) and used to make 10 mM Tris buffer, adjusted to pH 7.4 using HCl. Brain PS substitute 1,2-dioleoyl-sn-glycero-3-phospho-L-serine (sodium salt) (DOPS) was gifted from Avanti Polar Lipids Inc., Alabaster, AL, US. All solvents and chemicals used were of analytical grade.

2.4 Methods

2.4.1 Top-down liposome manufacture: Lipid-film hydration

The lipid-film hydration method for the manufacturing of liposomes was conducted in the following manner. Lipids were dissolved at specific concentrations in a chloroform:methanol mixture (v/v 9:1) in a round bottom flask. The flasks were then placed under rotatory evaporation for 6 minutes at 200 rpm, in a heated water bath (37°C) to remove solvent. The flasks then remained on the rotary evaporator for 10 minutes to allow trace organic solvent to evaporate. Hydration of the lipid film was

achieved by the addition of heated buffer solution (phosphate buffered saline, PBS) to the required transition temperature for each formulation (e.g. DSPC formulations: 55 °C), followed by multiple vortexing and re-heating cycles for 15 minutes.

2.4.1.1 Size reduction: Hand-held extrusion

Following lipid-film hydration, MLV must then be subsequently size reduced to produce SUVs. Hand-held extrusion experiments were conducted on a Mini Extruder from Avanti Polar Lipids Inc., Alabaster, AL, US. Liposome formulations (1 mg/mL) were extruded through specific pore size membrane filters, starting from 0.4 µm, followed by 0.2 µm and ending with a final filter pore size of 0.1 µm. Each sample is cycled through the membrane x10, while the sample is maintained at a temperature relevant to the transition temperature of the lipids within the formulation.

2.4.1.2 Size reduction: Probe sonication

Size reduction of MLV following lipid-film hydration using probe sonication was conducted on a Sonoplus HD 2070 (ultrasonic homogenizer, Bandelin, Berlin, Germany) at 40% amplitude in order to produce SUV. The probe tip was slightly submerged into the liposomal samples, and subjected to sonication over a specified time frame, with samples being removed every 1 minute for particle physicochemical analysis.

2.4.2 Bottom-up microfluidic manufacture of liposomes

The preparation of liposomes by microfluidics was conducted on the NanoAssemblr platform (Precision NanoSystems Inc., Vancouver, Canada). Selected lipids were dissolved in methanol (solvent phase) at specific concentrations and injected through one of the two inlets on the microfluidics staggered herringbone micromixer chip, whilst the aqueous phase (PBS; pH 7.3 ± 0.2 or TRIS; 10 mM pH 7.4) is injected into the second inlet. A number of production parameters can be controlled using the microfluidic platform software such as flow rate ratio (the ratio between the aqueous phase and the lipid phase) and the total flow rate (the speed at which the two inlets are injected through the chip). Flow rate ratios of 1:1, 3:1 and 5:1 were selected for testing as well as total flow rate speeds between 5 and 20 mL/min.

2.4.3 Purification of microfluidic formulations

2.4.3.1 Dialysis

In order to remove residual methanol after liposomal manufacture by microfluidics, dialysis was conducted. Briefly, 1 mL of the liposomal formulations were added to dialysis tubing (MWCO 14,000), clipped at both ends to stop sample leakage and subjected to magnetic stirring within 200 mL of appropriate buffer for 1 hour, in order for the concentration gradient to sufficiently remove the methanol from the liposome samples. Dialysis membrane (14,000 MWCO) was pre-treated in a solution of 2% sodium bicarbonate, 1 mM EDTA and 1 L of ultrapure water at 80°C for 2 hours under magnetic stirring. The membrane was then rinsed with water to remove any trace of pre-treated solution and stored in 20% EtOH.

2.4.3.2 Gel filtration

Sephadex® G-75 columns for solvent removal were prepared by weighing out 690 mg of Sephadex G-75 beads and adding 10.2 mL of deionized water, then allowing the mixture to swell for 3 h by subjection to 90°C heating. The slurry mixture was then added to a column, ready for sample addition. Briefly, 2 mL of sample was added on top of the column and the liquid was discarded (solvent section), then 3 mL of buffer as elution volume was added on top to flush the liposomes out for further analysis.

2.4.3.3 Tangential flow filtration

Liposome samples were purified using Krosflo Research lll tangential flow filtration (TFF) system fitted with an mPES (modified polyethersulfone) column with a pore size of 750 kD. For removal of solvent, liposomal samples were circulated through the column (21 mL/min) and purified through diafiltration, with fresh PBS being added at the same rate as the permeate leaving the column (for 12 diafiltrate volumes).

2.4.4 Liposome recovery using fluorescence tracking

To determine the recovery of liposomes across the different purification systems, liposomal formulations were prepared using microfluidics, with the addition of a lipophilic fluorescent dye 1,1'-dioctadecyl-3,3,3',3'-tetramethylindocarbocyanine (Dil excitation 549 nm, emission 565 nm). The dye was added to the solvent phase prior to liposome manufacture at a concentration of 0.2 mol%. The dye incorporates within the membrane of the liposomes during formation and liposome recovery can be quantified through the fluorescence readings of the dye post purification when compared

alongside a standard curve of known concentrations of liposomes in solvent with Dil incorporated. LOD and LOQ values for Dil curves were 0.06 and 0.19 mg/mL respectively.

2.4.5 Dynamic light scattering: Physicochemical analysis (off-line and at-line)

Dynamic light scattering (DLS) is a technique that can be used to measure particle size, generally below the micron range and dispersed within solution. DLS (Malvern Zetasizer Nano-ZS from Malvern Panalytical, Worcs., UK) was used to determine the Z-average (mean diameter) and polydispersity index (PDI) of the liposomal samples off-line. Measurements were maintained between attenuation 6-9 by diluting vesicles in buffer (1/10) and all readings were conducted in triplicate at 25°C, using a refractive index of 1.330 and 1.59 for the dispersant and the material respectively. For at-line analytics, the Zetasizer AT (Malvern Panalytical Ltd, Malvern, UK) was used, under the same dilution factors as the aforementioned off-line system, with a flow rate of 5 mL/min (buffer) and 0.5 mL/min (sample).

2.4.6 Gas chromatography: Quantification of residual solvent

To measure residual solvent levels in samples following purification, gas chromatography was carried out using a Fisons Instruments™ GC 8000 series with helium gas. Calibration curves of specific methanol levels were used, alongside an internal standard (butanol). For each sample, the internal standard of butanol was also added to act as a proportionality indicator for measurements with a run time of 3 minutes. LOD and LOQ values for the curve were 0.01 and 0.05% respectively.

2.4.7 Statistics

Results are represented as mean \pm SD with n = 3 independent batches unless stated otherwise. ANOVA tests were used to assess statistical significance between groups, with a Tukey's post adhoc test (p value of less than 0.05).

2.5 Results and Discussion

2.5.1 Comparison of liposomal manufacture: Top-down and bottom-up approaches

In order to investigate the development of microfluidics as a liposome manufacturing platform, initial studies focused on the production and characterisation of DSPC:Chol (10:5 w/w) liposomes following a traditional top-down manufacturing technique: lipid-film hydration for the production of MLV, followed by two common lab-scale down-sizing techniques, hand-held extrusion and probe sonication. Figure 2.1 indicates the down-sizing of MLV following lipid-film hydration (pre-extrusion) across a range of decreasing pore sized extrusion membranes. Following lipid-film hydration, the vesicles exhibited a high range of heterogeneity (885 ± 427 nm, 0.54 ± 0.19 PDI), and following subsequent extrusion cycles, a trend of decreasing vesicle size was observed (451 ± 101 nm, 177 ± 3 nm and 163 ± 19 nm) as the pore size of the extrusion membranes was reduced (400 nm, 200 nm and finally 100 nm). This trend of decreasing vesicle size was also observed in terms of heterogeneity of the liposome population (as indicated by a decrease in PDI values), with PDI values of 0.22 ± 0.16 , 0.10 ± 0.01 and 0.09 ± 0.03 following extrusion cycles.

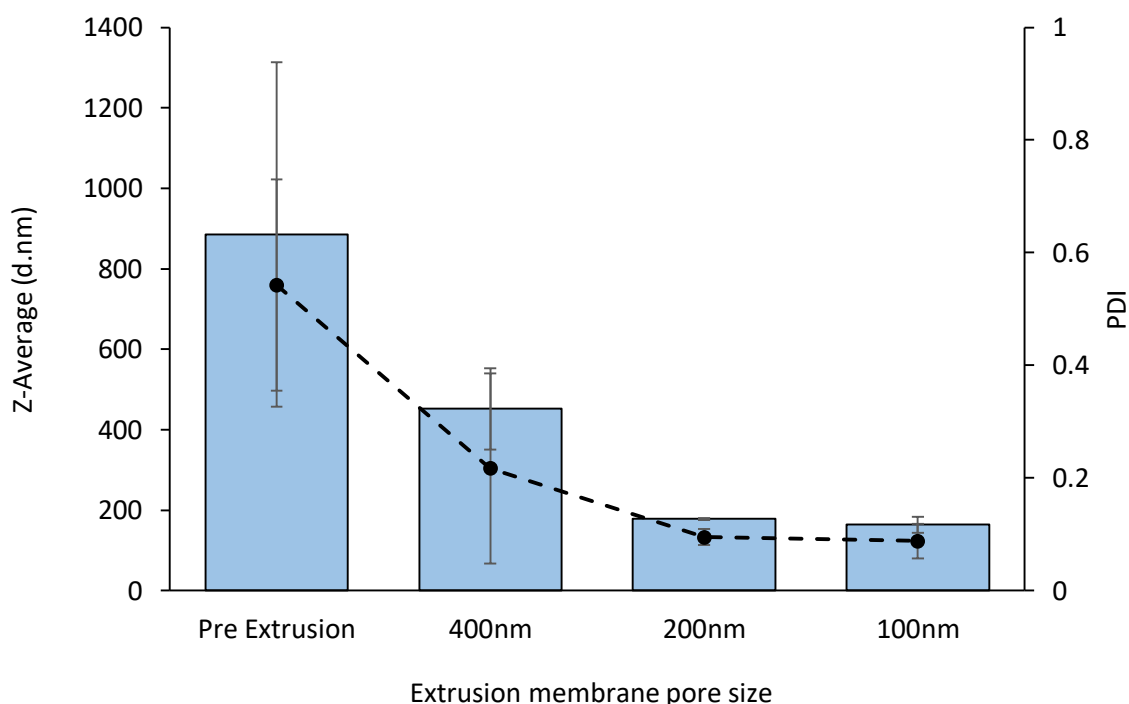


Figure 2.1 Down-sizing using hand-held extrusion: Evaluating particle size (columns) and polydispersity index (circle) through a series of decreasing pore sized membranes during hand-held extrusion for liposomal formulation DSPC:Chol 10.5 (w/w) at a total lipid concentration of 1 mg/mL. Results represent mean \pm SD, n =3 of independent batches.

Extrusion is a well-defined, common technique that can be used for the down-sizing of liposomes which also offers the additional benefit of some scalability (Wagner and Vorauer-Uhl, 2011). Extrusion of liposome samples involves the use of specific pore-sized membranes (commonly composed of polycarbonate), in which the liposome preparation (MLV) is forced through by either pressure pumps or syringe plunges. During this process, large vesicles elongate and rupture as they through the membrane, forming smaller vesicles, with the final size of the samples being dependent on the pressure applied and the number and choice of membrane sizes used (Patty and Frisken, 2003, Frisken et al., 2000b). For example, Mayer et al showed a direct correlation between mean diameter decreases in egg PC liposomes (243 ± 91 , 151 ± 36 and 103 ± 20 nm) as the filter pore size decreased across a 400, 200 and 100 nm range. However, these liposome samples were passed through each extrusion membrane for 20 cycles, as opposed to the 10 cycles as conducted in Figure 2.1. A comparison study between down-sizing techniques for non-ionic surfactant based vesicles (Tween 60:Cholesterol 60:40 molar ratio) prepared by lipid-film hydration found improved PDI values for extrusion (< 0.20) when compared to either homogenization (approximately 0.40) and probe sonication (approximately 0.45) after extrusion through 400 and 200 nm polycarbonate membranes (Nowroozi et al., 2018).

In addition to extrusion as a down-sizing technique for MLV, probe sonication was also examined. Probe sonication is based upon the use of acoustic energy to disrupt MLV into SUV. Following sonication of MLV for up to 2 minutes, a decrease in vesicle size was observed from ~ 700 nm prior to sonication, to ~ 360 nm after 1 minute of sonication and down to ~ 320 nm after 2-minute sonication (Figure 2.2). A similar decrease in PDI was also noted (from 0.65 to 0.28 after 2 min sonication) (Figure 2.2). A further drop in vesicle size was observed for the liposomal population after 3 minutes of sonication (~ 280 nm), although this corresponded with an increase in PDI (0.48). Further sonication did not produce an addition drop in vesicle size with a final size of ~ 260 nm and a PDI of 0.39 after 5 minutes (Figure 2.2).

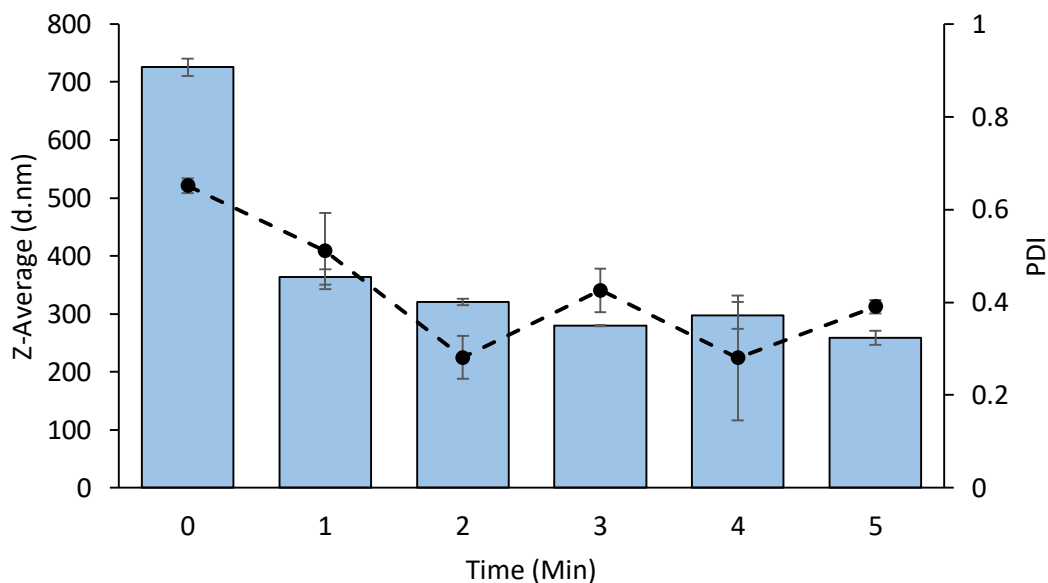


Figure 2.2 Particle size (columns) and polydispersity index (circles) during probe sonication for liposomal formulation DSPC:Chol 10:5 (w/w) at a total lipid concentration of 1 mg/mL. Samples were DLS analysis were removed every minute during sonication exposure. Results represent mean \pm SD, $n=3$ of independent batches.

Sonication for liposome down-sizing uses acoustic energy to generate cavitation within the sample to reduce MLV into SUV. The degree of down-sizing is dependent on a range of sonication parameters which each ultimately influence the final vesicle size obtained (Silva et al., 2010). The duration that the MLV sample is subjected to sonication is a key parameter for determining final vesicle size, as the longer the sonication occurs, the mean liposome diameter decreases. Nam et al showed the effect of sonication duration on vesicle size and PDI for DSPC:Chol:POPG (27:20:3 w/w/w) liposomes produced by lipid-film hydration. Prior to sonication, MLV size was 1433 ± 143 nm, but following 5 minutes of sonication a significant reduction in vesicle size was found (down to 337 ± 67 nm). Continued sonication for up to 40 minutes resulted in minimal changes in vesicle size. Polydispersity index of the sample was also found to decrease for the first 5 minutes of sonication from approximately 0.45 down to 0.30 before reaching a plateau (Nam et al., 2018). Similar results were found within the findings in Figure 2.2 with a plateau of both PDI and average vesicle size being reached. However, sonication past 5 minutes was not tested within this experimental design due to the excessive heat generated from the probe tip, which could lead to phospholipid degradation (Hong and Lim, 2015). Additional sonication parameters have previously been shown to impact upon final vesicle characteristics such as the intensity of the ultrasound energy during sonication, which leads to a decrease in the average diameter of the liposomes within the sample, as well as the distance of the probe sonicator source within the liposomal sample, although these parameters were outside of the scope of this investigation (Silva et al., 2010, Richardson et al., 2007).

In order to evaluate microfluidics as a potential manufacturing platform for liposomal formulations, the same formulation DSPC:Chol (10:5 w/w) was produced using the NanoAssemblr (Precision NanoSystems Inc.). Initially the microfluidic production parameters of flow rate ratio 3:1 and a total flow rate of 10 mL/min were chosen. To allow comparison to the lipid hydration/down-sizing methods, an initial lipid concentration of 4 mg/mL (resulting in a final total lipid concentration of 1 mg/mL across all techniques) was used. For removal of solvent following microfluidic production, dialysis was conducted. Figure 2.3 indicates the comparison of the physicochemical attributes of the three techniques. Both hand-held extrusion and microfluidics resulted in highly homogenous populations of vesicles (< 0.1 PDI), while probe sonication for 5 minutes resulted in a heterogeneous population (0.39 PDI). In terms of vesicle size, each technique could produce different sized vesicles, with extrusion resulting in particles around 160 nm, sonication around 250 nm while microfluidics could produce small vesicles around 45 nm.

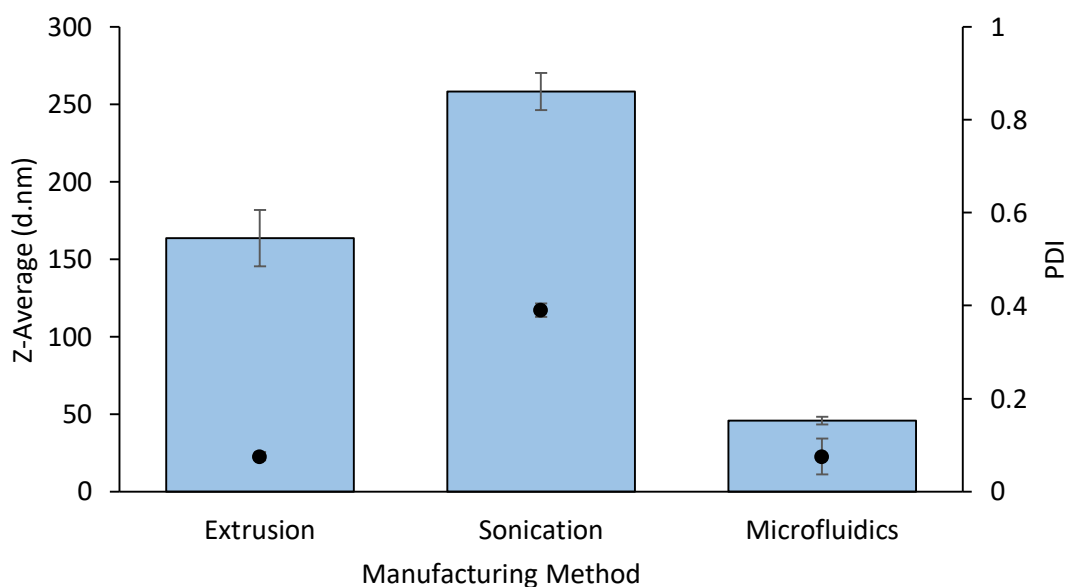


Figure 2.3 Liposome manufacturing comparison. Particle size (columns) and polydispersity index (circles) for hand-held extrusion (100 nm membrane), probe sonication (subjected to sonication for 5 minutes) and microfluidics (3:1 flow rate ratio, 10 mL/min total flow rate) for liposomal formulation DSPC:Chol 10:5 (w/w) at a final total lipid concentration of 1 mg/mL and purified using dialysis. Results represent mean \pm SD, n =3 of independent batches.

The need for homogenous, reproducible liposomal products is essential for a manufacturing system due to the impact this has on the pharmacokinetic profiles of the liposome samples. This has led to down-sizing techniques such as sonication and extrusion being widely used (Cho et al., 2013). While extrusion offers benefits such as ease of scalability and high reproducibility, disadvantages include the requirement of the product to be maintained above transition temperatures, which can present issues with thermo-sensitive drugs (e.g. proteins) within liposomal delivery systems. Furthermore, high levels

of product loss can result from down-sizing via extrusion, which can have detrimental financial implications for large-scale production (Wagner and Vorauer-Uhl, 2010). In the case of sonication, whilst it is an established tool for the generation of SUV from MLV within the laboratory setting, there remains some issues pertaining to contamination of the sample from the titanium probe tip, which therefore must be subsequently removed by additional down-stream processing such as centrifugation (Akbarzadeh et al., 2013). This potential contamination can be avoided through employing bath sonicators (Khadke et al., 2018); however, issues still remain in regards to scalability of the process. Alternative down-sizing techniques exist that address this lack of scalability, including high pressure homogenisation. The technique applies high shear processing, by forcing liposome mixtures through adaptable chambers that direct two fluid channels against each other, resulting in both impaction and shear, leading to a size reduction and improved PDI as the product is cycled repeatedly through (Anderluzzi et al., 2019). Although techniques such as this address scalability, the process is still inherently based upon batch production, where manufacturing and down-sizing are two separate components within the production chain. Microfluidics offers an alternative method for the production of liposomes. Manipulation of fluid streams in a microchannel environment allows for precise control and production of nanoparticles from a bottom up approach, circumventing the need for additional down-sizing. When comparing microfluidics to both sonication and extrusion, vesicles approximately 45 nm with high homogeneity were produced ($PDI < 0.1$) in a single step process (Figure 2.3). Microfluidics has previously been demonstrated to rapidly produce nanoscale vesicles with high population homogeneity (Jahn et al., 2004, Kastner et al., 2014). In addition, processing parameters can be identified and manipulated, allowing for control of desired vesicle size (Jahn et al., 2007). Furthermore, microfluidics offers ease of scale-up and can be incorporated into continuous manufacturing systems, de-risking and streamlining the production of liposome products (Deshpande and Dekker, 2018).

2.5.2 Cholesterol content can be adjusted to control vesicle size

Liposome production using traditional techniques such as lipid-film hydration generally require the phospholipid mixture to be above the transition temperature (T_c) of the lipid mixture in order for vesicles to form. This requirement of high temperature during manufacturing (for example DSPC lipid has a T_c of 55°C), presents challenges when working with thermosensitive moieties including proteins, where structural integrity is essential for therapeutic efficacy. Cholesterol is a common component in liposome formulations. Whilst cholesterol cannot form bilayers on its own, it can be incorporated into liposome bilayers at concentrations of up to 50 mol%. The inclusion of cholesterol within lipid mixtures has been shown to reduce/negate this requirement alongside DSPC lipid on a concentration basis, as well as increasing stability of the liposomes (Moghaddam et al., 2011, Mozafari, 2010). When using microfluidics, a heating block can be used to maintain solutions at specific, although production at ambient room temperature is preferable in terms of cost and stability. Therefore, in order to determine whether the bottom-up manufacturing method of microfluidics has the same T_c constraints as other methods, DSPC based liposomes with increasing concentrations of cholesterol were manufactured across a range of processing temperatures. Figure 2.4A indicates the average size of the vesicles following purification by dialysis. The addition of cholesterol to DSPC lipid at a weight to weight ratio of 10:1 (DSPC:Chol) resulted in vesicles around 150 nm, irrespective of the processing temperature. Increasing the cholesterol content resulted in a trend of decreasing vesicle size to 75 nm with the DSPC:Chol 10:3 (w/w) formulation down to 55 nm (10:4 DSPC:Chol w/w) and finally 45 nm (10:5 DSPC:Chol w/w) (Figure 2.4A). Again, the processing temperature during microfluidic manufacture did not impact upon vesicle size, with vesicles remaining the same size across all production temperatures tested (Figure 2.4A). The increasing cholesterol content and different production temperatures did not impact upon the homogeneity of the liposomal populations, with PDIs below 0.2 across all formulations and processing temperatures (Figure 2.4B).

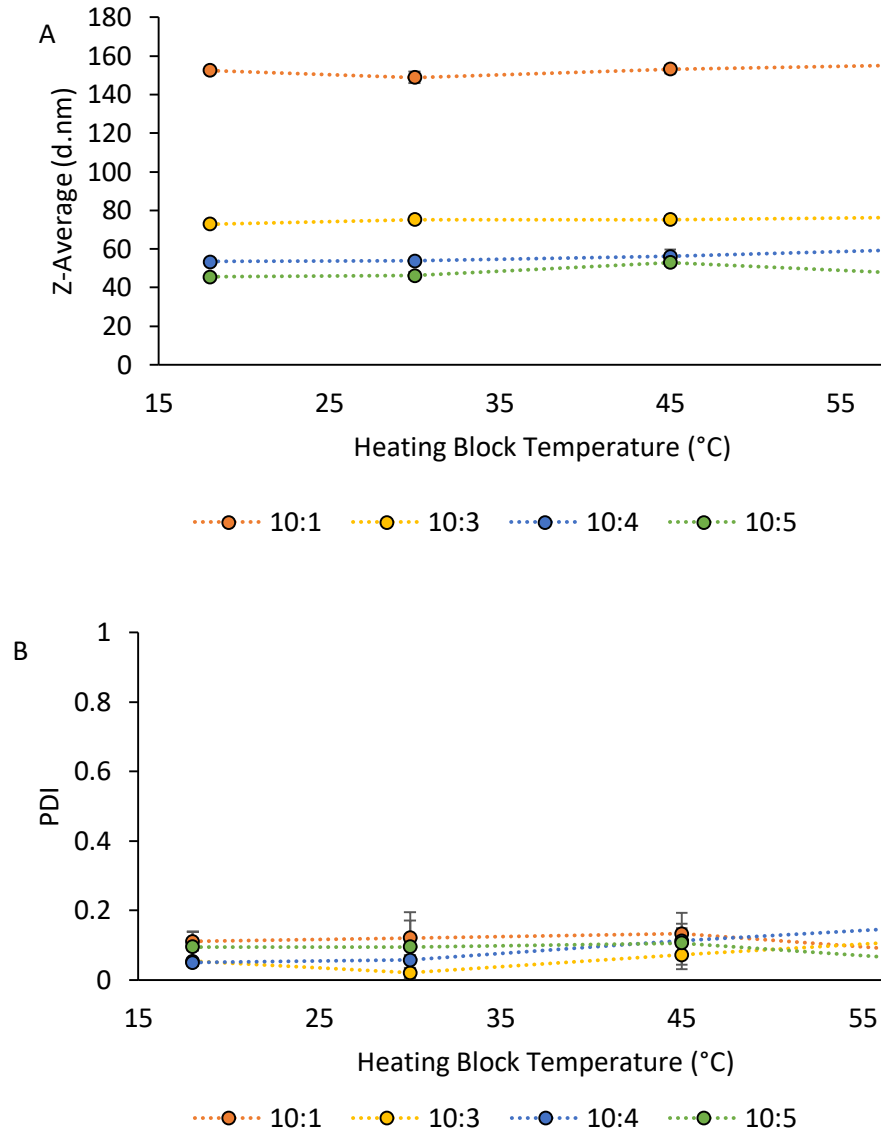


Figure 2.4. The effect of cholesterol content and heating block temperature during microfluidic manufacture for the high transition temperature lipid DSPC (and subsequently purified using dialysis) were investigated in regards to (A) z-average (particle size) and (B) PDI. Results represent mean \pm SD, $n = 3$ independent batches.

The inclusion of sterols, namely cholesterol, can induce structural changes within the bilayer of liposomes by increasing the packing of the phospholipid molecules by filling in molecular cavities, resulting in greater stability and a reduction in bilayer permeability (Bruglia et al., 2015, Moghaddam et al., 2011, Gregoriadis and Davis, 1979). Furthermore, the ability of cholesterol to influence transition temperatures (T_c) of lipids has previously been demonstrated using differential scanning calorimetry (DSC), with the addition of 33 - 50% cholesterol completely removing the T_c for DSPC lipid (T_c 55°C) (Moghaddam et al., 2011). During microfluidic manufacture, even the addition of low quantities of cholesterol within DSPC was shown to negate the requirement of temperatures above

DSPC T_c, with vesicle formation occurring across 10:1 – 10:5 DSPC:Chol w/w ratios (5 - 50% molar ratio).

Manufacture by microfluidics therefore offers an advantage when working with liposomal vesicles in order to incorporate thermosensitive compounds such as vaccine antigens, as the requirement for high temperatures during liposome formation is circumvented. The bottom-up approach of liposome formation from individual lipid monomers by microfluidics may mean that energy constraints during traditional manufacture (where lipid-films are hydrated into vesicles) are not required – as a result the different formation mechanisms involved when lipids dissolved in organic solvent are mixed with aqueous phase. The primary factor influencing the liposomal size during microfluidic manufacture appears not to be T_c constraints, but the concentration of cholesterol, with smaller vesicles forming when cholesterol content is increased. As described previously, cholesterol can intercalate within cavities in the bilayer, altering packing of the lipid molecules and reducing the volume of occupied space by ordering of the phospholipid tails (Falck et al., 2004). It is hypothesised that this improved packing and reduction in free space throughout the bilayer results in the formation of smaller vesicles as cholesterol content is increased when vesicles are formed by microfluidics.

2.5.3 Establishing normal operating parameters for microfluidics

Given the ability of microfluidics to manufacture DSPC:Chol SUV with high population homogeneity in a rapid manner, further studies were carried out to determine the critical processing parameters for this manufacturing platform. Figure 2.5 again focuses on liposomal formulation DSPC:Chol (10:5 w/w) across a range of initial lipid concentrations (the concentration of the lipids in solvent phase prior to liposome formation by microfluidics) with fixed microfluidic production parameters (3:1 FRR, 10 mL/min TFR) in PBS pH 7.4. Across low lipid concentrations (0.3 – 2 mg/mL), a trend of decreasing vesicle size was observed as initial lipid concentration is increased (61 nm down to 45 nm), along with a corresponding decrease in PDI values (0.27 to 0.12) ($p < 0.05$). As initial lipid concentration was further increased up to 4 mg/mL, vesicle size remained constant (around 45 nm), as well as PDI (< 0.1). At the highest concentration tested (10 mg/mL) a statistically significant increase in both Z-average and PDI was observed (51 nm, PDI 0.19) when compared to 4 mg/mL (Figure 2.5A) ($p < 0.05$). In terms of zeta potential, all values for this formulation remained neutral (between -1 mV and -6 mV) across all of the concentration ranges tested (Figure 2.5B).

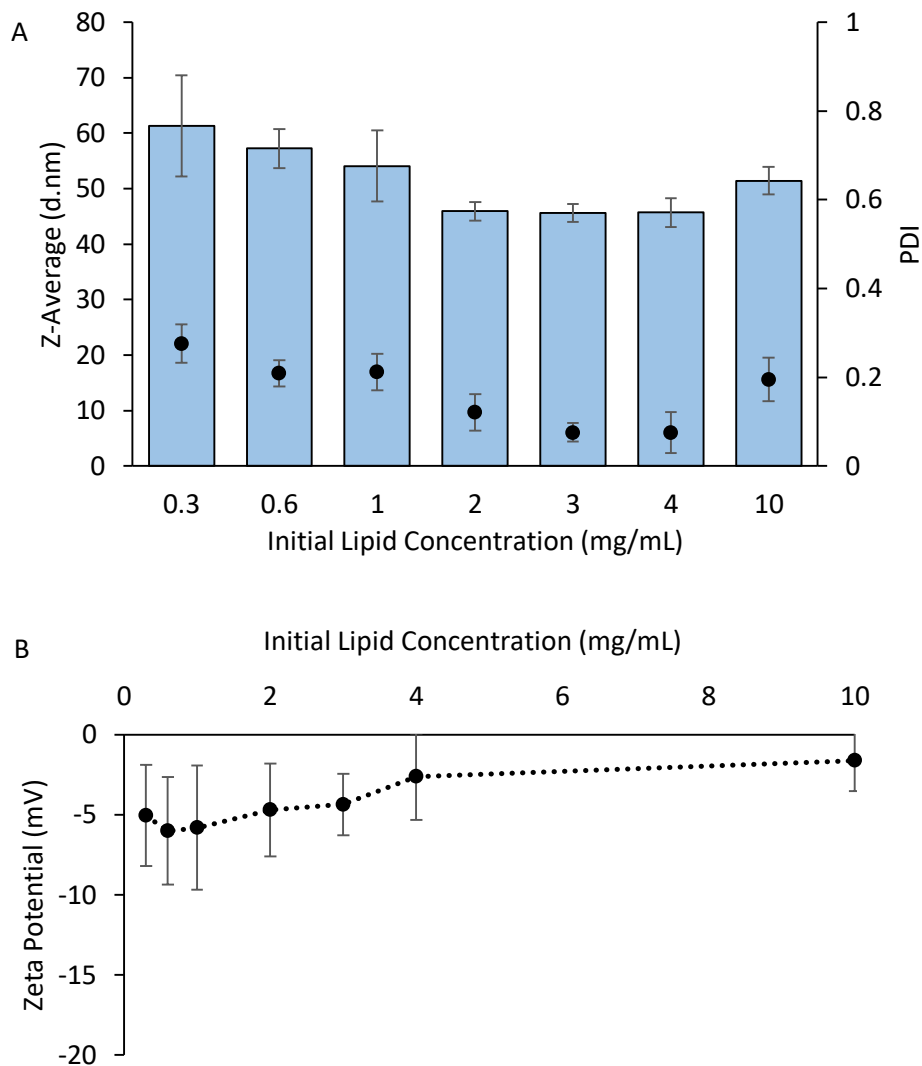


Figure 2.5. Liposomal formulation DSPC:Chol (10:5 w/w) in methanol, investigating the effect of initial total lipid concentration on physicochemical attributes: size (columns) and PDI (circle) (A) and zeta potential (B). Microfluidic parameters selected were flow rate ratio 3:1 and a total flow rate of 10 mL/min. Solvent purification was conducted by dialysis. Results represent mean \pm SD, $n = 3$ of independent batches.

During microfluidic production, a number of production parameters can be selected and adjusted, such as flow rate ratio and the total flow rate. In order to determine whether these production parameters ultimately impact upon the final attributes of the liposomes, the DSPC:Chol (10:5 w/w) formulation was selected for further analysis. Figure 2.6 indicates the effect of initial lipid concentration across three selected flow rate ratios: 1:1, 3:1 and 5:1, with a fixed total flow rate speed of 10 mL/min. In general, all three flow rate ratios exhibit the same trend of decreasing vesicle size as initial lipid concentration is increased from 0.3 – 2 mg/mL. This is also apparent for the polydispersity index across all of the flow rate ratios. When comparing between the flow rate ratios, 1:1 (equal solvent to aqueous phase) resulted in larger vesicles when compared to both 3 and 5:1. This larger

vesicle size across the concentration range (230 nm – 125 nm) did not result in a loss of population homogeneity, with PDI values for the 1:1 FRR remaining less than 0.22 across all of the tested concentrations (Figure 2.6). An increase in aqueous phase (or a corresponding decrease in solvent phase) for FRR 3:1 resulted in smaller vesicles when compared to FRR 1:1, with physicochemical attributes spanning a size range of 115 nm – 49 nm and PDI values between 0.30 and 0.18. Finally, a FRR of 5:1 produced vesicles with similar attributes to 3:1, with sizes between 103 nm – 48 nm and PDI values between 0.35 and 0.18 ($p>0.05$) (Figure 2.6).

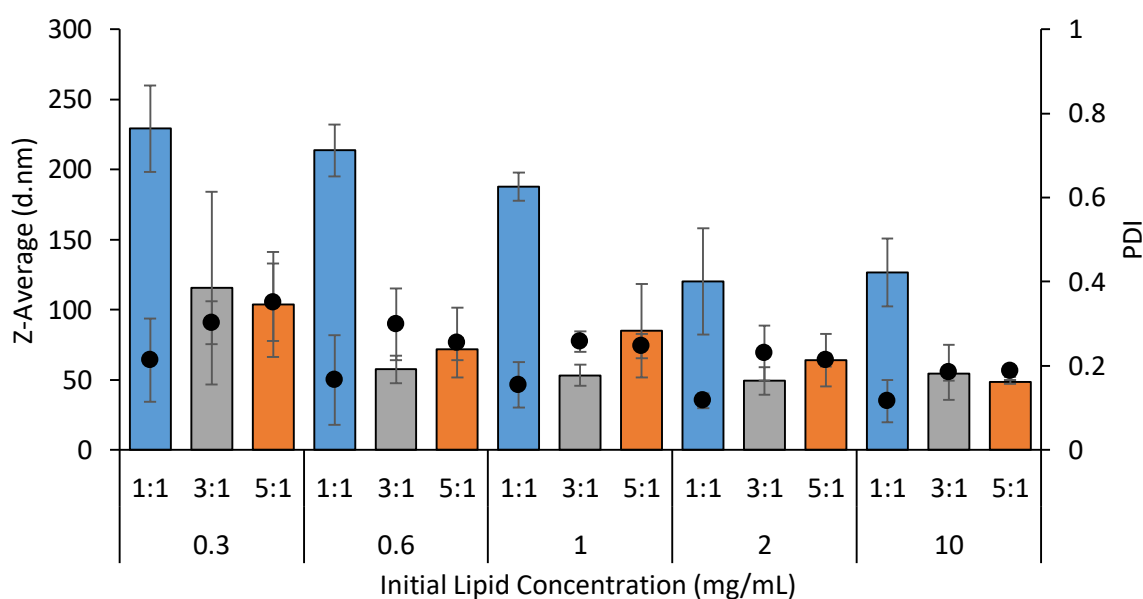


Figure 2.6 Liposomal formulation DSPC:Chol (10:5 w/w) in methanol, effect of initial total lipid concentration and flow rate ratio on physicochemical attributes: size (columns) and PDI (circles). Microfluidic parameters selected were flow rate ratio 1:1, 3:1 and 5:1 and a total flow rate of 10 mL/min. Solvent purification was conducted by dialysis. Results represent mean \pm SD, $n = 3$ of independent batches.

The final microfluidic parameter that can be adjusted is the total flow rate – the speed at which both the phases pass through the microfluidic cartridge. In order to determine the impact this processing parameter has on nanoparticle attributes, DSPC:Chol (10:5 w/w) was selected at an initial total lipid concentration of 4 mg/mL, with a fixed flow rate ratio of 3:1. A range of production speeds were then assessed, ranging between 5 and 20 mL/min. Across the speeds tested, no statistically significant impact upon both Z-average and PDI was observed (Figure 2.7A), with vesicle sizes remaining consistently between 49 nm – 52 nm and PDI values between 0.10 – 0.13 ($p>0.05$). Figure 2.7B shows the intensity plots derived from the DLS software, again indicating the similarities between the formulations across specific speeds of manufacture.

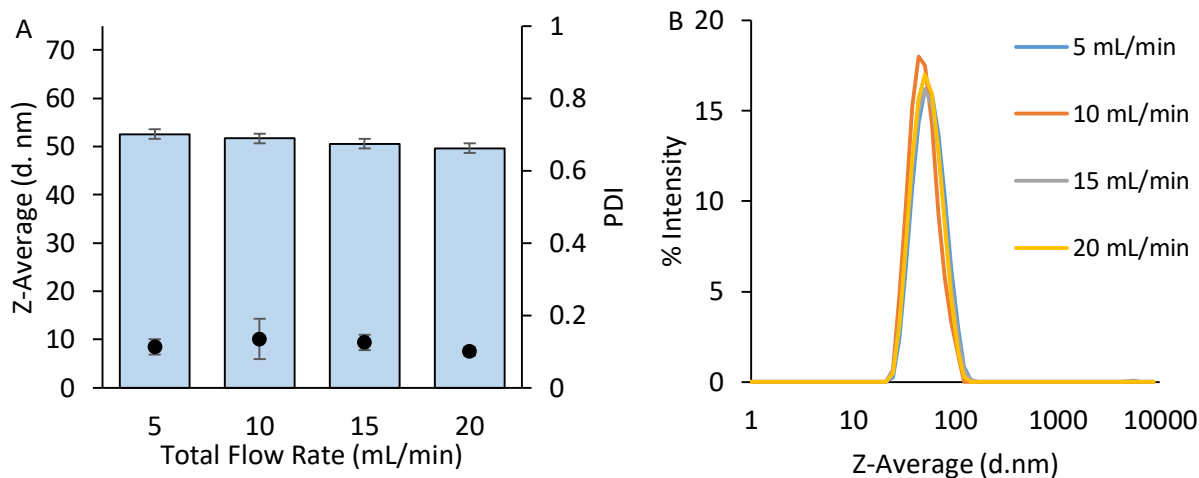


Figure 2.7. Liposomal formulation DSPC:Chol (10:5 w/w) in methanol, effect of total flow rate on physicochemical attributes: size (columns) and PDI (circles) (A) and Intensity (%) (B). Microfluidic parameters selected were flow rate ratio 3:1 and total flow rates between 5 – 20 mL/min. Solvent purification was conducted by dialysis. Results represent mean \pm SD, $n = 3$ of independent batches.

These results indicate the critical production parameters that influence the liposomal physicochemical characteristics following microfluidic manufacture for liposomal formulation DSPC:Chol (10:5 w/w). These studies indicate the influence of the initial total lipid concentration, with concentrations below 2 mg/mL resulting in vesicles with PDI > 0.2 and less reproducibility (indicated by the larger error bars). In terms of vesicle size reproducibility and PDI values less than 0.15, initial lipid concentrations between 2-4 mg/mL were the only concentrations tested that could attain this criterion. Similar results were found when identifying optimal lipid concentrations using the same microfluidic chip architecture (staggered herringbone micromixer) by Joshi et al, where concentrations below 1 mg/mL, resulted in larger vesicles with poor reproducibility being produced using PC:Cholesterol (2:1 w/w), and concentrations greater than 1 mg/mL resulted in improved reproducibility (Joshi et al., 2016). However, the choice of microfluidic manufacturing setup also impacts on the effect of initial lipid concentration, as shown by Mijailovic et al, where a general trend of increasing vesicle size was found as the initial POPC (1-palmitoyl-2-oleoyl-glycero-3-phosphocholine) concentration was increased when using microfluidic hydrodynamic focusing (where 3 micro channel inlets were etched into glass wafers) (Mijajlovic et al., 2013).

Flow rate ratio and total flow rate are both microfluidic production parameters that can be adjusted and controlled through a software interface. The results in Figure 2.6 indicate the large influence that adjusting flow rate ratio has on vesicle characteristics. When using a flow rate ratio of 1:1, larger vesicles were formed (230 – 120 nm) when compared to both 3 and 5:1, and this increase in size did

not correspond to an increase in PDI. When manufacturing at a 3:1 or 5:1 FRR, smaller vesicles (50-60 nm) can be manufactured, and at concentrations above 2 mg/mL, high population homogeneity can be maintained. Similar microfluidic results using a staggered herringbone micromixer have also indicated the influence that flow rate ratio has on the resulting vesicles, with average liposome size of the formulations at a flow rate ratio of 1:1 resulting in sizes above 200 nm, while a flow rate ratio of 5:1 generating sizes around 50 nm (Kastner et al., 2014, Kastner et al., 2015). This general decrease in vesicle size as flow rate ratio is increased was also shown by Jahn et al and is attributed to the influence the flow rate ratio has on the resulting alcohol content of the formulation. At low flow rate ratios (1:1), the alcohol content within the chip is 50% post mixing, thus when the lipids first meet with aqueous phase, partial liposome self-assembly occurs at the interface of the two streams. As the mixing of the fluid streams increases, the liposomes are exposed to differing alcohol – aqueous concentrations, resulting disassembly and re-assembly as the liposomes vary above and below the critical alcohol content. At higher flow rates (3:1 and 5:1), this disassembly and re-assembly cycle is reduced, thus limiting the size of the liposomes produced (Jahn et al., 2007, Jahn et al., 2010). In a similar explanation, Zizzari et al described the reduction in size at higher flow rate ratios as a result of the size of the solvent stream within the microfluidic chip. The lipid disc forms at the interface of the of the two streams and bend, eventually forming into vesicles as the solvent concentration they are exposed to decreases. The longer the discs are exposed to concentrations of solvent above a critical point, the larger the vesicles grow before forming liposomes, thus at high solvent concentrations (1:1), larger vesicles are subsequently formed (Zizzari et al., 2017).

While the microfluidic parameter FRR has been shown to impact upon vesicle characteristics through the exposure of different concentrations of solvent, the effect of the speed in which the vesicles are passed through the chip (between 5 – 20 mL/min) did not (Figure 2.7). Again, Joshi et al assessed the effect of total flow rate for PC:Chol (2:1 w/w) liposomes and found that manufacturing speeds between 5 – 15 mL/min did not impact significantly on liposomal average diameter and PDI (Joshi et al., 2016). Furthermore, an in depth investigation into the effect of total flow rate on liposomal formulations (using five formulations, representative of marketed liposomal products) using a Design of Experiments approach, using a staggered herringbone micromixer was conducted by Sedighi et al. While FRR was found to have a significant impact upon vesicle size, total flow rates above 8 mL/min resulted in no significant changes to vesicle attributes (Sedighi et al., 2019).

These results herein indicate that specific flow rate ratios can be adopted to tailor to specific vesicle size requirements (as long as normal operating parameters have been established for formulation concentration) and the speed of production can be increased to meet specific industrial demand, without impacting upon product quality.

2.5.4 The choice of organic solvent impacts upon formulation size

When using microfluidics as a production platform, choosing an organic solvent to work with can be an important parameter. The choice of solvent must not only be compatible with the choice of lipid components in regards to both solubility and water miscibility, but also an understanding of how the solvent can impact upon formulation characteristics is critical. For liposome formation, efficient fluid mixing must occur between both solvent and aqueous streams, therefore the water miscibility of the particular solvent must be suitable. As organic solvent carbon chain length increases, a decrease in water miscibility is observed (Forster et al., 1991). In order to assess the impact of different carbon chain length solvents on microfluidic manufacture, formulation DSPC:Chol (3:1 FRR, 15 mL/min) was selected. Figure 2.8 shows the average vesicle size of the liposomes manufactured using three different organic solvents, followed by purification by tangential flow filtration. Vesicles manufactured with methanol (MeOH) resulted in the smallest sizes (approximately 45 nm), this was then increased to 55.1 ± 3 nm when ethanol was tested. Finally, isopropyl alcohol (IPA) resulted in the largest liposomal sizes (83.3 ± 2 nm) (Figure 2.8). The PDI values for all of the formulations were found to be highly homogenous (<0.13 PDI for MeOH, EtOH and IPA).

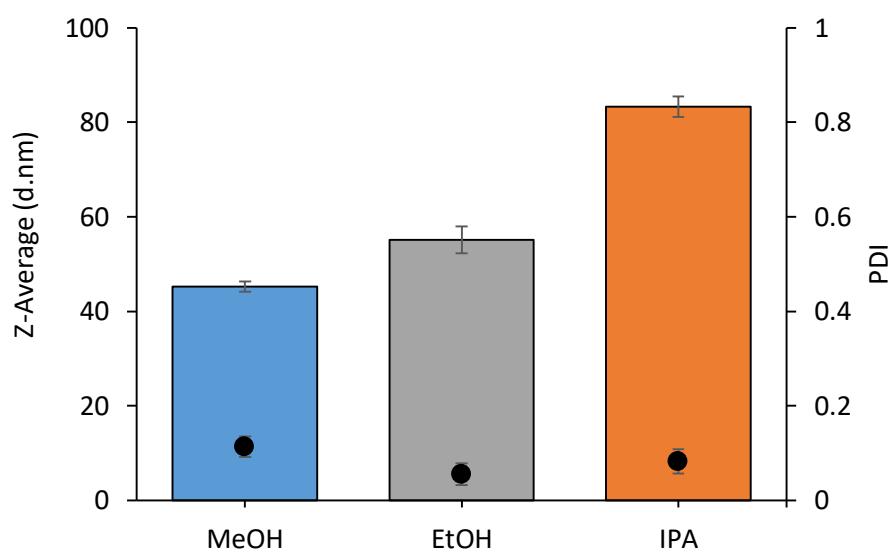


Figure 2.8. The effect of solvent during microfluidic manufacture of liposomal formulation DSPC:Chol (10:5 w/w) (3:1 FRR, 15 mL/min) in methanol (MeOH), ethanol (EtOH) and isopropyl alcohol (IPA): size (columns) and PDI (circles). Solvent purification was conducted by tangential flow filtration. Results represent mean \pm SD, $n = 3$ of independent batches.

This study has indicated the importance of solvent choice in regards to vesicle characteristics. The size of liposomal formulation (DSPC:Chol 10:5 w/w) can be adjusted by employing solvents with differing carbon chain lengths. This can be explained by the rate of polarity change seen when both fluid streams mix within the microfluidic cartridge. As organic solvent polarity is reduced (e.g. IPA), the rate

of polarity change is therefore reduced during mixing, thus lipid bilayer discs can expand for longer, before finally bending into larger liposomes. When employing a higher polarity solvent (e.g. MeOH), a steeper polarity shift is observed, thus the lipid discs have less time to expand, forming smaller liposome vesicles (Webb et al., 2019).

2.5.5 The effect of the inclusion of charged lipids on microfluidic manufacture

By adjusting liposome charge, the pharmacokinetic profile of the liposomal formulation can be manipulated in order to meet specific requirements. The modification of liposome charge can be achieved through the inclusion of lipids with negative or positively charged head groups (Beltrán-Gracia et al., 2019). For instance, cationic vesicles have been shown to have a preferential targeting ability towards angiogenic endothelium of tumours, as well as a strong association to cellular membranes – allowing them to be effective transfection systems for RNA and small proteins (Lonez et al., 2008, Krasnici et al., 2003). Furthermore, the inclusion of anionic lipids such as PS within liposomal formulations can actively target the vesicles to improve macrophage uptake, generating interest in terms of vaccine adjuvants (Geelen et al., 2012). Therefore, the next stage was to consider the formulation of charged liposomes using microfluidics.

2.5.5.1 The addition of phosphatidylserine (PS) within liposomal formulation DSPC:Chol

In order to determine the effect of anionic charged lipids, the addition of PS into the neutral formulation DSPC:Chol, PS was added incrementally and the impact investigated. PS was selected due to its potential as an immunostimulatory agent (Geelen et al., 2012). Three flow rate ratios were also assessed: 1, 3 and 5:1 in order to determine suitable operating parameters for the anionic formulation. As the concentration of PS was increased, a trend of increasing vesicle size was observed for flow rate ratio 1:1, increasing from approximately 80 nm up to 120 nm. This increase in vesicle size was not associated with an increase in PDI, with all values < 0.2. For flow rate ratios 3 and 5:1, vesicle size remained constant between approximately 40 - 50 nm irrespective of the amount of PS included within the formulation. Again, all vesicles measured were highly homogeneous (< 0.2 PDI) (Figure 2.8A). In terms of zeta potential (Figure 2.9B), flow rate ratio 1:1 showed an association with increasing PS resulting in a decrease in zeta potential (from approximately -24 mV to -50 mV), while flow rate ratios 3 and 5:1 showed less of a trend. When comparing between flow rate ratios, 1:1 resulted in the most negative zeta potential readings, followed by 3:1 (-17 mV to -22 mV) and finally 5:1 (-4 mV to -14 mV) (Figure 2.9B)

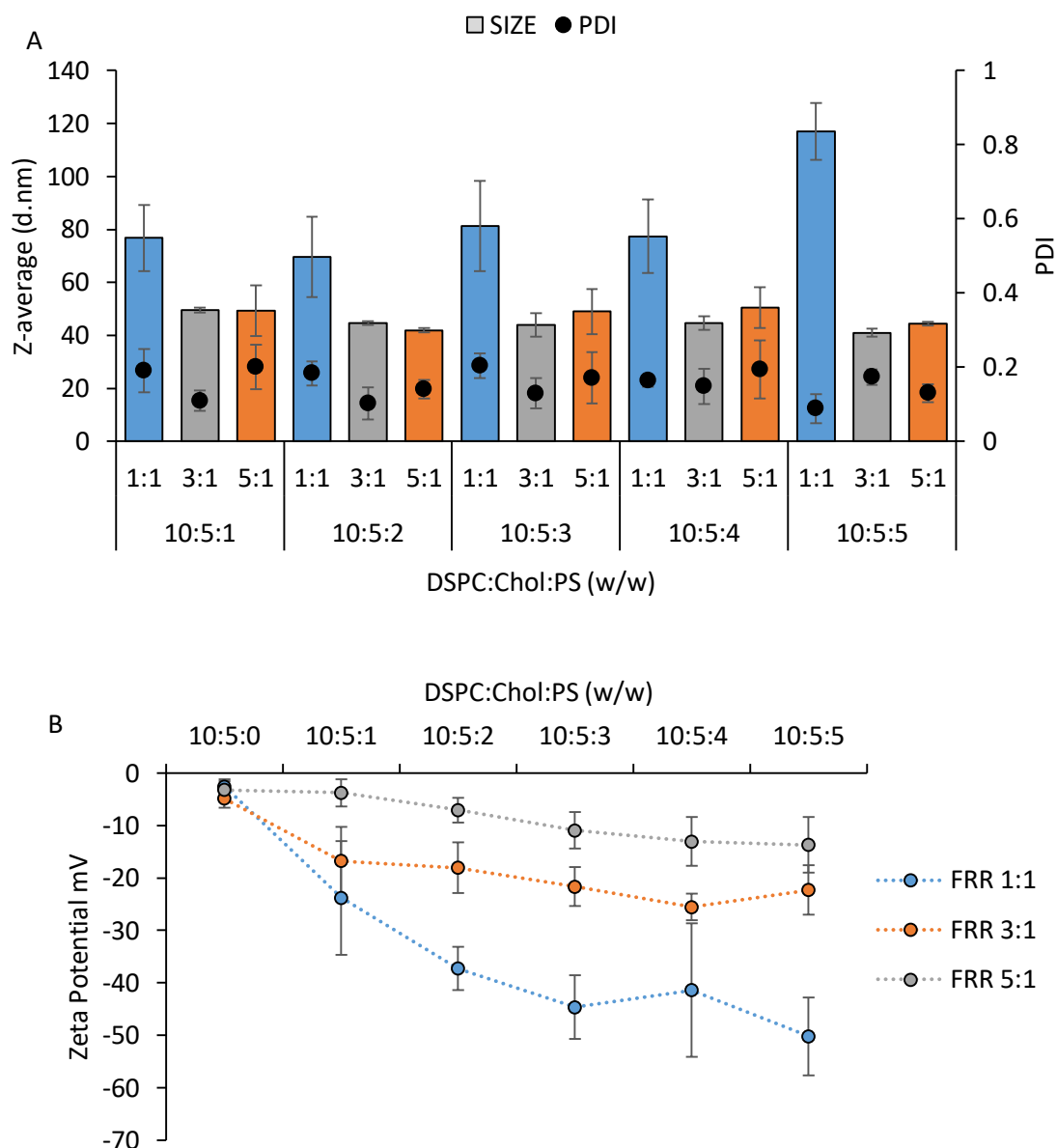


Figure 2.9. The effect of adding PS incrementally to the liposomal formulation DSPC:Chol, liposome size (bar) and PDI (circles) (A) and Zeta Potential (mV) (B) across three distinct flow rate ratios (1,3 and 5:1). Initial total lipid concentration was fixed at 4 mg/mL and purification was conducted using dialysis. Results represent mean \pm SD, n =3 of independent batches.

For further studies, a 3:1 flow rate ratio was selected as it exhibited good PDI values, as well as a narrow size distribution with an anionic zeta potential while retaining favourable levels of organic solvent within the formulation post production (25%). As previously shown (Figure 2.5), initial lipid concentration can impact upon physicochemical attributes of the formulation, therefore a range of concentrations for formulation DSPC:Chol:PS (10:5:4 w/w) were assessed. Across the concentration ranges tested, no statistically significant differences in terms of vesicle size could be found, apart from the lowest concentration used (0.3 mg/mL), where vesicle sizes were significantly larger than any

other concentrations tested ($p < 0.05$) (Figure 2.10). All PDI values across 0.6 – 10 mg/mL were found to be homogeneous (PDI values < 0.29); however, the lowest concentration tested resulted in a slight increase in PDI (0.3) (Figure 2.10). Concentrations between 3-10 mg/mL were found to have the highest particle homogeneity, statistically significant from all other concentrations tested (< 0.2) ($p < 0.05$). All zeta potentials for all concentrations (0.3 -10 mg/mL) were between -28 – -35 mV (data not shown).

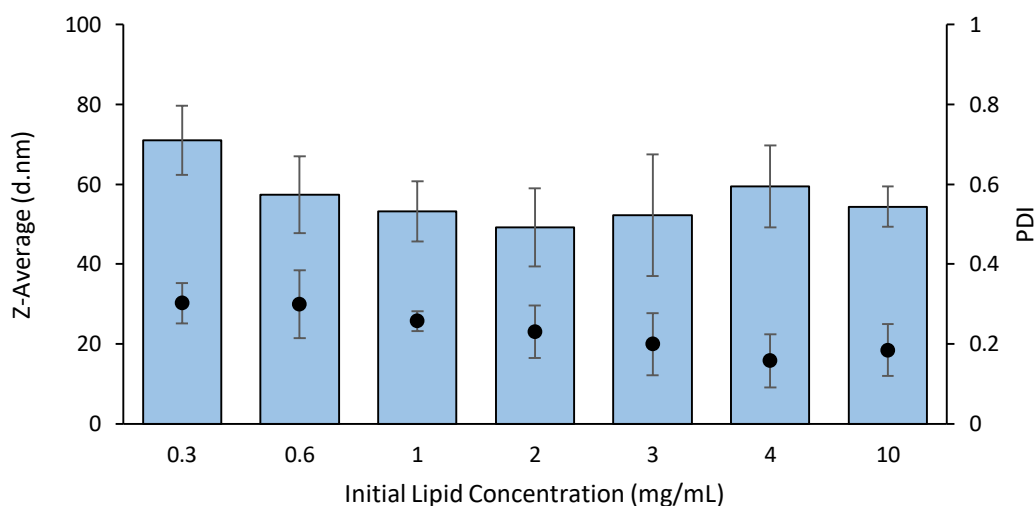


Figure 2.10. Liposomal formulation DSPC:Chol:PS (10:5:4 w/w) in methanol, effect of initial total lipid concentration on physicochemical attributes: size (columns) and PDI (circles). Microfluidic parameters selected were flow rate ratio 3:1 and a total flow rate of 10 mL/min. Solvent purification was conducted by dialysis. Results represent mean \pm SD, $n = 3$ of independent batches.

The inclusion of anionic lipid PS within DSPC:Chol when manufacturing through microfluidics was found to be most optimal for flow rate ratio 3:1, where comparably improved reproducibility was observed in terms of vesicle size, regardless of the quantities of PS added. Concentration ranges between 3 - 10 mg/mL were found to result in acceptable quality attributes (PDI < 0.2), with anionic zeta potentials (between -30 – -35 mV). This 3:1 flow rate ratio was also chosen by Khadke et al when manufacturing DSPC:Chol:PS (6:4:2.5 μ moles) by microfluidics with a staggered herringbone micromixer. While the vesicles were encapsulating H56 antigen, the PDI values for this formulation were found to be highly homogenous (< 0.15) (Khadke et al., 2019). When incorporating increasing levels of PS (0,6,12 and 37 mol%) within DSPC:cholesterol:PEG2000-DSPE liposomes, Geelen et al found a slight trend towards decreasing vesicle size. From 136 ± 3 nm (0%), 120 ± 7 nm (6%), 111 ± 10 nm (12%) to 97 ± 4 nm (37%). The PDI of the formulations remained below 0.3. While this manufacturing process is not entirely comparable to microfluidics (Geelen et al used lipid film hydration), and low levels of DSPE-PEG2000 were included, the data still exhibits the ability of homogenous vesicles to form with high quantities of PS within the bilayer (Geelen et al., 2012).

The studies conducted within this chapter involved the use of naturally occurring brain PS (porcine), which is a natural mixture of varying lipids with altered fatty acid distribution. Typically these natural phospholipids are purified by solvent extraction and chromatographic based techniques and offer some disadvantages compared to synthetic lipids due to challenges with stability and the need for improved testing for biological contamination (Avanti Polar Lipids). Issues with brain PS stability as a result of oxidation and hydrolysis may result in the poor reproducibility observed in Figure 2.9, indicated by the large error bars. Therefore, as an alternative, a synthetic brain PS counterpart was acquired, DOPS (1,2-dioleoyl-sn-glycero-3-phospho-L-serine) and assessed for its applicability as a synthetic substitute for brain PS during microfluidic manufacture.

Figure 2.11 shows a comparative study between lipid formulation DSPC:Chol containing either naturally occurring brain PS or DOPS at a weight to weight ratio of 10:5:4 to DSPC:Chol:PS/DOPS respectively. The initial total lipid concentration was incrementally increased between 0.3 to 4 mg/mL and particle size, PDI and zeta potential were measured to observe the physicochemical characteristics between naturally occurring PS and the synthetic DOPS following microfluidic production (3:1 FRR, 10 mL/min TFR) and dialysis for solvent removal. At the lowest total lipid concentration observed, there was no significant differences between the two formulations with naturally derived PS and synthetic DOPS both resulting in average particle sizes of 70 nm. As the initial total lipid concentration was increased, the PS formulation particle size generally decreased within a range between approximately 50 nm, while the DOPS formulation showed a gradual decrease in particle size until reaching 50 nm. At the final concentration tested (4 mg/mL), there was no significant difference between the particle size of both formulations (50 nm and 52 nm for DOPS and PS formulations respectively) ($p > 0.05$). Figure 2.11A additionally shows the PDI of the same formulations. As initial total lipid concentration is increased, a general trend in decreasing PDI can be observed. At the lowest concentration measured (0.3 mg/mL) PDI was measured at 0.24 and 0.29 for DOPS and PS formulations respectively. The general trend for both formulations shows a decrease in PDI as initial total lipid concentration is increased, however the rate of the decrease for DOPS formulation is much greater than that of the PS formulation. At the final concentration measured (4 mg/mL), DOPS formulation PDI was measured at 0.07, while the PS formulation showed a PDI of 0.22. In the case of the zeta potential of the different formulations, all values were found to be between -28 to -38 mV, with no significant differences found between PS and DOPS formulations at each concentration tested (Figure 2.11B).

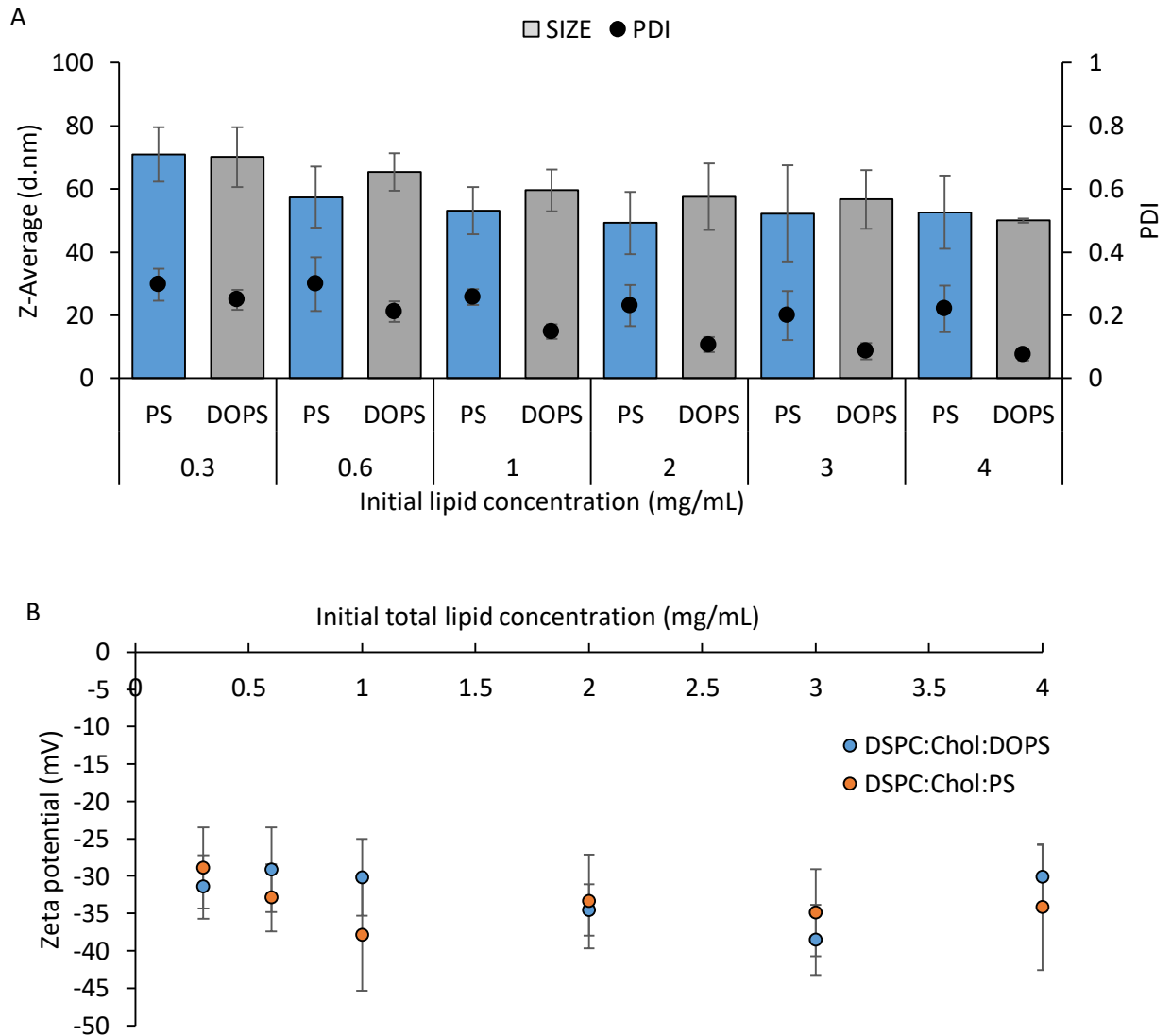


Figure 2.11. Liposomal bridging study for phosphatidylserine. Formulation DSPC:Chol:PS (10:5:4 w/w) and DSPC:Chol:DOPS (10:5:4 w/w) in methanol at a range of initial total lipid concentrations were compared for physicochemical attributes: size (columns) and PDI (circles) (A) and Zeta Potential (mV) (B). Microfluidic parameters selected were flow rate ratio 3:1 and a total flow rate of 10 mL/min. Solvent purification was conducted by dialysis. Results represent mean \pm SD, $n = 3$ of independent batches.

This bridging study was conducted in order to verify the applicability of a synthetic substitute for the naturally occurring brain PS. Across all lipid concentrations tested, the use of DOPS showed no statistically significant differences in terms of vesicle size and zeta potential when compared to the naturally occurring brain PS. When a concentration of DSPC:Chol:DOPS (10:5:4 w/w) at 4 mg/mL was used, highly reproducible particle attributes were obtained, with improved PDI values compared to the brain PS (PDI < 0.1). These results were expected since the synthetic PS lipid has a defined chemical structure and therefore a fixed transition temperature (-11°C). However, the naturally occurring brain

PS is a mixture of components and therefore, it has a range of transition temperatures (based upon the range of fatty acid distributions)(Avanti Polar Lipids). Thus, the DOPS liposome formulations result in more homogeneous size populations when compared to PS liposomes.

2.5.5.2 The effect of cationic lipid addition to DSPC:Chol formulation

It is now evident that the microfluidic parameter flow rate ratio has an impact upon vesicle characteristics for both neutral and anionic formulations (Figure 2.6 and 2.9). To further explore the effects of including charged lipids during microfluidic manufacture, addition of the cationic lipid DOTAP was investigated. This lipid was chosen due to its ease of availability and its extensive use in both *in vitro* and *in vivo* applications (Simberg et al., 2004). DOTAP was added alongside DSPC:Chol in the same manner as PS, with incremental increases of DOTAP and a fixed initial lipid concentration of 4 mg/mL. Three flow rate ratios were initially explored, with preliminary results indicating that flow rate ratios 3 and 5:1 resulted in highly heterogeneous populations (PDI > 0.6, data not shown), therefore further studies at the ratios were not carried out. For flow rate ratio 1:1, as DOTAP was added, a general trend of increasing vesicle size could be observed (approximately 62 nm – 86 nm), as well as an increase in PDI (0.07 – 0.32) (Figure 2.12A). In the case of zeta potential of the formulations, an increase was observed as more DOTAP was included within the formulation (26 mV – 58 mV), until a plateau was reached at 60 mV, where there were no further increases observed (Figure 2.12B).

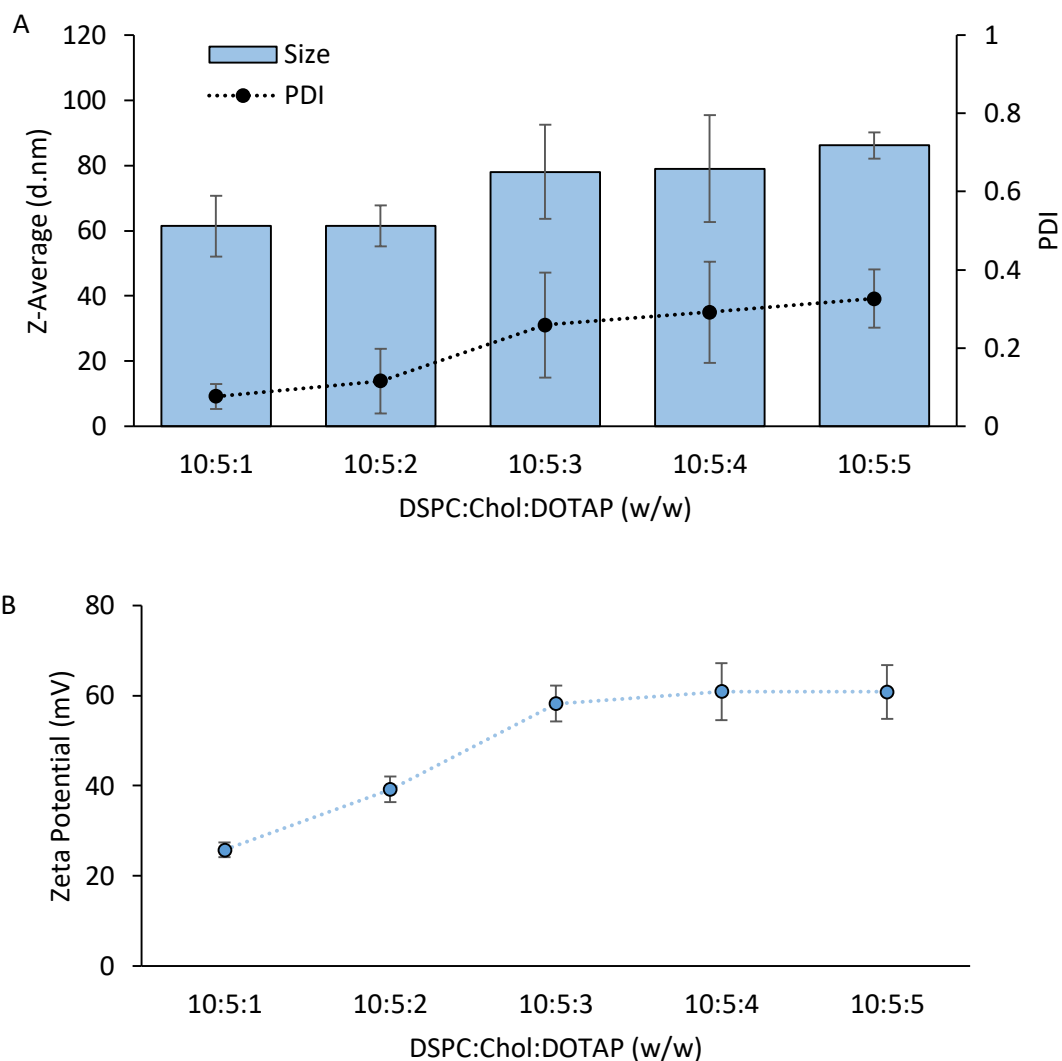


Figure 2.12. The effect of adding DOTAP incrementally to the liposomal formulation DSPC:Chol, liposome size (bar) and PDI (circles) (A) and Zeta Potential (mV) (B) for flow rate ratio 1:1. Initial total lipid concentration was fixed at 4 mg/mL while purification was conducted by dialysis. Results represent mean \pm SD, n =3 of independent batches.

Following on from preliminary optimisation studies, a weight to weight ratio of 10:5:4 was chosen along with a microfluidic manufacturing flow rate ratio of 1:1 for further formulation optimisation. Again, studies focused on the effect of initial lipid concentration where a general trend of decreasing vesicle size was found as lipid concentration was increased. The reproducibility of the formulation was also related to the concentration used, with larger error bars occurring at low concentrations. The population homogeneity however was largely unaffected, with most values found below 0.31 PDI (with the exception of the highest concentration used, 10 mg/mL) (Figure 2.13).

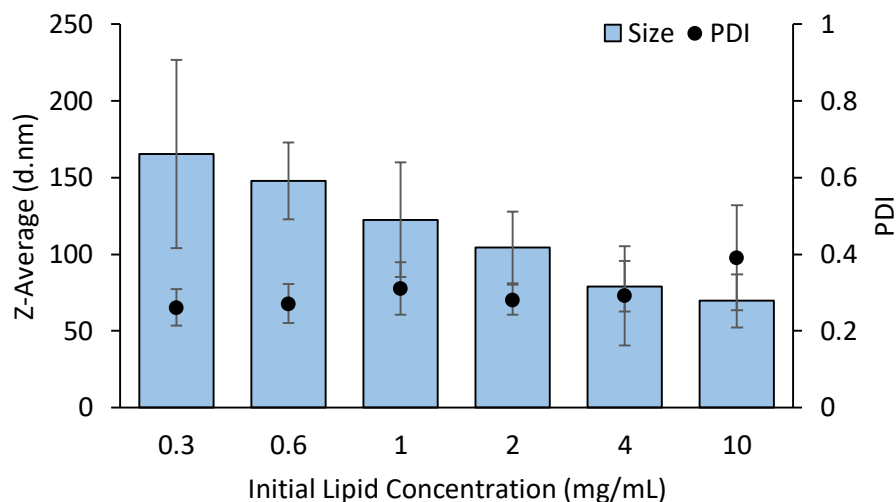


Figure 2.13. The effect of initial lipid concentration on cationic liposomal formulation DSPC:Chol:DOTAP (10:5:4 w/w) liposome size (bar) and PDI (circles) for flow rate ratio 1:1, total flow rate 10 mL/min. Purification was conducted using dialysis. Results represent mean \pm SD, n =3 of independent batches.

Cationic liposomes have been widely researched in relation to their potential as vaccine adjuvants (Christensen et al., 2011). Through the inclusion of charged lipids such as 3-beta-[N-(N',N'-dimethylaminoethane)-carbamoyl] cholesterol (DC-Chol) or 1,2-dioleoyl-3-trimethylammonium-propane (DOTAP), a positively charged liposome can effectively bind to the negatively charged membranes of cells as well as provide high encapsulation/association of negatively charged therapeutics such as siRNA or proteins (Petrilli et al., 2016). The inclusion of DOTAP into liposomes has been shown *in vitro* to stimulate DC maturation markers CD40, CD80 and CD86, while the substitution of the cationic lipid with a neutral phospholipid dioleoyl phosphatidyl ethanolamine (DOPE) resulted in a loss of maturation response (Soema et al., 2015). As well as indicating signs of innate immunity stimulation, DOTAP liposomes have shown promise generating both CD4⁺ and CD8⁺ T cell responses in mice when prepared by microfluidics, attributed by the authors to the small vesicle sizes (< 100 nm) obtained during this manufacturing method (Haseda et al., 2020). As a result of this relationship between vesicle size and charge and the resultant immunological profile, it is therefore crucial that operating parameters that are influential on vesicle characteristics are identified for cationic formulations. Investigation by Elsana et al using various DOTAP based liposomal formulations prepared by both lipid-film hydration and microfluidics found comparable results in relation to the effect of microfluidic operating parameters on liposomal vesicle size, where adjusting the flow rate ratio across 1,3 and 5:1 resulted in significant differences in vesicle size (Elsana et al., 2019). Furthermore, the use of flow rate ratio 1:1 for cationic formulation DOPE:DOTAP has been shown to generate particles below 100 nm with PDI values < 0.25 in TRIS buffer (100 mM) using a staggered herringbone micromixer chip (Lou et al., 2019). Conversely, microfluidic manufacture of cationic

adjuvant formulation DDA:TDB has been shown to be unsuitable using a 1:1 flow rate ratio with IPA. The formulation resulted in micron scale vesicles with poor homogeneity (>0.7) when manufactured at 1:1, however both 3 and 5:1 flow rate ratios resulted in nanoscale vesicles with improved PDI (<0.4) (Roces et al., 2019). The effect flow rate ratio has on cationic formulations is therefore substantial. However, it appears that specific formulations will require optimisation in order to determine the appropriate processing parameters. Therefore, as a result of the formulation optimisation conducted, normal operating parameters for liposomal formulation DSPC:Chol:DOTAP (10:5:4 w/w) were selected as 1:1 FRR, 4 mg/mL initial total lipid based on vesicle size (<100 nm), population homogeneity (< 0.3 PDI) and positive zeta potential (approximately 50 – 60 mV).

2.5.6 Down-stream processing: Formulation purification

Unlike the top-down approach to liposome production, one drawback for a bottom-up microfluidic approach is the residual solvent within the sample post production. During lipid-film hydration, solvent is evaporated off prior to hydration, however during microfluidic production, the solvent remains within the liposome suspension post manufacture. This results in the need for a solvent removal step post production. There are a number of options available in regards to solvent purification for liposomal samples such as dialysis and gel filtration columns. However, purification methods such as these are time-consuming techniques that are problematic for large scale manufacturing. For up-scale manufacturing of liposomes, solvent purification techniques must be employed which can deal with large volumes of sample and reliably produce consistent product. For up-scale liposome production, microfluidic systems can be connected to a cross-flow filtration system for large scale volumes of sample. Tangential Flow Filtration (TFF) is a process which utilises specific pore-sized membranes to remove salts or solvents from solutions and separate particulates based on size discrepancy principles. Unlike direct flow filtration, the solution stream is passed parallel to the membrane surface, where the permeate is filtered off, while the remainder of the product (in our case our liposome vesicles) is circulated and retained within the system.

In order to determine the suitability of these techniques for solvent purification, a range of liposomal formulations (neutral, anionic and cationic) were prepared by microfluidics, purified using either dialysis, gel filtration or TFF and then analysed for physicochemical attributes (Figure 2.14). For neutral formulation DSPC:Chol (10:5 w/w), dialysis and TFF showed no statistically significant differences in both vesicle size and PDI when compared to the vesicles manufactured by microfluidics ($p>0.05$). However, the use of the sephadex column for solvent purification resulted in an increase in both vesicle size and PDI (from approximately 54 nm, 0.14 PDI to 76 nm 0.25 PDI) ($p < 0.05$). When analysing

anionic formulation DSPC:Chol:PS (10:5:4 w/w), no substantial differences were observed in terms of vesicle size when comparing each technique to pre-purification vesicles, with all of the Z-average values between 44 – 59 nm. Cationic formulation DSPC:Chol:DOTAP showed no change following purification by dialysis, however this formulation could not be purified by sephadex column or TFF, due to column incompatibility with positively charged vesicles (as a result of the slightly negatively charged TFF column membrane) (Figure 2.14A). For both anionic and neutral formulations, the recovery post purification using dialysis was > 89%, while gel filtration recovery was found to be more inconsistent, with an average recovery greater than 83%. In the case of tangential flow filtration, high recovery was observed for both formulations tested (> 96%) (Figure 2.14B). Additionally, concentration of liposomal sample DSPC:Chol:PS (10:5:4 w/w) can be achieved using TFF (Figure 2.15) without negatively impacting upon vesicle size and PDI (56 – 63 nm, PDI approximately 0.24) up to a 4-fold concentration of sample.

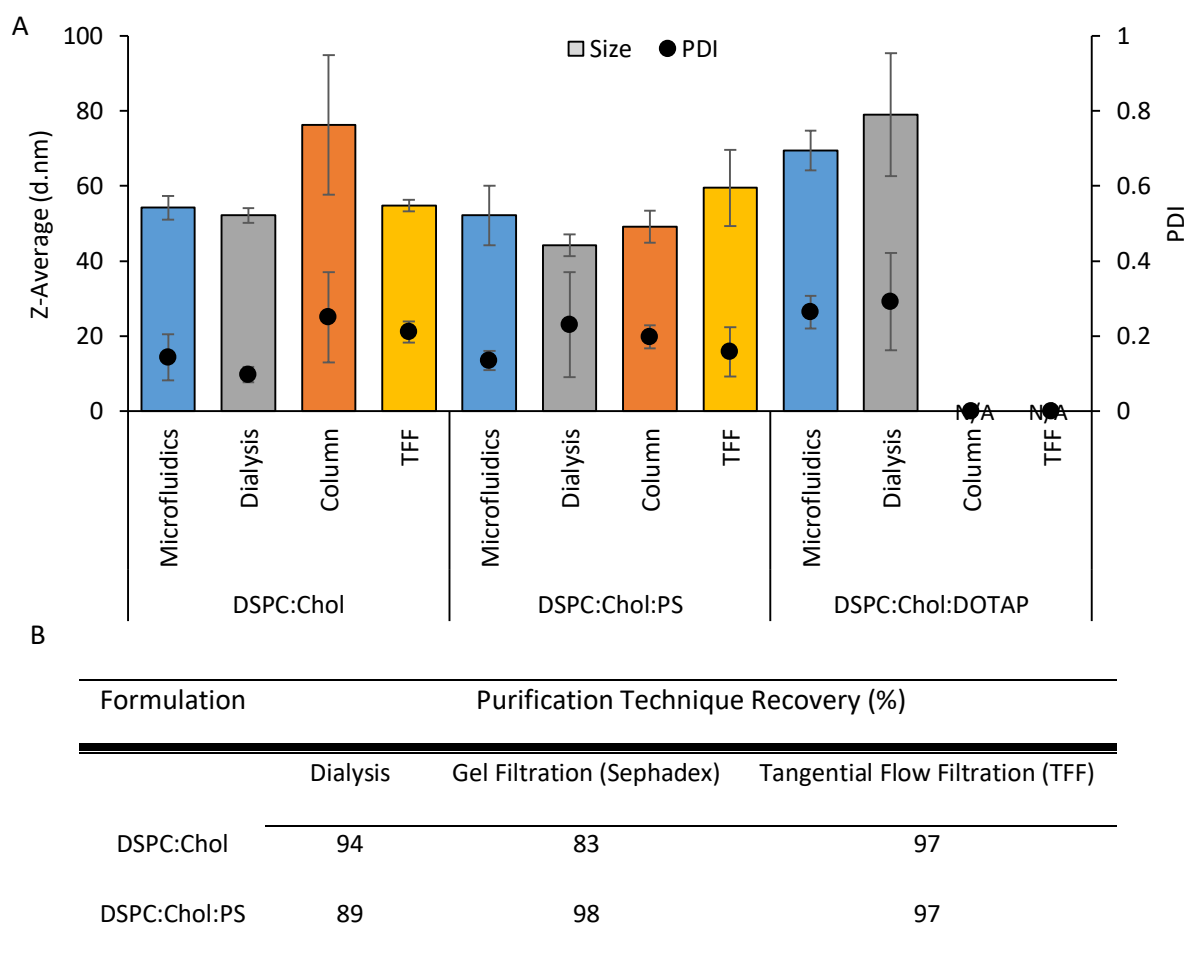


Figure 2.14. (A) The effect of the choice of purification method applied to liposomal formulations manufactured by microfluidics. The liposome size (bar) and PDI (circles) are shown for liposomal formulations DSPC:Chol (10:5 w/w), DSPC:Chol:PS (10:5:4 w/w) and DSPC:Chol:DOTAP (10:5:4 w/w) after microfluidics, dialysis, Sephadex column and tangential flow filtration. (B) Recovery rate (%) measured by Dil of liposomal formulations DSPC:Chol (10:5 w/w) and DSPC:Chol:PS (10:5:4 w/w) manufactured by microfluidics and subsequently purified by dialysis, sephadex column or tangential flow filtration. Results represent mean \pm SD, n = 3 of independent batches.

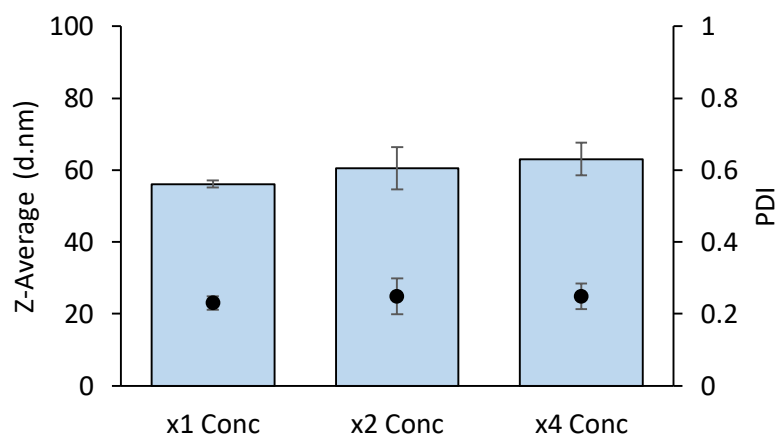


Fig 2.15. Concentration of liposomal formulation DSPC:Chol:PS (10:5:4 w/w) using tangential flow filtration. The liposomes were prepared at 4 mg/mL initial lipid concentration, 3:1 FRR, 10 mL/min TFR following microfluidics, followed by 1,2 and 4-fold concentration steps. Particle Size (Z-Avg; represented by bars) and PDI (represented by discrete points). Results represent mean \pm SD, n = 3 of independent batches.

To confirm removal of residual solvent following microfluidic manufacture, gas chromatography was conducted on samples post TFF and dialysis. The European Medicines Agency issues acceptable residual solvent levels based on the guidelines proposed by the International Council for Harmonisation of Technical Requirements for Pharmaceuticals for Human Use (ICH Q3C). Acceptable residual methanol levels are proposed to be 3000 ppm and below, and this cut off is compared to both TFF and dialysis residual methanol levels following a specified protocol (20 mL of wash cycles for TFF, 1 mL sample to 200 mL buffer for 1 hour under agitation for dialysis) (Figure 2.16). The results show that while 20 diafiltrate volumes during TFF purification is capable of reducing residual methanol levels well below ICH guidelines (< 0.05%), larger buffer volume than 200 mL may be required in order to reduce dialysis residual methanol levels below 0.3% v/v (3000 ppm).

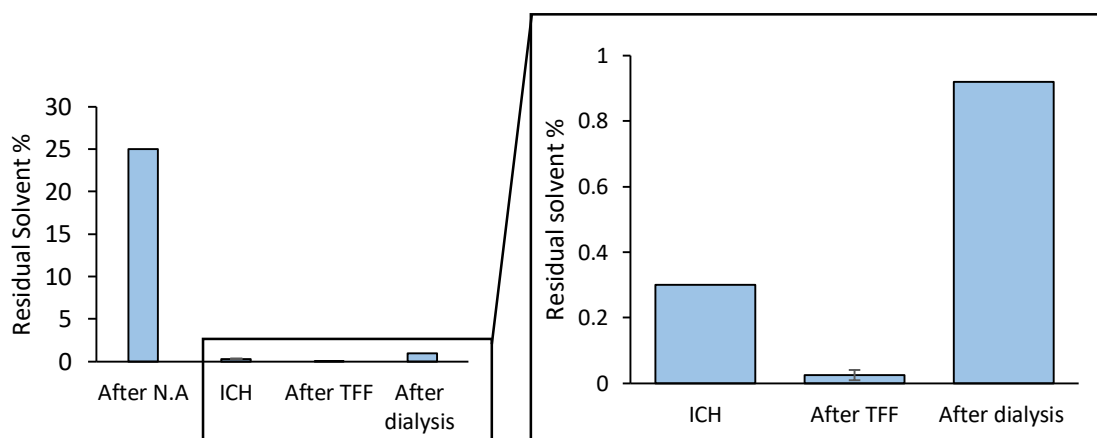


Figure 2.16. Residual solvent post TFF or dialysis for liposomal formulation DSPC:Chol (10:5 w/w) initial lipid concentration 4 mg/mL, prepared at a flow rate ratio of 3:1 and 10 mL/min TFR, compared to the ICH guideline benchmark for residual methanol. Results in collaboration with Pierce Lyons, at the University of Strathclyde. Results represent mean \pm SD, n =3 of independent batches.

Purification techniques such as sephadex size exclusion columns and dialysis can be well suited to lab scale purification of liposomes (Rashidinejad et al., 2014). Size exclusion columns (gel filtration) can separate small molecules from liposomes, although correct optimisation must be conducted in order to establish the elution volumes of the components or risk overlapping elution peaks, leading to incorrect purification (Grabielle-Mad尔蒙t et al., 2003) Liposome samples with different sizes would require further optimisation, as liposome size impacts upon elution time (Vemuri and Rhodes, 1994). The data indicated here shows while liposomes can be purified following size exclusion, there were issues associated with reproducibility in terms of vesicle physicochemical attributes and recovery rates for liposomal formulation DSPC:Chol, which partly could be attributed to the variation in column packing when preparing the sephadex G75. Furthermore, findings by Ruyschaert et al showed some liposome retention during purification, however the retention was only transitory and full liposome recovery could be achieved by further washing and column repacking/depacking cycles (Ruyschaert et al., 2005). Therefore, inadequacies in product purification consistency, as well as the issue of sample dilution when using excess buffer for washing, could pose major challenges for large scale liposome purification using gel filtration (Lin and Qi, 2018). Dialysis can be used to separate molecules of different molecular weights by employing a dialysis bag with a pore size suitable enough to retain vesicles and allow the free movement of smaller molecules for sample purification (Lin and Qi, 2018). The results shown within this chapter indicate this technique is suitable for liposome purification, with no significant differences occurring in the physicochemical attributes of the vesicles before and after purification. While methanol values were shown to be reduced below 1%, further reduction beyond ICH guidelines would require the addition of a slightly larger buffer volume or increased duration. Dialysis is a cost-effective technique, which can be used effectively in the lab scale environment, however translation of this technique to large scale production is not practical.

Tangential flow filtration is a well-established purification technique already applied throughout the food, biotechnology and pharmaceutical industry's to remove contaminants, improve quality and concentrate product (Musumeci et al., 2018). By continuous addition of buffer known as the "feed", washing of the sample occurs, with molecules above the molecular weight cut off of the column recirculating through the system – known as the "retentate", while smaller molecules flow freely through the membrane and are washed out as "permeate". As buffer is introduced at the same rate as leaving the system, over time the initial solvent concentrations are diluted out. Furthermore, sample concentration by tangential flow filtration during purification offers a potential solution to formulations which are limited by specific lipid solubility in solvents prior to microfluidic manufacture through concentration of low dose samples to required concentrations. The applicability of this

purification process shown here, combined with microfluidics, could improve the manufacturing and scalability prospects of liposomes.

2.5.7 Continuous at-line particle sizing

Using microfluidics as a high throughput production method, with a downstream purification system such as tangential flow filtration allows for an efficient manufacturing stream in contrast to bulky batch production. However, the ability to monitor critical quality attributes of the vesicles throughout the production/purification chain is essential in order to stop production and intervene if issues are detected with product quality. In order to determine whether this can be achieved in a liposome production chain, a real-time particle size monitor from Malvern (Zetasizer AT, Malvern Panalytical, UK) was investigated. The suitability of the system was compared to traditional off-line equipment (Zetasizer Nano ZS) for liposomal formulation DSPC:Chol (10:5 w/w) at two monitoring points: following microfluidic manufacture (post manufacture) and after solvent purification by TFF (post purification). The results indicate the ability of the at-line equipment to monitor vesicle size at both points (post manufacture and post purification), with no significant differences observed across at-line or off-line systems, indicating the potential to incorporate a rapid at-line particle size analysis tool into a continuous manufacturing chain for liposomal delivery systems (Figure 2.17).

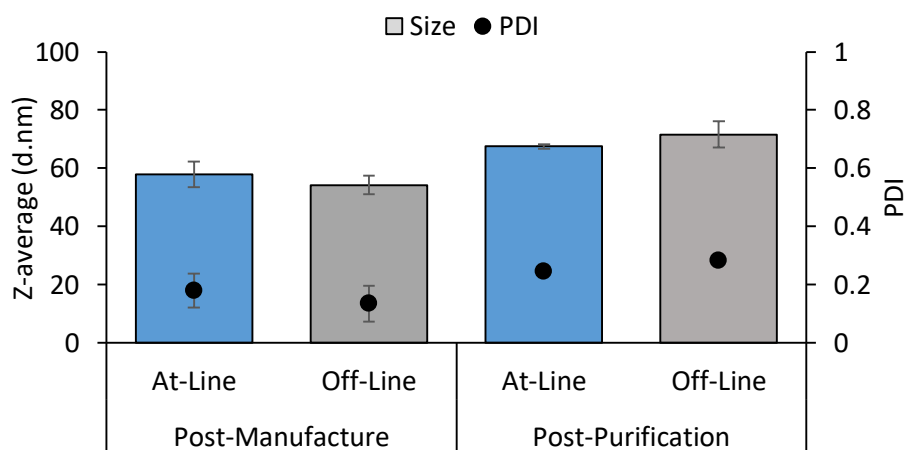


Figure 2.17. Size (bars) and PDI (circles) comparison for formulation DSPC:Chol (10:5 w/w) measured by two (At-line and Off-line) before and after purification by TFF. Results represent mean \pm SD, $n=3$.

The results indicate the ability of the at-line equipment to monitor vesicle size at both points (post manufacture, post purification), with no significant differences observed across at-line or off-line

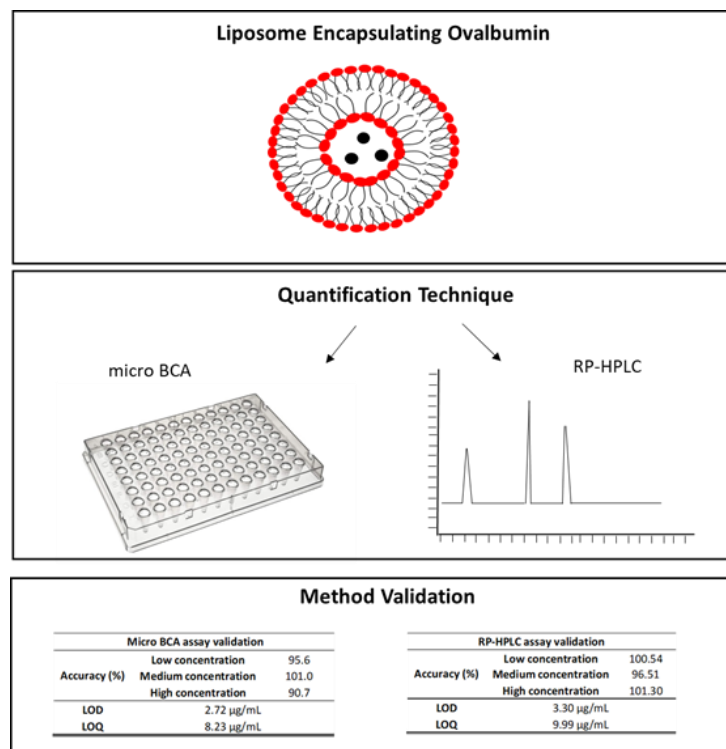
systems, indicating the potential to incorporate a rapid at-line particle size analysis tool into a continuous manufacturing chain for liposomal delivery systems (Figure 2.17).

2.6 Conclusions

The results within this chapter demonstrate the potential of microfluidics as a large scale manufacturing platform for liposome suspensions. A range of formulations were tested, and critical processing parameters were identified, including the impact of flow rate ratio and initial lipid concentration of the formulation. In the case of both neutral and anionic formulations DSPC:Chol (10:5 w/w) and DSPC:Chol:PS (10:5:4 w.w) manufacture at a flow rate ratio of 3:1 and initial concentrations above 2 mg/mL were identified as the most optimal based upon vesicle size and PDI values, while cationic formulation DSPC:Chol:DOTAP (10:5:4 w/w) was optimised for 1:1 FRR manufacture. The addition of tangential flow filtration as a down-stream purification system was shown to reduce residual solvent levels to below acceptable levels outlined by ICH guidelines, without impacting upon the vesicles physicochemical characteristics. Alongside the addition of at-line analytical tools such as dynamic light scattering, this setup demonstrates elements that can be adopted within a continuous manufacturing process for liposomes. Following on from this established work using empty liposomal formulations, the next step within the process was to determine the loading ability of these optimised formulations using model antigen ovalbumin.

Chapter 3

Method Validation for Protein Loading Quantification within liposomes



The work presented in this chapter has been published in:

HUSSAIN, M. T., FORBES, N. & PERRIE, Y. 2019. Comparative Analysis of Protein Quantification Methods for the Rapid Determination of Protein Loading in Liposomal Formulations. *Pharmaceutics*, 11, 39.

3.1 Introduction

Proteins have become increasing modalities as therapeutics for a wide range of diseases, with particular interest within the field of vaccine development (Carter, 2011, Leader et al., 2008). The immunogenicity of subunit antigens or highly purified protein recombinants as vaccine antigens can be enhanced with the inclusion of a suitable adjuvant. Furthermore, challenging routes of administration, such as oral or intranasal, may require a delivery system to enhance the stability of the subunit antigen in order to generate effective vaccine responses (Gupta et al., 2013). Liposomes have been thoroughly investigated as drug delivery platforms, improving stability, favourably altering biodistribution profiles of therapeutics and enhancing tissue and cellular uptake (Sercombe et al., 2015). The use of liposomal delivery systems as protein carriers offers flexibility in terms of how and where the protein is loaded – whether it is adsorbed onto the surface, or entrapped within the liposomal vesicles. These attributes have led to particular interest in the use of liposomes as vaccine carriers (Gregoriadis et al., 1999, Perrie et al., 2008, Perrie et al., 2017). Alongside advances in novel manufacturing techniques for liposomes such as microfluidics, a requirement for subsequent analytical techniques arises in order to rapidly quantify protein loading within liposomal delivery systems.

At present, there are a number of protein quantification techniques available for use to determine the loading efficiencies in drug delivery systems such as bicinchoninic acid assay (BCA), high-performance liquid based chromatography (HPLC) and the use of fluorescently / chemically / radio – labelled protein (Haidar et al., 2008, Huang et al., 2015, Li et al., 2011a, E Christine Lutsiak et al., 2002, Xu et al., 2012, Henriksen-Lacey et al., 2010b, Schiltz et al., 1977). Fluorescent based techniques employ the use of commercially available fluorescent molecules or by chemically conjugating fluorophores to proteins. The loading efficiencies of the protein can then be determined indirectly by measuring un-loaded protein fluorescence (Liau et al., 2015). However, fluorophores are often large molecules and the conjugation of these to proteins for quantification purposes could impact upon the solubility and structural folding of these molecules (Henriksen-Lacey et al., 2010a). The use of radioisotopes as a detection method for protein quantification can be used as an alternative, less invasive method. Henriksen-Lacey et al showed that quantification of antigen loading could be achieved using a tuberculosis antigen, Ag85B-ESAT-6 radiolabelled with ^{125}I (Henriksen-Lacey et al., 2010b). The BCA assay is a colorimetric based assay which is very common, simple to use and can be found within most laboratory settings (Krieg et al., 2005). The working solution depends upon colorimetric change, caused at first by the reduction of Cu^{2+} to Cu^{+} at a rate proportional to the amount of protein present. The Cu^{+} ions then bind two molecules of bicinchoninic acid, resulting in a colour change which can be measured through the adsorption of light at 562 nm. This two-step reaction establishes a direct

correlation between protein concentration and measureable colour change that can be conducted in a microplate, allowing for large scale screening (Walker, 1996). However, limitations of the assay include distinct protein concentration limits and the possibility of interference from other agents present in the sample such as lipids. Unlike colorimetric based assays (like the BCA assay), reverse phase high performance chromatography (RP-HPLC) involves the separation of molecules based upon hydrophobicity. In reverse-phase chromatography, the stationary phase is hydrophobic, and elution of analytes occurs as the gradient of organic solvent increases over time (Aguilar, 2004). The use of RP-HPLC is a commonly adopted method for protein and peptide analysis due to its high selectivity and reproducibility (Kanie et al., 2008, Josic and Kovac, 2010).

However, liposome loading using these methods tends to be achieved through quantification of free protein within the supernatant of the liposomes following separation by centrifugation; yet, this assumes that any protein not in the supernatant must be associated with the liposomes. Therefore, there is still a need to validate entrapment of protein within the liposomes, as opposed to the traditional, indirect approach. Furthermore, there is a need for a quantification technique that is rapid, which can be used to support formulation development and support large-scale protein loaded liposomal delivery system manufacture. In order to achieve this, two techniques (BCA and RP-HPLC) were compared to directly quantify encapsulated protein within liposomal vesicles.

3.2 Aim and Objectives

The aim of the work within this chapter was to develop a method to quantify protein loading within liposomes. To achieve this two protein quantification methods (BCA and RP-HPLC) were investigated and validated. Method validation was conducted following ICH guidelines for both assays in a systematic tiered approach. To achieve this, the objectives of this work were:

1. Compare the impact of liposome inclusion on protein quantification using BCA and HPLC.
2. Assessing the effect of the presence of liposomal formulations and concentrations on interference using BCA assay.
3. Comparing the impact of solubilisation mixture on protein quantification using BCA and HPLC.
4. Determine the suitability of the techniques to quantify protein loading for neutral, anionic and cationic liposomal formulations.

3.3 Materials

The lipids 1,2-distearoyl-sn-glycero-3-phosphocholine (DSPC), 1,2-dioleoyl-3-trimethylammonium-propane (DOTAP) and L- α -phosphatidylserine (Brain PS, Porcine) were all purchased from Avanti Polar Lipids Inc., Alabaster, AL, US. Cholesterol (cholesterol), Ovalbumin (OVA), trifluoroacetic acid and D9777-100ft dialysis tubing cellulose were purchased from Sigma Aldrich Company Ltd., Poole, UK. A Jupiter column (C18 (300 Å), 5 μ m, dimensions 4.60 \times 150 mm pore size 100 Å) was used for HPLC analysis, purchased from Phenomenex., Macclesfield, UK. The Pierce™ micro BCA Protein Assay kit, HPLC grade methanol and 2-propanol (IPA) were purchased from Fisher Scientific, Loughborough, England, UK. All water and solvents used were HPLC grade.

3.4 Methods

3.4.1 Protein quantification techniques

3.4.1.1 Micro BCA protein assay kit

Protein quantification using Micro BCA (Pierce™ BCA Protein Assay Kit, Sigma Aldrich, Poole, UK) was carried out under manufacturer's instructions. Briefly, samples were incubated up to 2 hours at 35°C, with 150 μ L of sample required (150 μ L) + 150 μ L of the working reagent (25:24:1 of reagent A, B and C respectively). Calibration curves were kept as similar to the sample as possible, with the concentration of all components (such as lipid and buffer concentration) matched to the sample concentration and appropriate blanks were subtracted. Absorbance was then measured at 562 nm using a Bio-rad 680 microplate reader.

3.4.1.2 Reversed-phase high performance chromatography (RP-HPLC)

To quantify the amount of model antigen ovalbumin on a Hewlett Packard 1100 series (California, USA), a Jupiter 5 μ C18 column with security guard, pore size 300A from Phenomenex (Macclesfield, UK) was used. The selected HPLC method was: Mobile Phase A (0.1% TFA in distilled water) B (0.1% TFA in Methanol); with a gradient flow for a total run time of 25 minutes. Initially, A:B mix of 95:5 was used, increasing to 5:95 (A:B) by minute 10. This was maintained for a following 5 minutes, before a return to 95:5 (A:B) by minute 20. UV detection was conducted at 210 nm, with a column temperature of 25°C and a flow rate of 1 mL/min, injection volume of 50 μ L.

3.4.2 Liposome production

The preparation of liposomes by microfluidics was conducted on the Nanoassembly Platform (Precision Nanosystems Inc., Vancouver, Canada). Selected lipids were dissolved in methanol (solvent phase) at specific concentrations and injected through one of the two inlets on the microfluidics staggered herringbone micromixer cartridge, whilst the aqueous phase (PBS; pH 7.3 ± 0.2 or TRIS; 10 mM pH 7.4) is injected into the second inlet. A flow rate ratio (FRR) of 3:1 was selected for neutral and anionic liposomal formulations, while 1:1 FRR was selected for cationic formulations as previously optimised. Total flow rates (TFR) between 10 -15 mL/min were selected.

3.4.3. Liposome purification

Following microfluidic production, purification of solvent from the sample is required. For “empty” liposomes, dialysis was conducted using Mw 14,000 Da membrane where the sample is loaded and sealed, before being submerged in 200 mL of equivalent buffer. The dialysis duration is 1 hour at room temperature under gentle agitation via magnetic stirring. Dialysis membrane (14,000 MWC) was pre-treated in a solution of 2% sodium bicarbonate, 1 mM EDTA and 1 litre of ultrapure water at 80°C for 2 hours under magnetic stirring. The membrane was then rinsed with water to remove any trace of pre-treated solution and stored in 20% EtOH. For purification of ovalbumin loaded liposomes, samples were purified using Krosflo Research Iii tangential flow filtration system fitted with an mPES (modified polyethersulfone) column with a pore size of 750 kDa to support effective separation of the protein (OVA; 45 kDa) and the liposomes. Liposomal samples were circulated through the column and purified through difiltration, with fresh PBS being added at the same rate as the permeate leaving the column.

3.4.4 Method validation

Method validation for the techniques was assessed under a number of select criteria; linearity, limit of detection (LOD), limit of quantification (LOQ), precision and accuracy.

3.4.4.1 Linearity

Calibration curves were designed across a concentration range of 0.5 – 40 µg/mL using 9 different concentrations. The signal output (area (mV) and absorbance for HPLC and BCA respectively), was plotted against known concentrations to determine the equation of the straight line and regression coefficient (R^2).

3.4.4.2 Limit of Detection and Limit of Quantification

Limit of detection (LOD) and limit of quantification (LOQ) were calculated using the following equations (Equation 3.1 and 3.2). The standard deviation of the response (σ), divided by the gradient of the slope, multiplied by 3.3 or 10 (LOD and LOQ respectively).

$$LOD = \left(3.3 * \left(\frac{\sigma}{S} \right) \right) \quad \text{Equation 3.1}$$

$$LOQ = \left(10 * \left(\frac{\sigma}{S} \right) \right) \quad \text{Equation 3.2}$$

3.4.4.3 Accuracy, Repeatability and Precision

Accuracy was calculated using the difference between theoretical and experimental values, taken at 3 separate concentrations across the assay in triplicate using a low, medium and high concentration value (Equation 3.3) (Umrethia et al., 2010). The accuracy is reported as the difference between the mean and the accepted true value together (Guideline, 2005).

$$Accuracy (\%) = \frac{(True Value - measured value) * 100}{True Value} \quad \text{Equation 3.3}$$

The determination of Precision during method validation can be summarised into two levels: Repeatability and Intermediate Precision. Repeatability examines how close a set of results are that have been generated in a short period of time, while intermediate precision requires a larger sample mean as well as an external variation such as days or analysts (Guideline, 2005).

Repeatability tests were conducted to examine intra-day precision for across three concentrations (low, medium and high) (Equation 3.4) (Guideline, 2005) .

$$Repeatability (\%) = \left(\frac{Std}{mean} \right) * 100\% \quad \text{Equation 3.4}$$

While precision (Intermediate) tests were conducted for inter-day analysis. Precision was calculated covering three concentrations in triplicate over 3 days (RP-HPLC) or 5 days (micro BCA) using the following equation (Equation 3.5).

$$Precision (\%) = \left(\frac{Std}{mean} \right) * 100\% \quad \text{Equation 3.5}$$

3.5 Results and Discussion

3.5.1 Quantification of ovalbumin to determine linearity

To assess the ability of both the micro BCA and RP-HPLC to quantify protein loading, the model antigen ovalbumin was chosen. Initially, calibration curves were designed using ovalbumin solubilised in water at protein concentration ranges between 0.5 – 40 µg/mL in order to determine linearity. Calibration curves were initially generated by micro BCA to establish detection and quantification limits for ovalbumin solubilised in water, with intra-day repeatability generating three separate curves within the same day (Figure 3.1A). For inter-day precision, five calibration curves were developed over five separate days (Figure 3.1B). Intra-day repeatability and inter-day precision were calculated using the %RSD (Figure 3.1C and D respectively), across three concentrations, with all values falling within the accepted criteria range of $\pm 5\%$, as well as the R^2 values of all calibration curves being > 0.99 . LOD and LOQ values of 1.85 µg/mL and 5.61 µg/mL respectively were calculated by the average of the previous curves (Figure 3.1E), as well as accuracy of the assay over three concentrations (a low, medium and high value) as per ICH guidelines. All calculated accuracy measurements fell within the accepted range (95-105%) (Figure 3.1F).

Following micro BCA analysis of ovalbumin in water, protein quantification was also measured using RP-HPLC using a gradient method across the same protein range (0.5 – 40 µg/mL). Linear relationships were observed ($R^2 > 0.99$) for both intra-day (Figure 3.2A) and inter-day (Figure 3.2B). Intra-day and inter-day precision presents %RSD values that again fall within the acceptable limits (within $\pm 5\%$) (Figure 3.2C, D). Using the average of the previous curves (Figure 3.2E), LOD and LOQ values were calculated at 2.41 and 7.31 µg/mL respectively, as well as accuracy values at all three concentrations tested again falling within the criteria range (95 – 105%) (Figure 3.2F).

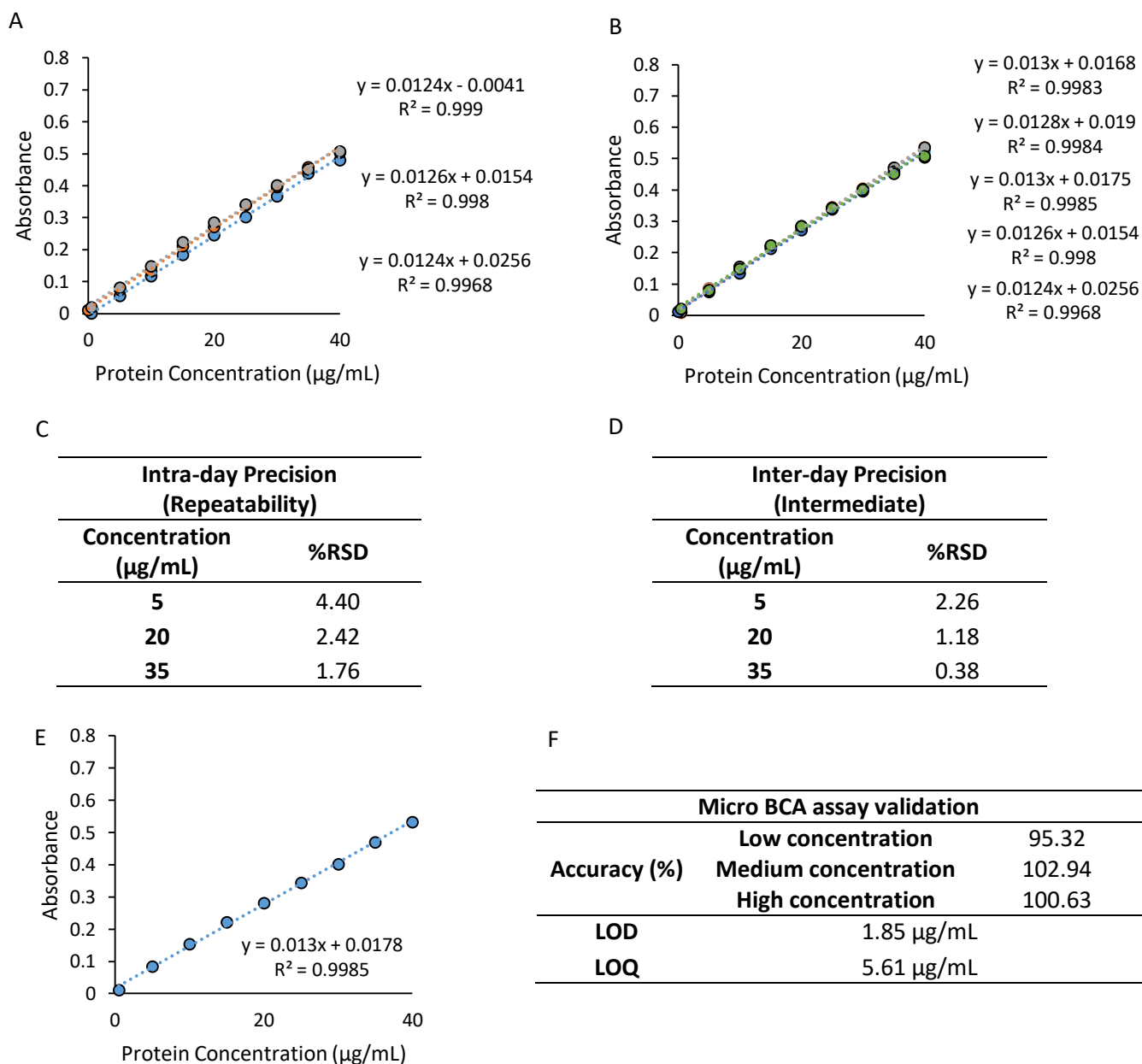


Figure 3.1 The calibration curves for micro BCA with ovalbumin in water: Intra-day curves (A), Inter-day curves (generated over 5 separate days) (B). Intra-day (C) and inter-day (D) precision were calculated across three different concentrations with %RSD shown. Finally, using the average curve (E), accuracy, LOD and LOQ values were determined (F). Results represent mean \pm SD, of at least $n = 3$ of independent batches.

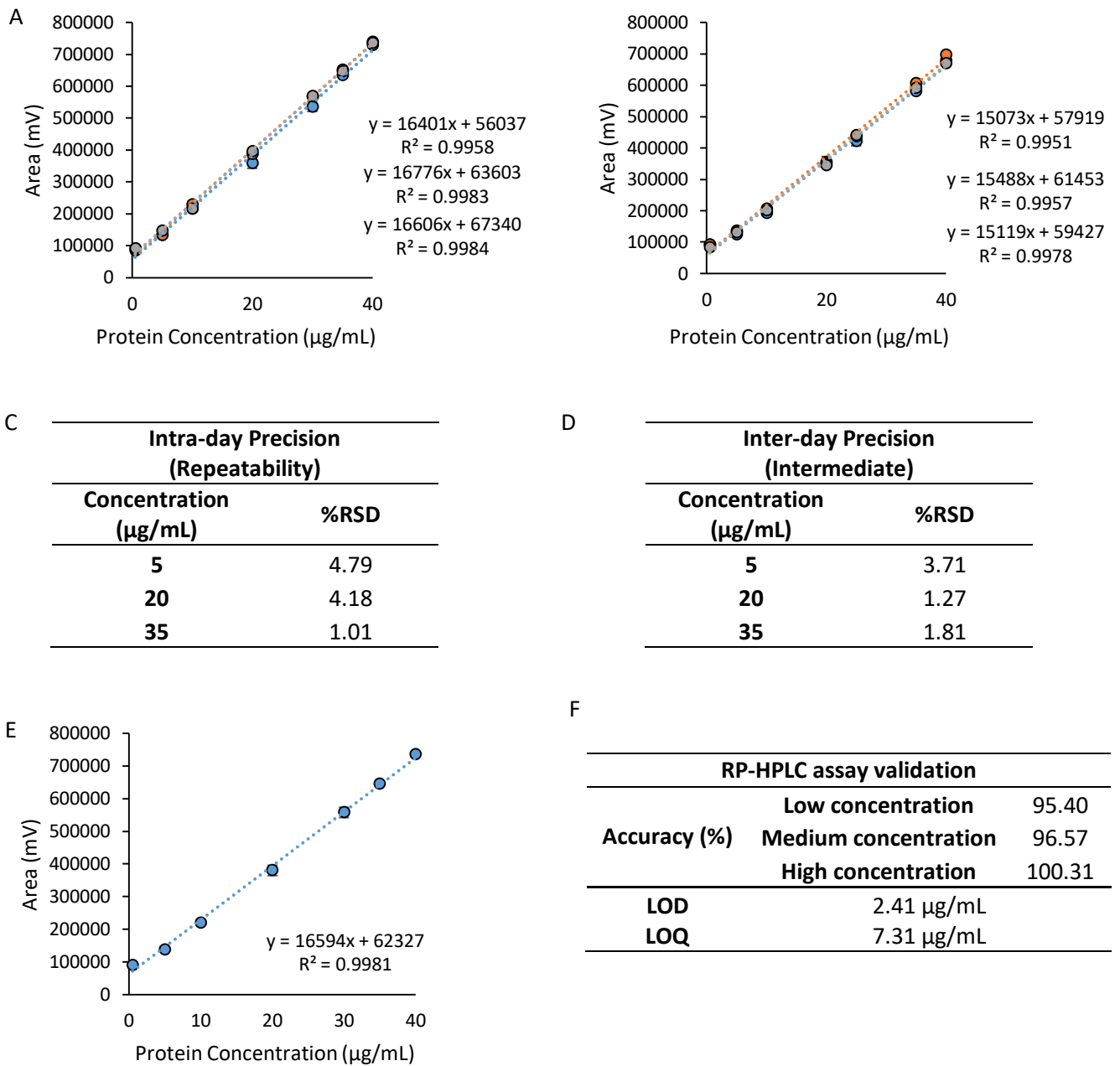


Figure 3.2 The calibration curves for RP-HPLC with ovalbumin in water: Intra-day curves (A), Inter-day curves (generated over 5 separate days) (B). Intra-day (C) and inter-day (D) precision were calculated across three different concentrations with %RSD shown. Finally, using the average curve (E), accuracy, LOD and LOQ values were determined (F). Results represent mean \pm SD, of at least $n = 3$ of independent batches.

Initial studies focused on the ability of these two techniques to quantify model antigen ovalbumin solubilised in water. Both techniques (micro BCA and RP-HPLC) were capable of determining ovalbumin concentrations to a high degree of linearity ($R^2 > 0.99$), with both of the techniques achieving precision and accuracy values within ICH guidelines (Figure 3.1F and 3.2F). Both LOD values from each of the techniques were approximately 2 $\mu\text{g/mL}$, however LOQ values for the RP-HPLC were found to be slightly less accurate (5.61 $\mu\text{g/mL}$ for micro BCA compared to 7.31 $\mu\text{g/mL}$). These results

are contrary to the majority of the literature (Umrethia et al., 2010, Grotefend et al., 2012), with most of the studies showing much improved detection limits using RP-HPLC. However, it should be noted that RP-HPLC methods can be highly refined and the inherent sensitivity of the technique can lead to compounding variables such as column packing, the structural integrity of the column and ambient room temperature resulting in reduced quantification accuracy (Chang et al., 2016).

3.5.2 Effect of liposome inclusion on protein quantification

Given the ability of the two methods to produce a linear relationship between ovalbumin and output signal, with $R^2 > 0.99$ in all cases and high degrees of accuracy and precision (falling within ICH guidelines for method validation), the next step was to determine the impact of the presence of lipids during the protein quantification process. Previous experimentation from our laboratory has shown that the inclusion of lipids using the same RP-HPLC method used here did not interfere with protein quantification (Hussain et al., 2019); however, phospholipids have previously been shown to interfere with the BCA protein assay (Kessler and Fanestil, 1986). Therefore, to determine the impact of liposome interference, initial studies focused on neutral liposomal formulation (DSPC:Chol 10:5 w/w, 3:1 FRR, 10 mL/min) produced using microfluidics, purified by dialysis, and mixed with the protein standards at a final concentration of 1 mg/mL per well. Protein was added at the same final concentration range as used previously (0.5 – 40 $\mu\text{g/mL}$) and the resulting blanks for micro BCA subtraction were produced with just liposomes (no ovalbumin present).

Intra-day repeatability (Figure 3.3A) was generated on the same day, while inter-day was generated across 5 distinct days (Figure 3.3B), each indicating a highly linear relationship ($R^2 > 0.99$) for protein concentration in the presence of liposomes using micro BCA. The intra and inter-day repeatability and precision was then calculated. Intra-day repeatability values of 5% and below were obtained across all concentrations tested, likewise with the medium and high concentrations for inter-day precision, however the lowest concentration tested resulted in %RSD value of 9.67% (Figure 3.3C and D). The presence of liposomes in the samples did not impact upon the LOD or LOQ values following blank subtraction (1.07 and 3.24 $\mu\text{g/mL}$ respectively) (Figure 3.3F), showing similar values to the micro BCA analysis of protein in water alone (Figure 3.2F). Accuracy values all fell within the accepted range (102.8 ± 0.61 , 99.4 ± 2.07 and $100.6 \pm 2.59\%$).

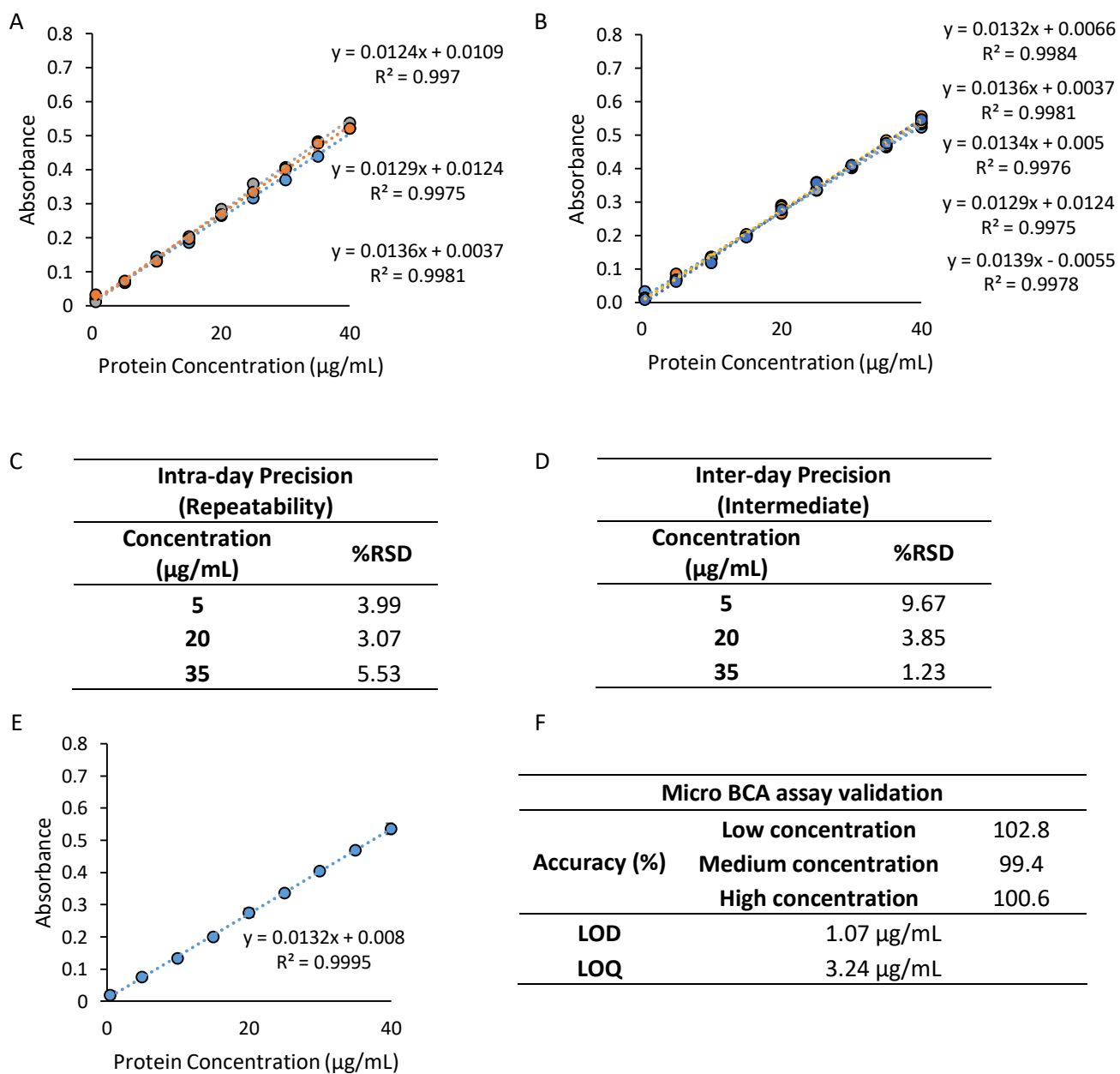


Figure 3.3 The calibration curves for micro BCA with ovalbumin and liposomes: Intra-day curves (A), Inter-day curves (generated over 5 separate days) (B). Intra-day (C) and inter-day (D) precision were calculated across three different concentrations with %RSD shown. Finally, using the average curve (E), accuracy, LOD and LOQ values were determined (F). Results represent mean \pm SD, of at least $n=3$ of independent batches.

As previously stated, phospholipids such as PC and PS have been shown to interfere with the BCA protein assay (Kessler and Fanestil, 1986). The results from a comprehensive study by Kessler et al indicated that while the interference was shown to be relatively linear with concentration, there was a risk associated with high liposome concentrations leading to a loss of linearity (Kessler and Fanestil, 1986). Furthermore, the authors state that the degree of interference is variable depending on the type of phospholipid used. Given our results so far have indicated that ovalbumin concentrations can be linearly measured using micro BCA in the presence of a fixed concentration of liposomal formulation DSPC:Chol (10:5 w/w), it was then important to determine the effect of liposome interference on the assay across a range of liposome concentrations, as well as the impact that different lipid formulations has on the rate of liposome interference. Formulations DSPC:Chol (10:5 w/w), DSPC:Chol:PS (10:5:4 w/w) and DSPC:Chol:DOTAP (10:5:4 w/w) were produced at a range of final concentrations (0.1 – 4 mg/mL) using microfluidics and purified through dialysis to remove solvent and then tested for interference. The results show a gradual increase in absorbance as liposome concentration is increased, with all three formulations showing a high degree of linearity between absorbance and increasing liposome concentration ($R^2 > 0.96$) (Figure 3.4). Differences between the degree of interference can be seen across the liposomal formulations, with the cationic DOTAP liposomes resulting in the least, followed by both the anionic and neutral formulation

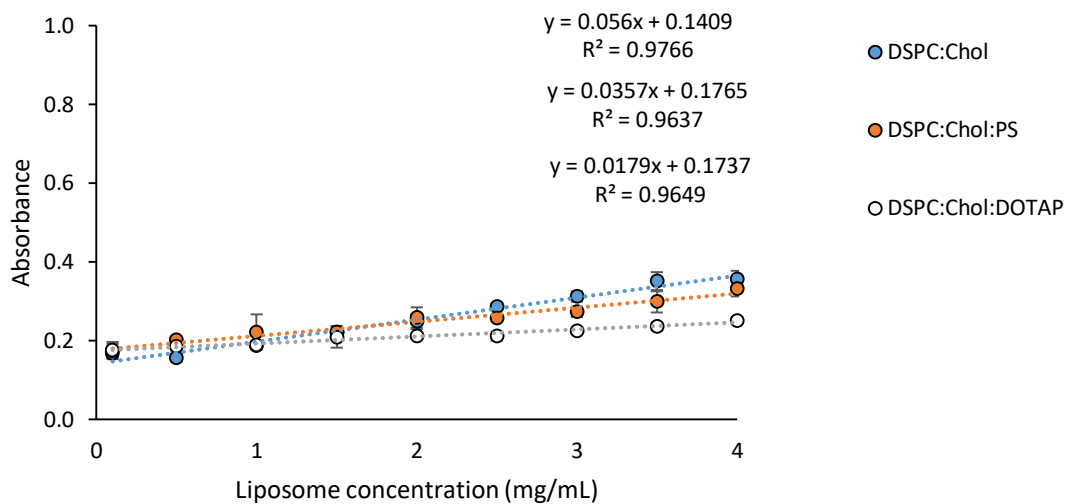


Figure 3.4 The effect of increasing liposome concentration on micro BCA absorbance with no ovalbumin added. Three liposomal formulations were produced using microfluidics (FRR 3:1 and 1:1, TFR 10 mL/min), DSPC:Chol, DSPC:Chol:PS and DSPC:Chol:DOTAP and assessed for BCA absorbance interference. Results represent mean \pm SD, of at least $n = 3$ of independent batches.

These results indicate issues associated with the use of micro BCA when quantifying protein loading in liposomal samples. A gradual increase in absorbance interference associated with high liposome concentrations adds a restriction on the ability of the assay to quantify samples in the presence of

large quantities of lipid. In the liposome concentration range tested here, linearity can still be maintained. However, at much higher liposome concentrations the assay would lose its linear association between absorbance and protein concentration as a result of the lipid interference. During protein loading, it is crucial that relevant liposome blanks are produced in order to accurately quantify the protein within the sample. This poses challenges when screening between different formulations, as individual formulation blanks will have to be produced in order to accurately quantify protein loading. At high lipid concentrations, when a potential loss of linearity can occur, it has been previously shown that the addition of 2% sodium dodecyl sulfate (SDS) can circumvent the interference increase by lipids (Morton and Evans, 1992).

3.4.3 Effect of solubilisation agent on ovalbumin quantification

Currently, it has been shown that it is possible to quantify 'free' (non-entrapped) protein in the presence of liposomes using both analytical techniques (micro BCA and HPLC). However, the aim of this chapter was to determine whether these techniques are capable of quantifying protein entrapped within liposomal vesicles. To achieve this, solubilisation of the liposomal bilayer is required to release the entrapped protein for quantification. Therefore, a previously published solubilisation technique (Fatouros and Antimisiaris, 2002) using 50/50 v/v IPA/buffer mixed with the liposomal sample at a ratio of 1:1 was initially tested. Ovalbumin was solubilised in water alongside solubilising solution (IPA/water 50/50 v/v), to a final protein concentration range between 0.5 – 40 µg/mL and subjected to both micro BCA and RP-HPLC analysis.

In the case of micro BCA, both intra-day and inter-day data was found to remain highly reproducible, with high degrees of linearity observed ($R^2 > 0.99$) in the presence of solubilisation agents (Figure 3.5A and B). The subsequent repeatability and precision analysis indicated that all concentrations remained within the $\pm 5\%$ acceptance range, aside from the lowest concentration for inter-day precision (%RSD of 13.49) (Figure 3.5C and D). The average of the curves was then produced (Figure 3.5E), yielding LOD and LOQ values of 2.72 and 8.23 µg/mL respectively (Figure 3.5F). When the accuracy of the curve was determined, it was found that at high concentrations (35 µg/mL), the accuracy of the assay was diminished to $90.73 \pm 8.92\%$ (Figure 3.5F). When these results were contrasted to RP-HPLC, again high degrees of linearity were observed ($R^2 > 0.99$) across both intra-day and inter-day measurements (Figure 3.6A and B). In the case of RP-HPLC, both repeatability and intermediate precision values fell within the acceptable range (Figure 3.6C and D), as well as accuracy values for the average of the curves at all three concentrations tested (Figure 3.6F).

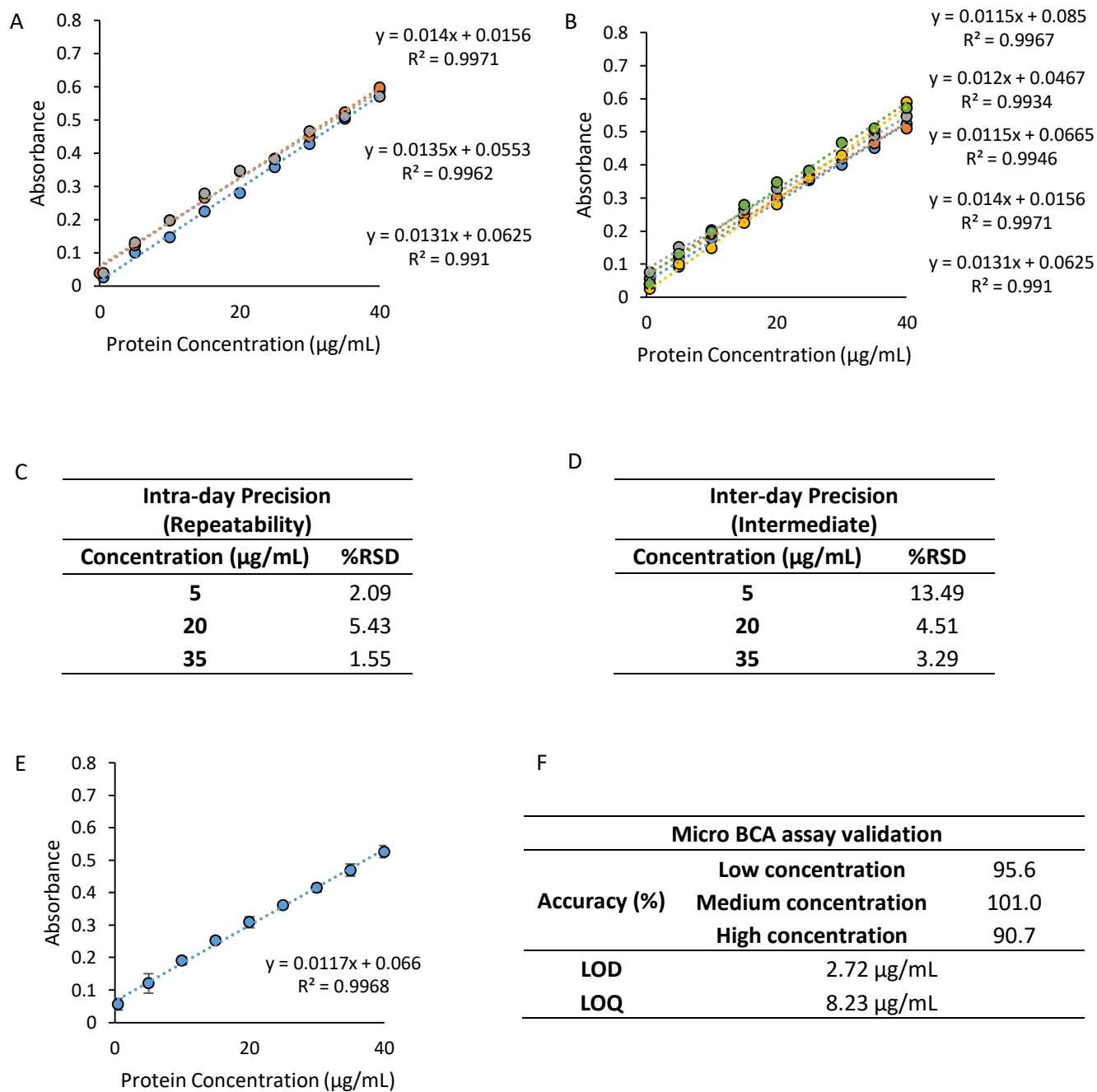


Figure 3.5 The calibration curves for micro BCA with ovalbumin in the presence of solubilisation mixture (IPA/Buffer 50/50 v/v): Intra-day curves (A), Inter-day curves (generated over 5 separate days) (B). Intra-day (C) and inter-day (D) precision were calculated across three different concentrations with %RSD shown. Finally, using the average curve (E), accuracy, LOD and LOQ values were determined (F). Results represent mean \pm SD, of at least $n=3$ of independent batches.

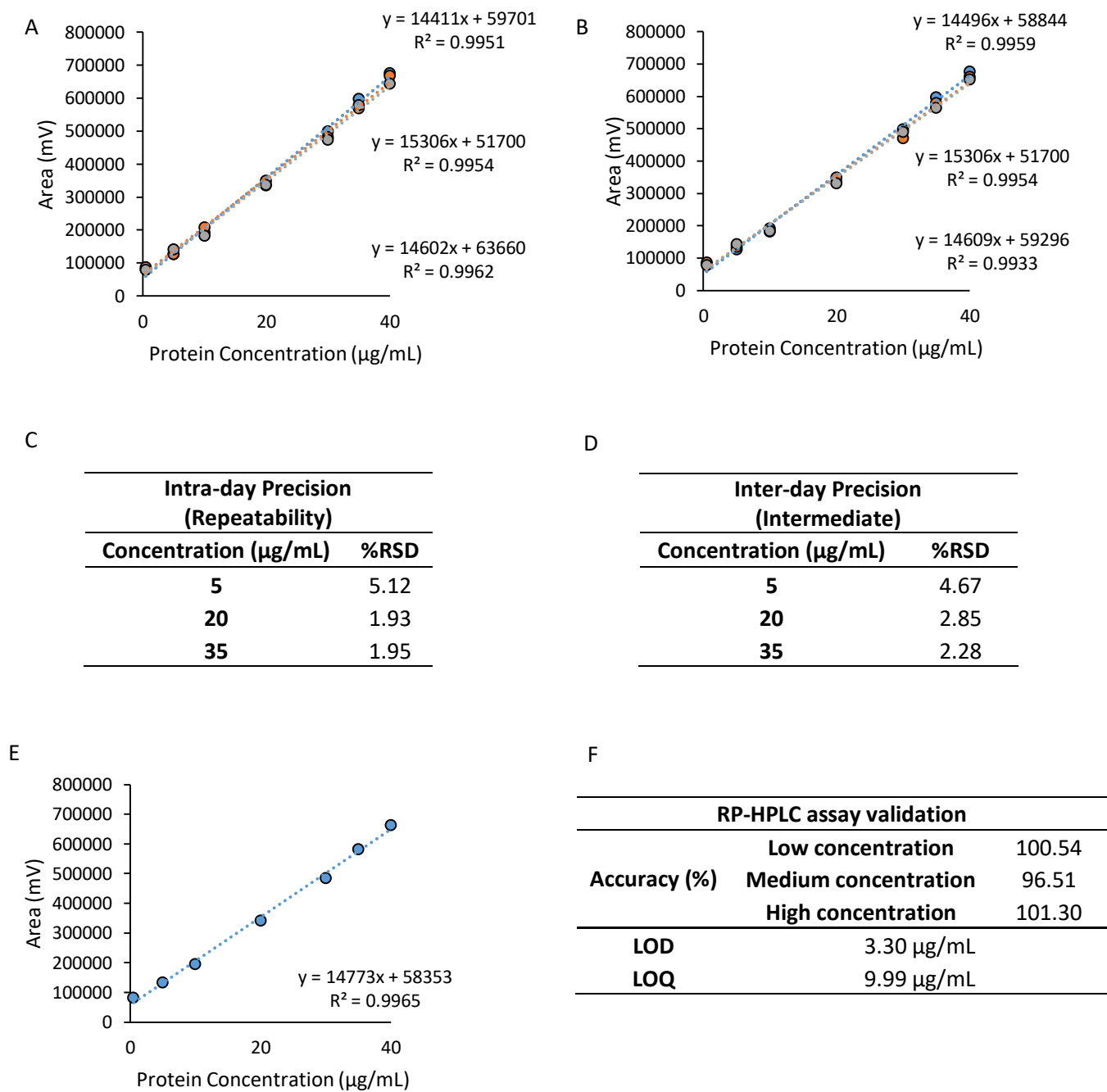


Figure 3.6 The calibration curves for RP-HPLC with ovalbumin in the presence of solubilisation mixture (IPA/Buffer 50/50 v/v): Intra-day curves (A), Inter-day curves (generated over 3 separate days) (B). Intra-day (C) and inter-day (D) precision were calculated across three different concentrations with %RSD shown. Finally, using the average curve (E), accuracy, LOD and LOQ values were determined (F). Results represent mean \pm SD, of at least $n=3$ of independent batches.

In the presence of a previously published liposome solubilisation technique, both micro BCA and RP-HPLC were capable of quantification of protein in a linear manner. Slight increases in LOD and LOQ values were found for both techniques when comparing against ovalbumin quantification in just water (Figure 3.1F and 3.2F). In the case of micro BCA, a loss in inter-day precision was observed for the lowest concentration. Interfering substances have previously been shown to affect protein quantification when using BCA. For example, when quantifying bovine serum albumin (BSA) in the presence of a cross-linking agent N-hydroxysuccinimide (NHS), it was found that errors in protein estimation was occurring due to the NHS interference with the Cu^{2+} ions in the working reagent. However, the inclusion of the NHS at a fixed concentration within the standard curve allowed for accurate protein estimation (Vashist and Dixit, 2011).

3.4.4 Effect of ovalbumin quantification in the presence of liposomes and solubilisation mixture for micro BCA protein quantification

Individually, both solvent and liposomes have been assessed to determine their impact on the ability of both RP-HPLC and micro BCA to quantify ovalbumin in a linear fashion. However, the quantification of protein loading within liposomal vesicles in a one-step process will require the ability of the assays to quantify the protein in the presence of both. As previously shown (Figure 3.4), liposomes result in an increase in interference in the BCA assay; yet, at the concentrations tested, this interference did not impact on the ability of the assay to determine protein concentration following blank control. Therefore, to test whether the inclusion of solubilisation agent in the presence of liposomes could result in a potentiation or inhibitory effect in the ability to quantify protein when present in combination, final protein concentrations of between 0.1 – 40 $\mu\text{g}/\text{mL}$ were added alongside solubilisation mixture (50/50 v/v IPA/water with neutral liposomal formulation DSPC:Chol (10:5 w/w) at a final concentration per well of 1 mg/mL .

Calibration curves were generated to determine intra and inter-day variability (Figure 3.7A and B), where all regression coefficients were found to be > 0.98 . Intra-day repeatability was determined using three calibration curves generated on the same day, with the lowest concentration tested falling outside of the acceptance criteria (7.64%) (Figure 3.7C), while inter-day precision was conducted using five curves over five separate days (Figure 3.7D), again resulting in a %RSD $> \pm 5\%$ for the lowest concentration. However, all other concentrations fell within the acceptable range. An average of the curves was then determined (Figure 3.7E), leading to LOD and LOQ values of 2.36 and 7.14 $\mu\text{g}/\text{mL}$ respectively. Accuracy of the assay was found to drift outside of the acceptable range at the highest concentration ($110.13 \pm 5.85\%$).

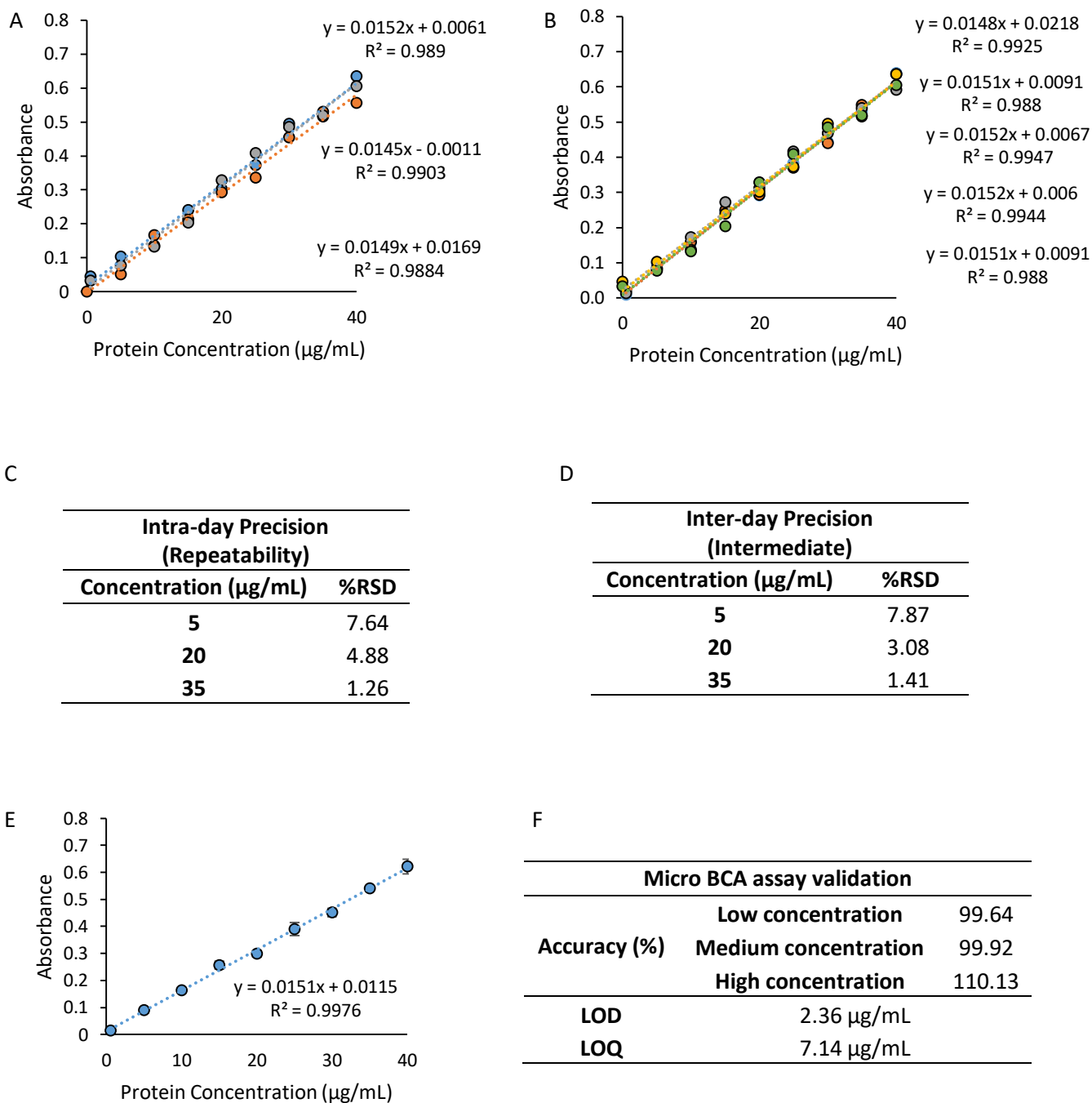


Figure 3.7 The calibration curves for micro BCA with ovalbumin in the presence of both liposomes (DSPC:Chol) and solubilisation mixture (IPA/Buffer 50/50 v/v): Intra-day curves (A), Inter-day curves (generated over 5 separate days) (B). Intra-day (C) and inter-day (D) precision were calculated across three different concentrations with %RSD shown. Finally, using the average curve (E), accuracy, LOD and LOQ values were determined (F). Results represent mean \pm SD, of at least $n=3$ of independent batches.

3.4.5 Protein loading quantification within liposomal formulations: Comparative study between RP-HPLC and micro BCA

Given the ability of both techniques to quantify protein in the presence of both liposomes and solubilisation agents, the final step was to compare the ability of both techniques to quantify loading of protein across a range of liposomal formulations. Three formulations were selected and protein was either entrapped (neutral and anionic liposomal formulations) or adsorbed onto the surface through electrostatic interactions (cationic liposomal formulation). Liposomal formulations were produced using microfluidics, with a flow rate ratio of 3:1 selected for neutral and anionic formulations and a flow rate ratio of 1:1 for cationic liposomal formulation and a total flow rate of 15 mL/min for all. Both neutral and anionic formulations were purified to remove unbound protein (while the unbound protein was not removed for the cationic formulation) and the samples were then subjected to both micro BCA and RP-HPLC to determine whether both techniques could quantify the protein loading efficiency. Table 3.1 shows the protein loading efficiency of each of the formulations, quantified by either BCA or HPLC over three replicates. Neutral formulation DSPC:Chol (10:5 w/w) showed an encapsulation efficiency of $36 \pm 0.9\%$ and $36 \pm 1.3\%$ for UV-HPLC and BCA respectively. Similarly, anionic formulation DSPC:Chol:PS (10:5:4 w/w) showed $20 \pm 0.0\%$ and $20 \pm 0.9\%$ for RP-HPLC and BCA respectively. Finally, cationic liposomal formulation DSPC:Chol:DOTAP (10:5:4 w/w) resulted in RP-HPLC readings of $82 \pm 3.1\%$ and micro BCA readings of $106 \pm 13.9\%$.

Table 3.1 Comparative protein loading for liposomal formulations DSPC:Chol (10:5 w/w), DSPC:Chol:PS (10:5:4 w/w) and DSPC:Chol:DOTAP (10:5:4 w/w) between two protein quantification techniques, RP-HPLC and micro BCA assay.

Liposomal formulation	Encapsulation Efficiency (%)		Protein Loaded ($\mu\text{g/mL}$)		
	RP-HPLC	BCA Assay	RP-HPLC	BCA Assay	
DSPC:Chol	n=1	37	35	55	53
	n=2	35	36	53	54
	n=3	35	38	53	56
	Average \pm SD	36 \pm 0.9	36 \pm 1.3	54 \pm 1	54 \pm 1.2
DSPC:Chol:PS	n=1	20	17	38	32
	n=2	20	19	37	35
	n=3	20	19	38	35
	Average \pm SD	20 \pm 0.0	18 \pm 0.9	38 \pm 0.5	34 \pm 1.4
DSPC:Chol:DOTAP	n=1	86	119	129	179
	n=2	80	113	120	170
	n=3	79	87	119	130
	Average \pm SD	82 \pm 3.1	106 \pm 13.9	123 \pm 4.5	160 \pm 21.3

With a wide range of analytical tools available for the use of protein quantification, understanding the limitations of these assays for determining protein loading within liposomal vesicles is essential (Lutsiak et al., 2002). Assessing the ability of two common protein quantification techniques, micro BCA and RP-HPLC to determine protein concentration within liposomal delivery systems has previously had limited robust testing. Understanding how these assays quantify protein in the presence of solubilisation agents and liposomes is essential if these methods are to be used for the quantification of protein loading in liposomal formulations in rapid manner.

The ability of these two techniques to quantify the protein loading in a range of liposomal formulations was tested (Table 3.1). The neutral and anionic formulations showed high similarity in protein loading values between both RP-HPLC and micro BCA, indicating the accurate ability of the two techniques to quantify the protein loading within liposomal vesicles. In terms of protein loading values within liposomes, the results presented here are in line with other studies. Using a neutral liposomal formulation (PC:Chol:Tween-80 and Vitamin E) the incorporation of BSA using thin layer dispersion method was found to yield 33.6% loading efficiency (Liu et al., 2015). Similarly, Lutsiak et al showed a loading efficiency of 29% following Hepatitis B core peptide encapsulation within a liposomal formulation containing 1,2-dipalmitoyl-sn-glycero-3-phosphocholine (DPPC), Cholesterol and 1,2-Dimyristoyl-sn-glycero-3-phosphoglycerol (DMPG) using a modified freeze-thaw method for liposome production. In the case of the cationic formulation (DSPC:Chol:DOTAP) with protein electrostatically

adsorbed on the surface, poor correlation of protein loading between the two techniques was observed (Table 3.1). However, this result cannot be directly attributed to the inability of either of the two techniques to quantify the loaded ovalbumin. It is hypothesised that aggregation of the formulation with protein on the surface led to the conflicting protein loading values obtained, as highlighted by the large variation between replicates.

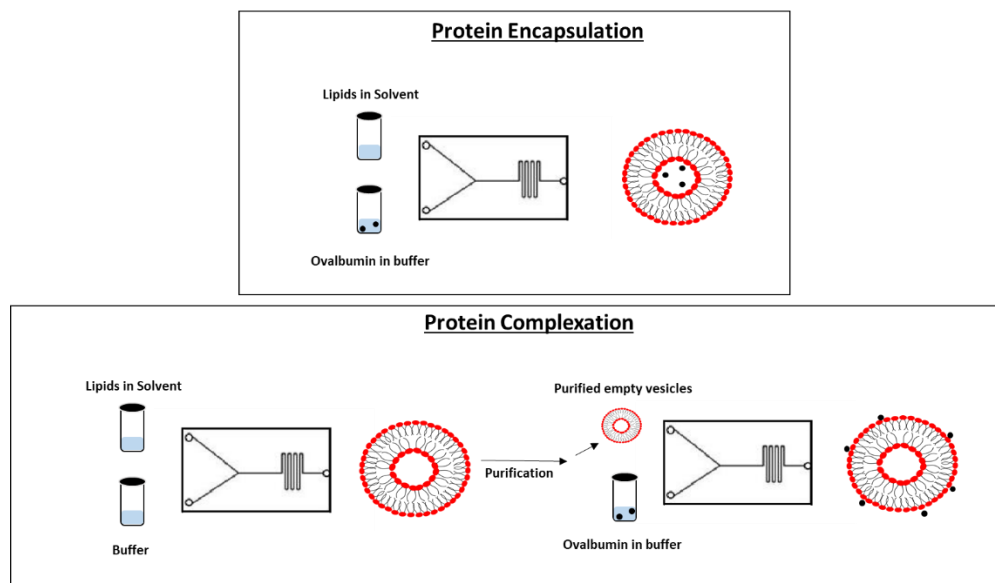
Each of the techniques studied have both advantages and disadvantages associated with their use, and the choice of whether to implement either one will be based on what the aim of the quantification is. For example, when analysing a large number of samples (using a fixed formulation and liposome concentration), micro BCA analysis can be useful given the multi-well setup allowing for high throughput screening. In comparison, RP-HPLC offers ease of quantification, without the need for establishing appropriate blanks. Furthermore, RP-HPLC has widely been reported throughout the literature for its ability to quantify to high degrees of precision (Grotefend et al., 2012). However, while ovalbumin quantification was found to not be affected by liposome inclusion for RP-HPLC, indirect loss of quantification accuracy can occur through lipid and or protein column fouling. Within the biopharmaceutical industry, chromatography is commonly employed during down-stream processing in order to purify products, however protein interactions with column resin has been shown to impact upon column performance over time, therefore care should be taken when using this method for high throughput analysis (Pathak et al., 2017).

3.6 Conclusions

Ovalbumin quantification techniques (RP-HPLC and micro BCA) were assessed for their ability to quantify loading within liposomal formulations. Both techniques were found to suitably detect protein concentrations (0.5 – 40 µg/mL) in a linear manner in the presence of liposomes and solubilisation agents. The choice of which method to select was found to be based upon the quantification need, where high-throughput screening for a single liposomal formulation would be suited to micro BCA analysis, while RP-HPLC analysis could be used for accurate determination of protein loading across different formulations. Given the suitability of the techniques to quantify protein loading within liposomal formulations, the following chapter can now assess the critical processing parameters involved when using microfluidics as a manufacturing platform for protein loaded liposomal formulations.

Chapter 4

Microfluidics as a manufacturing platform for protein loaded liposomal formulations



The work presented in this chapter has been published in:

FORBES, N., HUSSAIN, M. T., BRIUGLIA, M. L., EDWARDS, D. P., TER HORST, J. H., SZITA, N. & PERRIE, Y. 2019. Rapid and scale-independent microfluidic manufacture of liposomes entrapping protein incorporating in-line purification and at-line size monitoring. *International journal of pharmaceutics*, 556, 68-81.

4.1 Introduction

The use of adjuvants and/or delivery systems in the vaccine formulation can circumvent the reduction of immunogenicity found when administering subunit antigens by improving antigen delivery and uptake to relevant antigen presenting cells through mechanisms such as depot formation (Vartak and Sucheck, 2016, Silva et al., 2016, Henriksen-Lacey et al., 2010b). Since their inception as antigen carriers (Allison and Gregoriadis, 1974), liposomes have been broadly investigated as antigen delivery systems by adjusting lipid composition, membrane fluidity, particle size and charge as well as the localization of the antigen (surface adsorbed or encapsulated within) (Perrie et al., 2016). Owing to their versatility, liposomes offer tremendous possibilities as vaccine adjuvants for next generation vaccine therapies. For example, employing a cationic liposomal formulation can result in high loading efficiencies by exploiting electrostatic interactions with anionic proteins and peptides, while neutral and anionic formulations can incorporate antigen within the aqueous core of the vesicle to reduce degradation (Seelig, 2004). However, a major limitation pertaining to the use of liposomes within vaccine formulations is the lack of efficient manufacturing techniques for large scale production and processing. As shown in chapter 2, microfluidics can produce empty liposomal vesicles in a rapid and scalable manner, therefore the next stage was to determine the suitability of the technique to manufacture protein loaded liposomes. Using the quantification tools established in Chapter 3, the encapsulation efficiency of model antigen ovalbumin within the aqueous core of both neutral and anionic liposomal formulations will be determined. Furthermore, despite microfluidics emerging as a valuable manufacturing tool for liposome production (Forbes et al., 2019, Kastner et al., 2015, Roces et al., 2019, Jahn et al., 2007), there is little to no literature available for its use as a tool for controlling surface adsorption of protein onto preformed cationic liposomes. Currently, there are a range of methods available for the production of cationic liposomal adjuvants incorporating protein. Prior to liposome formation, lipid films can be hydrated in protein solutions leading to a mixture of entrapped and surface adsorbed protein (Heuts et al., 2018). Alternatively, following liposome production, the surface addition of protein can be typically added onto the surface of preformed liposomes by a number of techniques including dropwise addition or mixing liposome suspensions into protein mixtures under stirring followed by brief incubation times (Chatin et al., 2015, Varypataki et al., 2017, Milicic et al., 2012). Due to the lack of automation associated with these techniques, formulation physicochemical attributes can vary between users and laboratories as a number of important variables cannot be tightly controlled. The rate at which the reagents are mixed during dropwise addition, the speed of which both liposome and protein mixtures are stirred at can impact upon the formulations final characteristics, therefore it is hypothesised that microfluidics could aid in the automation of protein adsorption onto cationic liposomes. The work in this chapter examined

microfluidics as a tool to produce protein loaded liposomal formulations. Both antigen adsorption (cationic formulations) and encapsulation (anionic and neutral formulations) were tested in terms of loading efficiency and how this impacts upon vesicle characteristics.

4.2 Aim and objectives

Previously, optimisation of techniques capable of quantifying protein in the presence of liposomes was achieved (Chapter 3), therefore the next step was to evaluate the protein loading efficacies for a range of liposomal formulations using microfluidics. In order to achieve this, the objectives were:

1. Optimise and validate the purification processes for the removal of untrapped protein.
2. Identify the critical processing parameters for microfluidic production of neutral and anionic liposomes entrapping model antigen ovalbumin.
3. Determine the suitability of microfluidics as an automated tool for the surface adsorption of protein onto preformed cationic liposomes.

4.3 Materials

4.3.1 Materials used for the preparation of liposomes

The lipids 1,2-distearoyl-sn-glycero-3-phosphocholine (DSPC), 1,2-dioleoyl-3-trimethylammonium-propane (DOTAP) and L- α -phosphatidylserine (Brain PS, Porcine), cationic surfactant dimethyldioctadecylammonium bromide (DDA) and the immunopotentiator trehalose 6,6'-dibehenate (TDB) were all purchased from Avanti Polar Lipids Inc., Alabaster, AL, US. Cholesterol (cholesterol), ovalbumin (OVA), trifluoroacetic acid (TFA), 14,000 (MWCO) dialysis tubing cellulose and phosphate buffered saline (PBS; pH 7.4) in tablet form were purchased from Sigma Aldrich Company Ltd., Poole, UK. The Pierce™ BCA Protein Assay kit was purchased from Fisher Scientific, Loughborough, England, UK. Tris-base was obtained from IDN Biomedical Inc. (Aurora, OH, United States) and used to make 10 mM Tris buffer, adjusted to pH 7.4 using HCl. All solvents and chemicals used were of analytical grade.

4.4 Methods

4.4.1 Traditional manufacture of protein loaded liposomes: Lipid-film hydration

Lipids were dissolved at specific concentrations in a chloroform:methanol mixture (9:1 v/v) in round bottom flasks. The flasks were then placed under rotatory evaporation for 6 minutes at 200 rpm, in a heated water bath (37°C) to remove solvent. The flasks then remained on the rotary evaporator for 10 minutes to allow trace organic solvent to evaporate. Hydration of the lipid film was achieved by the addition of heated PBS 10 mM (to the appropriate transition temperature) with the inclusion of ovalbumin (0.25 mg/mL), followed by multiple vortexing and re-heating cycles for 15 minutes.

4.4.1.1 Size reduction: Hand-held extrusion

Following lipid-film hydration, MLV containing ovalbumin were then size reduced to produce SUV. Hand-held extrusion experiments were conducted on a Mini Extruder from Avanti Polar Lipids Inc., Alabaster, AL, US. Liposome formulations (1 mg/mL) were extruded through specific pore size membrane filters, starting from 0.5 µm, followed by 0.4 µm and ending with a final filter pore size of 0.2 µm. Each sample is cycled through the membrane x10, while the sample is maintained at a temperature relevant to the transition temperature of the lipids within the formulation.

4.4.2 Microfluidic manufacture of liposomes entrapping protein

The preparation of liposomes by microfluidics was conducted on the NanoAssemblr Platform (Precision Nanosystems Inc., Vancouver, Canada). Selected lipids were dissolved in methanol (solvent phase) at specific concentrations and injected through one of the two inlets on the microfluidics staggered herringbone micromixer cartridge, whilst the aqueous phase (PBS; pH 7.3 ± 0.2) containing ovalbumin (varied concentrations) was injected into the second inlet. Flow rate ratios of 1:1, 3:1 and 5:1 were selected and total flow rate speeds between 5 and 20 mL/min. Larger scale production of ovalbumin loaded liposomes was prepared using the NanoAssemblr® Blaze™ (10 mL to 1 L) using the same production parameters as previously optimised on the Benchtop system (3:1 FRR, 15 mL/min), using liposomal formulation DSPC:Chol.

4.4.2.1 Purification of liposomes entrapping protein

Liposome samples were purified using Krosflo Research lll tangential flow filtration (TFF) system fitted with an mPES (modified polyethersulfone) column with a pore size of 750 kD. For removal of solvent and untrapped protein, liposomal formulations were circulated through the column (21 mL/min) and purified through diafiltration, with fresh PBS being added at the same rate as the permeate leaving

the column. The diafiltrate volume was varied in order to determine the optimised volume needed to remove untrapped protein.

4.4.3 Microfluidic manufacture and complexation of cationic vesicles adsorbing protein

4.4.3.1 Manufacture of empty vesicles

For cationic liposomes, controlled surface antigen loading using microfluidics (complexation) was tested. Initially, empty cationic liposomes were manufactured in TRIS (10 mM pH 7.4), across a range of flow rate ratios and rates in order to determine suitable processing parameters. Two formulations (DSPC:Chol:DOTAP and DSPC:Chol:DDA) were prepared using methanol, while DDA:TDB was manufactured using IPA. The use of a heating block at 65°C was employed for formulation DDA:TDB in order to maintain the solubility of the lipids prior to microfluidic manufacture.

4.4.3.2 Purification of empty formulations

In order to remove residual solvent after liposomal manufacture by microfluidics, dialysis was conducted. Briefly, 1 mL of the liposomal formulations were added to dialysis tubing (MWCO 14,000), and subjected to magnetic stirring within 200 mL of appropriate buffer for 1 h. Dialysis membrane (14,000 MWCO) was pre-treated in a solution of 2% sodium bicarbonate, 1 mM EDTA and 1 L of ultrapure water at 80°C for 2 hours. The membrane was then rinsed with water to remove any trace of pre-treated solution and stored in 20% EtOH.

4.4.3.3 Complexation of protein

The controlled surface adsorption of protein onto preformed cationic vesicles (complexation) was tested by passing purified preformed cationic liposomes through the microfluidic system in one inlet, with TRIS (10 mM, pH 7.4) containing specific concentrations of ovalbumin added through the second inlet at a range of flow rate ratios (1, 3 and 5:1) and total flow rates (5-20 mL/min).

4.4.4 Circular Dichroism

The ovalbumin protein secondary structure was determined using Circular Dichroism (CD) after microfluidic manufacture and purification (TFF), as well as a comparison against native ovalbumin in PBS (0.3 mg/mL). The liposomes were made using 8 mg/mL initial lipid and 8 mg/mL initial ovalbumin at a 3:1 FRR and 15 mL/min TFR. The Chiroscan™- plus was used to analyse the samples with 20 µL placed in between two microscope slides and placed into a Suprasil® quartz absorption cuvette

(Hellma, Germany; path length of 1 mm). The measurement temperature was 25 °C and spectra was recorded between 180 to 260 nm, with each spectrum being the average of three runs.

4.4.5 Dynamic light scattering (off-line)

DLS (Malvern Zetasizer Nano-ZS from Malvern Panalytical, Worcs., UK) was used to determine the Z-average (mean diameter) and polydispersity index (PDI) of the liposomal samples off-line. Measurements were maintained between attenuation 6-9 by diluting vesicles in buffer (1/10) and all readings were conducted in triplicate at 25°C, using a refractive index of 1.330 and 1.59 for the dispersant and the material respectively

4.4.6 Protein quantification

Protein quantification using Micro BCA (Pierce™ BCA Protein Assay Kit, Sigma Aldrich, Poole, UK) was carried out as optimised in chapter 3. Briefly, samples were incubated up to 2 hours at 35°C, with 150 µL of sample required (150 µL) + 150 µL of the working reagent (25:24:1 of reagent A, B and C respectively). Calibration curves were kept as similar to the sample as possible, with the concentration of all components (such as lipid and solubilisation agents (50:50 v/v IPA: PBS)) matched to the sample concentration and appropriate blanks were subtracted. Absorbance was then measured at 562 nm using a Bio-rad 680 microplate reader. For larger scale samples manufactured by the NanoAssemblr Blaze, RP-HPLC (Shimadzu 2010-HT, Milton Keynes, UK) was used to quantify protein loading as previously described in Chapter 3. Briefly, a Jupiter 5 µ C18 column with security guard, pore size 300A from Phenomenex (Macclesfield, UK) was used. The selected HPLC method was: Mobile Phase A (0.1% TFA in distilled water) B (0.1% TFA in Methanol); with a gradient flow for a total run time of 25 minutes. Initially, A;B mix of 95:5 was used, increasing to 5:95 (A:B) by minute 10. This was maintained for a following 5 minutes, before a return to 95:5 (A:B) by minute 20. UV detection was conducted at 210 nm, with a column temperature of 25°C and a flow rate of 1 mL/min, injection volume of 50 µL.

4.4.7 Statistics

Results are represented as mean ± SD with n = 3 independent batches unless stated otherwise. ANOVA tests were used to assess statistical significance between groups, with a Tukey's post adhoc test (p value of less than 0.05).

4.5 Results and Discussion

4.5.1 Tangential flow filtration as a purification tool for liposomes entrapping protein

Prior to determining the suitability of microfluidics as a manufacturing platform for the production of protein loaded liposomes, it is crucial that a validated process for purification of these formulations is established. When determining the loading efficiency of neutral and anionic formulations following microfluidics, separation of untrapped protein from the protein loaded liposomes is necessary. As previously shown in chapter 2, tangential flow filtration (TFF) is a technique suitable for high throughput solvent purification for neutral and anionic liposomes. To ensure protein removal via TFF, empty neutral liposomes (DSPC:Chol 10:5 w/w) were produced via microfluidics and purified to remove solvent. The liposomes (1 mg/mL) were then mixed in the presence of ovalbumin at specific protein concentrations (500, 1000 and 2000 $\mu\text{g/mL}$) and subjected to 20 wash cycles of TFF. Protein concentration within the permeate was then quantified by micro BCA to determine ovalbumin removal in the presence of liposomes. Purification of up to 2000 $\mu\text{g/mL}$ (100% of initial content) of ovalbumin is achieved by 11 diafiltrate volumes, and given that none of the protein was entrapped within the vesicles, full removal of protein can therefore be achieved using this purification method (Figure 4.1).

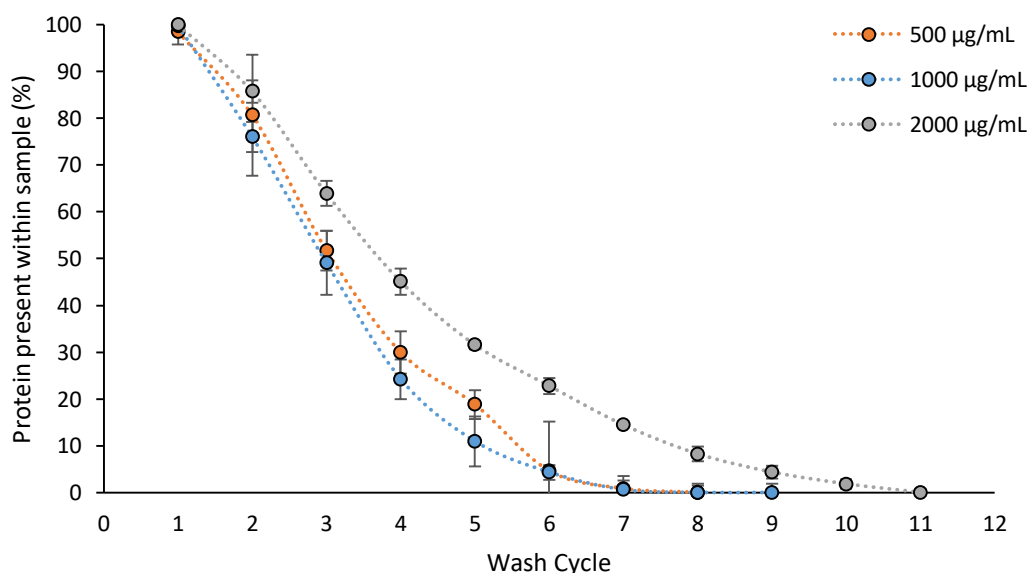


Figure 4.1 Removal of untrapped ovalbumin using tangential flow filtration. Preformed “empty” liposomes DSPC:Chol (10:5 w/w) prepared by microfluidics (4 mg/mL initial total lipid, 3:1 FRR and 15 mL/min TFR) were mixed with ovalbumin at final protein concentrations of 500, 1000 and 2000 $\mu\text{g/mL}$. Ovalbumin concentrations at each wash cycle was measured in the permeate using micro BCA. Results represent mean \pm SD, $n = 3$ of independent batches.

4.5.2 Microfluidic manufacture of vesicles entrapping protein

Once an appropriate purification technique was established for the removal of unentrapped protein, quantification of the protein loading efficiency of neutral and anionic formulations could be determined. Initial experiments compared the loading potential of formulations DSPC:Chol (10:5 w/w) and DSPC:Chol:PS (10:5:4 w/w) produced by microfluidics versus the traditional lipid film hydration followed by hand-held extrusion in order to down-size the vesicles. Both of the formulations manufactured by each technique were purified using tangential flow filtration in order to remove unentrapped ovalbumin and protein loading was then quantified using micro BCA (as per previously optimised in Chapter 3). Figure 4.2 shows the entrapment efficiency of both formulations, where liposomes produced by microfluidics resulted in high protein loading (29% and 20% for DSPC:Chol and DSPC:Chol:PS respectively; Figure 4.2A), while liposomes produced by lipid-film hydration and subsequent extrusion cycles through progressively smaller pore sizes yielded poor loading (3.5 and 1% respectively; Figure 4.2A). When comparing the vesicle size, in the case of DSPC:Chol, microfluidics produced smaller vesicles (65-70 nm) compared to lipid-film hydration and hand-held extrusion, with homogenous population distribution (<0.25 PDI). For formulation DSPC:Chol:PS, no differences could be observed in terms of vesicle size or PDI across both of the manufacturing methods (105 – 120 nm, <0.25 PDI) (Figure 4.2B).

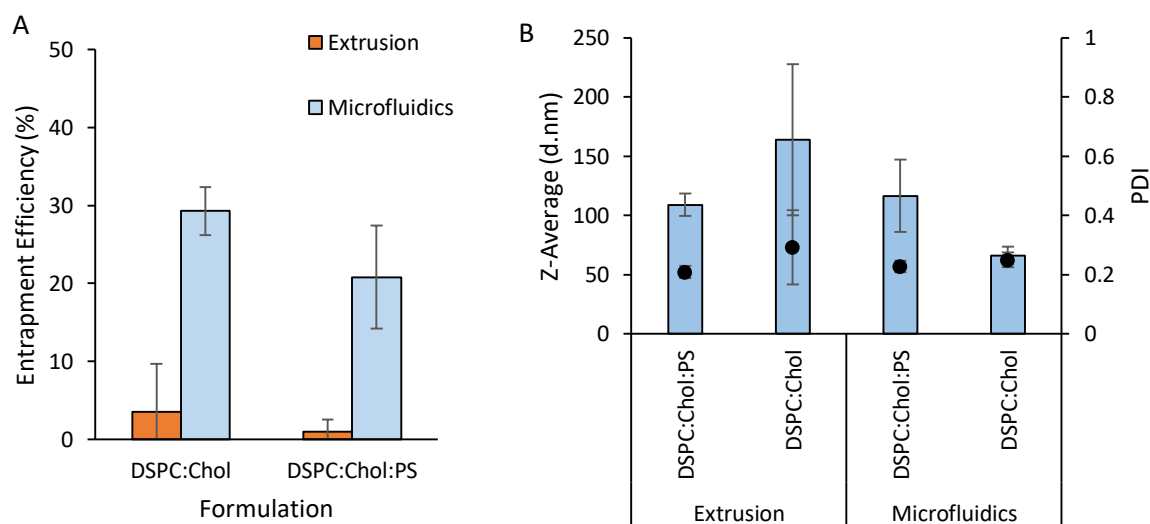


Figure 4.2 Manufacturing technique comparison for the production of protein loaded liposomal formulations entrapping protein. Neutral formulation DSPC:Chol (10:5 w/w) and anionic formulation DSPC:Chol:PS (10:5:4 w/w) were manufactured by microfluidics or lipid-film hydration followed by hand held extrusion. A final liposome and ovalbumin concentration of 1 mg/mL and 0.18 mg/mL respectively were maintained across both techniques. A) Entrapment efficiency of the formulations, B) physicochemical attributes of the same formulations. Results represent mean \pm SD, $n = 3$ of independent batches.

Protein entrapped within liposomes and subsequent extrusion cycles for particle size reduction has previously been reported to result in a rapid initial loss of enzyme loading using egg PC liposomes

entrapping acetylcholinesterase (Colletier et al., 2002). MLV loading efficiencies of the enzyme was found to be initially high (approximately 25%); however, a rapid drop to approximately 5% was observed following the initial extrusion cycles. Interestingly, recovery of protein loading was then observed as the extrusion cycles were continued, yet if a new extrusion membrane was used, the authors found no loading recovery. Membrane extrusion for liposome size reduction is thought to function through the process of large vesicles (above the membrane pore size) rupturing as pressure is applied, and re-forming as smaller vesicles as they pass through the membrane (Friskens et al., 2000a, Patti and Friskens, 2003). Therefore, MLV entrapping protein are likely disrupted during the extrusion process, leaking previously entrapped protein. It is likely that this free protein then interacts with the membrane and is retained, therefore if new membranes are applied for further size reduction (as they were in Fig 4.2), recovery of protein loading will be inhibited, resulting in poor loading efficiencies (Colletier et al., 2002). In comparison, microfluidics as a manufacturing platform followed by downstream purification by TFF for the production of protein loaded liposomes yields high protein entrapment in a rapid and scalable manner.

However, the ability of microfluidics to rapidly produce liposomes from lipids in organic solvents upon interaction with aqueous phase poses some issues in regards to solvent and protein interactions. Protein structural integrity, in particular relation to vaccine antigens, can determine how effective an immune response is, therefore ensuring ovalbumin secondary structure is retained throughout the production process is of high importance (Deressa et al., 2014). The native structure of protein tends to favour thermodynamically stable conformations under physiological conditions. The presence of organic solvents changes the polarity of the environment that the protein is exposed to, which can interfere with the hydrophobic interactions present within the protein, thus affecting structural folding (Taboada et al., 2007). Thus, circular dichroism was used to analyse and compare ovalbumin secondary structure following microfluidic manufacture (and subsequent TFF purification) against the native form of the protein in PBS pH 7.4 (Figure 4.3). Both spectra are similar to those reported within the literature, comprising of a mixture of α -helix and β -sheet with the characteristic minima peaks around 222 nm being slightly larger than the peak around 210 nm (Hu and Du, 2000). Therefore, it was concluded that the manufacture in the presence of 25% methanol, and subsequent TFF purification to return the sample to buffer conditions, did not impact upon the secondary structure of the final protein loaded liposome product.

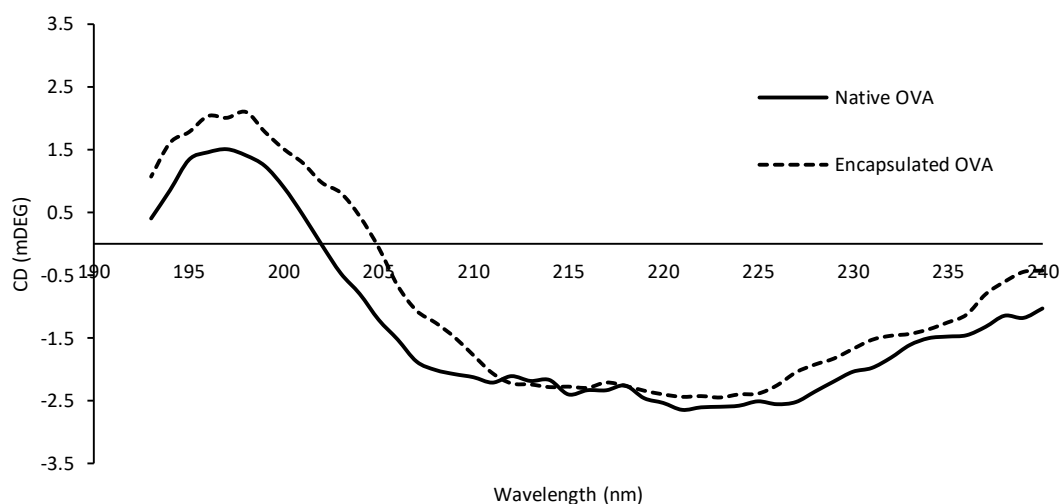


Figure 4.3 The structural integrity of ovalbumin loaded into the liposomes measured by circular dichroism. DSPC:Chol (10:5 w/w) liposomes were prepared with ovalbumin (8 mg/mL initial total lipid and OVA, 3:1 FRR, 15 mL/min TFR) and purified via TFF. Spectra was measured across 180 – 260 nm.

Following on from initial studies, the protein loading efficiency of the liposomal formulations was further studied with regards to the effect of increasing ovalbumin concentrations. Neutral formulation DSPC:Chol (10:5 w/w) and anionic formulation DSPC:Chol:PS (10:5:4 w/w) were selected at a fixed initial lipid concentration of 4 mg/mL. Figure 4.4A shows the entrapment efficiency of ovalbumin across a concentration range (0.1 – 20 mg/mL) as well as the amount of ovalbumin loaded for neutral DSPC:Chol (10:5 w/w). The data shows that up to approximately 2 mg/mL of initial ovalbumin, entrapment efficiencies remain above 25% (Figure 4.4A), while liposome size showed a slight increase from 55 – 85 nm, with PDI values < 0.3 for all concentrations (Figure 4.4B). The zeta potential for all of the ovalbumin concentrations remained near neutral (-5 mV to -10 mV) (Figure 4.4C). Further increases in initial ovalbumin concentration up to 20 mg/mL resulted in a significant drop in entrapment efficiency to 12% (Figure 4.4A) and a significant increase in particle physicochemical attributes (particle size > 700 nm, with poor polydispersity, data not shown).

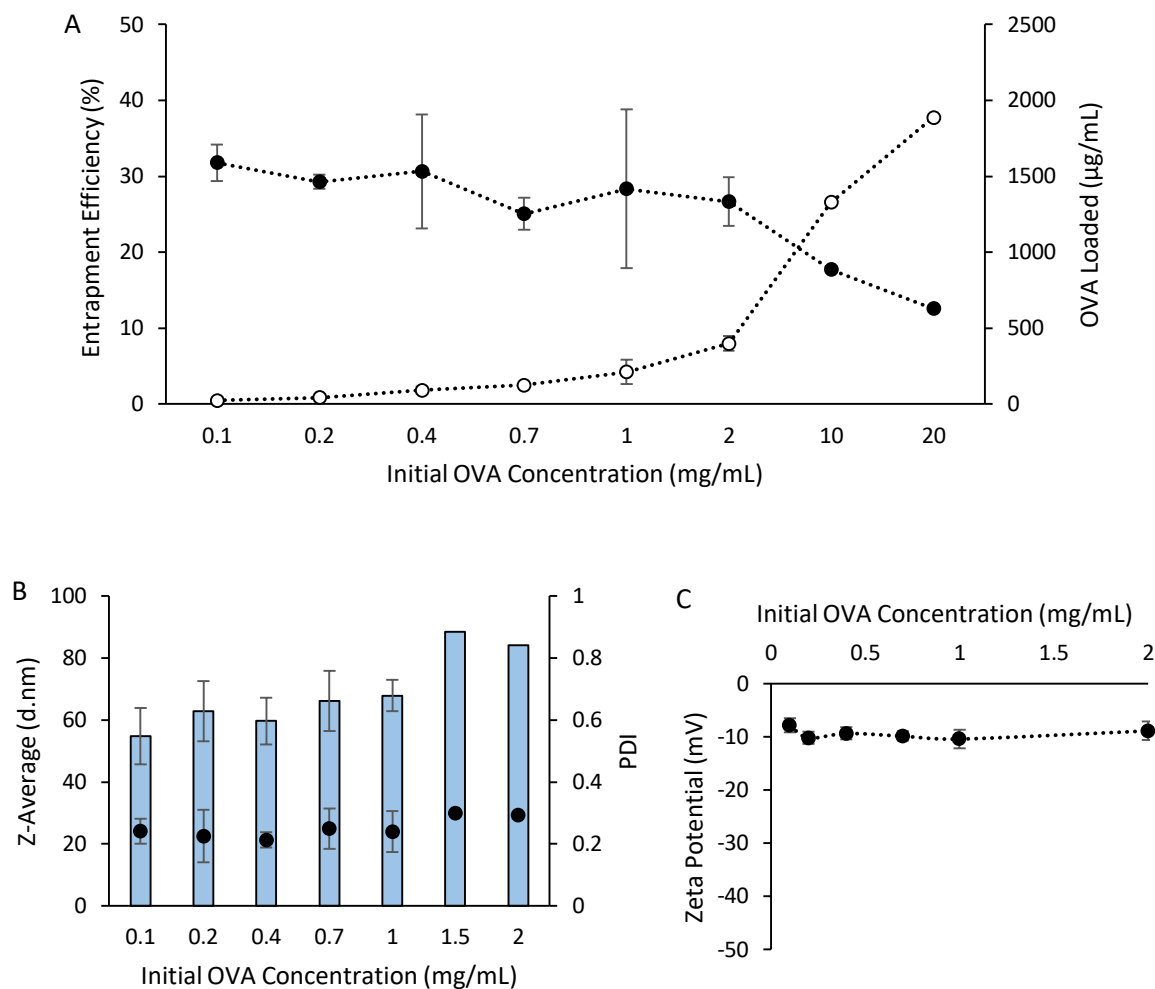


Figure 4.4 The effect of protein concentration in aqueous phase on entrapment efficiency and liposomal physicochemical characteristics for a neutral liposomal formulation (DSPC:Chol 10:5 w/w) using initial total lipid concentration of 4 mg/mL, 3:1 flow rate ratio and 15 mL/min TFR. (A) Entrapment efficiency (black circles) and protein loading (open circles) across initial ovalbumin concentrations for neutral liposomal formulation. (B) Average particle size and PDI, and (C) Zeta Potential for the same formulation. Results represent mean \pm SD, $n = 3$ of independent batches.

Anionic liposomal formulation DSPC:Chol:PS (10:5:4 w/w) was then tested under the same process conditions (4 mg/mL initial total lipid, 3:1 FRR, 15 mL/min TFR) with incremental increases of initial ovalbumin concentration. Across an initial protein concentration range between 0.1 to 2 mg/mL, entrapment efficiencies generally showed a gradual decrease between 22% and 18%, with an increase in the total ovalbumin loaded (Figure 4.5A). Particle size of the loaded liposomes was found to be between 100 nm and 116 nm, while maintaining homogenous populations at all protein concentrations (<0.25 PDI) (Figure 4.5B). The zeta potential of the formulation remained unaffected by the protein incorporation, ranging between -26 mV to -33 mV (Figure 4.5C).

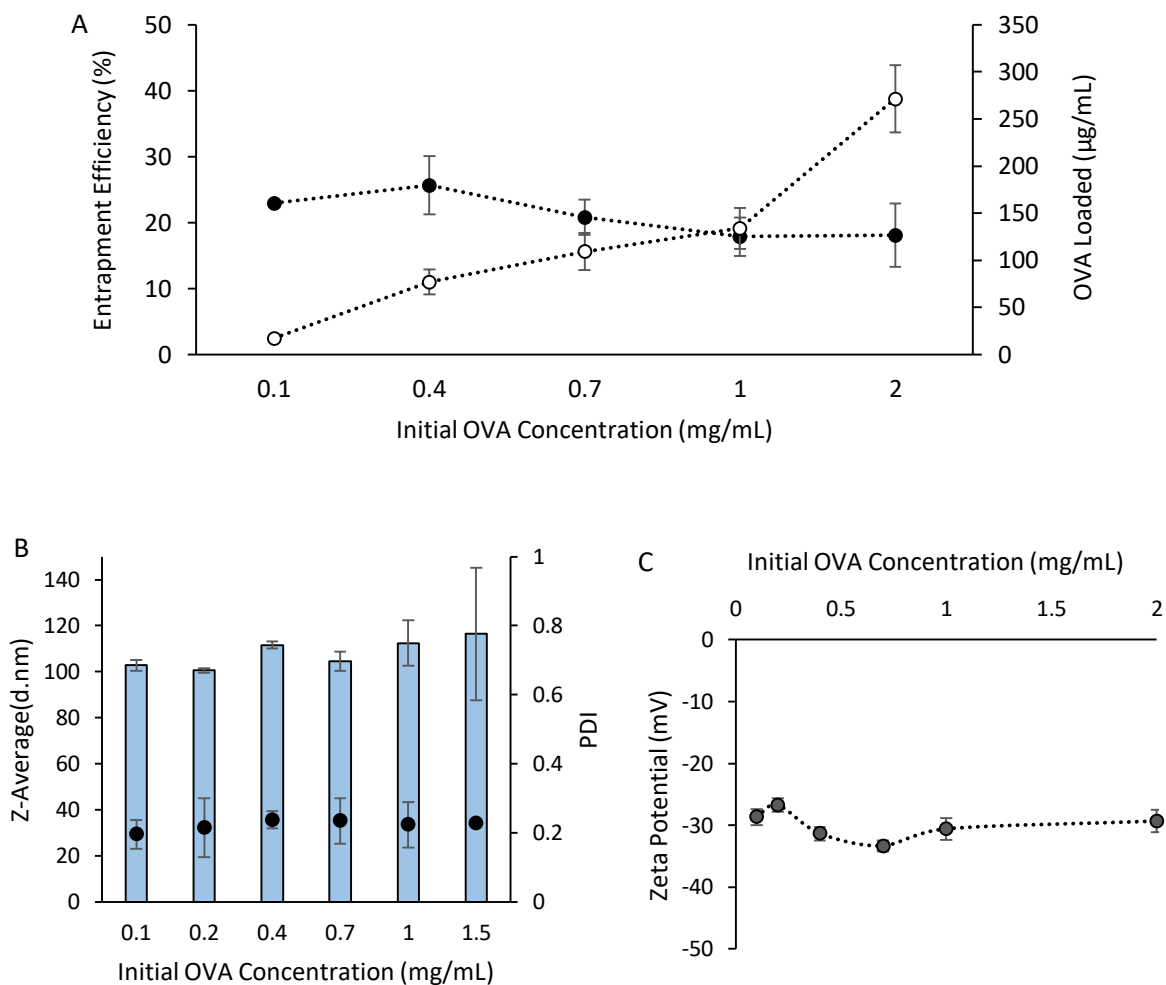


Figure 4.5 The effect of protein concentration in aqueous phase on entrapment efficiency and liposomal physicochemical characteristics for the anionic liposomal formulation (DSPC:Chol:PS 10:5:4 w/w) using an initial total lipid concentration of 4 mg/mL, 3:1 flow rate ratio and 15 mL/min TFR. A) Entrapment efficiency (black circles) and protein loading (open circles) across initial ovalbumin concentrations for anionic liposomal formulation. B) Average particle size and PDI, and C) Zeta Potential for the same formulation. Results represent mean \pm SD, $n = 3$ of independent batches.

While both neutral and anionic liposomal formulations showed good entrapment across protein concentrations up to 2 mg/mL, differences could be observed between the two formulations. The decrease in entrapment efficiency seen with the anionic formulation (around 20%) compared to neutral DSPC:Chol (approximately 28%) is not uncommon. The incorporation of acetylcholinesterase within a range of liposomal formulations was assessed in a comprehensive study by Colletier et al identifying key elements that impact upon encapsulation efficiency. Neutral surface charge based vesicles (POPC) were found to achieve encapsulation efficiencies greater than 35%, however when negatively charged POPS was used, encapsulation efficiency dropped below 20%. This is likely a result of the electrostatic repulsion that occurs between the polar head group of the phospholipids and the

overall anionic peripheral charge of the ovalbumin (which has an isoelectric point of approximately pH 4.50), leading to a decrease in encapsulation (Colletier et al., 2002, Niu et al., 2014).

4.5.3 Identification of critical microfluidic process parameters

4.5.3.1 The effect of FRR on protein entrapment efficiency for neutral and anionic vesicles

The microfluidic manufacture of liposomes allows for flexibility in relation to the choice of microfluidic operating parameters used during production. Given the effect these parameters such as flow rate ratio (FRR) and total flow rate (TFR) have on vesicle characteristics (shown in Chapter 2), understanding the effect these process parameters have on protein loading was studied next. Initially, the effect of FRR was studied for both DSPC:Chol and DSPC:Chol:PS formulations across 1:1, 3:1 and 5:1. In order to isolate the impact that this process parameter has on ovalbumin entrapment efficiency, initial lipid and protein concentrations were adjusted so that the final liposome and protein concentrations were fixed across all FRR (1 mg/mL and 0.525 mg/mL for lipid and protein respectively). Despite this, FRR was found to impact upon entrapment efficiency for formulation DSPC:Chol, where 3:1 resulted in approximately 25% and 5:1 14% (Figure 4.6A). When a FRR of 1:1 was applied, large levels of aggregation were observed, likely a result of interactions between 50% solvent and protein within the formulation, leading to poor purification (data not shown). Despite the decrease in encapsulation efficiency, vesicle size remained the same for both FRRs (60 – 70 nm); however, larger variance was observed when using the 5:1 (Figure 4.6B).

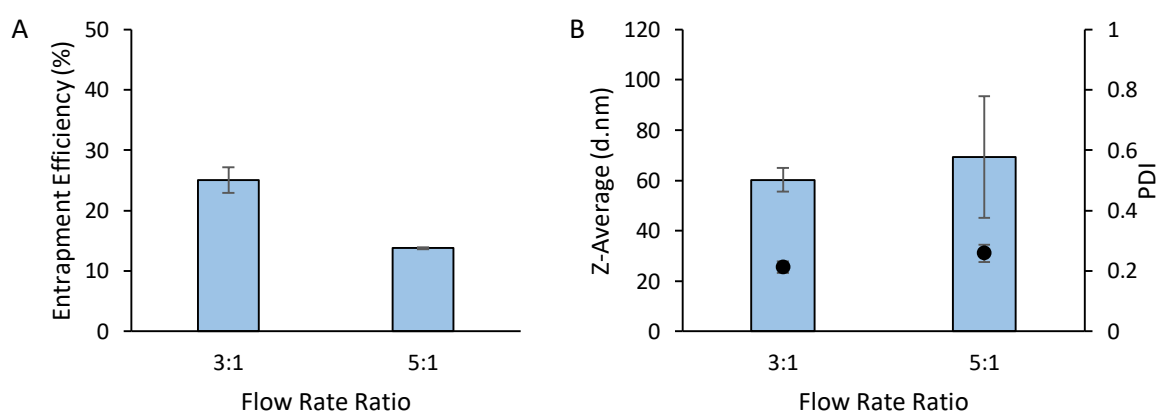


Figure 4.6 The effect of microfluidic process parameter flow rate ratio on entrapment efficiency and liposomal physicochemical characteristics for the liposomal formulation (DSPC:Chol 10:5 w/w) (A and B respectively). Total final lipid concentration was fixed at 1 mg/mL, with a final ovalbumin concentration of 0.525 mg/mL and a total flow rate of 15 mL/min. Results represent mean \pm SD, $n = 3$ of independent batches.

Similar results were found when employing the anionic liposomal formulation DSPC:Chol:PS, where an increase in flow rate ratio from 3:1 to 5:1 resulted in a decrease in encapsulation efficiency of ovalbumin (approximately 20% to 9%) (Figure 4.7A). This decrease in encapsulation efficiency also correlated with a slight, but statistically significant ($p < 0.05$) decrease in vesicle size from 111 nm to 102 nm (Figure 4.7B).

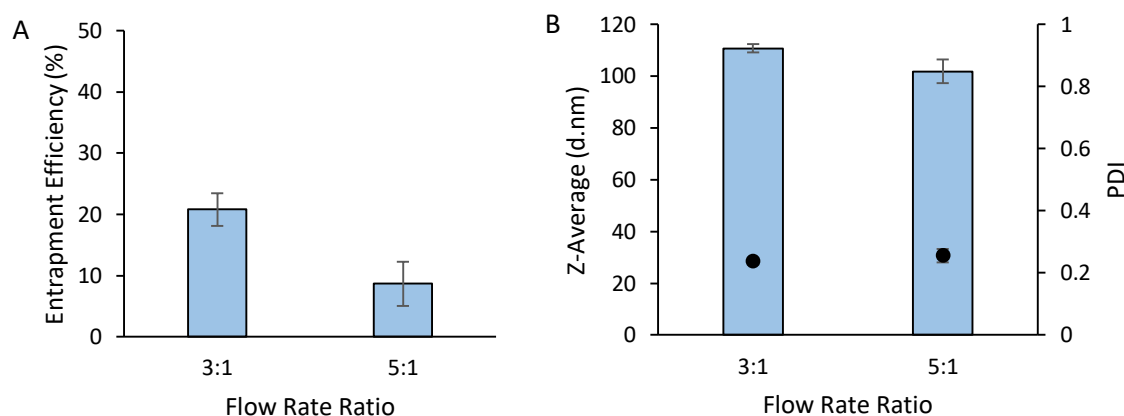


Figure 4.7 The effect of microfluidic process parameter flow rate ratio on entrapment efficiency and liposomal physicochemical characteristics for the liposomal formulation (DSPC:Chol:PS 10:5:4 w/w) (A and B respectively). Total final lipid concentration was fixed at 1 mg/mL, with a final ovalbumin concentration of 0.525 mg/mL and a total flow rate of 15 mL/min. Results represent mean \pm SD, $n = 3$ of independent batches.

When determining the effect of the manufacturing parameter flow rate ratio on vesicle characteristics, it is important that other factors which could influence vesicle attributes are controlled for. As previously shown in chapter 2, lipid concentration influences the final vesicle size, therefore in order to account for this, the final lipid and ovalbumin concentrations for all flow rate ratios were matched. Despite this, differences were observed with the higher flow rate ratio (5:1) resulting in a significant reduction in encapsulation efficiency. The effect that the flow rate ratio has on encapsulation efficiency of liposomes during microfluidics is well documented (Leung et al., 2018, Cheng et al., 2010, Forbes et al., 2019, Roces et al., 2020, Webb et al., 2020). This may be a result of the shift in the interface between aqueous and organic streams, where at equal flow rate ratios (1:1), the mixing interface occurs at the centre of the channel. When the flow rate ratios are then increased (3:1, 5:1), the liquid interface shifts, impacting upon the fluid stream (Oellers et al., 2017, Carugo et al., 2016). This shift in how the fluid streams merge within the channel could therefore have consequences on how the lipid and protein phases interact, resulting in a change in encapsulation efficiency.

4.5.3.2 The effect of TFR on protein entrapment efficiency for neutral and anionic vesicles

The next microfluidic parameter to assess was total flow rate. Both formulations (DSPC:Chol and DSPC:Chol:PS) were assessed for their ability to entrap ovalbumin across manufacturing flow rate speeds between 5-20 mL/min, while a fixed FRR of 3:1 was selected. At manufacturing speeds above 10 mL/min, encapsulation efficiencies approximately 20 -28% were found for both formulations, however at the lowest production total flow rate (5 mL/min), a reduction in entrapment efficiency was found (11-13%) (Figure 4.8A and C). Despite this, no significant changes in physicochemical attributes could be found across all flow rates for both formulations (Figure 4.8B and D), in accordance with the trends observed in chapter 2 (Figure 2.7).

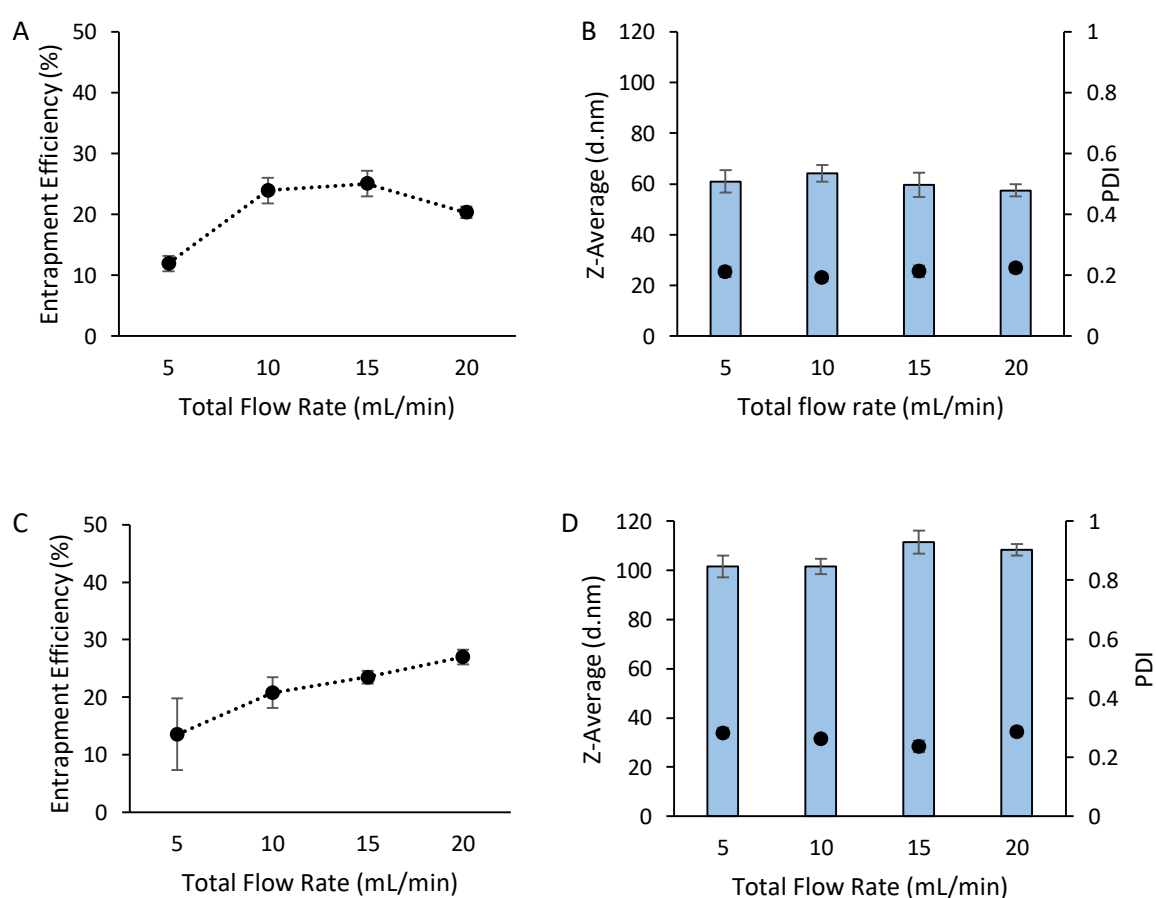


Figure 4.8 The effect of microfluidic process parameter total flow rate on entrapment efficiency and liposomal physicochemical characteristics for the liposomal formulation DSPC:Chol 10:5 w/w (A and B) and DSPC:Chol:PS 10:5:4 w/w (C and D). Total final lipid concentration was fixed at 1 mg/mL, with a final ovalbumin concentration of 0.525 mg/mL (initial concentrations of 4 mg/mL and 0.7 mg/mL respectively) and a flow rate ratio of 3:1. Results represent mean \pm SD, $n = 3$ of independent batches.

When production speeds of 10 mL/min and greater were applied, good encapsulation efficiencies were obtained (>20% for both formulations), however no apparent trends could be observed when operating above this total flow rate. Similar observations have been reported by Webb et al when

comparing microfluidic cartridge architectures (including a staggered herringbone micromixer, like the one used in these experiments), where encapsulation efficiencies of ovalbumin were found to be approximately 30% for 12, 15 and 20 mL/min with no significant differences observed (Webb et al., 2020). Furthermore, when optimising various PLGA nanoparticle formulations, total flow rate during microfluidic manufacture was shown to have no impact on antigen encapsulation efficiency for PLGA 75:25 and PLGA 85:15 (Roces et al., 2020). While flow rates above 10 mL/min have been found to result in little to no effect, slow production speeds (<10 mL/min) have previously been shown to exert a negative impact upon encapsulation efficiency. Roces et al found poor loading for PLGA 50:50 at 5 mL/min TFR (approximately 12%) (Roces et al., 2020). Additionally, total flow rate has been implicated to impact upon encapsulation when using phospholipid based nanoparticles, where higher mixing rates have been associated with improved loading using microfluidics (Correia et al., 2017). During large scale and GMP production of protein loaded nanoparticles, high throughput speeds are often employed (> 60 mL/min), therefore a loss of encapsulation efficiency as a result of low speeds (5 mL/min) will likely not be an issue (Webb et al., 2020, Forbes et al., 2019).

4.5.4 Tangential flow filtration as a tool for the concentration of protein loaded vesicles

Tangential flow filtration has been previously applied in a range of industries for the concentration of extracellular vesicles in an efficient and scalable manner with limited damage to the physicochemical characteristics of the product (Busatto et al., 2018, Casey et al., 2011, Cooper et al., 2011). Given the entrapment efficiencies shown here using microfluidics (typically between 20-30%), the ability to entrap high concentrations of protein in an efficient manner may be limited if there is a need for high dose therapeutics or vaccines. Therefore, to determine whether tangential flow filtration can be applied to concentrate protein loaded liposomes, anionic formulation DSPC:Chol:PS (10:5:4 w/w) was selected and manufactured by microfluidics, as a result of the lower protein loading found when using this anionic formulation. The sample was loaded with ovalbumin and subsequently purified as described previously. Following purification, a sample was removed for analysis of physicochemical characteristics, as well as protein quantification. Table 4.1 shows that as the sample is concentrated from 2 mL down to 1 mL, physicochemical attributes of the particles remain unchanged, while the protein concentration can be doubled.

Table 4.1 The effect of product concentration using Tangential flow filtration. Liposomal sample DSPC:Chol:PS (10:5:4 w/w) initial total lipid of 4 mg/mL, FRR 3:1 and TFR 10 mL/min was loaded with initial ovalbumin concentration of 15 mg/mL. The product was purified and then concentrated from 2 mL to 1 mL and assessed for protein concentration and vesicle physicochemical attributes.

Volume (mL)	Ovalbumin Concentration (mg/mL)	Z-Average (d.nm)	Polydispersity Index
2	0.51	182.7 ± 8	0.37 ± 0.01
1	0.94	188.5 ± 12	0.39 ± 0.02

4.5.5 Scale independent manufacture of protein loaded liposomes

Currently, various processing parameters influencing protein loading within neutral and anionic liposomal formulations have been established, including flow rate ratio, total flow rate and initial protein concentration. The next step was to determine whether the manufacturing and purification process could be scaled up in order to meet large scale production demands. Two batches of DSPC:Chol (10:5 w/w) loaded with ovalbumin were manufactured, one on bench-scale (NanoAssemblr, 1-15 mL production volume range) and the other larger scale (Blaze, 10 mL – 1 L production volume range). The formulations were then purified using TFF to remove untrapped protein and solvent and protein quantification was measured using RP-HPLC. Figure 4.9A indicates the reproducibility of the results across both of the manufacturing scales in terms of particle size (53 and 48 nm) and protein loading achieved (34 and 38%). When comparing intensity plots derived from dynamic light scattering for both formulations, highly comparable plots could be observed (Figure 4.9B). These results indicate the potential microfluidics has as both a large scale manufacturing and bench-scale developmental platform for protein loaded liposomal formulations entrapping protein, alongside down-stream processing techniques such as TFF.

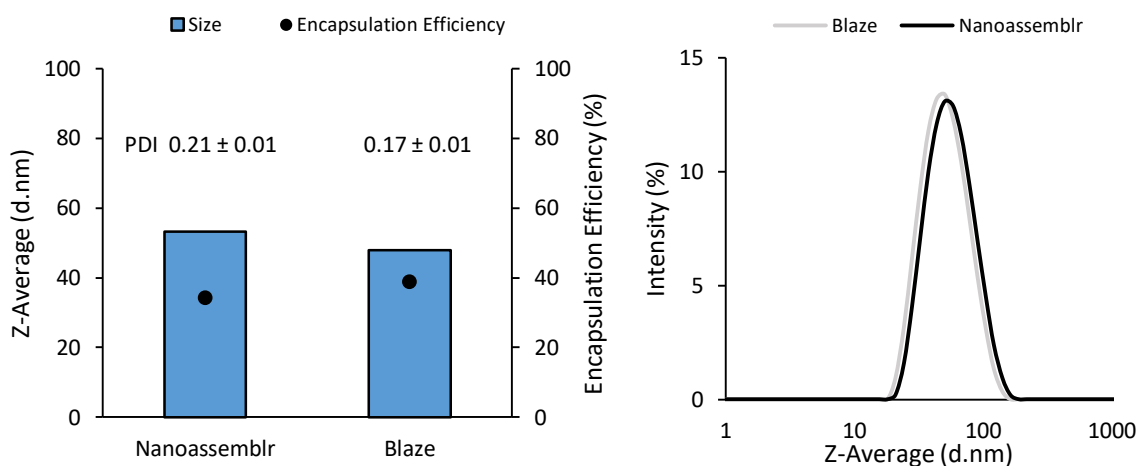


Figure 4.9 Scale-independent production study. Liposomal formulation DSPC:Chol (10:5 w/w) was manufactured at a 3:1 FRR, 15 mL/min TFR at a concentration of 4 mg/mL (initial 0.25 mg/mL ovalbumin) using both NanoAssemblr (2 mL) and Blaze (20 mL). (A) Particle size, PDI and loading efficiency for both batches, (B) overlay of the intensity plots derived from dynamic light scattering.

4.5.6 Microfluidic complexation using cationic vesicles

Up until now, the protein loading optimisation using microfluidics has been conducted using neutral and anionic formulations where the protein has been entrapped within the aqueous core of the vesicles. However, the inclusion of cationic lipids to vaccine adjuvant formulations is common practice to enhance immune responses towards specific antigens (Schwendener, 2014). When employing cationic liposomes as vaccine adjuvants, protein can be surface adsorbed to the cationic liposomes taking advantage of the electrostatic disparity between the vesicles surface and anionic moieties within the protein. Furthermore, increases in immunogenicity when compared to anionic and neutral vesicles have been observed, potentially a result of non-specific cellular toxicity as well as increases in depot formation at the site of injections, enhancing APC interaction (Agger et al., 2008, Shi and Rock, 2002, Henriksen-Lacey et al., 2010c). Therefore, in order to screen a range of formulations for both *in vitro* and *in vivo* efficacy, cationic formulations with surface adsorbed antigen were developed.

4.5.6.1 Optimisation of empty vesicles: Microfluidic parameters

Prior to protein adsorption optimisation, initial experiments focused on the microfluidic parameters for the manufacture of the empty vesicles. In order to determine the critical process parameters during microfluidic manufacture for positively charged vesicles, three cationic liposomal formulations were selected and screened for the effect of flow rate ratio (FRR) on particle size, PDI and surface charge while total flow rate was fixed at 15 mL/min, as a result of previous optimisation work done using this microfluidic system in our laboratory. Cationic formulations DSPC:Chol:DOTAP, DSPC:Chol:DDA were selected, using a weight to weight ratio of 10:5:4 as previously optimised

(chapter 2), while DDA:TDB was selected at 5:1 w/w (Christensen, 2017). Results in Figure 4.10 show that as the flow rate ratio between aqueous and solvent phases increases from 1:1 – 5:1 there is a gradual trend of increasing vesicle size for DSPC:Chol:DOTAP liposomes (72 ± 7 nm to 90 ± 10 nm). However, this increase in particle size resulted in a decrease in particle homogeneity with both 3 and 5:1 FRRs resulting in PDIs of approximately 0.6, while the 1:1 FRR resulted in a PDI value of 0.14 ± 0.06 (Figure 4.10). All three FRRs resulted in vesicles that were highly cationic (55 – 65 mV; Figure 4.10). To determine whether this trend could be found by substituting cationic lipid DOTAP with a cationic, micelle forming surfactant – DDA was selected due to its potential TH-1 stimulating effects. Unlike DOTAP, a 1:1 FRR resulted in vesicle sizes of 46 ± 1.6 nm while increasing the FRR to 3 and 5:1 led to no significant changes in particle sizes (46.5 ± 2.6 nm and 47 ± 3.4 nm respectively). Polydispersity index showed a slight increase as the FRR increases from 1 to 5:1 (0.22 ± 0.03 , 0.27 ± 0.04 and 0.26 ± 0.03 respectively; Figure 4.10). All of the vesicles exhibited highly cationic surface charges (30 – 50 mV). Finally, cationic adjuvant liposomal formulation DDA:TDB was produced by microfluidics to determine the impact of flow rate ratio on vesicle size and homogeneity. The effect of flow rate ratio on formulation DDA:TDB was much more apparent in comparison to the two previous cationic formulations tested. Flow rate ratio 1:1 resulted in micrometer scale vesicles > 2500 nm (data not shown) with high levels of heterogeneity (PDI 0.98). Following manufacture at 3:1 FRR, vesicle size decreased significantly to 142 ± 9.2 nm with a PDI of 0.3 ± 0.08 ($p < 0.05$). This trend of decreasing vesicle size was also found for FRR 5:1 (130 ± 51 nm); however, the homogeneity of the formulation was lost, with a PDI of 0.6 ± 0.3 . Zeta potentials were found to be between 40 – 50 mV across all three flow rate ratios (Figure 4.10)

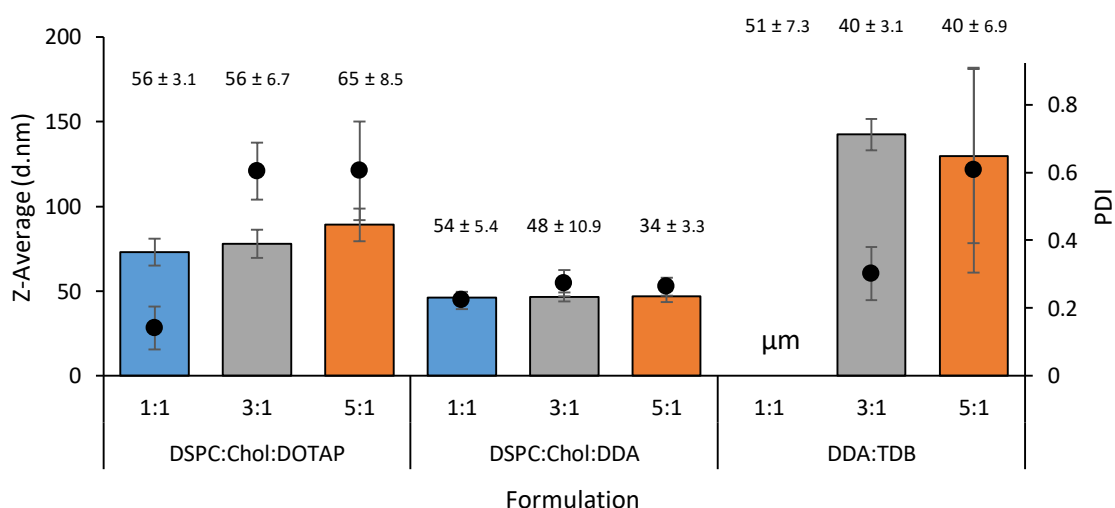


Figure 4.10 The effect of flow rate ratio on empty cationic liposomal formulations produced by microfluidics. Particles were prepared at at 3.6 mg/mL (DDA:TDB 5:1 w/w, IPA) and 4 mg/mL (DSPC:Chol:DOTAP/DDA 10:5:4 w/w, methanol) initial total lipid, with TRIS buffer 10 mM, pH 7.4 as aqueous phase. A total flow rate of 15 mL/min was selected, while flow rate ratios were increased through 1,3 and 5:1. For solvent purification, dialysis was conducted using TRIS buffer Average particle size (columns), polydispersity index (PDI) (circles) and Zeta Potential (mV) (values) are shown. Results represent mean \pm SD from three independent batches.

Previous work from our laboratory has shown the influence that flow rate ratio on the staggered herringbone micromixer has on particle size and homogeneity for both neutral and anionic formulations (Forbes et al., 2019, Webb et al., 2020, Roces et al., 2020). When manufacturing cationic vesicles, Lou et al selected the 1:1 flow ratio when formulating both DOPE:DDA and DOPE:DOTAP liposomes due to favourable PDI values (<0.25), while Kastner et al also showed agreeable PDI values when using the 1:1 FRR for DOPE:DOTAP (<0.25) when compared to 3 and 5:1 (Lou et al., 2019, Kastner et al., 2014). The unsuitability of DDA:TDB with a low FRR of 1:1 has previously been shown by Roces et al, where the resulting particles were micrometre in scale, alongside very high heterogeneity with PDI values greater than 0.7 (Roces et al., 2019). Similarly, a FRR of 3:1 was selected as the most optimal processing parameter, due to the low size and importantly, low PDI values (<0.3). The authors attributed this high variance in particle physicochemical attributes to the effect of the flow streams in the staggered herringbone micromixer chip. A FRR of 1:1 results in an equal stream size of aqueous to solvent, while increasing the FRR reduces the size of the aqueous stream, resulting in smaller particles forming. The results from these studies indicate that the influence flow rate ratio has on formulation characteristics may be formulation specific, and general rules and trends for formulations cannot be assumed.

4.5.6.2 Microfluidic complexation: Identifying critical process parameters

We have hypothesized that by automating the surface adsorption of ovalbumin onto cationic vesicles, the resulting particle physicochemical attributes can be tightly controlled through the use of microfluidic processing parameters. In order to determine whether microfluidics can be used to control the surface adsorption of model antigen ovalbumin onto preformed cationic liposomes, DSPC:Chol:DOTAP and DSPC:Chol:DDA were selected for further investigation. The formulations were manufactured, purified to remove solvent and re-injected into the microfluidics system inlet, with ovalbumin in buffer (TRIS 10 mM) going through the second inlet. In order to reduce any confounding variables and to keep the ratio of liposome to protein constant, both the liposome concentration and ovalbumin concentration were adjusted to maintain a final ratio of 1:0.1 mg/mL (10:1 liposome: protein).

Initial studies focused on the effect of total flow rate on vesicle physicochemical attributes following complexation. The cationic liposomal formulation, DSPC:Chol:DDA (initial total lipid concentration of 4 mg/mL) was initially manufactured using a flow rate ratio of 1:1 to produce the empty vesicles. Following dialysis for solvent purification, controlled complexation was conducted by passing the particles back through the microfluidics system at a flow rate ratio of 1:1, with a final ovalbumin concentration of 0.1 mg/mL (10:1 liposome to protein ratio). To evaluate the effect of processing

speeds on complexation characteristics, total flow rates between 5 and 20 mL/min were chosen. Figure 4.11 shows the particle size and PDI values for the four total flow rates tested. The slowest speed of 5 mL/min resulted in vesicle sizes of 204 ± 5.0 nm with a homogenous polydispersity index of 0.18. These results were highly comparable to the 10 mL/min speed, where the resulting particles were found to be 209 ± 9.3 nm with PDI values of 0.19. However, as the speed was increased to 15 and 20 mL/min, particle size variations could be observed. A total flow rate of 15 mL/min resulted in larger vesicles at 233 ± 8.8 nm, while 20 mL/min exhibited vesicles at 218 ± 7.4 nm. The polydispersity index of these two faster flow rates also showed higher values when compared to 5 and 10 mL/min, with values of 0.22 and 0.21 being found for 15 and 20 mL/min rates respectively. The surface charge of the four total flow rates remained unaffected, with all surface charges being found between 35 – 37 mV.

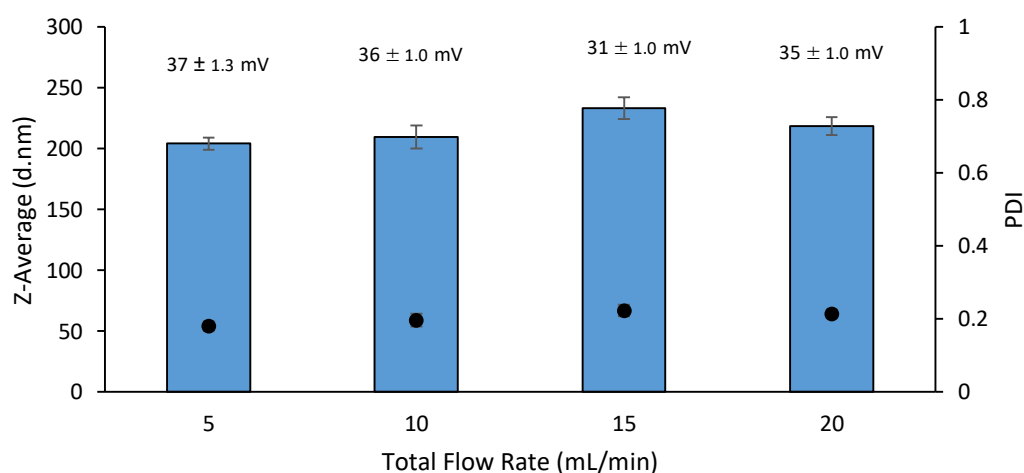


Figure 4.11 The effect of total flow rate on cationic liposomal formulations during complexation. Empty DSPC:Chol:DDA 10:5:4 w/w was prepared in TRIS buffer 10 mM, pH 7.4 at a flow rate ratio of 1:1 and purified by dialysis. The purified particles were then passed back through the NanoAssemblr in one inlet, with ovalbumin in TRIS passed through the second inlet using a fixed flow rate ratio of 1:1. Total flow rates of 5,10,15 and 20 mL/min were assessed and a final liposome: ovalbumin ratio of 10:1 w/w was chosen. Average particle size (columns) and polydispersity Index (PDI) (circles) are shown with zeta potential in text above. Results represent mean ± SD from three independent batches.

As shown previously, FRR has a significant impact upon vesicle formation by varying the size of the fluid streams, therefore 1, 3 and 5:1 FRRs were tested to assess the impact this could have on the ovalbumin surface adsorption onto the cationic vesicles, while the total flow rate was fixed at 15 mL/min. The results from Figure 4.12 show both DSPC:Chol:DOTAP and DSPC:Chol:DDA (final lipid concentration of 1 mg/mL) with 0.1 mg/mL ovalbumin surface adsorbed, across the three FRRs. A FRR of 1:1 results in larger vesicles of 224 ± 23 nm, while 3 and 5:1 resulted in smaller vesicles of 140 ± 2.3

nm and 151 ± 5.1 nm respectively for DSPC:Chol:DOTAP, with all flow rate ratios being significantly different ($p < 0.05$). Interestingly, the difference in the size of the vesicles did not correspond to a difference in homogeneity of the vesicle populations, with all three of the formulations resulting in PDI values less than 0.19 (Figure 4.12). Zeta potentials of the three FRRs were found to remain cationic, between 31 and 37 mV (Figure 4.12). Unlike the DOTAP formulation, there is a trend of low FRRs resulting in the smallest vesicle sizes following antigen adsorption for DSPC:Chol:DDA. FRR is shown to have a significant impact on vesicle size, with 1:1 resulting in vesicles around 233 ± 8.8 nm, while 3 and 5:1 increased the vesicle sizes to 272 ± 18.8 nm and 335 ± 34.8 nm respectively ($p < 0.05$). This trend was also observed slightly with the PDI values for the vesicles, with 1:1 resulting in the greatest homogeneity and 3 and 5:1 increasing the PDI value gradually (0.22, 0.23 and 0.29 respectively; Figure 4.12). The surface charge of the DSPC:Chol:DDA particles following ovalbumin adsorption was unaffected by the FRR chosen, with 1, 3 and 5:1 FRRs resulting in cationic surface charges of 34 ± 1 , 31 ± 1 and 29 ± 1 mV respectively (Figure 4.12).

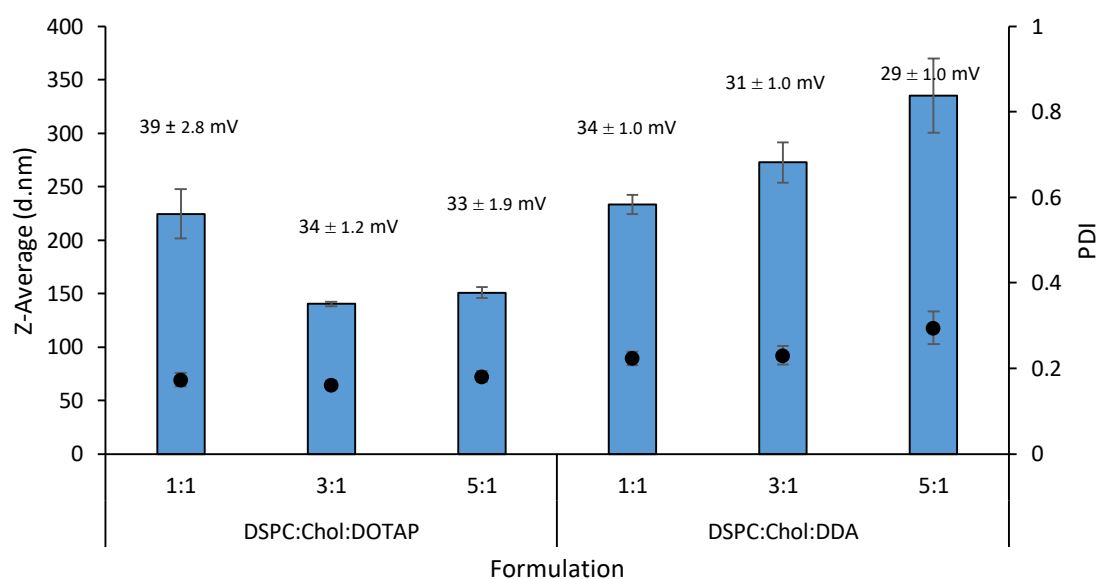


Figure 4.12 The effect of flow rate ratio on cationic liposomal formulations during complexation. Empty DSPC:Chol:DOTAP/DDA 10:5:4 w/w were prepared in TRIS buffer 10 mM, pH 7.4 at a flow rate ratio of 1:1 and purified by dialysis. The purified particles were then passed back through the NanoAssemblr in one inlet, with ovalbumin in TRIS passed through the second inlet at three flow rate ratios (1, 3 and 5:1) using a fixed total flow rate of 15 mL/min. Both final lipid and ovalbumin concentrations were fixed at 1 mg/mL and 0.1 mg/mL respectively. Average particle size (columns) and polydispersity Index (PDI) (circles) are shown with zeta potential in text above. Results represent mean \pm SD from three independent batches.

Despite all of the final liposome and ovalbumin concentrations being fixed, the flow rate ratios have a significant impact on the final size of the ovalbumin adsorbed vesicles. When cationic vesicles are

exposed to net negatively charged protein such as ovalbumin, the electrostatic binding can be described as a uniform coverage of the liposomal vesicles by the protein which is related to the overall surface charge of the liposomes, vesicle size and protein concentration (Letizia et al., 2007). Currently, complexation experiments have been conducted using a liposome to protein ratio of 10:1 (1 mg/mL final liposome concentration with 0.1 mg/mL ovalbumin). To determine whether this ratio is a key parameter for final particle physicochemical characteristics, cationic formulation DSPC:Chol:DDA (10:5:4 w/w) was again selected and liposome to protein ratio was incrementally adjusted from 10:1 w/w to 1:3 w/w. As the concentration of ovalbumin was increased from 10:1 to 3:1 ratio a trend of increasing vesicle size can be observed (Figure 4.13A). Across low concentrations of ovalbumin (10:1 – 7:1) vesicle sizes remained within the nanoscale and PDI remained <0.25 , however when ovalbumin concentrations increased to both 5 and 3:1 w/w ratios vesicle size dramatically increased (1248 ± 94 nm and 4551 ± 767 nm respectively), with heterogeneous PDI values (>0.3). However, when ovalbumin was increased to a 1:1 ratio with the liposomes, vesicle size greatly decreased again to 232 ± 12 nm with a PDI value of 0.14. This trend was then further observed as ovalbumin was increased to an excess ratio of 1:3, where vesicle size was measured at 168 ± 3 nm and a PDI value of 0.11 (Figure 4.13A). The surface charge of the vesicles surface coated with ovalbumin following complexation is shown in Figure 4.13B. As the ovalbumin concentration is increased, a steady decrease in surface charge can be observed from 53 mV (10:0) down to -19 mV (1:1), however a surface charge plateau can be seen after 1:1, where the addition of higher concentrations of ovalbumin did not affect the overall surface charge of the particles (Figure 4.13B).

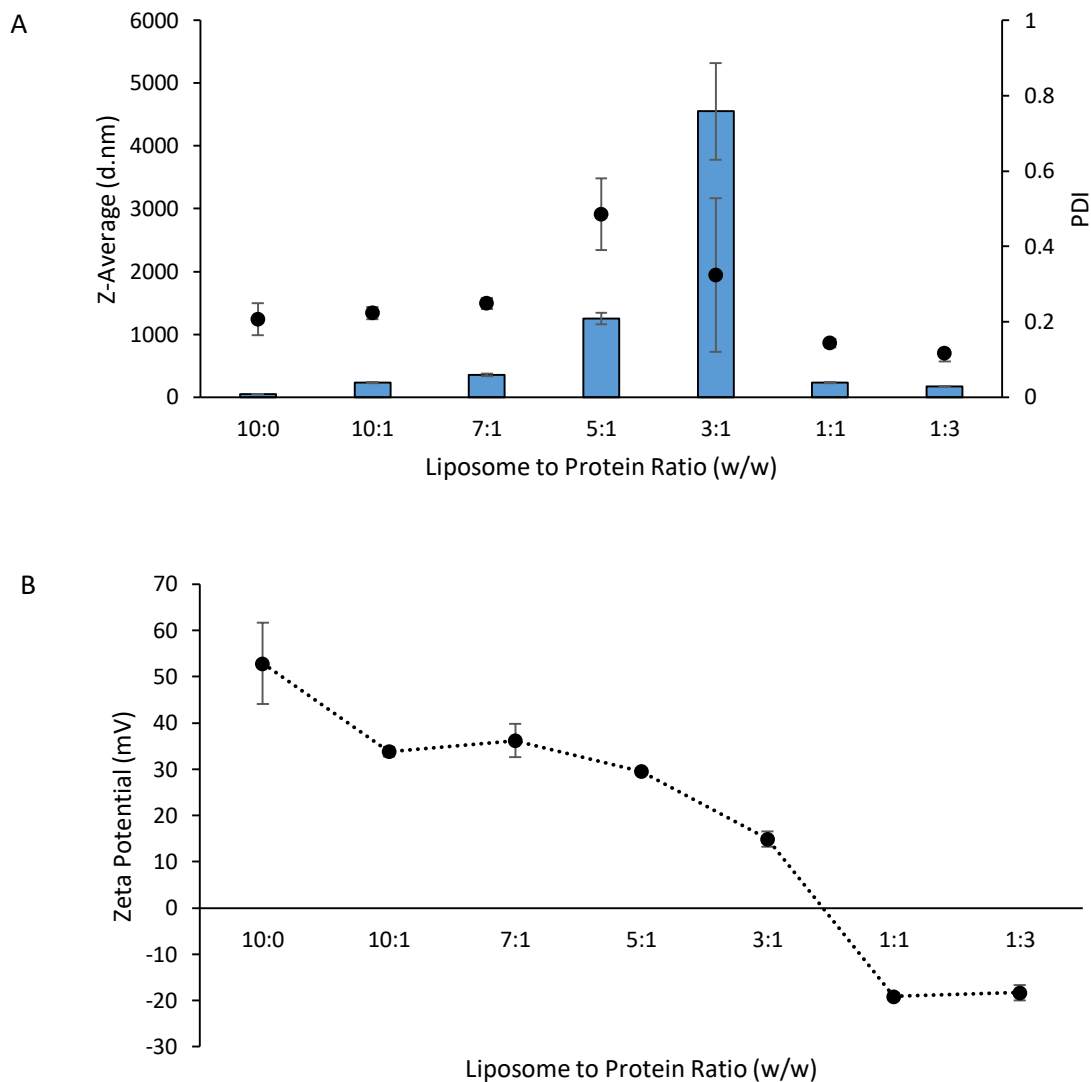


Figure 4.13 The effect of liposome to protein ratio following complexation. DSPC:Chol:DDA (10:5:4 w/w) was produced at an initial total lipid concentration of 4 mg/mL in methanol, with TRIS 10 mM pH 7.4 as aqueous phase. Following purification, complexation was conducted by passing the liposomes back through the NanoAssembler alongside ovalbumin in TRIS at a flow rate ratio of 1:1. Final albumin concentrations were scaled from 10:1 to 1:3. (A) Average particle size (columns) and polydispersity Index (PDI) (circles) are shown (B) Average Zeta Potential (mV). Results represent mean \pm SD from three independent batches.

The adsorption of the negatively charged protein (ovalbumin) onto the cationic vesicles surface has previously been shown within our laboratory to result in an increase in vesicle size as well as a reduction in the overall surface charge of the complexes (Chatzikleanthous et al., 2020). These results demonstrate that liposome to protein ratio is a critical process parameter, which will be essential for designing nanoscale systems with homogenous populations. Previous work conducted by Sarker et al have shown similar results when investigating the effect of synthetic cationic lipids and albumin ratios during complexation at pH 7.4. The team showed an increase in vesicle size as lipid concentration was decreased. At a ratio of 60:15 w/w lipid: albumin vesicle size was found to be 883 nm with a surface charge of 35 ± 3 mV, and as the lipid component was increased to 300:15 w/w lipid: albumin, vesicle

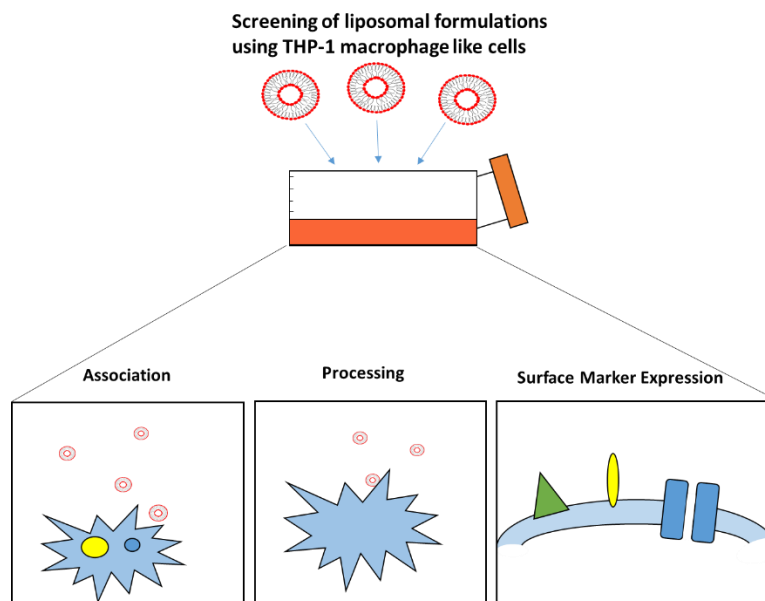
size decreased to 357 nm with a surface charge of 47 ± 2 mV. While the manufacturing method for this complexation was manual mixing, as opposed to microfluidics, it is evident that as protein increases in comparison to the cationic liposome component, vesicle size increases. However, the authors did not continue this investigation to protein excess (as was done here) and no polydispersity index values were mentioned. The authors did however attribute the decrease in surface charge to the gradual neutralization of the cationic vesicles surface, while size increases were a result of an increase in aggregation points for the albumin liposome complexes, resulting in larger vesicle aggregates (Sarker et al., 2014). Similar findings are also observed when producing lipoplexes (cationic liposome and DNA complexes). The ratio of lipid and DNA charge has been shown to be critical during the mixing process, where charge ratios between 1:1 and 2:1 (lipid to DNA charge) result in the largest vesicles, while less balanced ratios (e.g. 4:1 or 1:2) yielded smaller lipoplex diameters (Xu et al., 1999). Based on these results, this controlled microfluidic mixing protocol was adapted and used for the production of liposomal formulations used *in vitro* (Chapter 5) and *in vivo* (Chapter 6).

4.6 Conclusions

The results demonstrate the applicability of microfluidics as a manufacturing platform for the production of both neutral and anionic liposomal formulations incorporating model antigen ovalbumin. Critical process parameters for efficient loading are established, including both FRR and TFR, where the optimal conditions were found to be 3:1 and speeds of 10 mL/min and above. The use of tangential flow filtration as a purification and concentration system for formulations incorporating protein was demonstrated, as well as a proof-of-concept scale-out study where larger volumes of DSPC:Chol liposomes entrapping protein are mapped to the bench scale production. Finally, the use of microfluidics as an automated tool for controlling the surface adsorption of ovalbumin onto preformed cationic vesicles is shown and key processing parameters are identified to be FRR, as well as the ratio between the liposome and protein components. To see how these protein loaded formulations function as immune adjuvants, selected formulations will next be tested *in vitro* on a macrophage like cell line, where cellular association, antigen processing and effect on cell surface marker expression will be examined.

Chapter 5

In vitro vaccine study: cellular association, antigen processing and surface marker expression



5.1 Introduction

Mononuclear phagocytes such as monocytes, macrophages and dendritic cells (DCs) play a critical role within the immune system, connecting the innate branch of immunity to memory through antigen processing and presentation. Peripheral monocytes can act as precursors to both macrophages and DCs, differentiating into a range of specialised functions such as maturation into inflammatory macrophages in response to inflammation as a result of injury or infection (Jakubzick et al., 2017, Randolph et al., 2008). Previously, sessile classification of surface cellular markers was used to identify these cells. However advancements in techniques such as flow cytometry has led to the realisation that these markers are not so definitive and many are shared by different mononuclear phagocytes to varying degrees of expression, based on tissue localisation and the environmental stimuli they are exposed to (Guilliams et al., 2014, Daigneault et al., 2010). The recognition of foreign organisms (and self-associated antigens) through a range of pattern recognition receptors (PRRs) enables these cell types to orchestrate appropriate immune responses through cytokine and chemokine production and primary activation of naive T cells (Randolph et al., 2008). Antigen presenting cells (APC), such as macrophages and DCs, phagocytise foreign material, process the material, and load the peptide fragments onto their major histocompatibility complex (MHC) I or II for antigen-presentation (Savina and Amigorena, 2007). Once an APC has encountered and processed an antigen, a decrease in phagocytic ability and an altered expression rate of specific activation markers occurs including upregulation of MHC II expression on the cellular surface (Banchereau and Steinman, 1998, Berges et al., 2005). During this presentation phase, co-stimulatory molecules are necessary along with the primary binding of processed antigen to the T-cell antigen receptor (TCR). Examples of essential co-stimulatory molecules for T cell activation is the cluster of differentiation 40 and 80 (CD40, CD80) found on the APC (Martinez et al., 2008). For example, Lynch et al have previously shown that macrophages exposed to virulent ribotypes of *C. difficile* surface layer proteins produced high levels of pro-inflammatory cytokines and cell surface markers, such as the up regulation of CD40, CD80 and MHC II (Lynch et al., 2017, Ryan et al., 2011).

The use of nanocarrier systems, including liposomes, to promote antigen delivery and thus enhance vaccine efficacy offers a range of advantages given the inherent flexibility of these delivery systems. As shown in Chapter 4, liposomal formulations can be manufactured by microfluidics in a range of sizes, different lipid compositions and surface charges, as well as different antigen loading locations (entrapped or surface adsorbed). These attributes can greatly impact upon what type of immune response is generated. For example, *in vivo* studies have shown that through microfluidic manufacturing of small cationic vesicles (< 50 nm) composed of DOPE:DOTAP or DOPE:DDA, lymphatic accumulation can be increased when compared to their larger vesicle counterparts (500 – 750 nm),

which were found to persist longer at the injection site (Lou et al., 2019). Furthermore, the effect of bilayer rigidity has been shown to impact upon immune response through a bias towards Th1- type classification. Cationic liposomes composed of DDA:TDB (rigid) were found to result in an 100-fold increase in APCs expressing CD40 and CD86 co-stimulatory molecules when compared to a more fluid liposomal counterpart (DODA:TDB), a result of the retention of the DDA:TDB and antigen at the injection site (Christensen et al., 2012). The effect of modifying surface charge by employing cationic lipid components to produce positively charged vesicles as vaccine adjuvants has been thoroughly explored, taking advantage of the electrostatic attractions of the positively charged liposomal surface and negatively charged cell surface for high degrees of adsorption (Korsholm et al., 2012).

Given the diversity in physicochemical properties available when choosing a delivery system and the subsequent impact this has upon *in vivo* pharmacokinetic profile, a deeper understanding of how these physicochemical alterations affect cellular mechanisms could prove valuable. Currently, there remains some controversy in relation to the correlation between *in vitro* immunological models and their *in vivo* counterparts, making it difficult to translate between the two systems (Kelly et al., 2011). For example, monocyte/macrophage cytokine inhibition/ activation following exposure to various liposomal formulations (varying in size and charge) was found to show limited correlation to the bioactivity found in both rat and rabbit models (Epstein-Barash et al., 2010). Standard cell cultures are generally conducted in static fluid flow conditions, with foreign serum (FBS) and grown in a single-cell type environment, which can impact upon gene expression and therefore impact on *in vitro in vivo* correlations (Paunovska et al., 2018). However, despite the high degree of complexity associated with *in vivo* immunological models, *in vitro* models are often employed during the nonclinical stage of drug and vaccine development. Specific models can be used to predict blood compatibility and potential anaphylactic reactions are screened by monitoring complement activation *in vitro* (Zamboni et al., 2018). Furthermore, common markers such as phagocytosis and pro-inflammatory cytokine induction has been shown to generate predictive data across both *in vivo* and *in vitro* models, and in the case of identifying cytokine storm induction, the *in vitro* model employing human peripheral blood mononuclear cells was found to accurately predict outcomes when compared with both rat and non-human primate models (Zamboni et al., 2018, Dobrovolskaia, 2015).

In relation to the use of primary macrophages within *in vitro* experimentation, some challenges arise due to difficulties associated with the need for extraction from individual donors resulting in large phenotypic variability and low cell numbers, therefore immortalized monocytic cell lines can be employed to potentially overcome some of these issues (Daigneault et al., 2010). In these studies, the immortalized human monocytic cell line THP-1 was selected (originally sourced from the peripheral blood of an individual with acute leukaemia) as it is widely used as a model *in vitro* system for the

study of monocytes due to its ease of cultivation, relatively fast growth rate and homogenous genetic makeup. (Bosshart and Heinzelmann, 2016, Chanput et al., 2014). The THP-1 monocytic cell line has been shown to be capable of differentiation, through incubation of particular stimuli, into both macrophage-like phenotypes or immature and mature DCs with phenotypes comparable to that of donor cells (Berges et al., 2005, Daigneault et al., 2010). Here, a previously established protocol using VD3 has been adopted to differentiate the monocytes into cells that exhibit more macrophage-like characteristics.

The objectives of these studies were to determine whether a simplified *in vitro* model using macrophage-like cells could be used as a rapid screening tool for liposomal vaccine formulations in order to help direct the delivery system selection process for vaccine development. Vesicle association, antigen processing using DQ-OVA and the tracking of specific activation markers on the cells surface following exposure to the formulations is assessed.

5.2 Aim and Objectives

The aim of this chapter was to screen a range of liposomal formulations in an *in vitro* setting to determine their ability as vaccine adjuvants. A number of formulations were selected ranging in adjuvanticty, vesicle surface charge and where the antigen is located (entrapped within, or surface exposed). Using a monocyte/macrophage cell line, some of these cellular mechanisms which can impact upon the immunological efficacy of a delivery system *in vivo* are investigated. In order to achieve this, the objectives within this chapter were to:

- Determine the cellular association of the formulations incorporating antigen (ovalbumin).
- Evaluate the ability of the cells to then process the antigen (using a fluorescently labelled ovalbumin – DQ-OVA) across the formulations selected for testing.
- Finally, investigate whether these formulations (and their antigen) can impact upon the surface marker expression of the cells.

5.3 Materials

The lipids 1,2-distearoyl-sn-glycero-3-phosphocholine (DSPC), cationic surfactant dimethyldioctadecylammonium bromide (DDA) and immunopotentiator trehalose 6,6'-dibehenate (TDB) were all purchased from Avanti Polar Lipids Inc., Alabaster, AL, US. Cholesterol and ovalbumin (OVA) were purchased from Sigma Aldrich Company Ltd., Poole, UK. Tris-base was obtained from IDN Biomedical Inc. (Aurora, OH, United States) and used to make 10 mM Tris buffer, adjusted to pH 7.4 using HCl. For dialysis purification, Biotech CE Tubing MWCO 300 kD was used (Spectrum Inc., Breda, The Netherlands). Methanol, 2-propanol (IPA) and Dil Stain (1,1'-Dioctadecyl-3,3,3',3'-Tetramethylindocarbocyanine Perchlorate ('Dil'; DiIC18(3))) were purchased from Fisher Scientific, Loughborough, England, UK. Formaldehyde 4% in PBS was purchased from Alfa Aesar, Thermo Fisher Scientific, Lancashire, UK. $1\alpha,25$ -Dihydroxyvitamin D₃ (Vitamin D₃) was purchased from Enzo Life Sciences, Exeter, UK. RPMI medium 1640 (+ L-Glutamine), Phosphate buffered saline pH 7.4 (1x) and Fetal bovine serum (FBS) were ordered from Gibco, Life technologies, Thermo Scientific., Hampstead, England, UK. Monoclonal antibodies Anti-Hu HLA-DR (APC- eFluor), Anti-Hu CD40 (eFluor 450), Anti-hu CD80 (PE-Cyanine7), CD14 and DQtm ovalbumin conjugate and UltraComp eBeads were purchased from Invitrogen, Thermo Scientific (Life Technologies Ltd), Renfrew, UK. Fc Block (Human Trustain FcX) was purchased from Biolegend, London, UK. All water and solvents used were HPLC grade. THP-1 cells were kindly gifted from Dr. Dino Rotondo (SIPBS, University of Strathclyde, Glasgow) while 1,2-dioleoyl-sn-glycero-3-phospho-L-serine (sodium salt) (DOPS) was gifted from Avanti Polar Lipids Inc., Alabaster, AL, US.

5.4 Methods

5.4.1 Liposome manufacture and purification

The preparation of liposomes by microfluidics was conducted on the NanoAssemblr Platform (Precision NanoSystems Inc., Vancouver Canada). Formulations DSPC:Chol (2:1 w/w), DSPC:Chol:DOPS (10:5:4 w/w), DDA:TDB (5:1 w/w) and DSPC:Chol:DDA (10:5:4 w/w) were selected for investigation. Lipid stocks had 0.2 mol% of DiIC added following dissolution in methanol (or in the case of DDA: TDB, IPA). Liposomes were manufactured using a flow rate ratio of 3:1, 15 mL/min total flow rate to a final liposome concentration of 4 mg/mL. For the cationic formulations DSPC:Chol:DDA and DDA:TDB, TRIS buffer 10 mM pH 7.4 was used as aqueous phase. Following production, purification of residual solvent was conducted by dialysis (1 mL sample to 200 mL buffer for 1 h under magnetic stirring), before the addition of DQ-OVA to the surface of the liposomes at a final concentration of 100 μ g/mL. For neutral and anionic formulations DSPC:Chol and DSPC:Chol:DOPS respectively, DQ-OVA was loaded in-line

during manufacture at a final concentration of 0.525 mg/mL with PBS. The samples were then purified for both solvent and un-encapsulated ovalbumin using 24 h dialysis, with buffer exchange every 2 h, followed by overnight dialysis under fast magnetic stirring. Following purification, all the completed liposome formulations were then diluted in serum-free RPMI media, before treatment to the cells (at a final well concentration of 10 µg/mL).

5.4.2 THP-1 culture and differentiation

The human monocyte/macrophage-like cell line THP-1 was cultured in complete RPMI media (10% fetal bovine serum, 1% penicillin-streptomycin) and kept at 37°C, 5% CO₂. In order to differentiate the monocytic cells into macrophage like phenotypes, a previously published protocol was followed (Daigneault et al., 2010, Henriksen-Lacey et al., 2011b). Briefly, cells were adjusted to 5x10⁵/mL and 100nM Vitamin D3 was added before a 48h incubation at 37°C, 5% CO₂. Cell counting was conducted using a haemocytometer grid, where the average of the sets of 16 corner squares was counted by light microscopy, multiplied by 10⁴ and then multiplied by any dilution factors (as per manufacturer's instructions).

5.4.3 Liposome association and DQ-OVA studies

DQ-OVA is designed for the study of antigen processing, is a self-quenched conjugate of ovalbumin and upon proteolytic degradation, exhibits bright green fluorescence. DiIC is a hydrophobic dye (which exhibits red fluorescence) that accumulates within the liposomal bilayer, thus can be incorporated into the lipid stock prior to liposome manufacturing and used to evaluate liposome association to cells. Once differentiated, the macrophage-like THP-1 cells were added at a density of 1x10⁶ / mL (2.4 mL per well) to a 24-well plate in serum-free RPMI. Liposome formulations were added to the wells at a final concentration of 10 µg/mL containing both DQ-OVA and DiIC. For ovalbumin controls, DQ-OVA alone was added in TRIS buffer and serum-free RPMI at the same concentration as the liposome samples, while negative control wells received just serum-free RPMI. Time-points were mixed and removed from the incubator (37°C, 5% CO₂) at 0, 30, 60, 120, 180, 240 and 1440 minutes. After the 200 µL samples were removed, they were added to 500 µL FACS-buffer and centrifuged at 300 g for 5 minutes. The pellet was then resuspended in 4% paraformaldehyde and incubated for 20 minutes at 4°C in the dark. The FACS-buffer wash cycle was then repeated twice more before being resuspended in 200 µL FACS buffer and transferred to a 96-well plate for FACS analysis.

5.4.4 Activation markers

In order to assess the phenotypic changes of the differentiated THP-1 macrophage-like cells following liposome formulation exposure, a number of cellular markers were selected. The differentiated THP-1 cells were again plated at a final concentration of 1×10^6 /mL and exposed to the liposomal formulations, ovalbumin controls and negative controls as described above. Following a 24 h incubation, samples were removed and centrifuged with 500 μ L FACS buffer at 300 g for 5 minutes (twice), followed by the addition of 10 μ L of Fc-block. The samples were incubated for 10 minutes at 4°C, before the addition of 50 μ L of antibody mix (CD14, CD40, CD80 and MHC II diluted 1:200 in FACS-buffer). The samples and antibody mixtures were then further incubated for 30 minutes in the dark at 4°C. The samples were then washed in FACS buffer three more times, before being resuspended in 200 μ L of FACS buffer and transferred to a 96-well plate for FACS analysis.

5.4.5 Flow cytometry analysis

Flow cytometry was conducted on the Attune NxT Flow Cytometer coupled with an Attune NxT Autosampler for 96-well plate measurements, while data was analysed using the Kaluza analysis software v2.1.1. During analysis, a minimum of 10,000 events were recorded for each sample. Multi-colour compensation for the antibody panel was conducted on UltraComp ebeads from Invitrogen, briefly antibodies (1:200) were incubated with a drop of beads at 4°C in the dark, before wash cycles and transfer to a FACS tube. DQ-OVA and DiIC compensation were prepared in the same manner, however instead of beads, differentiated THP-1 cells and liposome formulation were used. MFI (median fluorescence intensity) and Geo-Mean was calculated using the Kaluza analysis software (v2.1)

5.4.6 Statistical analysis

Results are represented as mean \pm SD with n = 3 independent batches unless stated otherwise. ANOVA tests were used to assess statistical significance between groups with a Tukey's post adhoc test (p value of less than 0.05).

5.5 Results and Discussion

To investigate the impact of liposome formulation on cell association and/or uptake, antigen processing and expression of surface markers on differentiated THP-1 cells, four liposome formulations were selected. Table 5.1 outlines the physicochemical attributes of the four formulations: DSPC:Chol (10:5 w/w), DSPC:Chol:DOPS (10:5:4 w/w), DSPC:Chol:DDA (10:5:5 w/w) and DDA:TDB (5:1 w/w) following microfluidic manufacture. All formulations contained 0.2 mol% Dil within the bilayer of the liposomes, in order to detect the association ability of the formulations and the THP-1 differentiated cells. The physicochemical attributes of these formulations were in-line with the previous studies in Chapters 2 and 4. The liposome concentrations added per well (10 µg/mL) were selected based upon previously reported studies for cationic liposomes (DDA:TDB) using the THP-1 cell line (Kaur et al., 2013), while the DQ-OVA concentration was matched based on previous results from Chapter 4. The gating strategy used for analysis is shown in Figure 5.1, briefly singlets were selected (FSC-H vs FSC-A), followed by the gating of the THP-1 cells (SSC-A vs FSC-A). For the calculation of % positive cells, unstained controls were gated to ~2% in order to compensate for auto fluorescence.

Table 5.1 Physicochemical attributes (size, PDI and zeta potential) of the four formulations DSPC:Chol (10:5 w/w) DSPC:Chol:DOPS (10:5:4 w/w), DSPC:Chol:DDA (10:5:4 w/w) and DDA:TDB (5:1 w/w). Neutral and anionic formulations were dialyzed over night to remove untrapped DQ-OVA, while cationics were dialyzed for 1 h to remove solvent before the addition of fluorescent protein. Results represent mean \pm SD, n = 3.

Formulation	Size (d.nm)	PDI	Zeta Potential (mV)
DSPC:Chol	65.6 \pm 4	0.23 \pm 0.02	-5.5 \pm 3.0
DSPC:Chol:DOPS	111.8 \pm 4	0.22 \pm 0.05	-30.1 \pm 4.3
DSPC:Chol:DDA	44.8 \pm 1	0.25 \pm 0.01	48.0 \pm 9.8
DDA:TDB	141.4 \pm 4	0.23 \pm 0.01	39.4 \pm 3.0

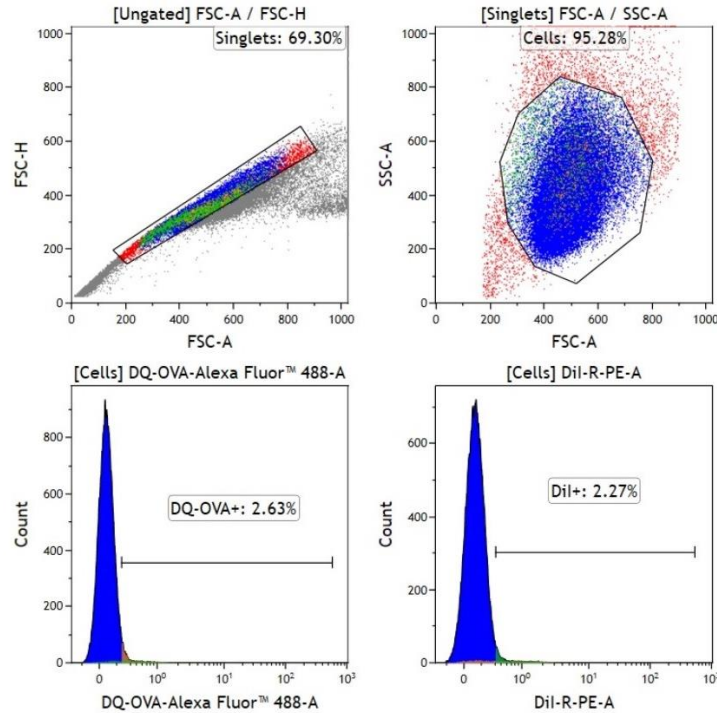


Figure 5.1 Gating strategy for the identification of differentiated THP-1 cells, with example DQ-OVA and DilC gating (selected at 2% for auto fluorescence). The example shown is the negative control (RPMI) THP-1 cells with no liposomal formulation added.

5.5.1 Determination of cellular association using a range of liposomal formulations

It should be stated that cellular association does not necessarily correlate to cellular internalisation, and without the use of optical or microscopic techniques, it can be a significant challenge when using cationic vesicles to differentiate between the two, therefore within this chapter the term association is used (Hou et al., 2016). Macrophage phagocytic receptors that are typically responsible for nanoparticle internalisation include TLRs, Mannose/lectin receptors (such as C-type lectin and mannan), Fc receptors and scavenger receptors (Gustafson et al., 2015). While determination of different uptake mechanisms can be achieved through incubation at 4°C to determine endocytosis, the scope of this study was focused primarily on simultaneous determination of association, followed by antigen processing (which is a critical factor in determining the suitability of a delivery system to enhance APC processing compared to free antigen alone). Figure 5.2 indicates the association of the formulations over a 24 h time period, as well as the control (cells without liposomes present). From these results it can be seen that both the neutral (DSPC:Chol) and anionic formulations (DSPC:Chol:DOPS) showed poor initial cellular association (Figure 5.2A). Initially, less than 3% of the THP-1 showed DSPC:Chol association (Figure 5.2B), however with this formulation an increase in % Dil positive cells was noted over time; within the following 4 h, up to 55% of the THP-1 exhibited Dil

fluorescence, and at 24 h the % of Dil positive cells was no different compared to the cationic formulations with all being >95% (Figure 5.2C). When considering the anionic liposome formulation (DSPC:Chol:DOPS), these liposomes promoted the slowest rate of cellular association (Figure 5.2A). Initially, a gradual association was observed, increasing up to 9% within the first 4 h of incubation (Figure 5.2B) and reaching ~ 70% of the cells showed Dil fluorescence after 24 h (Figure 5.2C). At both 4 h and 24 h, the % Dil positive cells were significantly ($p < 0.05$) lower than both the neutral and cationic formulations. Conversely, it can be seen that both cationic formulations DSPC:Chol:DDA and DDA:TDB showed high association with the THP-1 (greater than 80% of the cells showed Dil fluorescence) as soon as the formulations were added to the cell well. Formulation DSPC:Chol:DDA then displayed over 90% Dil positive cells across the following 4 h, while DDA:TDB indicated above 85% Dil positive cells (Figure 5.2B). At the final time point of 24 h, both cationic formulations and neutral formulation DSPC:Chol showed strong association (>95%), however anionic formulation DSPC:Chol:DOPS was found have significantly reduced association in comparison ($p < 0.05$) (Figure 5.2C).

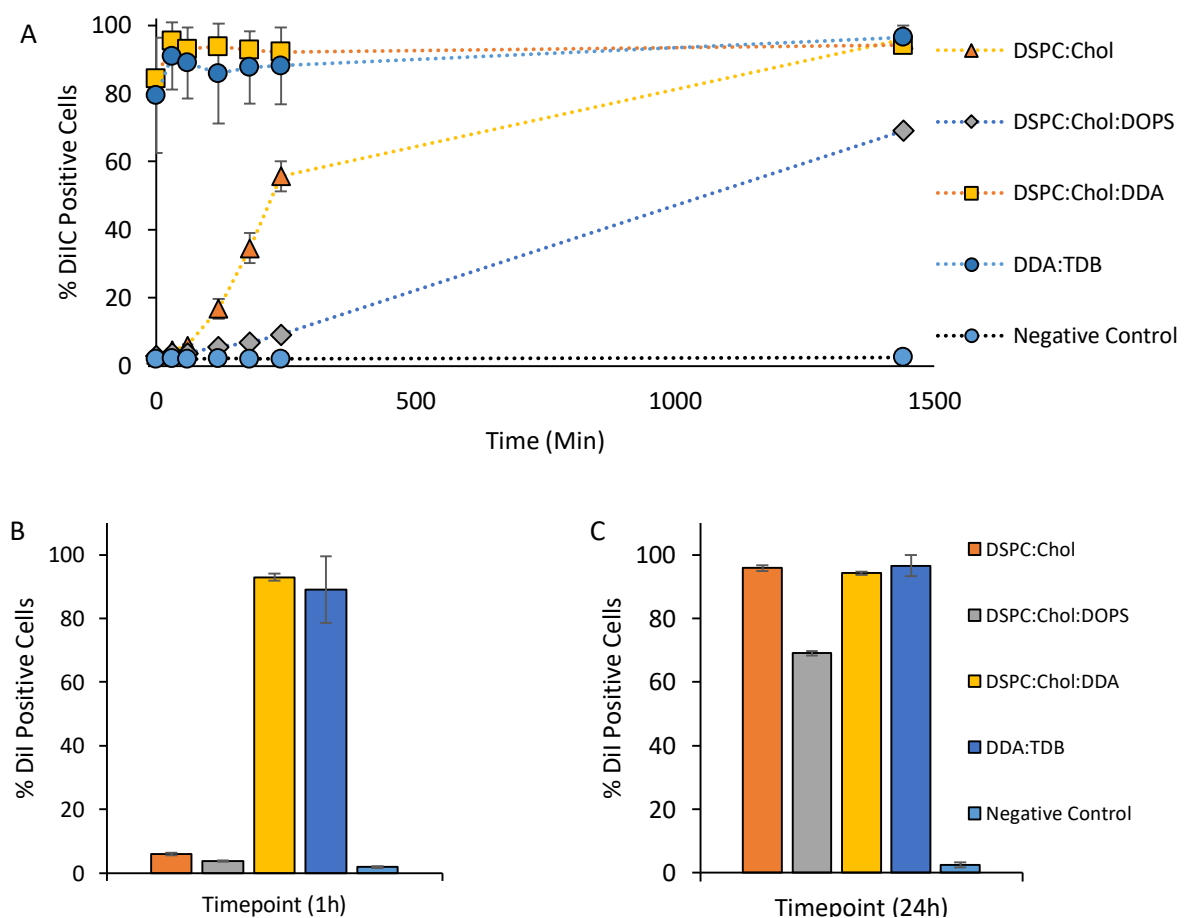


Figure 5.2 Differentiated THP-1 macrophage-like cells were co-cultured with four liposomal formulations containing DilC within the membrane. Time points were removed across 24 h incubation, with unstained controls receiving just serum-free RPMI (A). Time points 1 h (B) and 24 h (C) comparison for DilC %positive cells, with unstained controls receiving just serum-free RPMI. Results represent mean \pm SD, $n = 3$.

The use of fluorescent dyes within nanoparticles is a common strategy employed for *in vivo* and *in vitro* studies (Torchilin, 2005a, Hak et al., 2012). DiIC is a lipophilic membrane carbocyanine stain, which exhibits strong fluorescence when embedded within a lipid bilayer, yet weak fluorescence outside, making it an ideal marker for such studies. The applicability of a range of fluorescent dyes in nanoparticles was explored by Snipstad et al where a range of dyes and nanoparticle systems were tested *in vitro* at 37°C with PC3 cells. The results showed that the use of DiI within liposome systems was highly retained within the vesicle bilayer, and no fluorescent leakage was observed (Snipstad et al., 2017). This indicates that the association observed in Figure 5.2 is likely due to the delivery system association with the THP-1 cells, and not free dye. The highly associative cationic formulations shown in this study are in line with the current understanding of cationic vesicle interactions with cells. The electrostatic interactions between the cationic delivery system and anionic cellular surface has been used across a range of therapeutic areas, including the use of gene delivery (Kelly et al., 2011). In their studies to further elucidate the effect of liposome bilayer composition on monocyte derived dendritic cell uptake, Foged et al found that cationic TAP-based liposomes had strong association (over 90%), resulting in intracellular localisation, following a 2 h incubation period. The authors also reviewed the impact negatively charged liposome formulations had on association, using anionic formulations containing either phosphatidyl serine (PS) or phosphatidyl glycerol (PG). Following 2 h incubation, results shown are comparable to the data shown in Figure 5.2, with under 5% of the anionic formulations associating with the dendritic cells (Foged et al., 2004). Similarly, TAP-liposomes (dimyristoyl trimethylammonium propane), PS-based liposomes (anionic, targeting) and PG-based liposomes (anionic) have previously been compared for liposome interaction with dendritic cells. After 4 h, little interaction was observed outside of the TAP-based liposomes. However after 48 h incubation, almost all cells showed fluorescence regardless of the formulation. When the MFI was calculated, the cationic vesicles resulted in the greatest fluorescence, followed by PS-liposomes and then the anionic PG-liposomes (Arigita et al., 2003). In a similar study, Khadke et al compared SUV formulations composed of DSPC and cholesterol, with the addition of either PS or DMPG. At the final time point measured, DSPC:Chol:PS exhibited significantly higher %positive cells associated with liposomes when compared to the DMPG formulation (approximately 80% compared to 40%), again indicating the favourable association macrophages have for PS-based liposomal formulations (Khadke et al., 2019).

It should be noted that these associative studies within this chapter were conducted in serum-free RPMI. While under *in vivo* conditions within a biological system following parenteral injection, a protein corona will form around the cationic delivery system via electrostatic interactions with biomolecules in the blood, which has previously been demonstrated to affect cell interaction. The

composition of the biomolecules associated to the surface of the delivery system has shown to result in different uptake mechanisms, despite the composition of the delivery system remaining constant (Francia et al., 2019). Work within our laboratory has recently investigated the effect of cellular association exposed to DOTAP and DDA based cationic formulations in the presence of FCS-free media and complete media (5% FCS). When cellular association was plotted as a percentage of DiIC + cells, the presence of 5% FCS was found to have no impact, however MFI values indicated a lowering of intensity when conducted in FCS-free media, although the trends observed between +/-FCS were similar (Anderluzzi et al., 2020). Lou et al similarly investigated the effect FCS and FCS free media has on both cationic and ionizable lipid nanoparticle formulations in regards to cellular association and found no significant differences between FCS free and 5% FCS media when comparing MFI values (Lou et al., 2020).

When delivering oral nanoparticles, complex protein interactions are also likely to occur through-out the GI tract. Various enzymes, food components and other GI components may interact with the nanoparticles as they traverse, dependent on a wide range of factors including the nanoparticles physicochemical attributes (Berardi and Baldelli Bombelli, 2019).

While the associative nature of the cationic vesicles in Figure 5.2 is well documented within the literature, PS-based liposomal formulations have previously been shown to improve uptake and interaction with APCs when compared to neutral based compositions. The inclusion of PS into PC based MLVs enhanced the formulations phagocytosis by macrophages when compared to PC-based liposomes (Ahsan et al., 2002). Similarly, DOPS:Chol liposomes have shown a 5-fold increase in uptake compared to DOPC-based liposomes using a THP-1 model cell line (Kelly et al., 2011). The lipid ratio and PS molarity within the formulation has also been shown to impact upon association and internalisation when using murine macrophages. Liposomes containing DSPC, Gd-DOTA-DSPE, cholesterol, PEG2000-DSPE and varying mol% PS (0, 6, 12 and 37) found the optimum level of PS for internalization to be 6 mol%. The authors attributed this to the fact that within murine biological membranes, cells express between 2-10 mol% naturally occurring PS, thus it is likely that natural selection has tailored macrophages to effectively interact with these levels of PS (Geelen et al., 2012). Within the studies conducted in this chapter, PS was set at approximately 16 mol%, which would result in a more anionic zeta potential and therefore an increase in electrostatic repulsion between the vesicles and the cellular membranes, which may explain why DOPS based liposomes within this study showed poor cellular association in comparison to the other formulations at 24 h. In addition to this, the studies conducted by Geelan et al incorporated 5 mol% of PEG2000-DSPE within all of the formulations, which will reduce the electrostatic repulsion between the vesicles and cells, potentially enhancing association.

5.5.2 The effect of liposomal delivery systems on the rate of antigen processing using DQ-OVA

While associative studies using DiIC were conducted for determining formulation association with the differentiated THP-1 monocytes, a simultaneous investigation was carried out using DQ-OVA in order to understand the ability of the cells to process the antigen being delivered by the different liposomal formulations. DQ-OVA is a self-quenched substrate, that only exhibits fluorescence following breakdown by proteases. DQ-OVA was adsorbed onto the surface of the two cationic formulations (DDA:TDB and DSPC:Chol:DDA) and entrapped within DSPC:Chol and DSPC:Chol:DOPS to an approximate final concentration of 100 µg/mL prior to the addition of the formulation to serum-free RPMI as described in the methods section. Free DQ-OVA control was also added to the cells without a delivery system at the same concentration. Figure 5.3 shows the % positive cells marked with DQ-OVA fluorescence over time, analysed by flow cytometry. Delivering DQ-OVA using the neutral formulation (DSPC:Chol) promoted 11% of the cells being positive for DQ-OVA fluorescence after 4 h, with a steady increase to 67% at 24 h (Figure 5.3A). In the case of the anionic liposome formulation (DSPC:Chol:DOPS), 13% of the cells showed DQ-OVA fluorescence after 4 h (Figure 5.3B). However, following 24 h incubation, this increased to approximately 84% of the measured cells expressing DQ-OVA fluorescence, the highest out of all the formulations tested (Figure 5.3C). Free DQ-OVA control also resulted in protease breakdown over time, with approximately 50% of the cells measuring fluorescence positive after 24 h (Figure 5.3). Within the first 4 h, both cationic formulations exhibited the fastest fluorescence shift, with DDA:TDB resulting in approximately 20% of the cells being DQ-OVA positive after 4 h (Figure 5.3A). This trend was further pronounced with DSPC:Chol:DDA, where a sharp increase in DQ-OVA positive cells was found at 4 h (~ 65%). In the case of DDA:TDB, the final time point at 24 h showed a steady increase in DQ-OVA processing, reaching 64% DQ-OVA positive cells (Figure 5.3C). Interestingly, DSPC:Chol:DDA DQ-OVA positive cells remained relatively steady between 4 - 24 h, exhibiting no notable increase in DQ-OVA fluorescence, where 73% of the cells exhibited fluorescence at the final time point (Figure 5.3). By the 24 h time point, formulations DSPC:Chol, DSPC:Chol:DOPS and DSPC:Chol:DDA all resulted in statistically significant increases in %DQ-OVA positive cells when compared to free antigen alone ($p < 0.05$).

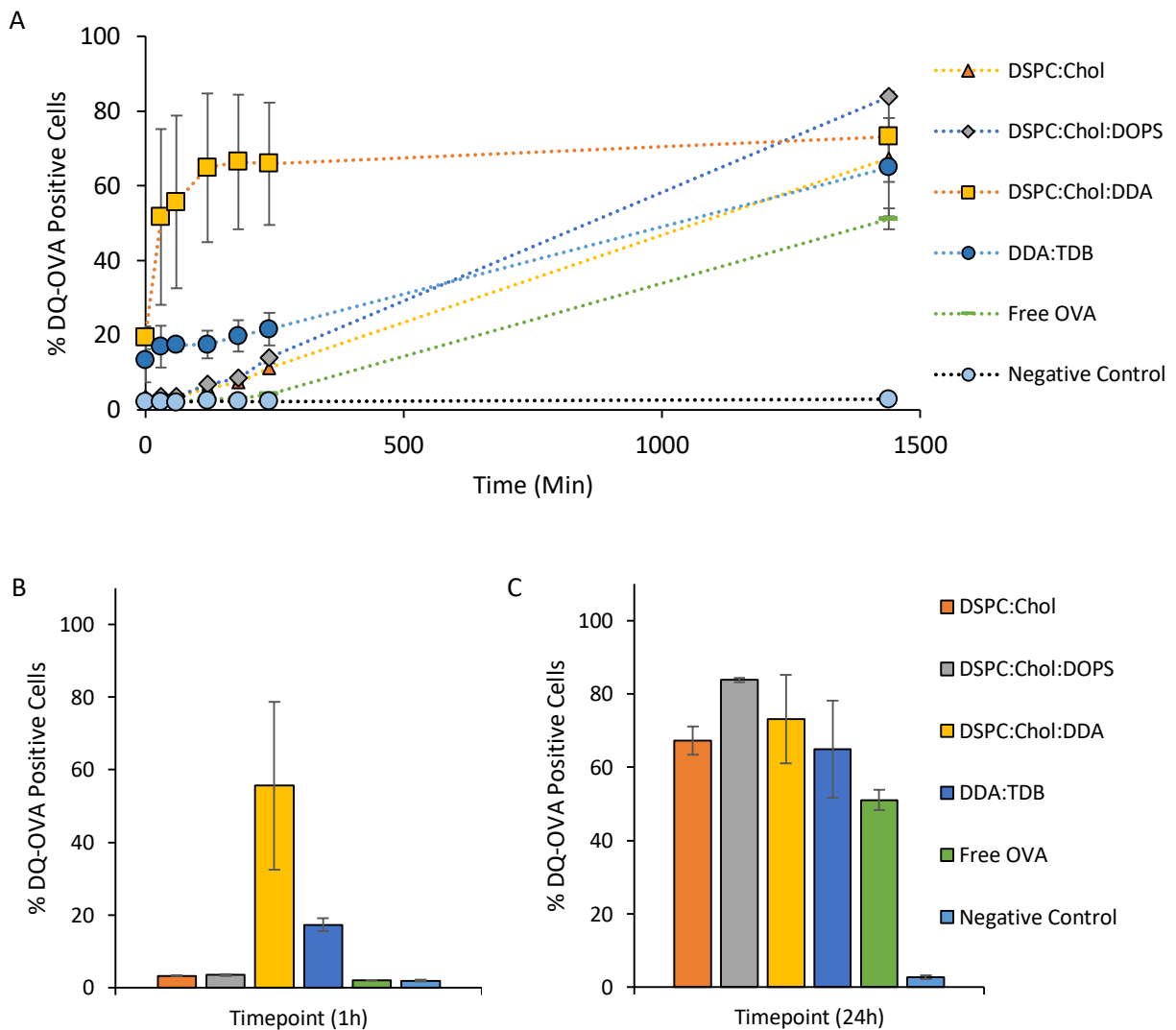


Figure 5.3 Differentiated THP-1 macrophage-like cells were co-cultured with four liposomal formulations containing DQ-OVA adsorbed to the surface or entrapped within. Time points were removed across 24 h incubation, with unstained controls receiving just serum-free RPMI or free OVA without a liposomal formulation (A). Time points 1 h (B) and 24 h (C) comparison for DQ-OVA % positive cells, with unstained controls receiving just serum-free RPMI. Results represent mean \pm SD, $n = 3$.

When comparing the rate of processing in relation to the association (% Processing / % Association), it can be seen that when using both neutral and anionic formulations (DSPC:Chol:DOPS, DSPC:Chol), poor association and processing occurs by the 1 h time point. In contrast, both cationic formulations result in rapid association, and in the case of DSPC:Chol:DDA, significant processing by 1 h. By 24 h, neutral formulation DSPC:Chol and both of the cationic formulations (DDA:TDB and DSPC:Chol:DDA) showed similar rates of processing / association, while anionic formulation DSPC:Chol:DOPS showed the highest degree of processing (Figure 5.4).

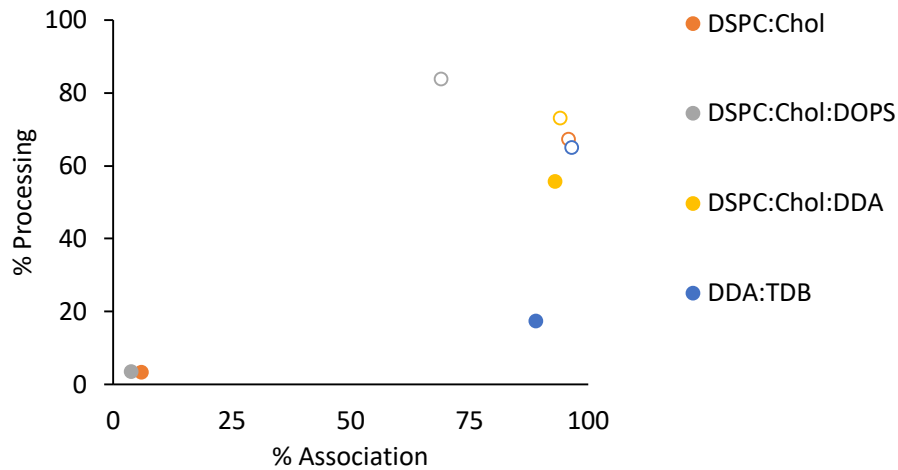


Figure 5.4 DQ-OVA processing (%) vs association (%) for the four liposomal formulations DSPC:Chol, DSPC:Chol:DOPS, DSPC:Chol:DDA and DDA:TDB at time points 1 h (closed symbol) and 24 h (open symbols). Results represent mean \pm SD, $n = 3$

The results in section 5.5.2 have indicated the benefits of using a liposome based delivery system for enhancing the processing of antigen when compared to free antigen alone, increasing DQ-OVA processing rates significantly (in case of DSPC:Chol, DSPC:Chol:DOPS and DSPC:Chol:DDA, $p < 0.05$). Employing the use of a liposomal delivery system is well documented for improving antigen uptake and processing *in vitro* by antigen processing cells (Cruz-Leal et al., 2014). By the 1 h time point, poor association and therefore processing can be seen with both neutral and anionic formulations – likely a result of limited interaction between THP-1 cells and liposomal vesicles. Both DSPC:Chol:DDA and DDA:TDB conversely show high association – due to the electrostatic disparities attracting and enhancing membrane interactions. However, the processing rate of DSPC:Chol:DDA initially was found to be accelerated in comparison to DDA:TDB. This could be explained by the difference in composition of the liposomal vesicles. Benne et al investigated the correlation between liposomal rigidity and the impact this has upon bone-marrow derived DCs (BMDCs) association and then subsequent regulatory T-cell activation. Using primarily anionic and neutral formulations, the study found that an increase in carbon chain length (by employing lipids such as DSPC), enhanced both association and subsequent adaptive immune response activation. While the mechanisms behind the enhanced regulatory T cell activation requires further investigation (whether or not rigidity enhances processing, presentation, co-stimulatory marker expression etc.), it is clear from the study that the composition of the liposomal formulation is a critical factor in how the vesicles interact with APCs (Benne et al., 2020).

By the 24 h time point, the results shown here indicate that the greatest number of cells expressing DQ-OVA fluorescence resulted from the anionic DSPC:Chol:DOPS formulation, despite the low association rate (Figure 5.4). This may indicate that for anionic vesicles, whilst initially association was

poor, potentially due to repulsive electrostatic interactions between the anionic liposomal vesicles and negative cellular surface, the inclusion of DOPS accelerates the processing of the delivered antigen. Indeed, the addition of DOPS within the DSPC:Chol formulation increased the DQ-OVA positive cells by approximately 17% when compared to DSPC:Chol alone (Figure 5.3). In a similar study, Mori et al investigated both PS and PC-based liposomal formulations with DQ-OVA conjugated to the surface of the liposomes and then subsequently incubated with macrophages (hybridoma clone No.39). The authors found that the liposomal formulation with PS included had improved antigen processing (2-fold increase in MFI) and presentation (approximately a 3-fold increase in MFI) when compared to the PC counterpart (Mori et al., 2005). Similarly, PS conjugated onto the surface of dioleoylphosphatidylethanolamine, dioleoylphosphatidylcholine, oleoyl phosphatidylglycerol acid and cholesterol (4:3:2:7 w/w) liposomes improved the delivery and subsequent T helper and cytotoxic T cell responses compared to non-PS liposomes. This is a result of the mechanisms that occur during apoptotic clearance by macrophages and dendritic cells. Phosphatidylserine is natively expressed in within the inner leaflet of all eukaryotic membranes, and therefore is hidden externally under normal conditions. However, upon cellular stress (or programmed apoptosis), the cell then externalises PS, presenting it within the outer membrane. This then acts as a potent signal for APC interactions, via the binding to Tim 4 and Tim 1 receptors on DCs and macrophages, enhancing uptake (Ichihashi et al., 2013, Birge et al., 2016).

Both cationic vesicles investigated within this study (Figure 5.3) resulted in 73% and 67% DQ-OVA positive cells for DSPC:Chol:DDA and DDA:TDB respectively (at the final time point), on average lower than the anionic DSPC:Chol:DOPS (84%) formulation (yet not statistically significant, $p>0.05$), despite an accelerated number of cells showing DQ-OVA fluorescence within the first 4 h. Cationic liposomes have been shown to show improved internalization by a range of APCs when compared to both neutral and anionic as a result of electrostatic interactions between the two membranes (Watson et al., 2012). As shown in Figure 5.2, high numbers of cells were found to have DiIC liposomes associated, yet this did not translate into comparable DQ-OVA fluorescence (Figure 5.4). There are a number of explanations as to why this could be occurring. Cationic liposomes have known cellular toxicity, dependent on both the choice of lipid composition and the liposome dose administered to the cells. The direct mechanisms of how cationic nanoparticles exert damage to biological cells remains unclear, however a number of mechanisms have been reported including excessive reactive oxygen species (ROS) production, autophagy and an increase in inflammatory cytokines (Petersen and Nelson, 2010, Tzeng et al., 2016). Using human liver-derived hepatoma cells (HepG2), DOTAP based cationic liposomes were screened for their cytotoxic effects and were found to be highly concentration dependent. At a dose of 25 $\mu\text{g}/\text{mL}$, cationic vesicles resulted in a loss of approximately 14% cell

viability, however this increased to above 90% when the liposome dose was increased to 3200 $\mu\text{g}/\text{mL}$ (Li et al., 2018). Data generated from our own laboratory has previously shown the differences in lipid composition and their impact upon cell viability on baby hamster kidney cells (BHK). Cationic liposome formulations (DOPE:DOTAP or DOPE:DDA, 1:1 w/w) manufactured by microfluidics were added at a range of concentrations, where DOTAP based formulations were found to be less cytotoxic (viability up to 33 $\mu\text{g}/\text{mL}$) when compared to DDA (viability up to 11 $\mu\text{g}/\text{mL}$) (Anderluzzi et al., 2020). In the case of the studies here in Figure 5.3, cationic liposome doses were kept to a final concentration of 10 $\mu\text{g}/\text{mL}$ in order to minimise any potential cytotoxicity, therefore the loss of processing found when comparing both cationic formulations to DSPC:Chol:DOPS may not be a result of cytotoxicity. In this case, aggregation between the cationic vesicles and cellular bodies could lead to poor surface area distribution, thus reducing the ability of the cell population within the well to gain access to the DQ-OVA adsorbed on the surface of the liposomes for processing. Additionally, cationic vesicles have been shown to release within the cytosol of the cell due to the rupturing of the endosomal and phagosomal membranes (Watson et al., 2012). This may impact upon the rate of the degradation process of the DQ-OVA when compared to anionic and neutral formulations as the reduced time within the endosome and therefore the subsequent lysosome, may reduce the rate of DQ-OVA fluorescence expression. Finally, cationic vesicles can associate with the cellular membrane through electrostatic interaction, however over time this association can damage the integrity of the cellular membrane, resulting in leakage of cytosolic material which can impact upon the cellular mechanisms for internalisation and therefore, the downstream antigen processing (Leroueil et al., 2007, Chen et al., 2009).

5.5.3 Cellular surface marker expression following liposomal delivery system incubation

In an attempt to understand how these specific delivery systems were impacting on macrophages, a range of co-stimulatory molecules were selected to track following 24 h incubation. The specific expression of these co-stimulatory molecules is essential for APCs during antigen presentation, as they determine the interaction with T-lymphocytes, therefore dictating which way the immune system generates adaptive immunity. Figure 5.5 indicates the % positive cells expression of co-stimulatory molecules CD14, CD40, CD80 and MHC II following 24 h incubation with formulations DSPC:Chol, DSPC:Chol:DOPS, DDA:TDB and DSPC:Chol:DDA and both controls, free ovalbumin and serum-free RPMI (negative control). These markers were selected because they are critical markers for APC maturation (Qu et al., 2018). When APCs process antigen, and upon presentation of peptidic fragments onto MHC II, T cells then bind via T cell receptors (TCR). Alongside this epitope specific

binding, co-stimulatory molecules must be present in order to activate T cell responses. These co-stimulatory molecules include CD80/86 and CD40 on the APC surface (Planelles et al., 2003).

For co-stimulatory cell surface molecules CD14 and CD40, no biologically relevant changes in expression compared to negative controls could be observed regardless of the liposomal formulation administered (Figure 5.5). However, co-stimulatory molecule CD80 showed significantly higher ($p < 0.05$) %positive cells expressing CD80 whenever a liposomal formulation (regardless of the formulation) was employed in comparison to free ovalbumin and the negative control (serum-free RPMI). When comparing between formulations, no statistically significant differences could be observed between any of the formulations with DSPC:Chol, DDA:TDB and DSPC:Chol:DOPS resulting in % positive CD80 expression of $13.49 \pm 2.3\%$, $12.42 \pm 0.4\%$ and $13.23 \pm 0.57\%$ respectively; while DSPC:Chol:DDA showed a slight decrease in CD80 % cells in comparison ($10.7 \pm 0.1\%$) ($p > 0.05$). When investigating the impact of the delivery systems on MHC II expression, no statistically significant differences could be observed across all formulations when compared to free antigen alone ($p > 0.05$; Figure 5.5). In the case of DDA:TDB, a statistically significant decrease in % positive MHC II cells could be observed when compared to both DSPC:Chol and DSPC:Chol:DOPS alone ($p < 0.05$). Similar results were found when analysing for mean fluorescence intensity (MFI). In the case of CD14, no statistically significant changes in MFI could be observed for all formulations when compared to free antigen alone ($p > 0.05$) with the exception of cationic formulation DSPC:Chol:DDA, where a statistically significant decrease in MFI was found ($p < 0.05$) (Figure 5.6A). For CD40, no statistically significant changes could be found for all formulations when compared against free antigen alone ($p > 0.05$) (Figure 5.6B). In the case of CD80, both DSPC:Chol and DSPC:Chol:DOPS formulations were found to show a statistically significant increase in MFI ($p < 0.05$), while cationic formulations DSPC:Chol:DDA and DDA:TDB were found to have no significant impact (Figure 5.6C). Finally, for MHC II MFI, DSPC:Chol:DDA was found to be the only formulation capable of eliciting a statistically significant increase ($p < 0.05$) (Figure 5.6D).

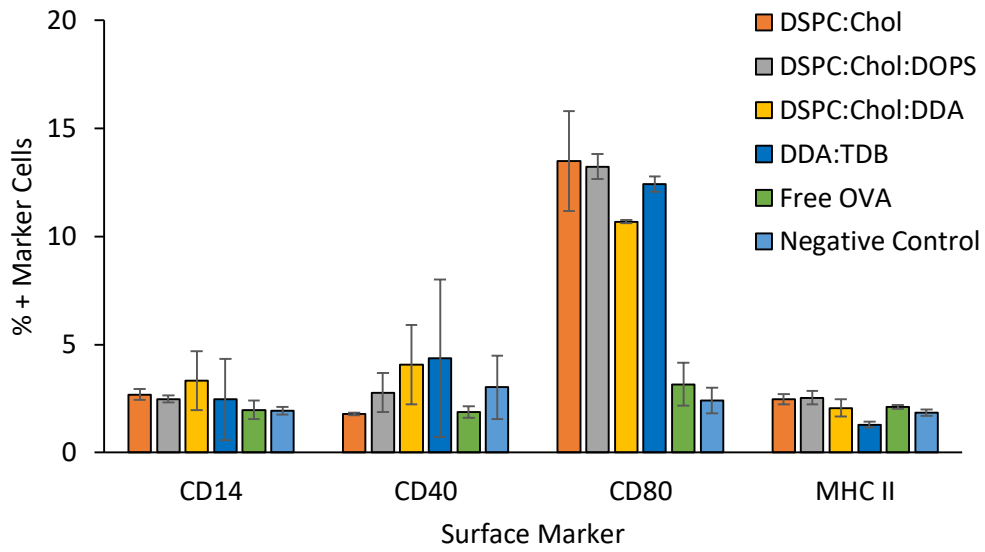


Figure 5.5 Differentiated THP-1 macrophage-like cells were co-cultured with four liposomal formulations for 24 h incubation, with negative controls receiving serum-free RPMI or just free ovalbumin. % Positive cells with surface co-stimulatory molecules CD14, CD40, CD80 and MHC II were analysed with FACs using specified antibodies. Results represent mean \pm SD, $n = 3$.

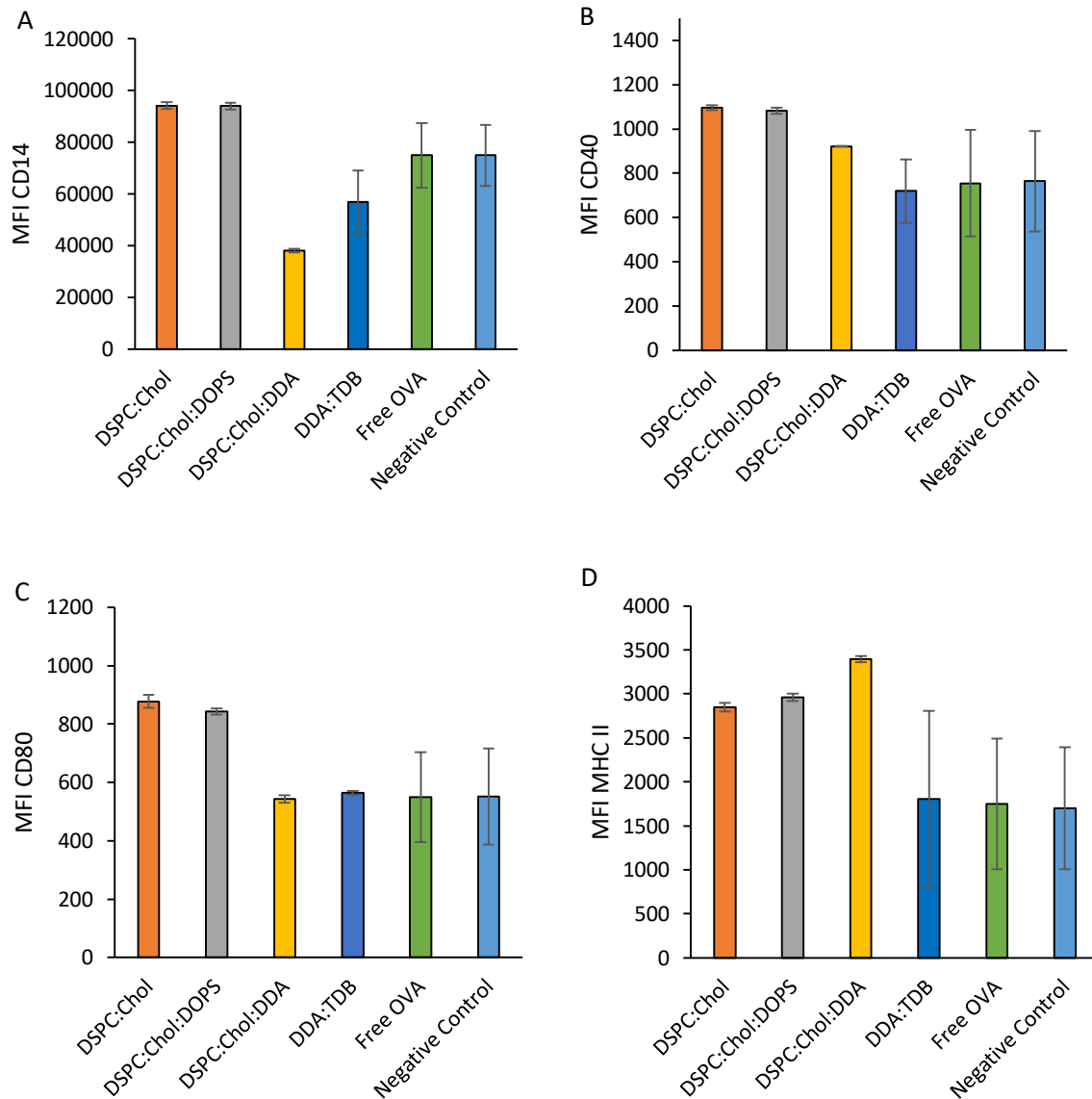


Figure 5.6 Differentiated THP-1 macrophage-like cells were co-cultured with four liposomal formulations for 24 h incubation, with negative controls receiving serum-free RPMI. MFI (median) of cell surface co-stimulatory molecules CD14, CD40, CD80 and MHC II (A, B, C and D respectively) were analysed with FACS using specified antibodies. Results represent mean \pm SD, $n = 3$.

Liposomes can be used to improve the delivery of antigen cargo to APCs and then ultimately to generate adaptive immunity. Nonetheless, the choice of liposome composition and the choice of antigen can impact upon how the antigen is processed and therefore subsequently determines the outcome and degree of the adaptive immunity. For example, novel liposomes incorporating lipids from non-pathogenic bacterial strains have been shown to elicit strong activation of BMDCs, increasing pro-inflammatory cytokines (IL-6, IL-12 and TNF- α) as well as increasing CD80, CD86 and MHC II expression when compared to conventional PC-based liposomes (EggPC:Cholesterol; (Faisal et al., 2011)). Therefore, the co-stimulation marker results shown within this chapter (Figures 5.5 – 5.6) can potentially give some insight into which type of immune response is being elicited. While

CD14 expression showed minimal differences in % positive cells, both cationic formulations resulted in a decrease in median fluorescence intensity, indicating reduced cellular surface expression. Conversely, both neutral and anionic formulations resulted in an increase of CD14 expression, however the number of % positive cells did not change when compared to the negative controls.

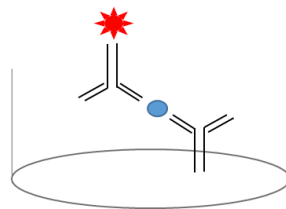
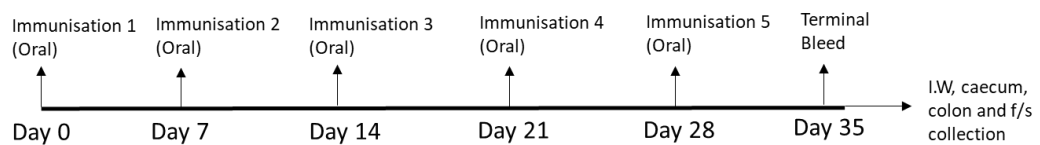
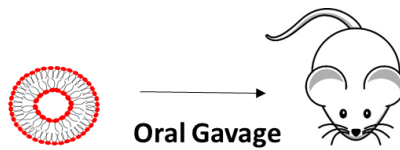
The effect of liposomal formulation incubation on cultured dendritic cells and the subsequent effect on activation markers was previously studied *in vitro* by Arigita et al. Dimyristoyl phosphatidylcholine and cholesterol based liposomes had PS, PG and 1,2-dimyristoyl-3-trimethylammonium-propane (14:0 TAP) added, and the formulations were exposed to DCs for 48 h with activation markers CD40, CD80 and MHC II expression subsequently being analysed by FACs. The authors found slight increases in activation across all the formulations, but the addition of PorA (an antigen from *Neisseria meningitides*) was found to enhance the markers expression rates. These results indicate that while the studies conducted within this chapter were terminated at the 24 h time point (half of that conducted by Arigita et al), the effect of the antigen associated with liposomes (in our case ovalbumin) may have more impact upon the route of APC activation when compared to the effect of the delivery system (Arigita et al., 2003). Similar results were shown when studying activation markers MHC II and CD80 on DCs incubated with plain (PC:PG:Chol) and mannosylated liposomes, little changes could be observed in expression levels of the dendritic cells without the inclusion of LPS (Espuelas et al., 2008). Again, the inclusion of tri-mannose containing liposomes, mono-mannose and PC-PS based liposomes was shown to only slightly impact upon markers CD40 and CD80 in murine dendritic cells, potentially due to down-regulation of immune responses as a result of a different uptake mechanism (via C-type lectin receptors) when compared to LPS, although mannosylated, PC and PS-based liposomes were found to significantly increase MHC II and CD80 expression when compared to free ovalbumin in solution alone, in accordance with some of the data shown within this chapter (White et al., 2006, Copland et al., 2003). It has also been shown that the extent of the activation marker expression may be linked to the delivery systems in a concentration dependent manner. Gordon et al using chitosan nanoparticles (CNPs) either unloaded or loaded with FITC-labelled ovalbumin and incubated with murine DCs found significant increases in MHC II and CD86 expression only at high dose concentrations (1 mg/mL) of particles. The delivery system doses used within this study were fixed at 10 µg/mL final concentration, therefore a potential dose optimisation may be required for these formulations to elicit significant changes in activation marker expression. Interestingly, the results also showed a significant loss of activation marker expression when ovalbumin was loaded with the CNPs compared to empty particles, furthering the understanding that the choice of antigen within the delivery system may act as a primary factor in determining the outcome of the immune response (Gordon et al., 2008).

5.6 Conclusions

Within this chapter, the *in vitro* applicability of four liposomal formulations was assessed for association, antigen processing and downstream activation marker expression following incubation with differentiated THP-1 macrophage-like cells. In line with current understanding of cellular interactions, both cationic formulations resulted in high degrees of association with the macrophage-like cells across all time points, while both neutral and anionic formulations showed strong, yet lagged association in comparison. The ability of the cells to then process the delivered antigen cargo was determined using a self-quenched model antigen, DQ-OVA. The results indicated that all of the liposomal formulations tested increased the rate of DQ-OVA fluorescence (and therefore antigen processing by the cells) when compared to the administered free DQ-OVA control by 24 h. Despite resulting in the lowest rate of association, DSPC:Chol:DOPS exhibited the highest degree of % positive cells for DQ-OVA fluorescence compared to neutral and both cationic formulations (DSPC:Chol:DDA and DDA:TDB). Following association and antigen processing studies, the liposomal formulations were then tested for their ability to activate specific cell surface markers and co-stimulatory molecules. Expression of CD14, CD40 and MHC II showed limited biologically relevant changes across all formulations tested, however a highly significant increase in both MFI and %positive cells was observed for CD80 when employing any of the delivery systems in comparison to free antigen and negative controls. The results within this chapter indicate the ability of the tested delivery systems to associate with THP-1 macrophage-like cells and therefore increase the rate of antigen processing when compared to free antigen alone. Given these *in vitro* results, the next step was to test the *in vivo* efficacy in regards to antibody responses following liposomal delivery of model antigen ovalbumin.

Chapter 6

Oral administration of liposomes manufactured by microfluidics: Mucosal and systemic antibody responses



6.1 Introduction

Vaccine immunisation via the oral route of administration allows for localised immune responses within specific locations throughout the G.I tract, allowing for effective defence systems against enteric pathogens (Cole et al., 2018). Through gut-associated lymphoid tissue (GALT) delivery, both localised mucosal antibody defences and systemic responses can be achieved, generally unlike parenteral administration routes (Parker et al., 2018). Alongside clinical advantages, further benefits in relation to ease of administration due to the lack of needle based injections and patient compliance further cement oral immunisation as a highly sought after administration route. However, challenges associated with poor uptake, antigen stability in the gastric environment as a result of the acidic pH and degradative enzymes has led to a very limited number of oral vaccines licensed for market (Davitt and Lavelle, 2015). In addition, evolutionary mechanisms has led to the development of a tolerant immunological state found throughout the GALT, a necessary adaption to limit the damage of potential inflammatory responses towards ingested antigen and commensal bacteria residing within the gut (Satitsuksanoa et al., 2018). It is believed that these limitations can be overcome by using nanoparticle delivery systems to offer protection to the antigen payload, enhance M cell uptake and therefore elicit immunologically relevant antibody responses (Lavelle and O'Hagan, 2006, Russell-Jones, 2000). A key component to the generation of an effective immune response against enteric pathogens and toxins is the generation of secretory IgA (sIgA). This antibody is the most abundant throughout the mucosal tissue and functions through the binding and therefore neutralisation of its specific epitope, rendering toxins and bacteria harmless, due to an inability to bind and interact with epithelial cells (Boyaka, 2017, Mantis et al., 2011). Liposomes have shown some promise in relation to oral vaccination, where enhanced IgA and IgG responses can be elicited to their respective antigen cargo (Shakya et al., 2016, Kang et al., 2018). To further investigate this, within this chapter a range of liposomal formulations were manufactured by microfluidics, both entrapping and surface loading model antigen ovalbumin. The formulations were characterised in terms of vesicle size and zeta potential, as well as the impact an acidic environment (pH 1.2) has on the vesicles physicochemical attributes and ability to retain antigen. Finally, the *in vivo* efficacy is determined for the formulations and their ability to generate both localised mucosal and systemic antibody responses is quantified through ELISA.

6.2 Aim and objectives

The aim of this chapter was to manufacture protein loaded liposomal formulations by microfluidics and determine the *in vivo* efficacy in regards to both mucosal and systemic IgA and IgG responses. These formulations covered a range of attributes including charge, antigen positioning (encapsulated or surface associated) and inclusion of different immunostimulatory components. In order to achieve this, the objectives were:

- Determine the physicochemical attributes and antigen retention of the formulations incorporating protein when subjected to acidic pH.
- Analyse the antibody responses of the liposomal formulations following oral administration.
- Assess the effect of the inclusion of immunostimulatory compounds in the formulations and their ability to enhance antibody responses.

6.3 Materials

6.3.1 Materials used for the preparation of liposomes

The 1,2-distearoyl-sn-glycero-3-phosphocholine (DSPC), 1,2-dioleoyl-3-trimethylammonium-propane (DOTAP), L- α -phosphatidylserine (PS) (Brain, Porcine) (sodium salt), cationic surfactant dimethyldioctadecylammonium bromide (DDA) and immunopotentiator trehalose 6,6'-dibehenate (TDB), were all purchased from Avanti Polar Lipids Inc., Alabaster, AL, US. Cholesterol and ovalbumin (OVA) were purchased from Sigma Aldrich Company Ltd., Poole, UK. Monopalmitoyl glycerol (MPG) was purchased from Larodan Labs, Sweden. Phosphate buffered saline was acquired from Oxoid Ltd., Basingstoke, UK. Tris-base was obtained from IDN Biomedical Inc. (Aurora, OH, United States) and used to make 10 mM Tris buffer, adjusted to pH 7.4 using HCl. For purification, Biotech CE Tubing MWCO 300 kD or a modified polyethersulfone (mPES) 750 kD MWCO hollow fibre column was used in conjunction with Tangential Flow Filtration (TFF) (Spectrum Inc., Breda, The Netherlands). TMB substrate solution, bovine serum albumin (BSA) as well as solvents (methanol (MeOH) and isopropanol (IPA)) were purchased from ThermoFisher Scientific, Loughborough, England, UK. Cholera Toxin from *Vibrio cholera* (95%), N-Succinimidyl 3-(2-pyridyldithio) propionate (SPDP), DL-Dithiothreitol (>98%) (DTT), L-Cysteine (>97%), L-Lysine (>98%) were purchased from Sigma Aldrich. Bio-Spin size exclusion chromatography column P-6 (approximately 6000 Da cut off) was purchased from Bio-Rad Laboratories Ltd., Perth, UK. Tween, Ethylenediaminetetraacetic acid (EDTA) and sodium carbonate

were purchased from commercial suppliers. Goat anti-mouse IgG and IgA H&L (HRP) were purchased from Abcam, Cambridge, England, UK. All water and solvents used were HPLC grade. Lipids 1,2-dioleoyl-sn-glycero-3-phospho-L-serine (sodium salt) (DOPS) and 1,2-dioleoyl-sn-glycero-3-phosphoethanolamine-N-[4-(p-maleimidomethyl) cyclohexane-carboxamide] (sodium salt) (18:1 PE MCC) were gifted from Avanti Polar Lipids Inc., Alabaster, AL, US.

6.4 Methods

6.4.1 Liposome manufacture and purification

6.4.1.1 Anionic and neutral formulations entrapping protein

The preparation of liposomes by microfluidics was conducted on the NanoAssemblr Platform (Precision Nanosystems Inc., Vancouver, Canada). Anionic and neutral formulations DSPC:Chol (2:1 w/w), DSPC:Chol:DOPS (10:5:4 w/w), DSPC:Chol:PS (10:5:4 w/w) and MPG:Chol:PS (10:5:4 w/w) were initially dissolved in methanol and manufactured using microfluidic parameters 3:1 FRR (flow rate ratio) and 15 mL/min TFR (total flow rate) with initial total lipid concentrations between 10 – 15 mg/mL. Ovalbumin was loaded in-line in PBS pH 7.4 in the second inlet at concentrations between 6 – 8.5 mg/mL. These formulations were purified using Krosflo Research Iii tangential flow filtration system (Waltham, MA, USA) fitted with an mPES (modified polyethersulfone) column with a pore size of 750 kD. For removal of solvent and untrapped protein, liposomal samples were circulated through the column and purified through difiltration, with fresh PBS being added at the same rate as the permeate leaving the column. Following purification, formulations entrapping protein were then concentrated using TFF, in order to have a final ovalbumin concentration of 1 mg/mL (as previously optimised).

6.4.1.2 Cationic formulations

For the cationic formulations manufactured by microfluidics, DSPC:Chol:DDA (10:5:5 w/w, initial total lipid 30 mg/mL), DSPC:Chol:DOTAP (10:5:2 w/w, initial total lipid 10 mg/mL) and DDA:TDB (5:1 w/w, initial total lipid 12 mg/mL) TRIS buffer 10 mM pH 7.4 was used as aqueous phase. The formulation DSPC:Chol:DOTAP was dissolved in MeOH and the microfluidic parameters used were: 1:1 FRR, 15 mL/min TFR. Following production, subsequent solvent removal was conducted by dialysis and then ovalbumin adsorption was conducted by re-circulating the pre-formed liposomes through the NanoAssemblr with ovalbumin in the second inlet (complexation) (FRR 5:1, 15 mL/min TFR). Formulation DDA:TDB was dissolved in IPA before manufacturing (FRR 3:1, 15 mL/min TFR). Addition of ovalbumin to the surface of the particles was then conducted via complexation (FRR 3:1, 15 mL/min

TFR). Finally, formulation DSPC:Chol:DDA was loaded in-line (liposome formation and ovalbumin addition was conducted at the same time using microfluidics) using the following production parameters FRR 3:1, 15 mL/min TFR. Dialysis was then conducted to remove solvent. The final ovalbumin concentration for all cationic formulations was the same as the neutral and anionic vesicles, 1 mg/mL.

6.4.1.3 Cholera Toxin conjugation process

The conjugation of modified cholera toxin (CT) protocol was adapted from a previously published protocol, based on the addition of thiol groups to lysine residues on the cholera toxin and then subsequent reaction with the maleimide group of the lipid component (Harokopakis et al., 1995). Briefly, cholera toxin was dissolved in PBS pH 7.4 and incubated with SPDP (amine-reactive reagent) at a molar ratio of CT:SPDP 1:10 for 30 minutes in a dark room. The reaction was quenched by the addition of 10 μ L of 20 mM L-Lysine (PBS pH 7.4), followed by a reduction reaction by the addition of 5 μ L of DTT (7.7 mg/mL in di H₂O). To purify the modified protein from unwanted by products, a Bio-Spin (Bio-Rad Laboratories) size exclusion chromatography column was used as per the manufacturer's instructions. For coupling of the cholera toxin thiol groups to the liposomes, 5% total lipid molarity of 18:1 PE MCC (PE lipid containing maleimide group) was added to formulation DSPC:Chol, and the manufactured liposomes were subsequently incubated with the modified CT overnight at 4°C. The reaction was quenched by the addition of 10 μ L of L-cysteine (20 mM in PBS pH 7.4). The liposome CT mix was then purified to remove unconjugated protein using TFF. The cholera toxin conjugation concentration was optimised to achieve approximately 100 μ g/mL (20 μ g / dose).

6.4.2 Dynamic light scattering: Physicochemical analysis and pH autotitration

Dynamic Light Scattering (DLS) was used to analyse the intensity mean diameter (z-average), polydispersity index (PDI) and zeta potential (mV) of the liposomal formulations using a Malvern Zetasizer Nano-ZS (Malvern Instruments, Worcs., UK). All measurements were undertaken in triplicate. All readings were between 6 and 9 attenuation and samples were diluted 1/10 with appropriate buffer. For vesicle analysis during acidic conditions, the Malvern Zetasizer Nano-ZS was equipped with a MPT-2 Autotitrator. The pH probe was calibrated following the manufacturers guide, using dissolvable pH tablets supplied by Malvern. Two concentrations of hydrochloric acid were used for the titration process 0.25 M and 0.025 M, following manufacturers guidelines and the programme automatically then adjusts the pH, measuring sample properties as the pH declines at specific levels.

6.4.3 Antigen retention following acidic exposure

Purified liposomal formulations (1mL) containing ovalbumin were added to 9 mL of PBS (adjusted to pH 1.2 with HCl) in a falcon tube at 37°C (maintained using a water bath under low mechanical agitation). Aliquots were removed at time points 30, 45, 60 and 120 minutes and added onto the tangential flow filtration for both neutralisation and removal of unbound antigen using PBS (pH 7.4) (pH neutralisation volumes were previously optimised). At the final time point, samples were neutralised and washed using tangential flow filtration and retained at neutral pH (7.4) for a further 2 hours to replicate the transition of the particles movement from the gastric environment to the more neutral pH found across the duodenum, jejunum and ileum (pH 6 – 7.4) (Fallingborg, 1999). The samples were then concentrated and the remaining antigen incorporated was determined using RP-HPLC (as previously optimised in Chapter 3). In case of cationic formulation DSPC:Chol:DOTAP, compatibility issues with the tangential flow filtration meant that dialysis was conducted to both neutralise and remove unbound antigen.

6.4.4 *In Vivo* studies

6.4.4.1 Immunisation schedule

All animal experiments were conducted at the National Institute for Biological Standards and Control (NIBSC). Female BALB/c mice (6–8 weeks old) and C57BL/6 mice 20g (6-12 weeks old) were obtained from Charles River Ltd. All animal procedures were conducted in accordance with the Home Office (scientific procedures) Act 1986. Mice were immunised weekly on five occasions at days 0, 7, 14, 21 and 28 by oral gavage (200 µL) with 200 µg of free ovalbumin (baseline control), 200 µg ovalbumin and 25 µg Cholera Toxin and ovalbumin 10 µg for subcutaneous immunisation (positive control) all in sodium bicarbonate pH 8.2. Nanoparticle formulations were administered (200 µL, oral gavage) as well as empty DSPC:Chol (no ovalbumin) for negative control. Mice were terminally bled on day 35, in order to collect blood samples for antibody analysis. The blood was then centrifuged in order to separate the supernatant from the blood plasma and stored at -80°C for further processing. Organ processing was then conducted, where colon, caecum and small intestine samples were isolated under sterile conditions. These organs were then added to individual vials containing PBSA containing protein inhibition solution and 10% FCS where they were subjected to homogenisation using scissors. Following homogenisation, the supernatant was separated by centrifugation and stored at -80°C. Finally, prior to termination, faecal samples were also collected (day 35), homogenised as previously described and stored in PBSA containing protein inhibition solution, centrifuged and the supernatant was then subsequently stored at -80°C for further processing.

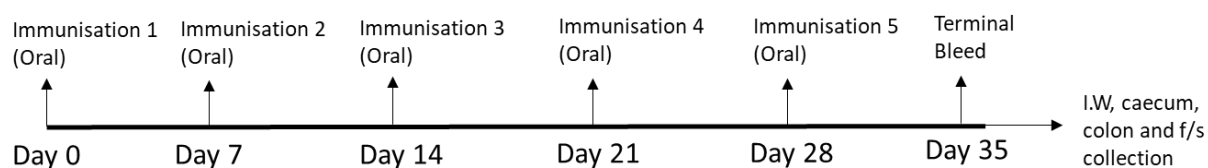


Figure 6.1 Immunisation schedule used for *in vivo* experimentation. Five mice per group were orally administered liposomal formulations (or *s/c* injection for positive control) weekly over a period of five weeks in order to evaluate systemic IgG and mucosal IgA.

6.4.4.2 Quantification of antibodies using ELISA

96-well plates were coated the previous day using 10 µg/mL ovalbumin in carbonate buffer (pH 9.6), kept at 37°C for 2 hours and then overnight at 4°C. The plates were then washed (x3) in wash buffer (PBS, 0.05% Tween) and blocked with 100 µL/well of assay diluent (1% BSA, 0.3% Tween, 0.01M EDTA in PBS) for 30 minutes at 37°C. Serum was diluted 1:50 in assay diluent while intestinal wash, colon, caecum and faecal samples were normalised and added to the wells neat. Samples were serially diluted across the plate, followed by 90-minute incubation at room temperature. The plates were then washed (x3), and either secondary antibody IgG or IgA was added (100 µL/well) (Goat pAb to Ms IgG (HRP, 1:4000 dilution and goat pAb to Ms IgA (HRP), 1:3000 dilution respectively), followed by a 90-minute incubation at room temperature. The plates were then washed (x3) and 100 µL TMB was added for approximately 20 minutes. The reaction was stopped by the addition of 2N sulphuric acid (50 µL) and the plates were subsequently read at 450 nm. Each sample/dilution was tested in duplicate and data are presented as endpoint titre. Both endpoint titre and OD 450 were used to represent the antibody responses. The endpoint titre was determined by the dilution where the optical density > the average blank multiplied by 2.

6.4.5 Statistics

ANOVA tests were used to assess statistical significance between groups for release studies, while the non-parametric Mann-Whitney U test was used for the analysis of antibody levels following ELISA, p values of <0.05 were considered statistically significant. Results are represented as mean ± SD with n = 3 independent batches unless stated otherwise. Antibody analysis is represented as the individual mice (circles) and the geo-mean (black bar) n=5.

6.5 Results and discussion

6.5.1 Liposomal vesicle characteristics and antigen retention under acidic conditions

The inherent physical properties of delivery systems such as vesicle size, composition and surface charge are closely linked to their *in vivo* efficacy (Ramirez et al., 2017). Therefore, understanding how the physicochemical attributes of the formulations behave as they transit through the stomach is an important element in designing an effective oral vaccine. Initial experiments focused on the effect that an acidic environment would have on the liposomal vesicle characteristics. Using the MPT-2 autotitrator adaption for the Malvern ZetaSizer NanoZS, software controlled addition of different titrants (1M HCL, 0.1M HCL and 1M NaOH) can closely regulate the pH environment where the liposomal vesicles are contained. The vesicles are then pumped into the Zetasizer chamber for analysis of both vesicle size and zeta potential. This allows for incremental pH changes through the addition of acids and then subsequent characterisation of the vesicles.

For this experiment, three formulations of differing charge were selected in order to determine how the acidic pH of the gastrointestinal tract would impact upon their stability. Neutral formulation DSPC:Chol (10:5 w/w), anionic formulation DSPC:Chol:PS (10:5:4 w/w) and cationic vesicle formulation DSPC:Chol:DOTAP (10:5:4 w/w) were chosen (Table 6.1). Initially, DSPC:Chol (10:5 w/w) vesicles were found to be approximately 45 nm, with a PDI of 0.13 and near neutral zeta potential (-3.2 mV) (Table 6.1), while DSPC:Chol:PS (10:5:4 w/w) were larger at 163 nm with a PDI of 0.15 and an anionic zeta potential of -49 mV. Finally cationic DSPC:Chol:DOTAP (10:5:4 w/w) were measured at 173 nm with a PDI of 0.29 and a zeta potential of 38 mV (Table 6.1).

Table 6.1 Liposomal formulations physicochemical characteristics prior to subjection to acidic autotitration. Results show neutral (DSPC:Chol), anionic (DSPC:Chol:PS) and cationic (DSPC:Chol:DOTAP) formulations with average size (d.nm), PDI and zeta potential (mV) indicated. Results represent mean \pm SD, n=3 of independent batches.

Liposomal Formulation (w/w)	Size (Z-Avg) (d.nm)	PDI	Zeta Potential (mV)
DSPC:Chol (10:5)	45.1 \pm 0.3	0.13 \pm 0.02	-3.2 \pm 0.5
DSPC:Chol:PS (10:5:4)	163.2 \pm 12.4	0.15 \pm 0.05	-49.3 \pm 2.3
DSPC:Chol:DOTAP (10:5:4)	173.2 \pm 23.7	0.29 \pm 0.13	38.1 \pm 1.5

For DSPC:Chol, at near neutral pH (6.5), vesicles were approximately 45.1 nm, however a steady increase in vesicle size was observed as the pH acidifies (up to approximately 451.9 nm) at pH 3.8. At this point, a plateau was observed, where the vesicle size did not change as the pH was decreased further to pH 1.3 (455.1 nm) (Figure 6.2). The zeta potential of the DSPC:Chol vesicles followed a similar trend, where initially a near neutral value was obtained at pH 6.5 (-3.2 mV), followed by an increase up to approximately 14.8 mV by pH 3.8. As the pH acidified further to pH 1.3, the vesicles were found to be cationic at 19.4 mV (Figure 6.2A). For anionic liposomal formulation DSPC:Chol:PS, a similar trend could be observed. A gradual increase in vesicle size is shown as the pH decreases towards pH 1.3, resulting in a final vesicle size of 291.3 nm. At neutral pH (6.5), the anionic vesicles were shown to have a surface charge of approximately -50 mV, however this increased up to 6.6 mV by pH 1.3 (Figure 6.2B). Finally, cationic liposomal formulation DSPC:Chol:DOTAP was shown to exhibit little changes in vesicle size between pH 6.5 – pH 2 (approximately 170 nm), however a sharp increase was found upon reaching pH 1.3 (278 nm). The zeta potential of the formulation remained highly cationic across all of the pH range tested (38 - 47 mV) (Figure 6.2C).

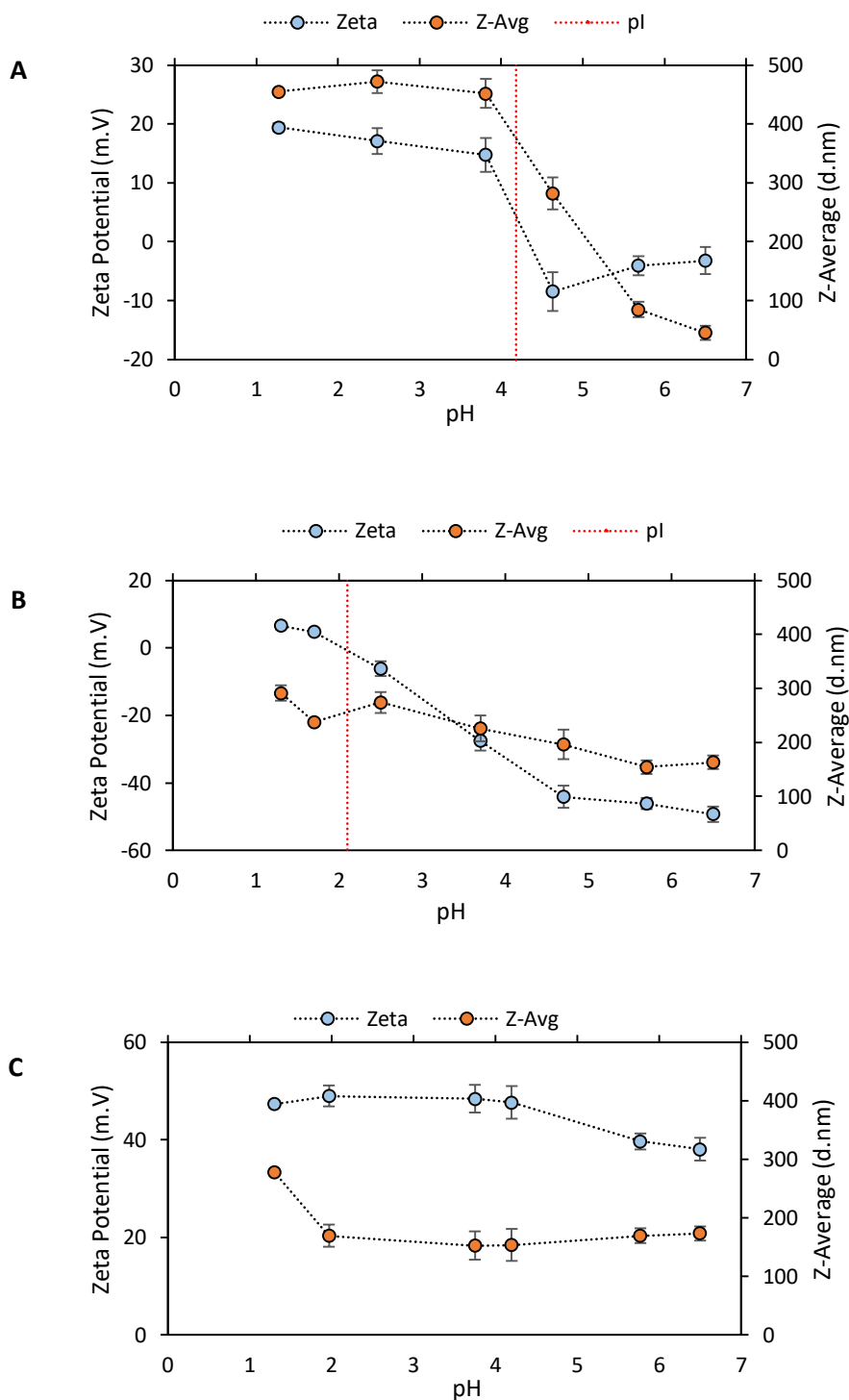


Figure 6.2 Average size (d.nm), PDI and zeta potential (mV) of three empty liposomal formulations A) DSPC:Chol (10:5 w/w) B) DSPC:Chol:PS (10:5:4 w/w) and C) DSPC:Chol:DOTAP (10:5:4 w/w) prepared by microfluidics and subjected to an increasing acidic environment using the MPT-2 Auto Titrator from Malvern Panalytical. The isoelectric point (pI) is indicated by the red dotted line. Results represent mean \pm SD, n=3 of independent batches.

While a definitive consensus is still lacking from the literature in regards to the most effective vesicle size for inducing oral immunisation, the majority of research indicates that particles under 10 μm are accessible through M cells, with some research indicating that particles under 1 μm being the most readily accessible (Davitt and Lavelle, 2015, Brayden and Baird, 2001, Wilkhu et al., 2013). While aggregation of all formulations was observed under highly acidic conditions (pH 1.2), none of the formulations tested aggregated outside of the range for accessibility and uptake at M cells. Furthermore, the adjuvanticity of particle formulations have been shown to be highly influenced by the overall surface charge of the administered formulations along with antigen (Nakanishi et al., 1999). The results shown here indicate a trend of increasing zeta potential as the pH steadily becomes more acidic. These results are likely due to the protonation of amino groups within the lipids, increasing the overall zeta potential of the vesicles as the concentration of hydrogen ions increases (Schmidt et al., 2018, Phayre et al., 2002).

Employing delivery systems for the delivery of antigens through the oral route of administration can enhance the immune response, partly as a result of the particulate nature of the delivery system. Particulate vesicles have inherent immune-stimulatory attributes as a result of increased uptake by both M cells and underlying APCs (Lavelle and O'Hagan, 2006). Given the results indicating the effect of an acidic environment on vesicle physicochemical attributes, it was then important to establish an overview of how low pH could affect antigen association with the liposomal vesicles. Therefore, ovalbumin loaded liposomal formulations were manufactured and subjected to highly acidic gastric pH (pH 1.2) in order to determine the antigen association over time. As described in the methods section, formulations were manufactured and purified before subjection to acidic pH and maintained at 37°C. At specific intervals, the samples were removed and washed using tangential flow filtration (for DSPC:Chol, DSPC:Chol:PS and MPG:Chol:PS) or dialysis (DPSC:Chol:DOTAP) to neutralise the pH, remove unbound protein and then analysed for protein concentration using RP-HPLC. The final liposome samples were retained at pH 1.2 and 37°C for a maximum of 2 hours, before neutralisation and then retained at a neutral pH for a further 2 hours before quantification of the antigen retention in order to attempt to replicate the pH change observed during transit from the gastric environment through to the more neutral environment of the duodenum, jejunum and ileum (Fallingborg, 1999).

The antigen retention of four liposomal formulations is shown in Figure 6.3. Neutral liposomal formulation DSPC:Chol encapsulating ovalbumin is shown to steadily release antigen in the presence of acidic pH, showing a loss of up to 40% of the initial antigen by the 2 hour time point. Upon return to neutral pH, no significant loss of antigen could be observed over the course of the following 2-hour period (Figure 6.3). A similar trend could be observed for anionic liposomal formulation DSPC:Chol:PS, where a steady loss of antigen is observed during acidic conditions, resulting in a loss of approximately

20% of the initial antigen by the 2-hour time point. By the final time point, no significant differences in terms of antigen retention could be observed between both DSPC:Chol and DSPC:Chol:PS ($p>0.05$) (Figure 6.3). Cationic liposomal formulation with surface adsorbed ovalbumin was then subjected to the same acidic conditions, where a more rapid disassociation between the antigen and delivery system was observed. By 30 minutes, 40% of the antigen was lost during acidic conditions and by the final time point at pH 1.2, approximately 20% of the initial antigen was retained. Upon restoration to neutral pH, no significant loss of ovalbumin could be observed (Figure 6.3). Finally, a fourth formulation was tested containing a non-ionic surfactant monopalmitoyl-glycerol (MPG) alongside the addition of cholesterol and phosphatidylserine in order to support vesicle formation. This niosomal formulation resulted in the greatest antigen retention when subjected to acidic pH. By 2 hours at pH 1.2, 89% of antigen was still associated with the vesicles and upon neutralisation of pH and a further 2 hours, no significant further loss of antigen was observed ($p>0.05$) (Figure 6.3).

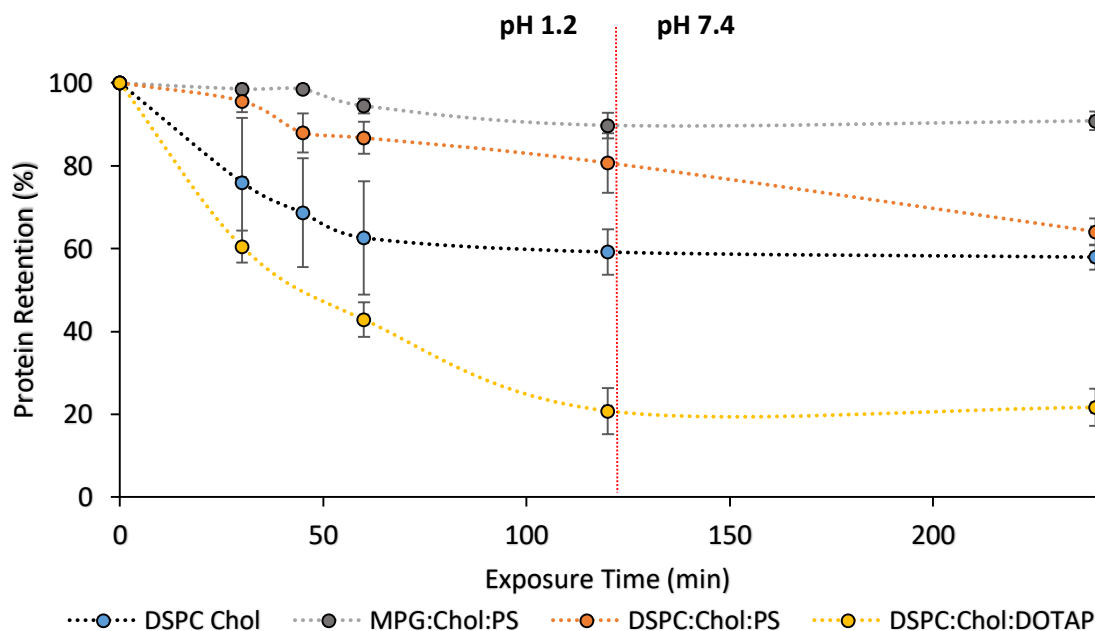


Figure 6.3 Formulations DSPC:Chol (10:5 w/w), MPG:Chol:PS (10:5:4 w/w), DSPC:Chol:PS (10:5:4 w/w) with ovalbumin encapsulated inside and DSPC:Chol:DOTAP (10:5:4 w/w) with surface adsorbed ovalbumin were subjected to acidic conditions (pH 1.2) for up to 120 minutes at 37 °C. Samples were removed, neutralised and washed to remove untrapped antigen using tangential flow filtration (DSPC:Chol, MPG:Chol:PS and DSPC:Chol:PS) or dialysis (DSPC:Chol:DOTAP). The final time point was further subjected to a neutralisation of pH (7.4) (indicated by the red-dotted line) and retained for an additional 120 minutes before sample removal and washing. Antigen retention within the vesicles was then determined using RP-HPLC. Results represent mean \pm SD, $n=3$ of independent batches.

While all formulations resulted in a significant loss of antigen retention during acidic exposure, there were large differences between formulations in regards to the rate of loss. Niosomal formulation MPG:Chol:PS (10:5:4 w/w) was found to retain approximately 90% of the encapsulated antigen after the 4 hour experiment. The use of non-ionic surfactants as oral delivery vehicles incorporating proteins

and peptides is well known within the literature. Niosomes have favourable stability attributes when administered *in vivo* and have been shown to protect insulin through the gastric tract, resulting in significantly lower levels of blood glucose levels, as well as stimulating IgG1 responses in relation to vaccine studies (Khaksa et al., 2000, Ge et al., 2019, Vangala et al., 2006). When determining the applicability of oral niosomal formulations as DNA vaccine carriers, formulations incorporating Span 60, cholesterol and stearylamine (6:3:1 molar ratio) with and without a *o*-palmitoyl mannan coating showed high DNA-vesicle retention in the presence of simulated gastric fluid (pH 1.2) ($77 \pm 6\%$ and $85 \pm 7\%$ for coated and uncoated vesicles respectively). When observing the antigen retention ability of the phospholipid based formulations, in the case of both DSPC:Chol and DSPC:Chol:PS, approximately 58 – 64% retention was observed. These specific lipid compositions were selected, as well as high cholesterol content, due to the long acyl chain length found with DSPC. Whilst the antigen retention observed was not as high as that found with the niosome formulation, the inclusion of lipids containing longer chains has been shown to greatly increase vesicle stability and retention of encapsulated material (Lu et al., 2012). In a similar study as to the one conducted here (Figure 6.3), Taira et al assessed the bovine serum albumin (BSA) retention in acidic conditions (pH 2, 37°C) for a range of liposomal formulations designed for oral delivery. Formulations containing EggPC, cholesterol (1:1 molar ratio) and binding ligands for M cell association were found to steadily release their protein contents over time, with approximately 60% release observed by the 2 hour time point (Taira et al., 2004). While the acidic conditions chosen in this study differ slightly to that conducted in Figure 6.3, the comparatively improved antigen retention is likely a result of the use of long chain lipids (DSPC carbon chain length – 18, PC carbon chain length – 12). The final formulation chosen was the cationic formulation DSPC:Chol:DOTAP with surface adsorbed antigen. It should be noted that the experimental procedure for this formulation was distinct to the other formulations encapsulating antigen, due to the incompatibility of the cationic formulation with the tangential flow filtration system. However, the apparent rapid loss of antigen association found at pH 1.2 is likely explained by how the antigen and vesicles interact. The antigen association for this cationic formulation was achieved through electrostatic adsorption of the negatively charged protein to the positively charged surface of the liposomes. Nevertheless, the isoelectric point of ovalbumin has been shown to be between pH 4 - 5, therefore at pH 1.2, is likely to be highly positively charged (with a zeta potential of approximately +35 mV) (Niu et al., 2014). Therefore, this rapid loss of antigen retention is likely due to a loss of electrostatic interaction, and upon neutralisation to pH 7, no further losses could be observed after 2 hours. It also should be noted that this acidic exposure experiment contained only water, NaCl and adjusted pH to 1.2 using HCl and a maximum acidic exposure time of 2 hours. These parameters were selected based upon the initial acidic exposure experiments conducted on the MPT-

2 autotitrator, yet the *in vivo* gastric and intestinal environments can vary dramatically. Typically, fasted human pH values can be between pH 1 - 3 (although can reach as neutral as pH 6 depending on ingested components), while the gastric volume can vary dramatically between 10 - 50 mL (with intake of exogenous fluid, this volume will rapidly increase). The transit time of the gastric environment has also shown wide variance, with some papers stating a median time of approximately 30 minutes (Koziolek et al., 2015). In addition to this, enzymatic degradation will additionally occur during *in vivo* transit, these include proteases such as pepsin, trypsin and groups of lipases, all of which will pose stability issues to both liposomes and antigen (Ramirez et al., 2017).

6.5.2 Mucosal and systemic antibody responses following oral administration of liposomal formulations

In order to determine the ability of nanoparticle formulations manufactured by microfluidics to induce antibody responses following oral administration, a wide range of formulations were developed (as optimised previously). These formulations focused on the inclusion of lipids with long acyl chain lengths (e.g. DSPC) as well as high cholesterol ratios to improve the stability of the antigen containing vesicles as they traverse through the gastric environment. Primarily, these formulations entrapped antigen within the aqueous core of the vesicles (DSPC:Chol, DSPC:Chol:PS and MPG:Chol:PS), with the exception of cationic formulation DSPC:Chol:DOTAP where the antigen was surface associated via electrostatic interactions between the positively charged membrane surface and the overall anionic charge of the ovalbumin. Phosphatidylserine was included in two of the formulations due to the potential improved uptake rates exhibited by macrophages observed in Chapter 5 (Shah et al., 2019).

Prior to immunisation, physicochemical characterisation of the formulations was conducted. In the case of both neutral and anionic formulations, a 3:1 FRR and 15 mL/min TFR were selected as the result of previous optimisation (Chapter 2 and 4). Following purification, these formulations were concentrated using tangential flow filtration in order to have a final ovalbumin concentration of 1 mg/mL. In the case of cationic formulation DSPC:Chol:DOTAP, the vesicles were manufactured via microfluidics using initial parameters 1:1 FRR, 15 mL/min followed by dialysis for solvent purification. The vesicles were then sent back through the microfluidic system in order to complex the ovalbumin onto the surface of the vesicles (FRR 5:1, 15 mL/min TFR). The final ovalbumin concentration was optimised in order to give the same final antigen concentration as the entrapped formulations (1 mg/mL).

After manufacture and purification, the formulations were then characterised in terms of vesicle size and zeta potential. Figure 6.4 indicates the average vesicle characteristics of the formulations used

prior to oral administration. For neutral formulation DSPC:Chol (10:5 w/w) entrapping ovalbumin, the vesicles were found to be approximately 76.6 ± 6 nm with a near neutral zeta potential (-4.5 ± 2 mV) and a PDI of approximately 0.3. Anionic formulation incorporating PS was found to be slightly larger with an average size of 94 ± 27 nm and a zeta potential of -20 ± 3 mV as well as a homogenous population distribution (0.24 PDI). For niosomal formulation incorporating non-ionic surfactant monopalmitoyl glycerol (MPG) alongside cholesterol and PS, an average diameter of 70 ± 15 nm with an anionic zeta potential of -28 ± 7 mV and a PDI value of 0.24. Finally, cationic liposomal formulation DSPC:Chol:DOTAP with surface adsorbed antigen was found to be the largest at 198 ± 43 nm and a homogenous PDI value of 0.18, with an overall negative surface charge of -13 ± 2 mV as a result of the ovalbumin coating (Figure 6.4).

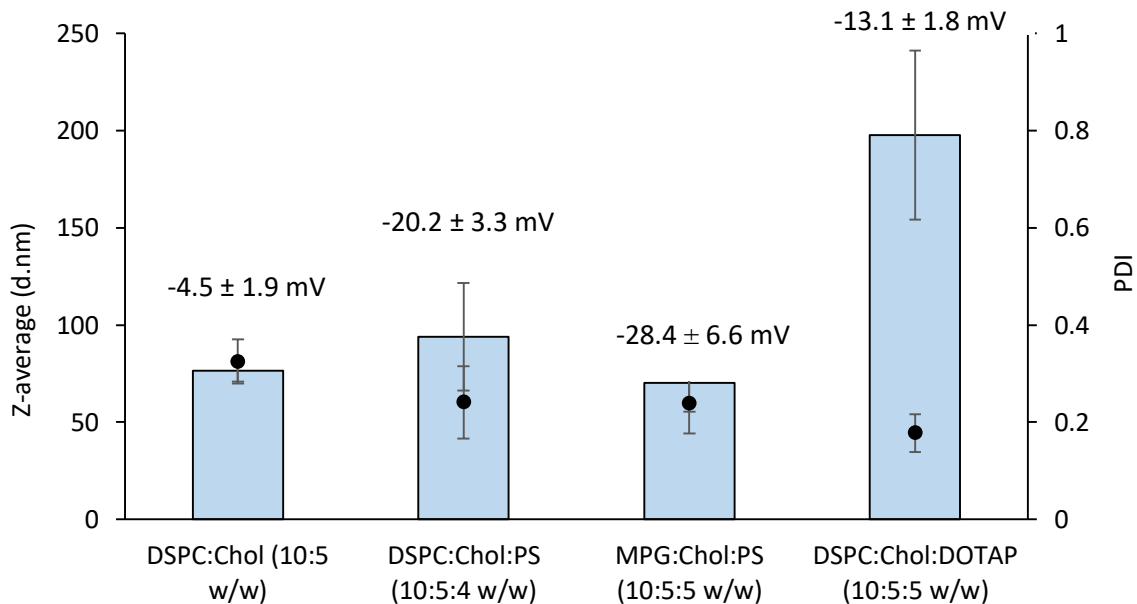


Figure 6.4 Average size (d.nm) (bars), PDI (circles) and zeta potential (mV) (values) of the four formulations prior to oral administration. Microfluidic manufacture of DSPC:Chol (10:5 w/w), DSPC:Chol:PS (10:5:4 w/w) and MPG:Chol:PS (10:5:5 w/w) (3:1 FRR, 15 mL/min TFR) with a final OVA concentration of 1 mg/mL entrapped. Cationic formulation DSPC:Chol:DOTAP (10:5:2 w/w) (1:1 FRR, 15 mL/min TFR) with a final ovalbumin concentration of 1 mg/mL adsorbed on the surface. Results represent mean \pm SD, $n = 5$ of independent batches.

To assess these formulations *in vivo*, female C57BL/6 mice were immunised by oral gavage (as well as a subcutaneous injection of ovalbumin as a positive control group) on 0, 7, 14, 21 and 28 days. Terminal bleeds were conducted on day 35, where serum was kept for determination of systemic IgG responses. In order to determine mucosal IgA responses, the colon, caecum and small intestine were removed and stored with protein inhibition solution and FCS at -80°C alongside sera samples. Figure 6.5 shows the OD 450 values of the antibody immune response data quantified by ELISA. Positive controls (subcutaneous ovalbumin), negative controls (oral empty DSPC:Chol and oral ovalbumin) are

compared to the four nanoparticle formulations in terms of either IgG or IgA responses. Figure 6.5A indicates the systemic IgG responses on day 35, where no statistically significant increases in IgG levels could be observed across any of the administered formulations in comparison to oral ovalbumin alone ($p>0.05$). Conversely, subcutaneous ovalbumin generated comparatively high levels of systemic IgG within the serum ($p<0.05$). When comparing IgA levels within the serum, subcutaneous ovalbumin is shown to generate very low IgA levels (Figure 6.5B). An increase in IgA is observed when ovalbumin was administered orally and administered entrapped within liposomal formulation DSPC:Chol:PS (10:5:4 w/w) (not statistically significant) ($p>0.05$). However, IgA sera levels of formulations DSPC:Chol (10:5 w/w), MPG:Chol:PS (10:5:4 w/w) and DSPC:Chol:DOTAP (10:5:4 w/w) failed to increase IgA responses above baseline.

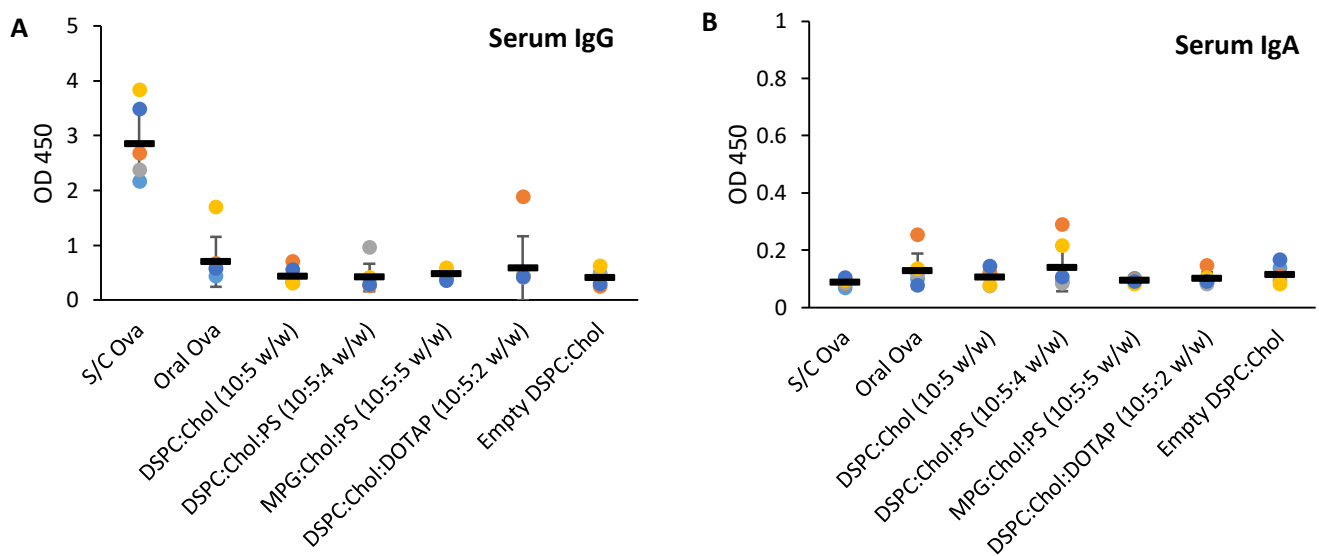


Figure 6.5 Anti-OVA antibody systemic immune responses following oral administration of liposomal formulations in mice (BALB/c mice 6–8 weeks old). Mice were terminally bled on day 35 and serum antibody analysis was conducted using ELISA. (A) Serum IgG response and (B) Serum IgA response. Each sample/dilution was tested in duplicate and data are presented as mean optical density (OD 450) with each individual sample (circle) and Geo-mean (black line) shown. Results represent geo-mean \pm SD, $n=5$ of independent batches

When comparing localised mucosal antibody responses, first intestinal washes from the small intestine were analysed. Results from Figure 6.6A indicate poor IgA responses for all four formulations tested, with no significant differences observed across all test parameters. When analysing the caecum data, subcutaneous ovalbumin resulted in the greatest increase in localised IgA, while none of the formulations significantly increased antibody levels above baseline (Figure 6.6B) ($p>0.05$). A similar story was observed for the IgA colon samples, where no significant increases in IgA could be found across all groups (Figure 6.6C). In the case of DSPC:Chol:PS and DSPC:Chol:DOTAP, some mice were shown to have 3-5 fold increases in IgA when compared to both subcutaneous and oral

ovalbumin, however no statistically significant increases could be found overall ($p > 0.05$). Finally, faecal samples were taken from the individual mice on day 35 for IgA analysis. No significant changes in anti-ovalbumin IgA levels could be found across all formulations when compared to oral ovalbumin alone (Figure 6.6D).

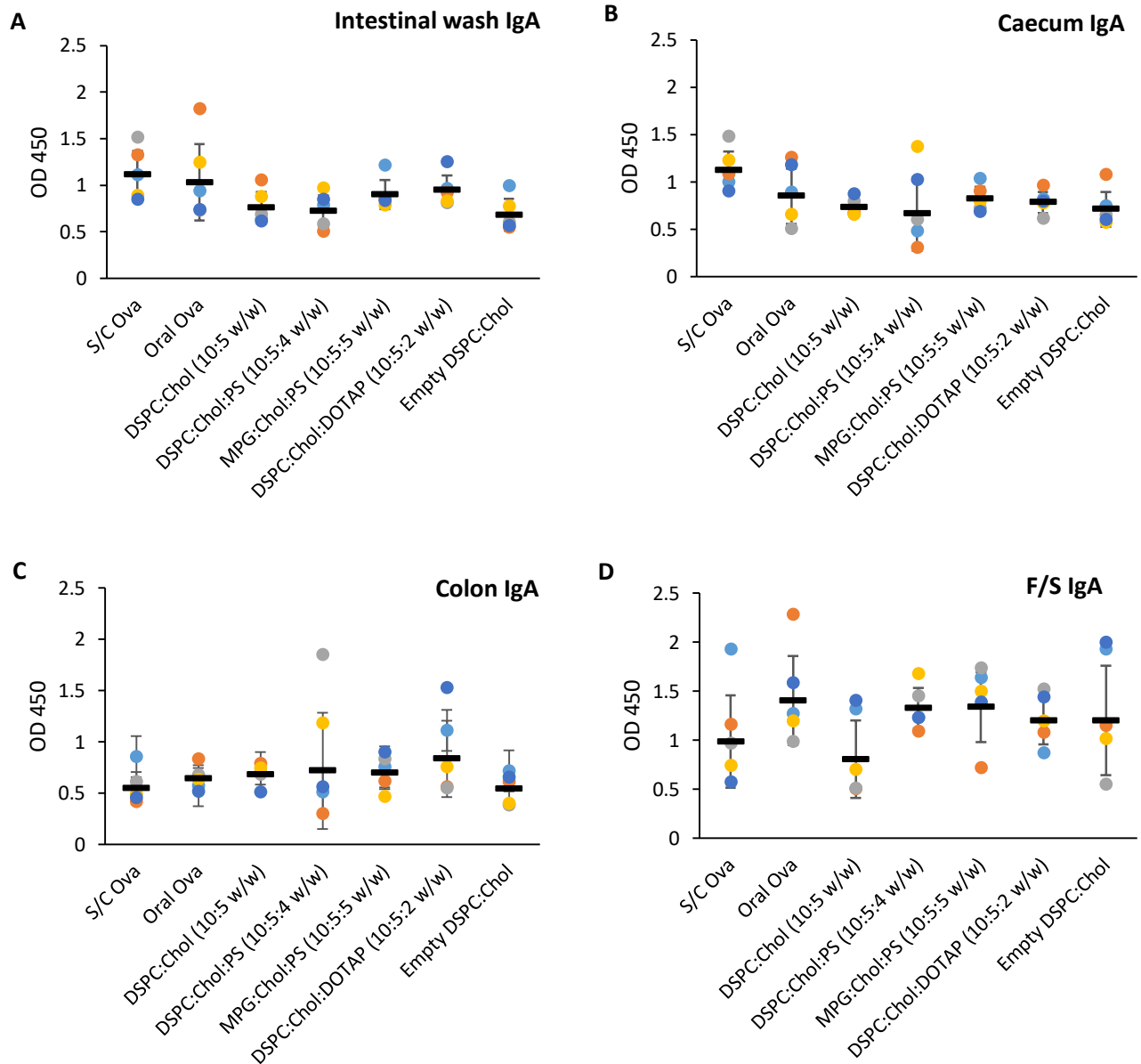


Figure 6.6 Anti-OVA antibody mucosal immune responses following oral administration of liposomal formulations in mice (BALB/c mice 6–8 weeks old). (A) Intestinal wash (B) caecum (C) colon and (D) faecal samples were analysed for IgA antibody response using ELISA. Each sample/dilution was tested in duplicate and data are presented as mean optical density (OD 450) with each individual sample (circle) and Geo-mean (black bar) shown. Results represent geo-mean \pm SD, $n = 5$ of independent batches.

Once antigen has traversed through the stomach and enters the small intestine, there are a number of uptake pathways possible which can then result in an adaptive immune response. The uptake of antigen can occur through entry and transcytosis through M cells, before uptake by APCs such as DCs and macrophages. Furthermore, epithelial cells lining the vast majority of the small intestine are capable of antigen uptake and finally DCs can directly sample antigen within the lumen by extending appendages through epithelial tight junctions (Weiner et al., 2011). Currently, there remains some ambiguity in regards to the most effective particle size for oral immunisation (highlighting the complexity and challenges involved with this route of administration); nonetheless, it has generally been shown that vesicles under 1 μm are readily taken up by M cells (Davitt and Lavelle, 2015, des Rieux et al., 2006). Despite all of the formulations within this study being sub-micron in size, poor antibody responses were observed for all. This is typically a result of the intricacies involved when dealing with the mucosal immune system. It is well established that the mucosal immune system is a separate entity compared to the systemic, where high degrees of compartmentalization can be found. This is a result of the existence of homing receptors on APCs and lymphocytes resulting in immune responses being largely confined within the MALT (Janeway et al., 1999). The results shown in Figure 6.5A highlight this compartmentalisation, where subcutaneous ovalbumin results in high systemic IgG responses, yet unresponsive localised (intestinal wash, caecum and colon) IgA in comparison. Contrarily, oral ovalbumin antigen alone resulted in both poor systemic IgG and localised IgA (Figure 6.5). This is a result of the tolerogenic default environment found within the gut, where a range of cells exert controls over each other to actively pursue a state of higher tolerance in comparison to the systemic immune system. Interactions between our gut microorganisms, epithelial cells and then subsequently DCs results in CD103⁺ retinoic acid-dependent types, which then induces a number of different regulatory T cells (including IL-10, foxp3⁺ and transforming growth factor- β dependent types) promoting tolerance to an antigen (Weiner et al., 2011). This indicates why adjuvants (and in this case, delivery systems) are a crucial component to the success of an oral vaccine comprising of a subunit antigen (Rhee et al., 2012). While it has been shown that particulate systems can enhance vaccine delivery and are inherently immunogenic, a comprehensive understanding of the specific immune-stimulating properties are still lacking (Lavelle and O'Hagan, 2006). While some mice showed 3 - 5 fold increases in IgA levels (colon samples) after DSPC:Chol and DSPC:Chol:DOTAP administration, despite the particulate nature of the liposomes, it was not enough to significantly overcome these tolerance mechanisms, resulting in overall poor localised anti-OVA IgA levels. Cationic formulations, as a result of electrostatic repulsions, can be beneficial for oral vaccination due to their mucoadhesive properties as well as improved resistance to enzyme degradation (He et al., 2019). In particular, chitosan – ovalbumin complexes can boost localised IgA responses compared to ovalbumin alone when

administered orally (Cole et al., 2018). However, DSPC:Chol:DOTAP liposomes with surface adsorbed antigen failed to improve baseline systemic and mucosal antibody levels compared to oral antigen alone. This could be a result of the exposure of the antigen to the gastric environment, where the benefit of protection from complexed or encapsulated antigen is lost, as well as a lack of immunostimulation from the vesicles (Davitt and Lavelle, 2015).

For neutral formulation DSPC:Chol entrapping ovalbumin within the aqueous core, it was hypothesised that the use of long acyl chain lengths could protect antigen degradation and therefore improve antibody responses, however it is likely that the formulation required a more potent adjuvant (Bernasconi et al., 2016). Previous studies working with DSPC:Chol (10:5 molar ratio) liposomes encapsulating ovalbumin (with and without PEGylation) following oral administration found similar levels of intestinal wash IgA across the liposomal formulations and ovalbumin in solution, yet this effect was shown to be liposome-concentration dependent (Minato et al., 2003). Phosphatidylserine (PS) was then added to two formulations, liposomal DSPC:Chol and non-ionic surfactant formulation MPG:Chol encapsulating ovalbumin. As previously stated, PS was incorporated within these formulations to enhance macrophage phagocytosis, therefore potentially improving the antigen presentation and subsequent adaptive immune response (Bernasconi et al., 2016, Tseng et al., 2009). PS is a highly abundant, negatively charged glycerophospholipid found mainly within the inner leaflet of eukaryotic membranes. However, during cellular stress or the process of apoptosis, the cell begins to externalise PS from the inner membrane leaflet to the outer-leaflet. Externalised PS on the cells surface then serves as a potent “eat-me” signal for macrophages and DCs. The immune cells recognise the externalised PS through direct cell-cell interactions as well as indirectly through third party molecules (Birge et al., 2016). The process is designed to recycle old and damaged cells, however in relation to vaccine delivery, the addition of PS to liposomal formulations can serve as a unique way for the vaccine delivery system to improve the presentation of antigen to the hosts immune system. Furthermore, the results from Chapter 5 indicate the synthetic version of PS, DOPS, as having enhanced processing properties for THP-1 derived macrophages. Nevertheless, the data in Figure 6.5 and 6.6 indicates no significant increase in both systemic IgG and localised IgA levels being found when compared to negative controls. While initially these results may seem contrary, a study published in 2018 indicated that while PS-liposomes entrapping insulin peptides were indeed up taken at an accelerated rate through apoptotic pathways, the downstream effects of this internalisation choice resulted in tolerogenic presentation (typically useful for autoantigen in regards to apoptosis) and therefore a subsequent down regulation of the adaptive immune response (Rodriguez-Fernandez et al., 2018). Therefore, from the results shown here in Figure 6.5 and 6.6, it is possible that particulate liposome systems comprising of components such as DSPC and cholesterol may in fact require further

immunostimulatory components incorporated in order to overcome the inherent bias of the mucosal immune system towards tolerance in the face of oral antigens.

6.5.3 Inclusion of immunostimulatory components to liposomal formulations and the effect on mucosal and systemic antibody response

Given the poor antibody responses generated from the liposomal formulations, the next step was to improve the immunogenicity of the formulations in order to overcome the tolerogenic mucosal environment. The use of cholera toxin (CTX) as an oral adjuvant has been studied for a number of decades. The toxin is produced by *Vibrio cholera* and can stimulate potent IgA responses against a non-related antigen when co-administered (Lycke and Holmgren, 1986). The mechanism of action is dependent on the animal model in question, however CTX is believed to upregulate presentation by a range of APCs as well as promoting B cell isotype differentiation towards IgA secretion and enhancing mucosal membrane permeability. Furthermore, in conjunction with antigen, CTX can enhance antigen uptake at M cells (likely due to targeting of the G_{m1} ganglioside), indicating its strengths as an effective oral vaccine adjuvant when administered at the correct dose (Holmgren et al., 1992). Therefore, in order to boost the mucosal antibody response to ovalbumin within liposomal particulate vesicles, CTX was chosen. Following a previously published protocol, CTX was both conjugated to the surface of DSPC:Chol modified liposomes via maleamide-thiol interactions as well as co-administered without chemical conjugation (Harokopakis et al., 1995, Harokopakis et al., 1998).

In addition to cholera toxin, further immunostimulatory components were included within the previous round of *in vivo* formulations in order to boost the antibody responses. The cationic surfactant dimethyldioctadecylammonium bromide (DDA) has previously been shown to be an effective adjuvant in regards to both enhanced antibody and cell mediated immune responses (Hilgers and Snippe, 1992). Therefore, DOTAP was replaced with DDA, and the manufacturing protocol was adjusted. Previously, cationic DSPC:Chol:DOTAP was manufactured, purified and then surface coated with antigen via electrostatic interactions. However, it is hypothesised that this may lead to poor protection from the acidic and enzymatic degradation. Therefore, a new cationic formulation composing DSPC:Chol:DDA was manufactured in-line with the ovalbumin (one microfluidic inlet contained the lipid components while the second inlet contained the ovalbumin in TRIS buffer 10 mM, pH 7.4). Following manufacture, the liposome – ovalbumin complex was purified by dialysis.

Finally, a potent cationic adjuvant formulation CAF01 was investigated to determine the ability of this formulation to generate mucosal immune responses following oral administration. This adjuvant formulation consists of cationic surfactant DDA and the immunopotentiator α,α' -trehalose 6,6'-

dibehenate (TDB) (Hamborg et al., 2014). TDB is a synthetic mycobacterial cord factor and in conjunction with DDA, can generate both potent cell-mediated and humoral immune responses (Agger et al., 2008).

6.5.3.1 Development of the liposomal CTX conjugates

The coupling between cholera toxin and liposomes via a thioether bond was achieved following a previously published protocol by Harokopakis et al. Chemical modification is initially required in order to add thiol groups (necessary for the thiol-maleimide reaction) to lysine residues of the cholera toxin. This was achieved through the use of SPDP, an amine reactive reagent added at a 1:10 molar ratio (protein:SPDP). Specific lipid containing maleimide groups (18:1 PE:MCC) was then added within the liposomal formulation DSPC:Chol at 5% of the total lipid molarity (additional information for the conjugation process can be found within the methods section 6.4.1.3). In order to confirm conjugation, initial experiments used fluorescently labelled ovalbumin (Alexa Fluor™ 488) as an easily quantifiable substitution for the cholera toxin. Initial experiments resulted in poor conjugation efficiency (1.5%) following the published protocol (Table 6.2). This poor conjugation was likely due to the insolubility of the SPDP within aqueous buffer during the incubation with the protein, therefore prior to SPDP addition, DMSO was used as a solubilisation agent. This process was then found to increase the conjugation efficiency dramatically (up to 24%) (Table 6.2). Further optimisation of the protocol was then investigated by adjusting the pH of the protein: SPDP reaction, given the importance of maintaining a neutral pH close to 7.5 (ThermoFisher). Increasing the pH from 6.8 to 7.3 resulted in a high conjugation efficiency (66%) between the modified ovalbumin and the liposome surface (containing PE:MCC for conjugation).

Table 6.2 Conjugation efficiency of fluorescent ovalbumin (Alexa Fluor) to liposome surface (DSPC:Chol) containing 5% PE:MCC. The effect of DMSO for SPDP solubilisation and buffer pH during SPDP and protein incubation is shown, with % conjugation efficiency measured by fluorescence.

DMSO for SPDP dissolution	Buffer pH	Conjugation efficiency (%)
X	6.8	1.5
✓	6.8	24
✓	7.3	66

6.5.3.2 Formulation of adjuvanted liposome systems.

Following on from the inclusion of more potent adjuvants, characterisation of these new formulations was conducted in terms of vesicle physicochemical properties. Figure 6.7 indicates the formulations encapsulating ovalbumin: DSPC:Chol CTX Co-mix, DSPC:Chol CTX Conjugate, DSPC:Chol:DDA – ovalbumin complex and cationic adjuvant DDA:TDB with surface adsorbed ovalbumin. Again, all formulations were loaded with a final antigen concentration of 1 mg/mL. The data represents the average of n=5 formulations prior to oral administration. In the case of DSPC:Chol (10:5 w/w) encapsulating ovalbumin with CTX co-administered, the vesicles were found to be approximately 63.2 ± 10 nm with a homogenous population distribution (PDI 0.24) (Figure 6.6). For liposomal formulation DSPC:Chol:PE:MCC (10:5 w/w) encapsulating ovalbumin with CTX conjugated onto the surface, larger vesicles were characterised (approximately 246.9 ± 117 nm) yet a homologous population distribution was still retained (PDI 0.24) (Figure 6.7). In the case of cationic liposomal formulation DSPC:Chol:DDA (10:5:5 w/w) complexed in-line with ovalbumin, vesicles were found to average approximately 318.4 ± 39 nm (PDI 0.2) (Figure 6.7). The final formulation, DDA:TDB with surface adsorbed ovalbumin resulted in micron sized vesicles (data not shown) with a relatively heterogeneous population distribution (PDI 0.5) due to the particular dose restrictions of DDA:TDB (250 μ g: 50 μ g) and ovalbumin (1mg/mL). In the case of zeta potential, DSPC:Chol co-administered with CTX was found to be -11.6 ± 3.6 mV, while the conjugated formulation showed a more negative zeta potential (-29.1 ± 7.3 mV) (Figure 6.7). Cationic formulation DSPC:Chol:DDA complexed with ovalbumin remained positively charged (37.5 ± 1.8 mV) as did DDA:TDB with surface adsorbed ovalbumin (23.4 ± 3.3 mV) (Figure 6.7).

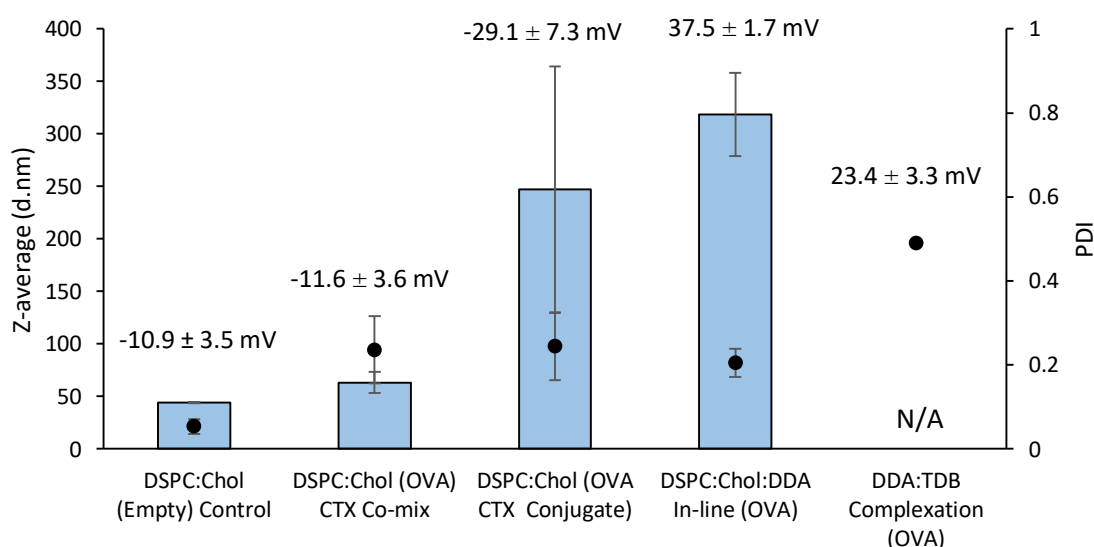


Figure 6.7 Average size (d.nm) (bars), PDI (circles) and zeta potential (mV) (values) of the four formulations prior to oral administration. Microfluidic manufacture of empty DSPC:Chol (10:5 w/w), DSPC:Chol (10:5 w/w) encapsulating ovalbumin with co-mixed CTX, DSPC:Chol (10:5 w/w) encapsulating ovalbumin with surface conjugated CTX, DSPC:Chol:DDA (10:5:4 w/w) in-line loaded with ovalbumin and DDA:TDB (5:1 w/w) with surface complexed ovalbumin. All formulations had a final antigen concentration of 1 mg/mL. Results represent mean \pm SD, n=5 of independent batches.

6.5.3.3 Systemic antibody response

Female BALB/c mice (8 - 12 weeks old) were immunised under the same schedule as previous (0, 7, 14, 21, 28 days with termination bleeds being conducted on day 35). Serum was analysed by ELISA for systemic IgG responses, while intestinal wash samples, caecum and colon were analysed for both IgA and IgG. A number of controls were also kept within the experimental setup, with subcutaneous injection of ovalbumin, oral ovalbumin, oral ovalbumin and CTX as well as oral empty DSPC:Chol vesicles.

Serum was analysed at termination (day 35) for systemic anti-ovalbumin IgG. Figure 6.8 shows the endpoint titre antibody response for all groups. In the case of subcutaneous ovalbumin, strong IgG responses were observed (51200 endpoint titre), while oral ovalbumin alone resulted in poor IgG levels (1212 endpoint titre) (Figure 6.8). When ovalbumin was then administered in the presence of CTX, IgG levels increased by 32-fold (38802). The same endpoint titre was then reached by the liposomal formulation encapsulating ovalbumin in the presence of co-administered CTX (Figure 6.8). When the CTX was then conjugated onto the liposomal surface, a significant ($p < 0.05$) decrease in mean titre was observed compared to both of the co-mixed formulations and subcutaneous ovalbumin injection (1392). Similar baseline levels of IgG response was observed for all other delivery systems, with no significant increase being found for DDA:TDB and DSPC:Chol:DDA (1212, 263 respective mean titres; $p > 0.05$; Figure 6.8).

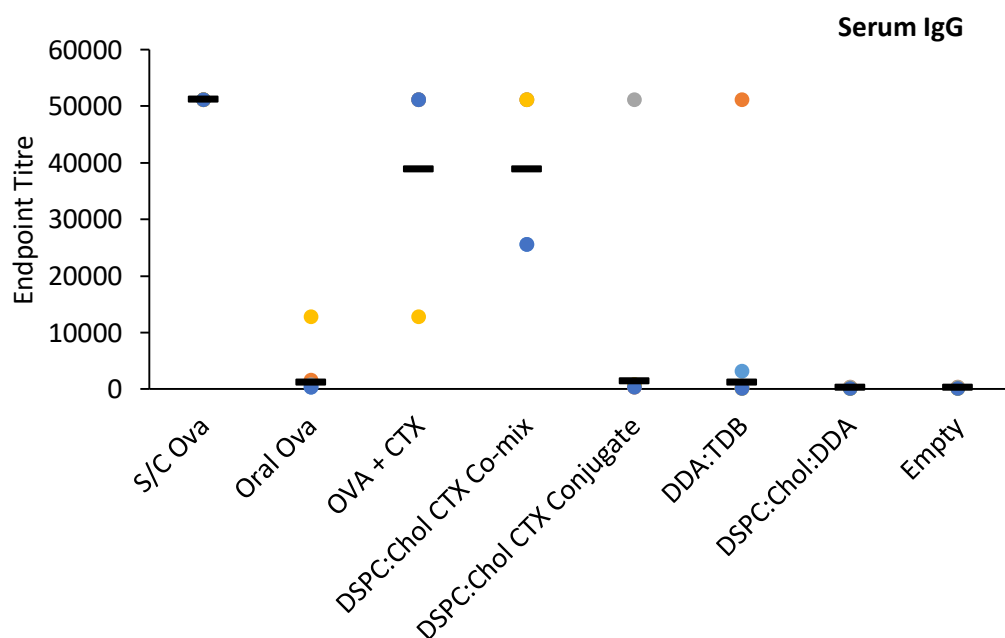


Figure 6.8 Anti-OVA antibody systemic immune responses following oral administration of liposomal formulations in mice (C57BL/6 mice 20g, 6-12 weeks old). Mice were terminally bled on day 35 and serum IgG antibody analysis was conducted using ELISA. Each sample/dilution was tested in duplicate and data are presented as mean optical density (OD 450) with each individual sample (circle) and Geo-mean (black bar) shown. Results represent geo-mean \pm SD, $n=5$ of independent batches.

6.5.3.4 Mucosal antibody response

Determination of local mucosal antibody responses were then conducted on intestinal wash, caecum and colon samples, where both IgG and IgA levels were quantified through ELISA. In the case of the intestinal wash samples, both subcutaneous and oral ovalbumin resulted in baseline levels, however ovalbumin with CTX significantly ($p < 0.05$) increased IgA (Figure 6.9A). While liposomal DSPC:Chol co-mixed with CTX only slightly improved IgA, none of the formulations resulted in any significant increases in endpoint titres when compared to oral ovalbumin alone (Figure 6.9A). When analysing the IgG responses, subcutaneous ovalbumin yielded high titres (1024 mean titre, Figure 6.9B), while oral ovalbumin resulted in a poor antibody response. Both ovalbumin and CTX, and liposomal formulation DSPC:Chol encapsulating antigen with co-mixed CTX significantly ($p < 0.05$) improved IgG responses (891 and 675 mean titres respectively, Figure 6.9B) when compared to oral ovalbumin alone (Figure 6.9B). All other formulations tested showed baseline IgG levels (Figure 6.9B). Caecum IgA levels showed both subcutaneous and oral ovalbumin groups yielding baseline IgA antibody levels (21 and 16 mean titres respectively, Figure 6.9C). However, the addition of CTX alongside ovalbumin resulted in the highest IgA levels among all groups (776 mean titre, Figure 6.9C). In the case of the liposomal formulations, no statistically significant increases could be observed when compared to oral antigen alone; DSPC:Chol ovalbumin co-mixed with CTX (64 mean titre, Figure 6.9C), DSPC:Chol ovalbumin with conjugated CTX, DDA:TDB and DSPC:Chol:DDA ($p > 0.05$) (48.5, 32 and 21 mean titres respectively, Figure 6.9C). Finally, colon samples were analysed in regards to both IgA and IgG responses. Figure 6.9D indicates the IgA responses, where the only statistically significant ($p < 0.05$) increase in antibody levels found was from oral ovalbumin with CTX. No formulations tested showed significant increases in IgA responses compared to oral ovalbumin alone (Figure 6.9D). In case of colon IgG levels, significant increases in IgG were found for subcutaneous, ovalbumin + CTX and DSPC:Chol CTX groups. When comparing between the oral antigen with CTX and the liposomal antigen with CTX, no statistically significant differences could be found ($p > 0.05$). No other formulations were found to significantly impact ($p > 0.05$) upon IgG levels when compared to oral antigen alone (Figure 6.9E).

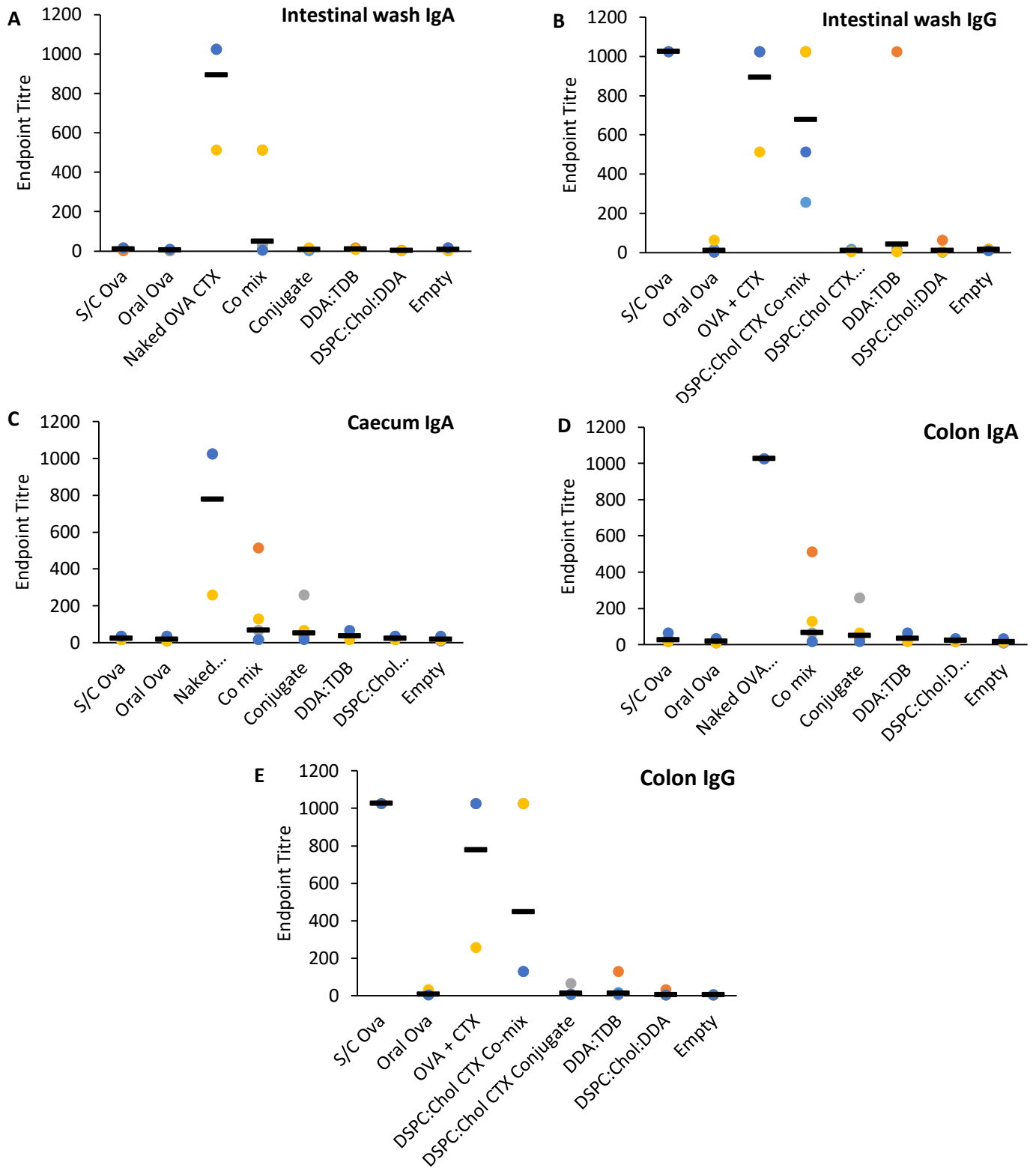


Figure 6.9 Anti-OVA antibody mucosal immune responses following oral administration of liposomal formulations in mice (C57BL/6 mice 20g, 6-12 weeks old). (A-B) Intestinal wash IgA and IgG respectively, (C) caecum IgA (D-E) colon IgA and IgG respectively were analysed for antibody responses using ELISA. Each sample/dilution was tested in duplicate and data are presented as the endpoint titre with each individual sample (circle) and Geo-mean (black bar) shown. Results represent geo-mean \pm SD, n=5 of independent batches.

Given the lack of antibody responses found when administering conventional liposomal formulations (Figure 6.5 and 6.6), it is hypothesised that the inclusion of components that are capable of eliciting immunostimulatory properties may boost immune responses following liposomal oral administration. When determining the suitability of liposomes as oral vaccine adjuvants using ovalbumin as a model antigen, Li et al found that egg phosphatidylcholine: cholesterol (3:2 molar ratio) vesicles encapsulating ovalbumin failed to elicit both IgA and IgG levels above that of ovalbumin solution alone. However, following the inclusion of the polar lipid fraction E (from purified *Sulfolobus acidocaldarius*) within the formulation, the archaosomes were capable of eliciting much higher titres of both mucosal IgA and systemic IgG due to improved stability and adjuvant activity (Li et al., 2011b).

In the case of the formulations tested within this experiment, both of the cationic based formulations (DSPC:Chol:DDA and DDA:TDB) failed to elicit significant antibody titres following oral administration. The immunogenicity of cationic formulations administered parenterally has been well documented, a result of enhanced interaction with APCs (Christensen et al., 2007). However, this adjuvant activity is not simply a result of the electrostatic interactions found between the positively charged vesicle surface and the negatively charged cell membranes. The cationic lipid choice has been shown to greatly impact upon a range of immunological responses, with DDA (in combination with TDB) yielding much higher Interferon Gamma (IFN γ) responses in mice when compared to a DOTAP counterpart following intramuscular injection (Henriksen-Lacey et al., 2011a). However, the results shown in Figures 6.8–6.9 indicate no enhanced IgG or IgA responses following oral administration with DSPC:Chol:DDA, when compared to oral antigen alone or DSPC:Chol:DOTAP formulation shown previously in Figures 6.5–6.6. It should be noted that a direct comparison between both DDA and DOTAP formulations cannot be conducted due to the different strains of mice used between the *in vivo* experiments. However, it is likely that both formulations are not adequately immunogenic enough to generate significant anti-ovalbumin antibody responses following oral administration.

The adjuvant activity of DDA:TDB is well-known, eliciting both strong humoral and cell mediated immune responses following parenteral vaccination (Agger et al., 2008, Christensen, 2017). Some research pertaining to effective mucosal stimulation using this delivery system has emerged, prompting some intrigue towards using DDA:TDB for oral immunisation. *In vitro* studies using bone-marrow derived DCs (BMDCs) found that DDA:TDB could enhance both cell uptake and maturation and then when subsequently administered intranasally, significantly increased IgA titres from the nasal tissue compared to H3N3 antigen alone were observed (Qu et al., 2018). Similarly, mucosal immunological responses have been observed using DDA:TDB as a delivery system for the protein ScpA to the airway. Initial subcutaneous priming followed by two intranasal immunisations resulted in the migration of Th17 cells to the lung parenchyma and then subsequent IgA secretion through B

cell production (Christensen et al., 2017). However, this intranasal prime-pull strategy has been shown to result in poor mucosal responses at distal sites (Pedersen et al., 2018). While these mucosal IgA responses are highly desirable for enteric protection, intranasal administration is a much less hostile environment for both antigen and delivery system when compared to the gastric environment. Oral administration using DDA:TDB and ovalbumin may therefore require an initial parenteral priming immunisation, in order to generate an increased level of Th17 cells within the small intestine to stimulate effective IgA responses.

In order to boost antibody responses towards encapsulated ovalbumin in DSPC:Chol based liposomes, cholera toxin was both co-administered with and conjugated onto the surface of the liposomal vesicles. The cholera toxin B (CTB) subunit is currently used within an oral vaccine for cholera toxin known as Dukoral. However, strong immune responses to other non-related antigens can also occur when administered in the presence of CTX (New, 2019, Davitt et al., 2019). The results shown in Figures 6.8-6.9 indicate significantly enhanced IgG responses towards both free antigen and encapsulated antigen (DSPC:Chol) when co-administered with CTX for both serum and localised tissue samples. When comparing the immunostimulatory effect of a recombinant CTB protein on antibody responses to an antigen (saliva-binding region, SBR) encapsulated in POPC-based liposomes, similar results were shown, where significantly increased IgG (Serum) and IgA (Vaginal) levels were observed when rCTB was co-mixed compared to liposome-SBR alone (Harokopakis et al., 1998). However, this enhanced immune response was also found when the rCTB was surface conjugated to the POPC-based liposomes. While the antigen, delivery system composition and immunostimulant (CTX and rCTB) used were slightly different, the results shown in Figures 6.8–6.9 conversely indicate a loss of antibody response when the CTX was conjugated to the DSPC:Chol liposomes. This apparent loss of immunogenicity through conjugation has been demonstrated when the conjugation occurs directly between the CTB and the specific antigen. It is believed that while the conjugation process does not inhibit the beneficial binding activity of the CTB to the M cells, some downstream disruption may be occurring limiting the interaction of the toxin to lipid rafts (Sun et al., 2010). Furthermore, it is believed that a loss of CTB binding sites may occur as a result of the antigen conjugation, a process which may also be occurring within these results (Figures 6.8–6.9) between the maleimide-thiol bonds between the CTX and lipid components, explaining the apparent loss of immunogenicity (New, 2019).

The results shown in Figures 6.8 and 6.9 indicate a stark difference in the antibody response when comparing between subtypes (IgA and IgG). In the case of DSPC:Chol encapsulating ovalbumin with co-administered CTX, significant increases in systemic IgG and localised IgG throughout the intestine could be observed, yet IgA responses were found to be largely unaffected. Furthermore, the antigen alone with co-administered CTX was found to generate both IgG and IgA responses.

The apparent loss in IgA production when ovalbumin is encapsulated within DSPC:Chol liposomes may be a result of the alteration of how the immune system interacts with the antigen. In the process of designing delivery systems that are capable of providing some protection to the antigen against gastric degradation (e.g. using long-chain lipids such as DSPC along with cholesterol), this means that the majority of the antigen uptake at the Peyer's patches is being done in the liposomal form. Whilst particulate vesicles under the size of 10 μm have been shown to be readily up taken by Peyer's patches, smaller vesicles preferentially drain (and move with APCs) to the mesenteric lymph nodes and circulatory system (Eldridge et al., 1989). The size dependent movement of antigen containing vesicles may mean that systemic IgG responses are pursued by employing smaller particulate delivery systems, while larger vesicles are retained and processed more within the Peyer's patches leading to more potent localised IgA responses (Kunisawa et al., 2012). With the Peyer's patches being the primary site for IgA class switching upon antigen recognition and activation for B cells, the particulate liposomal drainage of these sub 100 nm vesicles towards the mesenteric lymph nodes and systemic circulation may bias a more systemic IgG response, as observed through-out the IgG responses for encapsulated (DSPC:Chol) ovalbumin co-administered with CTX (Bernasconi et al., 2016).

Naïve B cells residing in B cell follicles bind antigen and become activated via CD40 interactions (and other chemokine signals) with the approval from follicular helper T cells (Tfh). While T cell activation can occur through peptidic fragments mounted on MHC II APCs, B cell binding requires antigen in the native 3-D structure form (Lung et al., 2020). This antigen binding through B cell receptor (BCR) then triggers the differentiation of the B cells into plasmablasts (IgM secreting), and subsets of these populations then initiate GC formation. Within the GC, Tfh cells regulate both the somatic hypermutation (SHM) and class switch recombination (CSR), the mechanisms behind improved Ig affinity and Ig class switching respectively, in the presence of antigen. If there is not enough readily available antigen in its native form, the GC will not proceed, therefore limiting the class switching ability of the B cells from IgM to IgA producers (Janeway, Brandtzaeg and Johansen, 2005). Therefore, liposomal vesicles entrapping antigen may not have released adequate levels of native antigen at the mucosal inductive sites in order to maintain GC formation and subsequent Ig class switching. Moon et al tested this hypothesis when delivering malaria antigen (recombinant *Plasmodium vivax* antigen) in nanoparticle lipid-based carriers. The authors found that enhanced GC formation and a subsequent 9-fold increase in antigen specific antibody responses was observed when the antigen was both encapsulated within the aqueous core and anchored to the surface of the vesicles when compared to entrapped within the aqueous core alone (Moon et al., 2012). This resulted in enhanced BCR activation, yielding strong humoral responses, however it should be noted that this paper focused on

subcutaneous injection, thus the surface anchored antigens were not subjected to the degradative environment of the gastric tract.

6.6 Conclusions

The oral administration for vaccination remains a highly sought after route of administration, yet significant challenges remain in regards to vaccine stability, uptake and efficacy. Within this chapter, the manufacturing of lipid-based nanoparticles through microfluidics incorporating model antigen ovalbumin is shown. The vesicle characteristics remained within the acceptable size ranges for effective M cell uptake, and significant antigen retention was observed for formulations entrapping antigen when exposed to acidic conditions. Finally, antibody responses were analysed following oral administration. Initial formulations resulted in a poor local and systemic antibody response, likely a result of a lack of immunostimulatory components overcoming the tolerant immune environment found within the GALT. All cationic vesicles were found to result in no significant increases in antibody responses, therefore an additional priming immunisation may be required. The addition of cholera toxin was shown to greatly improve IgG levels when antigen was encapsulated, however localised IgA response was limited when the antigen was delivered in liposomal form.

Chapter 7

Overall Conclusions

7.1 Introduction

The prevalence and subsequent financial burden of *Clostridium difficile* within Europe has been estimated to cost over 2 billion pounds annually. Clinical manifestations of the bacterial spore former can range from asymptomatic carriers to, in rare cases, fatality as a result of complications relating to extreme inflammation throughout the small intestine and colon. In healthy individuals, *C. difficile* can be controlled by other symbiotic microorganisms that are found within the gut, however following administration of drugs or therapies commonly administered in healthcare settings (such as antibiotics and chemotherapeutics), alteration of microbiome diversity occurs, leading to rapid *C. difficile* proliferation. Virulence is a result of a number of exotoxins (such as Toxin A and Toxin B) that bind to epithelial cells within the gut and glycosylate a host of proteins that are integral to cytoskeletal function, leading to eventual cellular apoptosis. Epithelial cells exposed to large quantities of *C. difficile* toxins results in neutrophil infiltration, ROS generation and upregulation of pro-inflammatory cytokines and chemokines leading to extensive epithelial damage and the loss of gut integrity.

Oral vaccination as a means for protection against *C. difficile* infection is a promising avenue for generating effective immune responses against the bacterium. The oral route of administration has many practical advantages over parenteral administration including ease of patient compliance and the ability to be conducted without the need of a specialist to administer needle based vaccines. Furthermore, oral vaccination has been shown to generate both systemic immune response as well as localised mucosal responses – a feat that cannot easily be achieved through parenteral vaccination alone. Currently a number of vaccines are undergoing clinical trials, focusing largely on the use of inactivated toxoids (either chemically or genetically) alongside an adjuvant such as aluminium hydroxide. However, poor phase III data has recently emerged in regards to Sanofi Pasteur's vaccine efficacy, resulting in the decision to discontinue development. Challenges pertaining to effective oral vaccines are a result of the environment found throughout the gastrointestinal tract. Acidic pH, the presence of bile salts and a host of enzymes designed to cleave and degrade proteins and fats exist throughout the stomach (and parts of the intestine), in order to aid the adsorption of nutrients across the epithelial barrier. This poses a challenge for oral vaccines, in particular subunit vaccines, as the structural integrity of the vaccine antigen is key to generating effective protection. Therefore, delivery systems can be employed to help protect the subunit antigen through the stomach and direct uptake at relevant sites for immune induction, such as Peyer's patches.

Liposomes are a highly versatile delivery system platform that have been extensively studied as drug delivery vehicles due to their biocompatibility and low toxicity. This is represented by their market representation, ranging from anti-cancer therapies, anti-fungals and recently the first FDA approved

siRNA therapy (Patisiran). Despite the success of liposomes as delivery systems, issues exist within the manufacturing chain of these products. Liposomal manufacture and down-stream processing still largely relies on lab-scale production methods which often require a host of further processing techniques to achieve suitable product attributes. This leads to extensive batch style manufacturing steps, which can last across numerous days.

7.2 Microfluidics as a manufacturing platform for liposomal vaccines

Microfluidics is a relatively novel technique for liposome production that relies upon the manipulation of fluid streams in a microenvironment – producing SUV liposomes. When comparing empty liposomal vesicles manufactured by lipid-film hydration (and subsequent downsizing by extrusion or sonication) against the same formulation manufactured by microfluidics, nanoscale homogenous vesicles were formed in a single step. Key processing parameters were then investigated, with cholesterol content being shown to play a critical role in vesicle size. When cholesterol was included alongside DSPC lipid (55°C T_c), the requirement of a heating block was not necessary to form vesicles using microfluidics. Critical processing parameters were then investigated, where both initial lipid concentration and the flow rate ratio (FRR) were shown to impact upon vesicle size and PDI for neutral formulation DSPC:Chol (10:5 w/w) – with 1:1 FRR resulting in larger vesicle size. When total flow rate was investigated, little to no impact upon both vesicle size and homogeneity was observed. The same trend was then observed with anionic formulation DSPC:Chol:PS (10:5:4 w/w), with FRR, initial lipid concentration and the molarity of PS included in the formulation all being critical factors in influencing vesicle size. Following microfluidic manufacture, down-stream purification is necessary in order to either dilute or completely remove residual solvent within the sample. A significant advantage of microfluidics is the potential for this platform to be part of a continuous manufacturing chain, therefore purification techniques were investigated for their suitability alongside this manufacturing system. Tangential flow filtration (TFF) is a well-established technique that can be found across food, biotechnology and pharmaceutical industries and the ability of the technique to purify solvent from empty liposomal samples was compared against traditional batch techniques such as dialysis and gel-filtration columns (sephadex). TFF was shown to rapidly remove residual methanol concentrations below ICH guidelines (0.3%) within 12 diafiltration volumes with minimal impact upon the liposomes physicochemical characteristics. Unlike dialysis (which similarly did not affect liposome attributes), TFF can be incorporated within a continuous manufacturing stream, giving the manufacturers improved efficiency over liposomal production. Following down-stream purification, a real-time particle size analysis technique was shown to be successfully incorporated at specific points during the

manufacturing chain (post microfluidic production and post TFF purification), supporting continuous monitoring during production.

7.3 Validation of protein quantification tools

Prior to the investigation of the protein loading ability of liposomes manufactured by microfluidics, suitable protein quantification techniques were required. Commonly, the protein loading ability of formulations is quantified indirectly through the quantification of free protein. Two techniques were compared for their ability to determine model antigen ovalbumin concentration within liposomal vesicles in a linear fashion, micro BCA and RP-HPLC. Initially, determination of naked antigen was assessed, where both techniques could quantify protein with high degrees of linearity, with calculated LOD values < 8 µg/mL. Determination of loading within liposomal vesicles requires solubilisation of the liposomes, therefore the effect of the two techniques to quantify ovalbumin in the presence of solubilisation mixture IPA: Buffer was assessed. Both micro BCA and RP-HPLC could similarly quantify protein concentration with high degrees of linearity, and calculated LODs of <10 µg/mL were observed. Finally, the inclusion of lipids was found to not impact upon RP-HPLC, and was shown to interfere minimally at this concentration (1 mg/mL) when applying micro BCA following appropriate blank subtraction. The microplate setup of the microBCA allows for high-throughput screening, however the inclusion of appropriate blanks within the calibration curves is necessary to maintain interference across the curve and samples, therefore limiting the ability of the technique when quantifying different formulations and concentrations. RP-HPLC was found to accurately quantify protein loading irrespective of the choice of formulations tested within this thesis.

7.4 Microfluidic manufacture of liposomal formulations incorporating protein

Upon determination of suitable techniques to quantify liposomal protein loading within vesicles, identification of critical processing parameters that impact upon protein loading ability of a range of liposomal formulations during manufacture were identified. Across initial protein concentration ranges between 0.1 – 2 mg/mL, loading efficiencies between approximately 25-30% were achieved for neutral formulation DSPC:Chol, however above ovalbumin concentrations of 10 mg/mL resulted in a significant decrease in encapsulation efficiency (approximately 15%). When anionic formulation DSPC:Chol:PS was investigated, electrostatic repulsion between the antigen and vesicle membrane resulted in lower loading efficiencies between approximately 18-25%. Microfluidic manufacturing parameter FRR was shown to impact significantly upon encapsulation ability, with 3:1 resulting in

higher loading than 5:1, while total flow rates below 10 mL/min yielded statistically lower loading than faster speeds between 10-20 mL/min.

In the case of cationic liposomal formulations loading antigen, surface adsorption through manual mixing is a common approach. This thesis investigated the ability of microfluidics to tightly control this surface adsorption process, taking advantage of the automation involved in the microfluidic software. Surface adsorption of antigen onto preformed cationic vesicles by microfluidics was demonstrated successfully, with critical processing parameters being the FRR and the liposome to protein ratio during automated manufacture. A key principal of the microfluidic production platform is the ease of scalability across the formulation development landscape. Formulation development can be optimised at small scale and then translated to pre-clinical / clinical manufacture. Translation of bench-scale (1-15 mL) loading to large scale production (10 mL – 1L) was shown for neutral formulation DSPC:Chol entrapping model antigen ovalbumin, with comparable loading and physicochemical attributes across both production platforms, de-risking the adoption of liposome based delivery systems for wide-scale application.

7.5 *In vitro* screening of liposomal formulations

Given the diversity available when choosing liposomal delivery systems (charge, vesicle size and localisation of the antigen), four formulations were then selected and screened *in vitro* using a human macrophage-like cell line as part of a down-selection process for immunological activity. While correlation between *in vitro* and *in vivo* data remains controversial, specific models and markers can help direct and predict some *in vivo* efficacy. Within this thesis, delivery systems association to THP-1 like macrophage cells followed by antigen processing ability and then subsequent specific cell marker expression was determined through FACs analysis. Predictably (and in line with the vast majority of literature), cationic formulations with surface adsorbed antigen quickly associated with the differentiated THP-1 cells due to electrostatic attractions, while neutral and anionic liposomal formulations entrapping antigen showed a more gradual association over time. By the 24 hour time point, both cationic formulations (DDA:TDB and DSPC:Chol:DDA) and neutral formulation DSPC:Chol resulted in >95% association, while anionic DSPC:Chol:DOPS showed a more lagged association response (70%). Interestingly, the high degrees of association did not directly translate into improved antigen processing (using a self-quenched model antigen DQ-OVA protocol). While all formulations tested showed improved antigen processing compared to free antigen alone, anionic formulation DSPC:Chol:DOPS was found to have the highest % positive DQ-OVA cells at 24 hours compared to both cationic and neutral formulations. Despite the initial electrostatic repulsion delaying liposome and

cellular interactions, the inclusion of DOPS within the formulation accelerated the antigen processing (increasing the DQ-OVA positive cells by approximately 20% when compared to DSPC:Chol alone), in line with our current understanding of macrophage and PS interaction. Finally, a selection of four surface markers (CD14, CD40, CD80 and MHC II) that are critical for both presentation of antigen peptide and co-stimulation of T cells by APCs were measured following liposomal incubation. In the case of CD14, CD40 and MHC II expression at 24 hours, none of the liposomal delivery systems incorporating ovalbumin resulted in biologically relevant changes in surface marker expression. However, significant increases (8-12%) in CD80 surface marker expression was found when employing any of the delivery systems tested within this experiment compared to both free antigen alone and negative control groups.

7.6 *In vivo* vaccine efficacy: Antibody responses

Given the ability of these liposomal delivery systems to enhance both association and antigen processing of THP-1 macrophage like cells *in vitro*, the next phase of development was to establish *in vivo* efficacy.

Establishing effective mucosal and systemic antibody responses requires the passage of antigen through the gastric environment and along the intestine to then interact with specific immunological inductive sites. These sites can be Peyer's patches with specialised M cells for access to lymphoid associated cells underneath, lymphoid follicles or even DCs sampling antigen from the lumen through epithelial tight junctions. Delivery systems can enhance antigen interactions with APCs by a range of mechanisms including ligand targeting, electrostatic interactions and even just by the particulate nature of the vesicles. In addition to this, it is widely believed that vesicles below 10 μm can be taken up by Peyer's patches, with some studies indicating enhanced uptake for vesicles below 1 μm . In light of this, initial experimentation focused on the selection of four liposomal formulations incorporating model antigen ovalbumin, delivered via the oral route of administration and then subsequent antibody responses (IgA and IgG) determined via ELISA. The formulations selected focused on long chain hydrocarbon lipids such as DSPC and cholesterol to improve formulation stability, alongside phosphatidylserine (as a macrophage targeting modality) and the inclusion of positively charged lipids such as DOTAP. Both surface adsorbed antigen and encapsulated antigen were trialled and all formulations were within the nanoscale range, however minimal antibody responses could be observed for all formulations both mucosally and systemically following oral administration. It was therefore hypothesised that potent immunogens must be incorporated within the liposomal formulations in order to overcome the highly tolerogenic environment of the gut associated lymphoid

tissue. By this means, immunostimulatory components such as cholera toxin (CTX) (co-administered and conjugated to DSPC:Chol liposomes) and trehalose 6,6'-dibehenate (TDB) were included due to their known ability to enhance mucosal antibody responses. Formulations DSPC:Chol CTX co-mix, DSPC:Chol CTX Conjugate and DSPC:Chol:DDA were found to be <500 nm, while cationic formulation DDA:TDB was within the micron range. Both systemic and mucosal anti-ovalbumin antibody responses were measured following oral administration with control groups including empty DSPC:Chol, free ovalbumin and ovalbumin co-administered with CTX. The addition of co-administered CTX was found to significantly increase both the systemic and localised (Intestinal wash and colon) IgG response for both free ovalbumin and ovalbumin loaded liposomal formulation DSPC:Chol. All other formulations failed to elicit significant IgG responses compared to free antigen alone. In the case of IgA, only the positive control group (free ovalbumin and co-administered CTX) statistically increased above the baseline, with all other liposomal formulations failing elicit meaningful antibody responses.

7.7 Concluding Remarks and future work

The work within this thesis has demonstrated the use of microfluidics as a manufacturing tool for the production of protein loaded liposomes. A range of formulations varying in surface charge (neutral, anionic and cationic) entrapping or surface adsorbing model antigen ovalbumin have been shown. Using the microfluidic software to adjust manufacturing parameters, liposomal formulations of varying size and particle homogeneity can be manufactured – allowing for tailor-made physicochemical attributes dependent upon the specific needs of the application. The microfluidic process was shown to be highly efficient, creating SUV liposomes in a single step process. When downstream purification techniques such as tangential flow filtration and real-time particle size analysis are incorporated, the demonstration of a scale-independent production platform for protein loaded liposomes is shown. The use of these liposomal vesicles was shown to enhance both antigen association and processing when studied *in vitro* and the inclusion of immunostimulatory components such as CTX resulted in enhanced IgG antibody responses following oral administration. While IgA responses were found to be lacking when employing any liposomal delivery system tested here (IgA response is a hallmark of effective mucosal antibody vaccination), the work within this thesis has set out foundations for wider scale applications. Oral vaccination will likely continue to pose challenges as a route of administration to researchers, however the work within thesis has de-risked the large scale manufacture of liposomes as delivery system. Protein based-therapeutics within healthcare are steadily increasing, however issues relating to stability, half-life and biodistribution remain. Delivery systems such as liposomes can help overcome these issues, and with a scale-independent chain for

the manufacture, purification and monitoring of liposomal vesicles, the push towards the next generation of protein therapeutics can be supported.

Further studies should focus on the screening of additional liposomal formulations as mucosal adjuvants, incorporating modalities that are capable of eliciting mucosal antibody responses orally. In order to support large-scale manufacturing through microfluidics, ideally these modalities should aim to be easily incorporated within liposomal formulations, avoiding complex processes that will detract from the continuous manufacturing chain developed here. In regards to vaccination against *C. difficile*, further work could focus on the design of recombinant antigens that are non-toxic and could enhance the immunogenicity of the antigen itself, through the selection of well-defined epitopes such as the receptor binding domain for Toxin A and B.

References

- ABRAHAM, S., JUEL, H. B., BANG, P., CHEESEMAN, H. M., DOHN, R. B., COLE, T., KRISTIANSEN, M. P., KORSHOLM, K. S., LEWIS, D. & OLSEN, A. W. 2019. Safety and immunogenicity of the chlamydia vaccine candidate CTH522 adjuvanted with CAF01 liposomes or aluminium hydroxide: a first-in-human, randomised, double-blind, placebo-controlled, phase 1 trial. *The Lancet Infectious Diseases*.
- ABT, M. C., MCKENNEY, P. T. & PAMER, E. G. 2016. Clostridium difficile colitis: pathogenesis and host defence. *Nature Reviews Microbiology*, 14, 609.
- AGGER, E. M., ROSENKRANDS, I., HANSEN, J., BRAHIMI, K., VANDAHL, B. S., AAGAARD, C., WERNINGHAUS, K., KIRSCHNING, C., LANG, R. & CHRISTENSEN, D. 2008. Cationic liposomes formulated with synthetic mycobacterial cordfactor (CAF01): a versatile adjuvant for vaccines with different immunological requirements. *PLoS one*, 3.
- AGUILAR, M.-I. 2004. Reversed-phase high-performance liquid chromatography. *HPLC of Peptides and Proteins*. Springer.
- AHN, H. & PARK, J.-H. 2016. Liposomal delivery systems for intestinal lymphatic drug transport. *Biomaterials Research*, 20, 36.
- AHSAN, F., RIVAS, I. P., KHAN, M. A. & SUÁREZ, A. I. T. 2002. Targeting to macrophages: role of physicochemical properties of particulate carriers—liposomes and microspheres—on the phagocytosis by macrophages. *Journal of Controlled Release*, 79, 29-40.
- AKBARZADEH, A., REZAEI-SADABADY, R., DAVARAN, S., JOO, S. W., ZARGHAMI, N., HANIFEHPOUR, Y., SAMIEI, M., KOUHI, M. & NEJATI-KOSHKI, K. 2013. Liposome: classification, preparation, and applications. *Nanoscale research letters*, 8, 1.
- AKINC, A., MAIER, M. A., MANOHARAN, M., FITZGERALD, K., JAYARAMAN, M., BARROS, S., ANSELL, S., DU, X., HOPE, M. J. & MADDEN, T. D. 2019. The Onpatro story and the clinical translation of nanomedicines containing nucleic acid-based drugs. *Nature Nanotechnology*, 14, 1084-1087.
- ALLISON, A. & GREGORIADIS, G. 1974. Liposomes as immunological adjuvants. *Nature*, 252, 252.
- ANDERLUZZI, G., LOU, G., GALLORINI, S., BRAZZOLI, M., JOHNSON, R., O'HAGAN, D. T., BAUDNER, B. C. & PERRIE, Y. 2020. Investigating the impact of delivery system design on the efficacy of self-amplifying RNA vaccines. *Vaccines*, 8, 212.
- ANDERLUZZI, G., LOU, G., SU, Y. & PERRIE, Y. 2019. Scalable manufacturing processes for solid lipid nanoparticles. *Pharmaceutical Nanotechnology*, 7, 444-459.
- ANGSANTIKUL, P., FANG, R. H. & ZHANG, L. 2017. Toxoid vaccination against bacterial infection using cell membrane-coated nanoparticles. *Bioconjugate chemistry*, 29, 604-612.
- APOSTÓLICO, J. D. S., LUNARDELLI, V. A. S., COIRADA, F. C., BOSCARDIN, S. B. & ROSA, D. S. 2016. Adjuvants: classification, modus operandi, and licensing. *Journal of immunology research*, 2016.
- APOSTOLOPOULOS, V., THALHAMMER, T., TZAKOS, A. G. & STOJANOVSKA, L. 2013. Targeting antigens to dendritic cell receptors for vaccine development. *Journal of drug delivery*, 2013.
- ARIGITA, C., BEVAART, L., EVERSE, L. A., KONING, G. A., HENNINK, W. E., CROMMELIN, D. J., VAN DE WINKEL, J. G., VAN VUGT, M. J., KERSTEN, G. F. & JISKOOT, W. 2003. Liposomal meningococcal B vaccination: role of dendritic cell targeting in the development of a protective immune response. *Infection and immunity*, 71, 5210-5218.
- AVANTI POLAR LIPIDS, I. "What Are The Differences Between (Advantages Of) Synthetic And Natural Phospholipids?" [Online]. Available: <https://avantilipids.com/tech-support/faqs/synthetic-vs-natural-phospholipids> [Accessed].
- AWATE, S., BABIUK, L. A. B. & MUTWIRI, G. 2013. Mechanisms of action of adjuvants. *Frontiers in immunology*, 4, 114.
- AZZOUZ, L. L. & SHARMA, S. 2019. Physiology, Large Intestine. *StatPearls [Internet]*. StatPearls Publishing.

- BANCHEREAU, J. & STEINMAN, R. M. 1998. Dendritic cells and the control of immunity. *Nature*, 392, 245-252.
- BANGHAM, A., STANDISH, M. M. & WATKINS, J. C. 1965. Diffusion of univalent ions across the lamellae of swollen phospholipids. *Journal of molecular biology*, 13, 238-277.
- BELTRÁN-GRACIA, E., LÓPEZ-CAMACHO, A., HIGUERA-CIAPARA, I., VELÁZQUEZ-FERNÁNDEZ, J. B. & VALLEJO-CARDONA, A. A. 2019. Nanomedicine review: clinical developments in liposomal applications. *Cancer Nanotechnology*, 10, 11.
- BENNE, N., LÉBOUX, R. J., GLANDRUP, M., VAN DUIJN, J., VIGARIO, F. L., NEUSTRUP, M. A., ROMEIJN, S., GALLI, F., KUIPER, J. & JISKOOT, W. 2020. Atomic force microscopy measurements of anionic liposomes reveal the effect of liposomal rigidity on antigen-specific regulatory T cell responses. *Journal of Controlled Release*, 318, 246-255.
- BERARDI, A. & BALDELLI BOMBELLI, F. 2019. Oral delivery of nanoparticles-let's not forget about the protein corona. Taylor & Francis.
- BERGER, J. L., SMITH, A., ZORN, K. K., SUKUMVANICH, P., OLAWAIYE, A. B., KELLEY, J. & KRIVAK, T. C. 2014. Outcomes analysis of an alternative formulation of PEGylated liposomal doxorubicin in recurrent epithelial ovarian carcinoma during the drug shortage era. *OncoTargets and therapy*, 7, 1409.
- BERGES, C., NAUJOKAT, C., TINAPP, S., WIECZOREK, H., HÖH, A., SADEGHI, M., OPELZ, G. & DANIEL, V. 2005. A cell line model for the differentiation of human dendritic cells. *Biochemical and biophysical research communications*, 333, 896-907.
- BERNASCONI, V., NORLING, K., BALLY, M., HÖÖK, F. & LYCKE, N. Y. 2016. Mucosal vaccine development based on liposome technology. *Journal of immunology research*, 2016.
- BÉZAY, N., AYAD, A., DUBISCHAR, K., FIRBAS, C., HOCHREITER, R., KIERMAYR, S., KISS, I., PINL, F., JILMA, B. & WESTRITSCHNIG, K. 2016. Safety, immunogenicity and dose response of VLA84, a new vaccine candidate against *Clostridium difficile*, in healthy volunteers. *Vaccine*, 34, 2585-2592.
- BILSBOROUGH, J. & VINEY, J. L. 2004. Gastrointestinal dendritic cells play a role in immunity, tolerance, and disease. *Gastroenterology*, 127, 300-309.
- BIRGE, R., BOELTZ, S., KUMAR, S., CARLSON, J., WANDERLEY, J., CALIANESE, D., BARCINSKI, M., BREKKEN, R., HUANG, X. & HUTCHINS, J. 2016. Phosphatidylserine is a global immunosuppressive signal in efferocytosis, infectious disease, and cancer. *Cell Death & Differentiation*, 23, 962-978.
- BOSSHART, H. & HEINZELMANN, M. 2016. THP-1 cells as a model for human monocytes. *Annals of translational medicine*, 4.
- BOYAKA, P. N. 2017. Inducing mucosal IgA: a challenge for vaccine adjuvants and delivery systems. *The Journal of Immunology*, 199, 9-16.
- BRANDTZAEG, P. & JOHANSEN, F. E. 2005. Mucosal B cells: phenotypic characteristics, transcriptional regulation, and homing properties. *Immunological reviews*, 206, 32-63.
- BRAYDEN, D. J. & BAIRD, A. W. 2001. Microparticle vaccine approaches to stimulate mucosal immunisation. *Microbes and infection*, 3, 867-876.
- BRIUGLIA, M.-L., ROTELLA, C., MCFARLANE, A. & LAMPROU, D. A. 2015. Influence of cholesterol on liposome stability and on in vitro drug release. *Drug delivery and translational research*, 5, 231-242.
- BULBAKE, U., DOPPALAPUDI, S., KOMMINENI, N. & KHAN, W. 2017. Liposomal Formulations in Clinical Use: An Updated Review. *Pharmaceutics*, 9, 12.
- BUSATTO, S., VILANILAM, G., TICER, T., LIN, W.-L., DICKSON, D. W., SHAPIRO, S., BERGESE, P. & WOLFRAM, J. 2018. Tangential flow filtration for highly efficient concentration of extracellular vesicles from large volumes of fluid. *Cells*, 7, 273.
- CARSTENS, M. G., CAMPS, M. G., HENRIKSEN-LACEY, M., FRANKEN, K., OTTENHOFF, T. H., PERRIE, Y., BOUWSTRA, J. A., OSSENDORP, F. & JISKOOT, W. 2011. Effect of vesicle size on tissue localization and immunogenicity of liposomal DNA vaccines. *Vaccine*, 29, 4761-4770.

- CARTER, P. J. 2011. Introduction to current and future protein therapeutics: A protein engineering perspective. *Experimental Cell Research*, 317, 1261-1269.
- CARUGO, D., BOTTARO, E., OWEN, J., STRIDE, E. & NASTRUZZI, C. 2016. Liposome production by microfluidics: potential and limiting factors. *Scientific reports*, 6.
- CASEY, C., GALLOS, T., ALEKSEEV, Y., AYTURK, E. & PEARL, S. 2011. Protein concentration with single-pass tangential flow filtration (SPTFF). *Journal of membrane science*, 384, 82-88.
- CERUTTI, A. 2008. The regulation of IgA class switching. *Nature reviews immunology*, 8, 421-434.
- CHADWICK, S., KRIEGEL, C. & AMIJI, M. 2009. Delivery strategies to enhance mucosal vaccination. *Expert opinion on biological therapy*, 9, 427-440.
- CHAN, Y. H., CHEN, B. H., CHIU, C. P. & LU, Y. F. 2004. The influence of phytosterols on the encapsulation efficiency of cholesterol liposomes. *International journal of food science & technology*, 39, 985-995.
- CHANG, Y., WANG, L.-X., LI, Y.-P. & HU, C.-Q. 2016. Factors influencing the HPLC determination for related substances of azithromycin. *Journal of chromatographic science*, 54, 187-194.
- CHANPUT, W., MES, J. J. & WICHERS, H. J. 2014. THP-1 cell line: an in vitro cell model for immune modulation approach. *International immunopharmacology*, 23, 37-45.
- CHATIN, B., MÉVEL, M., DEVALLIÈRE, J., DALLEY, L., HAUDEBOURG, T., PEUZIAT, P., COLOMBANI, T., BERCHEL, M., LAMBERT, O. & EDELMAN, A. 2015. Liposome-based formulation for intracellular delivery of functional proteins. *Molecular Therapy-Nucleic Acids*, 4, e244.
- CHATZIKLEANTHOUS, D. 2020. *Design of vaccine nanotechnology-based delivery systems : the effect of CpGODN TLR9 agonist-protein antigen conjugates anchored to liposomes*. Ph.D., University of Strathclyde.
- CHATZIKLEANTHOUS, D., CUNLIFFE, R., CARBONI, F., ROMANO, M. R., O'HAGAN, D. T., ROBERTS, C. W., PERRIE, Y. & ADAMO, R. 2020. Synthesis of protein conjugates adsorbed on cationic liposomes surface. *MethodsX*, 100942.
- CHEN, J., HESSLER, J. A., PUTCHAKAYALA, K., PANAMA, B. K., KHAN, D. P., HONG, S., MULLEN, D. G., DIMAGGIO, S. C., SOM, A. & TEW, G. N. 2009. Cationic nanoparticles induce nanoscale disruption in living cell plasma membranes. *The journal of physical chemistry B*, 113, 11179-11185.
- CHENG, X., LIU, R. & HE, Y. 2010. A simple method for the preparation of monodisperse protein-loaded microspheres with high encapsulation efficiencies. *European Journal of Pharmaceutics and Biopharmaceutics*, 76, 336-341.
- CHIU, M. L., GOULET, D. R., TEPLYAKOV, A. & GILLILAND, G. L. 2019. Antibody structure and function: The basis for engineering therapeutics. *Antibodies*, 8, 55.
- CHO, N.-J., HWANG, L. Y., SOLANDT, J. J. & FRANK, C. W. 2013. Comparison of extruded and sonicated vesicles for planar bilayer self-assembly. *Materials*, 6, 3294-3308.
- CHRISTENSEN, D. 2017. Development and Evaluation of CAF01. *Immunopotentiators in Modern Vaccines*. Elsevier.
- CHRISTENSEN, D., HENRIKSEN-LACEY, M., KAMATH, A. T., LINDENSTRØM, T., KORSHOLM, K. S., CHRISTENSEN, J. P., ROCHAT, A.-F., LAMBERT, P.-H., ANDERSEN, P. & SIEGRIST, C.-A. 2012. A cationic vaccine adjuvant based on a saturated quaternary ammonium lipid have different in vivo distribution kinetics and display a distinct CD4 T cell-inducing capacity compared to its unsaturated analog. *Journal of controlled release*, 160, 468-476.
- CHRISTENSEN, D., KORSHOLM, K. S., ANDERSEN, P. & AGGER, E. M. 2011. Cationic liposomes as vaccine adjuvants. *Expert review of vaccines*, 10, 513-521.
- CHRISTENSEN, D., KORSHOLM, K. S., ROSENKRANDS, I., LINDENSTRØM, T., ANDERSEN, P. & AGGER, E. M. 2007. Cationic liposomes as vaccine adjuvants. *Expert review of vaccines*, 6, 785-796.
- CHRISTENSEN, D., MORTENSEN, R., ROSENKRANDS, I., DIETRICH, J. & ANDERSEN, P. 2017. Vaccine-induced Th17 cells are established as resident memory cells in the lung and promote local IgA responses. *Mucosal immunology*, 10, 260-270.

- CLARK, M. A., BLAIR, H., LIANG, L., BREY, R. N., BRAYDEN, D. & HIRST, B. H. 2001. Targeting polymerised liposome vaccine carriers to intestinal M cells. *Vaccine*, 20, 208-217.
- CLARO, T., DANIELS, S. & HUMPHREYS, H. 2014. Detecting *Clostridium difficile* spores from inanimate surfaces of the hospital environment: which method is best? *Journal of clinical microbiology*, 52, 3426-3428.
- COCCIA, M., COLLIGNON, C., HERVÉ, C., CHALON, A., WELSBY, I., DETIENNE, S., VAN HELDEN, M. J., DUTTA, S., GENITO, C. J. & WATERS, N. C. 2017. Cellular and molecular synergy in AS01-adjuvanted vaccines results in an early IFN γ response promoting vaccine immunogenicity. *NPJ vaccines*, 2, 1-14.
- COFFMAN, R. L., SHER, A. & SEDER, R. A. 2010. Vaccine adjuvants: putting innate immunity to work. *Immunity*, 33, 492-503.
- COLE, H., BRYAN, D., LANCASTER, L., MAWAS, F. & VLLASALIU, D. 2018. Chitosan nanoparticle antigen uptake in epithelial monolayers can predict mucosal but not systemic in vivo immune response by oral delivery. *Carbohydrate polymers*, 190, 248-254.
- COLLETIER, J.-P., CHAIZE, B., WINTERHALTER, M. & FOURNIER, D. 2002. Protein encapsulation in liposomes: efficiency depends on interactions between protein and phospholipid bilayer. *BMC Biotechnology*, 2, 9.
- COLLINS, J. T. & BADIREDDY, M. 2019. Anatomy, abdomen and pelvis, small intestine.
- COOPER, A. R., PATEL, S., SENADHEERA, S., PLATH, K., KOHN, D. B. & HOLLIS, R. P. 2011. Highly efficient large-scale lentiviral vector concentration by tandem tangential flow filtration. *Journal of virological methods*, 177, 1-9.
- COPLAND, M. J., BAIRD, M. A., RADES, T., MCKENZIE, J. L., BECKER, B., RECK, F., TYLER, P. C. & DAVIES, N. M. 2003. Liposomal delivery of antigen to human dendritic cells. *Vaccine*, 21, 883-890.
- CORREIA, M. G. S., BRIUGLIA, M. L., NIOSI, F. & LAMPROU, D. A. 2017. Microfluidic manufacturing of phospholipid nanoparticles: Stability, encapsulation efficacy, and drug release. *International journal of pharmaceutics*, 516, 91-99.
- CRUZ-LEAL, Y., MACHADO, Y., LÓPEZ-REQUENA, A., CANET, L., LABORDE, R., ALVARES, A. M., LUCATELLI LAURINDO, M. F., SANTO TOMAS, J. F., ALONSO, M. E. & ÁLVAREZ, C. 2014. Role of B-1 cells in the immune response against an antigen encapsulated into phosphatidylcholine-containing liposomes. *International immunology*, 26, 427-437.
- CZEPIEL, J., DRÓZDŹ, M., PITUCH, H., KUIJPER, E. J., PERUCKI, W., MIELIMONKA, A., GOLDMAN, S., WULTAŃSKA, D., GARLICKI, A. & BIESIADA, G. 2019. *Clostridium difficile* infection. *European Journal of Clinical Microbiology & Infectious Diseases*, 1-11.
- DA SILVA, C., WAGNER, C., BONNARDEL, J., GORVEL, J.-P. & LELOUARD, H. 2017. The Peyer's patch mononuclear phagocyte system at steady state and during infection. *Frontiers in immunology*, 8, 1254.
- DAIGNEAULT, M., PRESTON, J. A., MARRIOTT, H. M., WHYTE, M. K. & DOCKRELL, D. H. 2010. The identification of markers of macrophage differentiation in PMA-stimulated THP-1 cells and monocyte-derived macrophages. *PloS one*, 5.
- DAVITT, C. J. & LAVELLE, E. C. 2015. Delivery strategies to enhance oral vaccination against enteric infections. *Advanced drug delivery reviews*, 91, 52-69.
- DAVITT, C. J., LONGET, S., ALBUTTI, A., AVERSA, V., NORDQVIST, S., HACKETT, B., MCENTEE, C. P., ROSA, M., COULTER, I. S. & LEBENS, M. 2019. Alpha-galactosylceramide enhances mucosal immunity to oral whole-cell cholera vaccines. *Mucosal Immunology*, 12, 1055-1064.
- DE BRUYN, G., SALEH, J., WORKMAN, D., POLLAK, R., ELINOFF, V., FRASER, N. J., LEFEBVRE, G., MARTENS, M., MILLS, R. E. & NATHAN, R. 2016. Defining the optimal formulation and schedule of a candidate toxoid vaccine against *Clostridium difficile* infection: A randomized Phase 2 clinical trial. *Vaccine*, 34, 2170-2178.
- DE GUNZBURG, J., GHOZLANE, A., DUCHER, A., LE CHATELIER, E., DUVAL, X., RUPPÉ, E., ARMAND-LEFEBVRE, L., SABLIER-GALLIS, F., BURDET, C. & ALAVOINE, L. 2018. Protection of the human gut microbiome from antibiotics. *The Journal of infectious diseases*, 217, 628-636.

- DE, M., GHOSH, S., SEN, T., SHADAB, M., BANERJEE, I., BASU, S. & ALI, N. 2018. A novel therapeutic strategy for cancer using phosphatidylserine targeting stearylamine-bearing cationic liposomes. *Molecular Therapy-Nucleic Acids*, 10, 9-27.
- DEL GIUDICE, G., RAPPUOLI, R. & DIDIERLAURENT, A. M. Correlates of adjuvanticity: a review on adjuvants in licensed vaccines. *Seminars in immunology*, 2018. Elsevier, 14-21.
- DERESSA, T., STOECKLINGER, A., WALLNER, M., HIMLY, M., KOFLER, S., HAINZ, K., BRANDSTETTER, H., THALHAMER, J. & HAMMERL, P. 2014. Structural integrity of the antigen is a determinant for the induction of T-helper type-1 immunity in mice by gene gun vaccines against E. coli beta-galactosidase. *PLOS one*, 9.
- DES RIEUX, A., FIEVEZ, V., GARINOT, M., SCHNEIDER, Y.-J. & PRÉAT, V. 2006. Nanoparticles as potential oral delivery systems of proteins and vaccines: a mechanistic approach. *Journal of controlled release*, 116, 1-27.
- DESAI, M. P., LABHASETWAR, V., AMIDON, G. L. & LEVY, R. J. 1996. Gastrointestinal uptake of biodegradable microparticles: effect of particle size. *Pharmaceutical research*, 13, 1838-1845.
- DESPANDE, S. & DEKKER, C. 2018. On-chip microfluidic production of cell-sized liposomes. *Nature protocols*, 13, 856-874.
- DIMOV, N., KASTNER, E., HUSSAIN, M., PERRIE, Y. & SZITA, N. 2017. Formation and purification of tailored liposomes for drug delivery using a module-based micro continuous-flow system. *Scientific reports*, 7, 1-13.
- DING, B. 2018. Pharma industry 4.0: Literature review and research opportunities in sustainable pharmaceutical supply chains. *Process Safety and Environmental Protection*, 119, 115-130.
- DOBROVOLSKAIA, M. A. 2015. Pre-clinical immunotoxicity studies of nanotechnology-formulated drugs: Challenges, considerations and strategy. *Journal of Controlled Release*, 220, 571-583.
- DONALD, R. G., FLINT, M., KALYAN, N., JOHNSON, E., WITKO, S. E., KOTASH, C., ZHAO, P., MEGATI, S., YURGELONIS, I. & LEE, P. K. 2013. A novel approach to generate a recombinant toxoid vaccine against *Clostridium difficile*. *Microbiology*, 159, 1254-1266.
- DU, P., CAO, B., WANG, J., LI, W., JIA, H., ZHANG, W., LU, J., LI, Z., YU, H. & CHEN, C. 2014. Sequence variation in *tcdA* and *tcdB* of *Clostridium difficile*: ST37 with truncated *tcdA* is a potential epidemic strain in China. *Journal of clinical microbiology*, 52, 3264-3270.
- E CHRISTINE LUTSIAK, M., KWON, G. & SAMUEL, J. 2002. *Analysis of peptide and lipopeptide content in liposomes*.
- ELDRIDGE, J. H., HAMMOND, C. J., MEULBROEK, J. A., STAAS, J. K., GILLEY, R. M. & TICE, T. R. 1990. Controlled vaccine release in the gut-associated lymphoid tissues. I. Orally administered biodegradable microspheres target the Peyer's patches. *Journal of Controlled Release*, 11, 205-214.
- ELDRIDGE, J. H., MEULBROEK, J. A., STAAS, J. K., TICE, T. R. & GILLEY, R. M. 1989. Vaccine-containing biodegradable microspheres specifically enter the gut-associated lymphoid tissue following oral administration and induce a disseminated mucosal immune response. *Immunobiology of proteins and peptides V*. Springer.
- ELHISSI, A., PHOENIX, D. & AHMED, W. 2015. Some approaches to large-scale manufacturing of liposomes. *Emerging Nanotechnologies for Manufacturing*. Elsevier.
- ELSANA, H., OLUSANYA, T. O., CARR-WILKINSON, J., DARBY, S., FAHEEM, A. & ELKORDY, A. A. 2019. Evaluation of novel cationic gene based liposomes with cyclodextrin prepared by thin film hydration and microfluidic systems. *Scientific reports*, 9, 1-17.
- EPSTEIN-BARASH, H., GUTMAN, D., MARKOVSKY, E., MISHAN-EISENBERG, G., KOROUKHOV, N., SZEBENI, J. & GOLOMB, G. 2010. Physicochemical parameters affecting liposomal bisphosphonates bioactivity for restenosis therapy: internalization, cell inhibition, activation of cytokines and complement, and mechanism of cell death. *Journal of controlled release*, 146, 182-195.

- ESPUELAS, S., THUMANN, C., HEURTAULT, B., SCHUBER, F. & FRISCH, B. 2008. Influence of ligand valency on the targeting of immature human dendritic cells by mannosylated liposomes. *Bioconjugate chemistry*, 19, 2385-2393.
- FAISAL, S. M., CHEN, J.-W., MCDONOUGH, S. P., CHANG, C.-F., TENG, C.-H. & CHANG, Y.-F. 2011. Immunostimulatory and antigen delivery properties of liposomes made up of total polar lipids from non-pathogenic bacteria leads to efficient induction of both innate and adaptive immune responses. *Vaccine*, 29, 2381-2391.
- FALCK, E., PATRA, M., KARTTUNEN, M., HYVÖNEN, M. T. & VATTULAINEN, I. 2004. Lessons of slicing membranes: interplay of packing, free area, and lateral diffusion in phospholipid/cholesterol bilayers. *Biophysical journal*, 87, 1076-1091.
- FALLINGBORG, J. 1999. Intraluminal pH of the human gastrointestinal tract. *Danish medical bulletin*, 46, 183.
- FATOUROS, D. G. & ANTIMISIARIS, S. G. 2002. Effect of amphiphilic drugs on the stability and zeta-potential of their liposome formulations: a study with prednisolone, diazepam, and griseofulvin. *Journal of colloid and interface science*, 251, 271-277.
- FITZPATRICK, F., SKALLY, M., BRADY, M., BURNS, K., ROONEY, C. & WILCOX, M. H. 2018. European practice for CDI treatment. *Updates on Clostridium difficile in Europe*. Springer.
- FLANNIGAN, K. L., GEEM, D., HARUSATO, A. & DENNING, T. L. 2015. Intestinal antigen-presenting cells: key regulators of immune homeostasis and inflammation. *The American journal of pathology*, 185, 1809-1819.
- FOGED, C. 2011. Subunit vaccines of the future: the need for safe, customized and optimized particulate delivery systems. *Therapeutic delivery*, 2, 1057-1077.
- FOGED, C., ARIGITA, C., SUNDBLAD, A., JISKOOT, W., STORM, G. & FROKJAER, S. 2004. Interaction of dendritic cells with antigen-containing liposomes: effect of bilayer composition. *Vaccine*, 22, 1903-1913.
- FOGLIA, G., SHAH, S., LUXEMBURGER, C. & PIETROBON, P. J. F. 2012. Clostridium difficile: development of a novel candidate vaccine. *Vaccine*, 30, 4307-4309.
- FORBES, N., HUSSAIN, M. T., BRIUGLIA, M. L., EDWARDS, D. P., TER HORST, J. H., SZITA, N. & PERRIE, Y. 2019. Rapid and scale-independent microfluidic manufacture of liposomes entrapping protein incorporating in-line purification and at-line size monitoring. *International journal of pharmaceutics*, 556, 68-81.
- FORSTER, S., BUCKTON, G. & BEEZER, A. E. 1991. The importance of chain length on the wettability and solubility of organic homologs. *International journal of pharmaceutics*, 72, 29-34.
- FOSTER, J. A., RINAMAN, L. & CRYAN, J. F. 2017. Stress & the gut-brain axis: regulation by the microbiome. *Neurobiology of stress*, 7, 124-136.
- FRANCIA, V., YANG, K., DEVILLE, S., REKER-SMIT, C., NELISSEN, I. & SALVATI, A. 2019. Corona composition can affect the mechanisms cells use to internalize nanoparticles. *ACS nano*, 13, 11107-11121.
- FRISKEN, B., ASMAN, C. & PATTY, P. 2000a. Studies of vesicle extrusion. *Langmuir*, 16, 928-933.
- FRISKEN, B. J., ASMAN, C. & PATTY, P. J. 2000b. Studies of Vesicle Extrusion. *Langmuir*, 16, 928-933.
- FUJII, Y., ARAMAKI, Y., HARA, T., YACHI, K., KIKUCHI, H. & TSUCHIYA, S. 1993. Enhancement of systemic and mucosal immune responses following oral administration of liposomes. *Immunology letters*, 36, 65-69.
- FULLER, D. H. & BERGLUND, P. 2020. Amplifying RNA vaccine development. *New England Journal of Medicine*, 382, 2469-2471.
- GAUDINO, S. J. & KUMAR, P. 2019. Cross-talk between antigen presenting cells and T cells impacts intestinal homeostasis, bacterial infections, and tumorigenesis. *Frontiers in immunology*, 10.
- GE, X., WEI, M., HE, S. & YUAN, W.-E. 2019. Advances of non-ionic surfactant vesicles (niosomes) and their application in drug delivery. *Pharmaceutics*, 11, 55.

- GEELLEN, T., YEO, S. Y., PAULIS, L. E., STARMANS, L. W., NICOLAY, K. & STRIJKERS, G. J. 2012. Internalization of paramagnetic phosphatidylserine-containing liposomes by macrophages. *Journal of nanobiotechnology*, 10, 37.
- GERDING, D. N., JOHNSON, S., RUPNIK, M. & AKTORIES, K. 2014. Clostridium difficile binary toxin CDT: mechanism, epidemiology, and potential clinical importance. *Gut microbes*, 5, 15-27.
- GHIMIRE, T. R. 2015. The mechanisms of action of vaccines containing aluminum adjuvants: an in vitro vs in vivo paradigm. *Springerplus*, 4, 1-18.
- GORDON, S., SAUPE, A., MCBURNEY, W., RADES, T. & HOOK, S. 2008. Comparison of chitosan nanoparticles and chitosan hydrogels for vaccine delivery. *Journal of Pharmacy and Pharmacology*, 60, 1591-1600.
- GOTO, Y. 2019. Epithelial cells as a transmitter of signals from commensal bacteria and host immune cells. *Frontiers in immunology*, 10, 2057.
- GRABIELLE-MADELMONT, C., LESIEUR, S. & OLLIVON, M. 2003. Characterization of loaded liposomes by size exclusion chromatography. *Journal of biochemical and biophysical methods*, 56, 189-217.
- GREGORIADIS, G. 2006. *Liposome technology: interactions of liposomes with the biological milieu*, CRC press.
- GREGORIADIS, G. & DAVIS, C. 1979. Stability of liposomes in vivo and in vitro is promoted by their cholesterol content and the presence of blood cells. *Biochemical and biophysical research communications*, 89, 1287-1293.
- GREGORIADIS, G., MCCORMACK, B., OBRENOVIC, M., SAFFIE, R., ZADI, B. & PERRIE, Y. 1999. Vaccine entrapment in liposomes. *Methods*, 19, 156-162.
- GROTEFEND, S., KAMINSKI, L., WROBLEWITZ, S., DEEB, S. E., KÜHN, N., REICHL, S., LIMBERGER, M., WATT, S. & WÄTZIG, H. 2012. Protein quantitation using various modes of high performance liquid chromatography. *Journal of Pharmaceutical and Biomedical Analysis*, 71, 127-138.
- GUIDELINE, I. H. T. Validation of analytical procedures: text and methodology Q2 (R1). International Conference on Harmonization, Geneva, Switzerland, 2005. 11-12.
- GUILLIAMS, M., GINHOUX, F., JAKUBZICK, C., NAIK, S. H., ONAI, N., SCHRAML, B. U., SEGURA, E., TUSSIWAND, R. & YONA, S. 2014. Dendritic cells, monocytes and macrophages: a unified nomenclature based on ontogeny. *Nature Reviews Immunology*, 14, 571-578.
- GUO, S., YAN, W., MCDONOUGH, S. P., LIN, N., WU, K. J., HE, H., XIANG, H., YANG, M., MOREIRA, M. A. S. & CHANG, Y.-F. 2015. The recombinant Lactococcus lactis oral vaccine induces protection against C. difficile spore challenge in a mouse model. *Vaccine*, 33, 1586-1595.
- GUPTA, P. N. & VYAS, S. P. 2011. Investigation of lectinized liposomes as M-cell targeted carrier-adjuvant for mucosal immunization. *Colloids and Surfaces B: Biointerfaces*, 82, 118-125.
- GUPTA, S., JAIN, A., CHAKRABORTY, M., SAHNI, J. K., ALI, J. & DANG, S. 2013. Oral delivery of therapeutic proteins and peptides: a review on recent developments. *Drug Delivery*, 20, 237-246.
- GUSTAFSON, H. H., HOLT-CASPER, D., GRAINGER, D. W. & GHANDEHARI, H. 2015. Nanoparticle uptake: the phagocyte problem. *Nano today*, 10, 487-510.
- HABJANEC, L., FRKANEC, R., HALASSY, B. & TOMAŠIĆ, J. 2006. Effect of liposomal formulations and immunostimulating peptidoglycan monomer (PGM) on the immune reaction to ovalbumin in mice. *Journal of liposome research*, 16, 1-16.
- HABTEZION, A., NGUYEN, L. P., HADEIBA, H. & BUTCHER, E. C. 2016. Leukocyte trafficking to the small intestine and colon. *Gastroenterology*, 150, 340-354.
- H Aidar, Z. S., HAMDY, R. C. & TABRIZIAN, M. 2008. Protein release kinetics for core-shell hybrid nanoparticles based on the layer-by-layer assembly of alginate and chitosan on liposomes. *Biomaterials*, 29, 1207-1215.
- HAK, S., HELGESEN, E., HEKTOEN, H. H., HUUSE, E. M., JARZYNA, P. A., MULDER, W. J., HARALDSETH, O. & DAVIES, C. D. L. 2012. The effect of nanoparticle polyethylene glycol surface density on

- ligand-directed tumor targeting studied in vivo by dual modality imaging. *ACS nano*, 6, 5648-5658.
- HAMBORG, M., ROSE, F., JORGENSEN, L., BJORKLUND, K., PEDERSEN, H. B., CHRISTENSEN, D. & FOGED, C. 2014. Elucidating the mechanisms of protein antigen adsorption to the CAF/NAF liposomal vaccine adjuvant systems: effect of charge, fluidity and antigen-to-lipid ratio. *Biochimica et Biophysica Acta (BBA)-Biomembranes*, 1838, 2001-2010.
- HAROKOPAKIS, E., CHILDERS, N. K., MICHALEK, S. M., ZHANG, S. S. & TOMASI, M. 1995. Conjugation of cholera toxin or its B subunit to liposomes for targeted delivery of antigens. *Journal of immunological methods*, 185, 31-42.
- HAROKOPAKIS, E., HAJISHENGALLIS, G. & MICHALEK, S. M. 1998. Effectiveness of liposomes possessing surface-linked recombinant B subunit of cholera toxin as an oral antigen delivery system. *Infection and immunity*, 66, 4299-4304.
- HASEDA, Y., MUNAKATA, L., MENG, J., SUZUKI, R. & AOSHI, T. 2020. Microfluidic-prepared DOTAP nanoparticles induce strong T-cell responses in mice. *Plos one*, 15, e0227891.
- HE, H., LU, Y., QI, J., ZHU, Q., CHEN, Z. & WU, W. 2019. Adapting liposomes for oral drug delivery. *Acta pharmaceutica sinica B*, 9, 36-48.
- HELLMIG, S., VON SCHÖNING, F., GADOW, C., KATSOUNIS, S., HEDDERICH, J., FÖLSCH, U. R. & STÜBER, E. 2006. Gastric emptying time of fluids and solids in healthy subjects determined by ¹³C breath tests: influence of age, sex and body mass index. *Journal of gastroenterology and hepatology*, 21, 1832-1838.
- HENRIKSEN-LACEY, M., BRAMWELL, V. & PERRIE, Y. 2010a. Radiolabelling of antigen and liposomes for vaccine biodistribution studies. *Pharmaceutics*, 2, 91-104.
- HENRIKSEN-LACEY, M., BRAMWELL, V. W., CHRISTENSEN, D., AGGER, E.-M., ANDERSEN, P. & PERRIE, Y. 2010b. Liposomes based on dimethyldioctadecylammonium promote a depot effect and enhance immunogenicity of soluble antigen. *Journal of controlled release*, 142, 180-186.
- HENRIKSEN-LACEY, M., CHRISTENSEN, D., BRAMWELL, V. W., LINDENSTRØM, T., AGGER, E. M., ANDERSEN, P. & PERRIE, Y. 2010c. Liposomal cationic charge and antigen adsorption are important properties for the efficient deposition of antigen at the injection site and ability of the vaccine to induce a CMI response. *Journal of controlled release*, 145, 102-108.
- HENRIKSEN-LACEY, M., CHRISTENSEN, D., BRAMWELL, V. W., LINDENSTRØM, T., AGGER, E. M., ANDERSEN, P. & PERRIE, Y. 2011a. Comparison of the depot effect and immunogenicity of liposomes based on dimethyldioctadecylammonium (DDA), 3β-[N-(N', N'-dimethylaminoethane) carbonyl] cholesterol (DC-Chol), and 1, 2-dioleoyl-3-trimethylammonium propane (DOTAP): prolonged liposome retention mediates stronger Th1 responses. *Molecular pharmaceutics*, 8, 153-161.
- HENRIKSEN-LACEY, M., DEVITT, A. & PERRIE, Y. 2011b. The vesicle size of DDA: TDB liposomal adjuvants plays a role in the cell-mediated immune response but has no significant effect on antibody production. *Journal of controlled release*, 154, 131-137.
- HEUTS, J., VARYPATAKI, E. M., VAN DER MAADEN, K., ROMEIJN, S., DRIJFHOUT, J. W., VAN SCHELTINGA, A. T., OSSENDORP, F. & JISKOOT, W. 2018. Cationic Liposomes: A Flexible Vaccine Delivery System for Physicochemically Diverse Antigenic Peptides. *Pharmaceutical research*, 35, 207.
- HILGERS, L. & SNIPPE, H. 1992. DDA as an immunological adjuvant. *Research in immunology*, 143, 494-503; discussion 574-6.
- HOH, R. A. & BOYD, S. D. 2018. Gut Mucosal Antibody Responses and Implications for Food Allergy. *Frontiers in Immunology*, 9, 2221.
- HOLMGREN, J. & CZERKINSKY, C. 2005. Mucosal immunity and vaccines. *Nature medicine*, 11, S45-S53.
- HOLMGREN, J., CZERKINSKY, C., LYCKE, N. & SVENNERHOLM, A.-M. 1992. Mucosal Immunity: Implications for Vaccine Development. *Immunobiology*, 184, 157-179.

- HONG, H. A., HITRI, K., HOSSEINI, S., KOTOWICZ, N., BRYAN, D., MAWAS, F., WILKINSON, A. J., VAN BROEKHOVEN, A., KEARSEY, J. & CUTTING, S. M. 2017. Mucosal antibodies to the C terminus of toxin A prevent colonization of *Clostridium difficile*. *Infection and immunity*, 85, e01060-16.
- HONG, S.-S. & LIM, S.-J. 2015. Laboratory scale production of injectable liposomes by using cell disruptor to avoid the probe sonication process. *Journal of Pharmaceutical Investigation*, 45, 73-78.
- HOU, S., SIKORA, K. N., TANG, R., LIU, Y., LEE, Y.-W., KIM, S. T., JIANG, Z., VACHET, R. W. & ROTELLO, V. M. 2016. Quantitative differentiation of cell surface-bound and internalized cationic gold nanoparticles using mass spectrometry. *ACS nano*, 10, 6731-6736.
- HU, H. & DU, H. 2000. α -to- β structural transformation of ovalbumin: heat and pH effects. *Journal of Protein Chemistry*, 19, 177-183.
- HUA, S. 2014. Orally administered liposomal formulations for colon targeted drug delivery. *Frontiers in pharmacology*, 5.
- HUANG, J.-H., WU, C.-W., LIEN, S.-P., LENG, C.-H., HSIAO, K.-N., LIU, S.-J., CHEN, H.-W., SIU, L.-K. & CHONG, P. 2015. Recombinant lipoprotein-based vaccine candidates against *C. difficile* infections. *Journal of biomedical science*, 22, 1.
- HUANG, Y.-Y. & WANG, C.-H. 2006. Pulmonary delivery of insulin by liposomal carriers. *Journal of Controlled Release*, 113, 9-14.
- HUNYADY, B., MEZEY, E. & PALKOVITS, M. 2000. Gastrointestinal immunology: cell types in the lamina propria--a morphological review. *Acta physiologica Hungarica*, 87, 305-328.
- HUSSAIN, M. T., FORBES, N. & PERRIE, Y. 2019. Comparative Analysis of Protein Quantification Methods for the Rapid Determination of Protein Loading in Liposomal Formulations. *Pharmaceutics*, 11, 39.
- ICHIHASHI, T., SATOH, T., SUGIMOTO, C. & KAJINO, K. 2013. Emulsified phosphatidylserine, simple and effective peptide carrier for induction of potent epitope-specific T cell responses. *PLoS One*, 8.
- ISLAM, M. A., FIRDOUS, J., BADRUDDOZA, A. Z. M., REESOR, E., AZAD, M., HASAN, A., LIM, M., CAO, W., GUILLEMETTE, S. & CHO, C. S. 2019. M cell targeting engineered biomaterials for effective vaccination. *Biomaterials*, 192, 75-94.
- JAHN, A., STAVIS, S. M., HONG, J. S., VREELAND, W. N., DEVOE, D. L. & GAITAN, M. 2010. Microfluidic Mixing and the Formation of Nanoscale Lipid Vesicles. *ACS Nano*, 4, 2077-2087.
- JAHN, A., VREELAND, W. N., DEVOE, D. L., LOCASCIO, L. E. & GAITAN, M. 2007. Microfluidic Directed Formation of Liposomes of Controlled Size. *Langmuir*, 23, 6289-6293.
- JAHN, A., VREELAND, W. N., GAITAN, M. & LOCASCIO, L. E. 2004. Controlled vesicle self-assembly in microfluidic channels with hydrodynamic focusing. *Journal of the American Chemical Society*, 126, 2674-2675.
- JAKUBZICK, C. V., RANDOLPH, G. J. & HENSON, P. M. 2017. Monocyte differentiation and antigen-presenting functions. *Nature Reviews Immunology*, 17, 349-362.
- JANEWAY, C. Immunobiology 5th edition: The immune System in Health and Disease. 5th. New York: Garland Science.
- JANEWAY, C. A., CAPRA, J. D., TRAVERS, P. & WALPORT, M. 1999. *Immunobiology: the immune system in health and disease*.
- JANEWAY JR, C. A., TRAVERS, P., WALPORT, M. & SHLOMCHIK, M. J. 2001. B-cell activation by armed helper T cells. *Immunobiology: The Immune System in Health and Disease. 5th edition*. Garland Science.
- JOSHI, S., HUSSAIN, M. T., ROCES, C. B., ANDERLUZZI, G., KASTNER, E., SALMASO, S., KIRBY, D. J. & PERRIE, Y. 2016. Microfluidics based manufacture of liposomes simultaneously entrapping hydrophilic and lipophilic drugs. *International journal of pharmaceutics*, 514, 160-168.
- JOSIC, D. & KOVAC, S. 2010. Reversed-phase high performance liquid chromatography of proteins. *Current protocols in protein science*, 61, 8.7. 1-8.7. 22.

- KALEKO, M., BRISTOL, J. A., HUBERT, S., PARSLEY, T., WIDMER, G., TZIPORI, S., SUBRAMANIAN, P., HASAN, N., KOSKI, P. & KOKAI-KUN, J. 2016. Development of SYN-004, an oral beta-lactamase treatment to protect the gut microbiome from antibiotic-mediated damage and prevent *Clostridium difficile* infection. *Anaerobe*, 41, 58-67.
- KANG, S. H., HONG, S. J., LEE, Y.-K. & CHO, S. 2018. Oral Vaccine Delivery for Intestinal Immunity—Biological Basis, Barriers, Delivery System, and M Cell Targeting. *Polymers*, 10, 948.
- KANIE, Y., ENOMOTO, A., GOTO, S. & KANIE, O. 2008. Comparative RP-HPLC for rapid identification of glycopeptides and application in off-line LC-MALDI-MS analysis. *Carbohydrate Research*, 343, 758-768.
- KASTNER, E., KAUR, R., LOWRY, D., MOGHADDAM, B., WILKINSON, A. & PERRIE, Y. 2014. High-throughput manufacturing of size-tuned liposomes by a new microfluidics method using enhanced statistical tools for characterization. *International journal of pharmaceuticals*, 477, 361-368.
- KASTNER, E., VERMA, V., LOWRY, D. & PERRIE, Y. 2015. Microfluidic-controlled manufacture of liposomes for the solubilisation of a poorly water soluble drug. *International journal of pharmaceuticals*, 485, 122-130.
- KAUR, R., HENRIKSEN-LACEY, M., WILKHU, J., DEVITT, A., CHRISTENSEN, D. & PERRIE, Y. 2013. Effect of incorporating cholesterol into DDA: TDB liposomal adjuvants on bilayer properties, biodistribution, and immune responses. *Molecular pharmaceuticals*, 11, 197-207.
- KELLY, C., JEFFERIES, C. & CRYAN, S.-A. 2011. Targeted liposomal drug delivery to monocytes and macrophages. *Journal of drug delivery*, 2011.
- KELLY, C. P. & KYNE, L. 2011. The host immune response to *Clostridium difficile*. *Journal of medical microbiology*, 60, 1070-1079.
- KESSLER, R. J. & FANESTIL, D. D. 1986. Interference by lipids in the determination of protein using bicinchoninic acid. *Analytical Biochemistry*, 159, 138-142.
- KHADKE, S., ROCES, C. B., CAMERON, A., DEVITT, A. & PERRIE, Y. 2019. Formulation and manufacturing of lymphatic targeting liposomes using microfluidics. *Journal of Controlled Release*, 307, 211-220.
- KHADKE, S., STONE, P., ROZHIN, A., KROONEN, J. & PERRIE, Y. 2018. Point of use production of liposomal solubilised products. *International journal of pharmaceuticals*, 537, 1-8.
- KHAKSA, G., D'SOUZA, R., LEWIS, S. & UDUPA, N. 2000. Pharmacokinetic study of niosome encapsulated insulin.
- KHALIL, R. A. & AL-HAKAM, A. Z. 2014. Theoretical estimation of the critical packing parameter of amphiphilic self-assembled aggregates. *Applied surface science*, 318, 85-89.
- KOKKONA, M., KALLINTERI, P., FATOUROS, D. & ANTIMISIARIS, S. G. 2000. Stability of SUV liposomes in the presence of cholate salts and pancreatic lipases: effect of lipid composition. *European Journal of Pharmaceutical Sciences*, 9, 245-252.
- KORSHOLM, K. S., ANDERSEN, P. L. & CHRISTENSEN, D. 2012. Cationic liposomal vaccine adjuvants in animal challenge models: overview and current clinical status. *Expert review of vaccines*, 11, 561-577.
- KOZIOLEK, M., GRIMM, M., BECKER, D., IORDANOV, V., ZOU, H., SHIMIZU, J., WANKE, C., GARBACZ, G. & WEITSCHIES, W. 2015. Investigation of pH and temperature profiles in the GI tract of fasted human subjects using the Intellicap® system. *Journal of pharmaceutical sciences*, 104, 2855-2863.
- KRASNICI, S., WERNER, A., EICHHORN, M. E., SCHMITT-SODY, M., PAHERNIK, S. A., SAUER, B., SCHULZE, B., TEIFEL, M., MICHAELIS, U. & NAUJOKS, K. 2003. Effect of the surface charge of liposomes on their uptake by angiogenic tumor vessels. *International journal of cancer*, 105, 561-567.
- KRIEG, R. C., DONG, Y., SCHWAMBORN, K. & KNUECHEL, R. 2005. Protein quantification and its tolerance for different interfering reagents using the BCA-method with regard to 2D SDS PAGE. *Journal of Biochemical and Biophysical Methods*, 65, 13-19.

- KUNISAWA, J., KURASHIMA, Y. & KIYONO, H. 2012. Gut-associated lymphoid tissues for the development of oral vaccines. *Advanced drug delivery reviews*, 64, 523-530.
- KYNE, L., WARNY, M., QAMAR, A. & KELLY, C. P. 2000. Asymptomatic carriage of *Clostridium difficile* and serum levels of IgG antibody against toxin A. *New England Journal of Medicine*, 342, 390-397.
- KYNE, L., WARNY, M., QAMAR, A. & KELLY, C. P. 2001. Association between antibody response to toxin A and protection against recurrent *Clostridium difficile* diarrhoea. *The Lancet*, 357, 189-193.
- LAVELLE, E. C. & O'HAGAN, D. 2006. Delivery systems and adjuvants for oral vaccines. *Expert opinion on drug delivery*, 3, 747-762.
- LAZAR, V., DITU, L.-M., PIRCALABIORU, G. G., GHEORGHE, I., CURUTIU, C., HOLBAN, A. M., PICU, A., PETCU, L. & CHIFIRIUC, M. C. 2018. Aspects of gut microbiota and immune system interactions in infectious diseases, immunopathology, and cancer. *Frontiers in immunology*, 9, 1830.
- LEADER, B., BACA, Q. J. & GOLAN, D. E. 2008. Protein therapeutics: a summary and pharmacological classification. *Nature Reviews Drug Discovery*, 7, 21.
- LEE, S. L., O'CONNOR, T. F., YANG, X., CRUZ, C. N., CHATTERJEE, S., MADURAWA, R. D., MOORE, C. M., LAWRENCE, X. Y. & WOODCOCK, J. 2015. Modernizing pharmaceutical manufacturing: from batch to continuous production. *Journal of Pharmaceutical Innovation*, 10, 191-199.
- LEROUEIL, P. R., HONG, S., MECKE, A., BAKER JR, J. R., ORR, B. G. & BANASZAK HOLL, M. M. 2007. Nanoparticle interaction with biological membranes: does nanotechnology present a Janus face? *Accounts of chemical research*, 40, 335-342.
- LETIZIA, C., ANDREOZZI, P., SCIPIONI, A., LA MESA, C., BONINCONTRO, A. & SPIGONE, E. 2007. Protein binding onto surfactant-based synthetic vesicles. *The Journal of Physical Chemistry B*, 111, 898-908.
- LEUNG, S. S., MORALES, S., BRITTON, W., KUTTER, E. & CHAN, H.-K. 2018. Microfluidic-assisted bacteriophage encapsulation into liposomes. *International journal of pharmaceutics*, 545, 176-182.
- LEVIE, K., GJORUP, I., SKINHØJ, P. & STOFFEL, M. 2002. A 2-dose regimen of a recombinant hepatitis B vaccine with the immune stimulant AS04 compared with the standard 3-dose regimen of Engerix-B in healthy young adults. *Scandinavian journal of infectious diseases*, 34, 610-614.
- LI, N., PENG, L.-H., CHEN, X., NAKAGAWA, S. & GAO, J.-Q. 2011a. Effective transcutaneous immunization by antigen-loaded flexible liposome in vivo. *International Journal of Nanomedicine*, 6, 3241-3250.
- LI, Y., CUI, X.-L., CHEN, Q.-S., YU, J., ZHANG, H., GAO, J., SUN, D.-X. & ZHANG, G.-Q. 2018. Cationic liposomes induce cytotoxicity in HepG2 via regulation of lipid metabolism based on whole-transcriptome sequencing analysis. *BMC Pharmacology and Toxicology*, 19, 43.
- LI, Z., ZHANG, L., SUN, W., DING, Q., HOU, Y. & XU, Y. 2011b. Archaeosomes with encapsulated antigens for oral vaccine delivery. *Vaccine*, 29, 5260-5266.
- LIAU, J. J., HOOK, S., PRESTIDGE, C. A. & BARNES, T. J. 2015. A lipid based multi-compartmental system: Liposomes-in-double emulsion for oral vaccine delivery. *European Journal of Pharmaceutics and Biopharmaceutics*, 97, 15-21.
- LIN, M. & QI, X.-R. 2018. Purification Method of Drug-Loaded Liposome. In: LU, W.-L. & QI, X.-R. (eds.) *Liposome-Based Drug Delivery Systems*. Berlin, Heidelberg: Springer Berlin Heidelberg.
- LIU, J., WU, J., WANG, B., ZENG, S., QI, F., LU, C., KIMURA, Y. & LIU, B. 2014. Oral vaccination with a liposome-encapsulated influenza DNA vaccine protects mice against respiratory challenge infection. *Journal of medical virology*, 86, 886-894.
- LIU, W., YE, A., LIU, W., LIU, C., HAN, J. & SINGH, H. 2015. Behaviour of liposomes loaded with bovine serum albumin during in vitro digestion. *Food Chemistry*, 175, 16-24.
- LOMBARDO, D., CALANDRA, P., BARRECA, D., MAGAZÙ, S. & KISELEV, M. A. 2016. Soft interaction in liposome nanocarriers for therapeutic drug delivery. *Nanomaterials*, 6, 125.
- LONEZ, C., VANDENBRANDEN, M. & RUYSSCHAERT, J.-M. 2008. Cationic liposomal lipids: from gene carriers to cell signaling. *Progress in lipid research*, 47, 340-347.

- LOU, G., ANDERLUZZI, G., SCHMIDT, S. T., WOODS, S., GALLORINI, S., BRAZZOLI, M., GIUSTI, F., FERLENGHI, I., JOHNSON, R. & ROBERTS, C. W. 2020. Delivery of self-amplifying mRNA vaccines by cationic lipid nanoparticles: The impact of cationic lipid selection. *Journal of Controlled Release*.
- LOU, G., ANDERLUZZI, G., WOODS, S., ROBERTS, C. W. & PERRIE, Y. 2019. A novel microfluidic-based approach to formulate size-tuneable large unilamellar cationic liposomes: Formulation, cellular uptake and biodistribution investigations. *European Journal of Pharmaceutics and Biopharmaceutics*, 143, 51-60.
- LU, T., WANG, Z., MA, Y., ZHANG, Y. & CHEN, T. 2012. Influence of polymer size, liposomal composition, surface charge, and temperature on the permeability of pH-sensitive liposomes containing lipid-anchored poly (2-ethylacrylic acid). *International journal of nanomedicine*, 7, 4917.
- LUNG, P., YANG, J. & LI, Q. 2020. Nanoparticle formulated vaccines: opportunities and challenges. *Nanoscale*, 12, 5746-5763.
- LUTSIK, M., KWON, G. S. & SAMUEL, J. 2002. Analysis of peptide and lipopeptide content in liposomes. *Journal of pharmacy & pharmaceutical sciences: a publication of the Canadian Society for Pharmaceutical Sciences, Societe canadienne des sciences pharmaceutiques*, 5, 279-84.
- LYCKE, N. & HOLMGREN, J. 1986. Strong adjuvant properties of cholera toxin on gut mucosal immune responses to orally presented antigens. *Immunology*, 59, 301.
- LYNCH, M., WALSH, T. A., MARSZALOWSKA, I., WEBB, A. E., MACAOGAIN, M., ROGERS, T. R., WINDLE, H., KELLEHER, D., O'CONNELL, M. J. & LOSCHER, C. E. 2017. Surface layer proteins from virulent *Clostridium difficile* ribotypes exhibit signatures of positive selection with consequences for innate immune response. *BMC evolutionary biology*, 17, 90.
- MANTIS, N. J., ROL, N. & CORTHÉSY, B. 2011. Secretory IgA's complex roles in immunity and mucosal homeostasis in the gut. *Mucosal immunology*, 4, 603-611.
- MARTINEZ, F. O., SICA, A., MANTOVANI, A. & LOCATI, M. 2008. Macrophage activation and polarization. *Front Biosci*, 13, 453-461.
- MCKAY, P. F., HU, K., BLAKNEY, A. K., SAMNUAN, K., BROWN, J. C., PENN, R., ZHOU, J., BOUTON, C. R., ROGERS, P. & POLRA, K. 2020. Self-amplifying RNA SARS-CoV-2 lipid nanoparticle vaccine candidate induces high neutralizing antibody titers in mice. *Nature communications*, 11, 1-7.
- MIJAJLOVIC, M., WRIGHT, D., ZIVKOVIC, V., BI, J. X. & BIGGS, M. J. 2013. Microfluidic hydrodynamic focusing based synthesis of POPC liposomes for model biological systems. *Colloids and Surfaces B: Biointerfaces*, 104, 276-281.
- MILICIC, A., KAUR, R., REYES-SANDOVAL, A., TANG, C.-K., HONEYCUTT, J., PERRIE, Y. & HILL, A. V. 2012. Small cationic DDA: TDB liposomes as protein vaccine adjuvants obviate the need for TLR agonists in inducing cellular and humoral responses. *PLoS one*, 7, e34255.
- MINATO, S., IWANAGA, K., KAKEMI, M., YAMASHITA, S. & OKU, N. 2003. Application of polyethyleneglycol (PEG)-modified liposomes for oral vaccine: effect of lipid dose on systemic and mucosal immunity. *Journal of controlled release*, 89, 189-197.
- MINOR, P. D. 2015. Live attenuated vaccines: historical successes and current challenges. *Virology*, 479, 379-392.
- MOGHADDAM, B., ALI, M. H., WILKHU, J., KIRBY, D. J., MOHAMMED, A. R., ZHENG, Q. & PERRIE, Y. 2011. The application of monolayer studies in the understanding of liposomal formulations. *International Journal of Pharmaceutics*, 417, 235-244.
- MONTILLA, N. A., BLAS, M. P., SANTALLA, M. L. & VILLA, J. M. 2004. Mucosal immune system: a brief review. *Inmunología*, 23, 207-216.
- MOON, J. J., SUH, H., LI, A. V., OCKENHOUSE, C. F., YADAVA, A. & IRVINE, D. J. 2012. Enhancing humoral responses to a malaria antigen with nanoparticle vaccines that expand Tfh cells and promote germinal center induction. *Proceedings of the National Academy of Sciences*, 109, 1080-1085.
- MORI, M., NISHIDA, M., MAEKAWA, N., YAMAMURA, H., TANAKA, Y., KASAI, M., TANEICHI, M. & UCHIDA, T. 2005. An increased adjuvanticity of liposomes by the inclusion of

- phosphatidylserine in immunization with surface-coupled liposomal antigen. *International archives of allergy and immunology*, 136, 83-89.
- MORTON, R. E. & EVANS, T. A. 1992. Modification of the bicinchoninic acid protein assay to eliminate lipid interference in determining lipoprotein protein content. *Analytical biochemistry*, 204, 332-334.
- MOWAT, A. M. 2003. Anatomical basis of tolerance and immunity to intestinal antigens. *Nature Reviews Immunology*, 3, 331-341.
- MOZAFARI, M. 2010. Nanoliposomes: preparation and analysis. *Liposomes*. Springer.
- MUSUMECI, T., LEONARDI, A., BONACCORSO, A., PIGNATELLO, R. & PUGLISI, G. 2018. Tangential Flow Filtration Technique: An Overview on Nanomedicine Applications. *Pharmaceutical nanotechnology*, 6, 48-60.
- NAKANISHI, T., KUNISAWA, J., HAYASHI, A., TSUTSUMI, Y., KUBO, K., NAKAGAWA, S., NAKANISHI, M., TANAKA, K. & MAYUMI, T. 1999. Positively charged liposome functions as an efficient immunoadjuvant in inducing cell-mediated immune response to soluble proteins. *Journal of controlled release*, 61, 233-240.
- NAM, J. H., KIM, S.-Y. & SEONG, H. 2018. Investigation on physicochemical characteristics of a nanoliposome-based system for dual drug delivery. *Nanoscale research letters*, 13, 101.
- NDIBEWU, P. P. & NGOBENI, P. 2013. *Use of Analytical Methods and In-silico Techniques in Public Health Research*.
- NEW, R. 2019. Formulation technologies for oral vaccines. *Clinical & Experimental Immunology*, 198, 153-169.
- NIU, F., SU, Y., LIU, Y., WANG, G., ZHANG, Y. & YANG, Y. 2014. Ovalbumin–gum arabic interactions: Effect of pH, temperature, salt, biopolymers ratio and total concentration. *Colloids and Surfaces B: Biointerfaces*, 113, 477-482.
- NKANGA, C. I., BAPOLISI, A. M., OKAFOR, N. I. & KRAUSE, R. W. M. 2019. General Perception of Liposomes: Formation, Manufacturing and Applications. *Liposomes-Advances and Perspectives*. IntechOpen.
- NOWROOZI, F., ALMASI, A., JAVIDI, J., HAERI, A. & DADASHZADEH, S. 2018. Effect of Surfactant Type, Cholesterol Content and Various Downsizing Methods on the Particle Size of Niosomes. *Iranian journal of pharmaceutical research: IJPR*, 17, 1.
- OELLERS, M., BUNGE, F., VINAYAKA, P., DRIESCHE, S. V. D. & VELLEKOOP, M. J. Flow-ratio monitoring in a microchannel by liquid-liquid interface interferometry. *Multidisciplinary Digital Publishing Institute Proceedings*, 2017. 498.
- OWEN, J. L., SAHAY, B. & MOHAMADZADEH, M. 2013. New generation of oral mucosal vaccines targeting dendritic cells. *Current opinion in chemical biology*, 17, 918-924.
- PARKER, E. P., RAMANI, S., LOPMAN, B. A., CHURCH, J. A., ITURRIZA-GOMARA, M., PRENDERGAST, A. J. & GRASSLY, N. C. 2018. Causes of impaired oral vaccine efficacy in developing countries. *Future microbiology*, 13, 97-118.
- PASETTI, M. F., SIMON, J. K., SZTEIN, M. B. & LEVINE, M. M. 2011. Immunology of gut mucosal vaccines. *Immunological reviews*, 239, 125-148.
- PATHAK, M., LINTERN, K., CHOPDA, V., BRACEWELL, D. G. & RATHORE, A. S. 2017. Fluorescence based real time monitoring of fouling in process chromatography. *Scientific reports*, 7, 45640.
- PATI, R., SHEVTSOV, M. & SONAWANE, A. 2018. Nanoparticle Vaccines Against Infectious Diseases. *Frontiers in immunology*, 9.
- PATTY, P. J. & FRISKEN, B. J. 2003. The pressure-dependence of the size of extruded vesicles. *Biophysical journal*, 85, 996-1004.
- PAUNOVSKA, K., SAGO, C. D., MONACO, C. M., HUDSON, W. H., CASTRO, M. G., RUDOLTZ, T. G., KALATHOOR, S., VANOVER, D. A., SANTANGELO, P. J. & AHMED, R. 2018. A direct comparison of in vitro and in vivo nucleic acid delivery mediated by hundreds of nanoparticles reveals a weak correlation. *Nano letters*, 18, 2148-2157.

- PÉCHINÉ, S., JANOIR, C., BOUREAU, H., GLEIZES, A., TSAPIS, N., HOYS, S., FATTAL, E. & COLLIGNON, A. 2007. Diminished intestinal colonization by *Clostridium difficile* and immune response in mice after mucosal immunization with surface proteins of *Clostridium difficile*. *Vaccine*, 25, 3946-3954.
- PEDERSEN, G. K., ANDERSEN, P. & CHRISTENSEN, D. Immunocorrelates of CAF family adjuvants. *Seminars in immunology*, 2018. Elsevier, 4-13.
- PELED, J. U., HANASH, A. M. & JENQ, R. R. 2016. Role of the intestinal mucosa in acute gastrointestinal GVHD. *Blood, The Journal of the American Society of Hematology*, 128, 2395-2402.
- PENNOCK, N. D., WHITE, J. T., CROSS, E. W., CHENEY, E. E., TAMBURINI, B. A. & KEDL, R. M. 2013. T cell responses: naive to memory and everything in between. *Advances in physiology education*, 37, 273-283.
- PERRIE, Y., CROFTS, F., DEVITT, A., GRIFFITHS, H. R., KASTNER, E. & NADELLA, V. 2016. Designing liposomal adjuvants for the next generation of vaccines. *Advanced drug delivery reviews*, 99, 85-96.
- PERRIE, Y., KASTNER, E., KHADKE, S., ROCES, C. B. & STONE, P. 2017. Manufacturing methods for liposome adjuvants. *Vaccine Adjuvants*. Springer.
- PERRIE, Y., MOHAMMED, A. R., KIRBY, D. J., MCNEIL, S. E. & BRAMWELL, V. W. 2008. Vaccine adjuvant systems: Enhancing the efficacy of sub-unit protein antigens. *International Journal of Pharmaceutics*, 364, 272-280.
- PETERSEN, E. J. & NELSON, B. C. 2010. Mechanisms and measurements of nanomaterial-induced oxidative damage to DNA. *Analytical and Bioanalytical Chemistry*, 398, 613-650.
- PETRILLI, R., ELOY, J. O., DE SOUZA, M. C., BARCELLOS, J. P. A., MARCHETTI, J. M., YUNG, B. & LEE, R. J. 2016. Lipid nanoparticles as non-viral vectors for siRNA delivery: Concepts and applications. *Nanobiomaterials in Drug Delivery*. Elsevier.
- PETROVIC, A., ALPDOGAN, O., WILLIS, L. M., ENG, J. M., GREENBERG, A. S., KAPPEL, B. J., LIU, C., MURPHY, G. J., HELLER, G. & VAN DEN BRINK, M. R. 2004. LPAM ($\alpha 4\beta 7$ integrin) is an important homing integrin on alloreactive T cells in the development of intestinal graft-versus-host disease. *Blood*, 103, 1542-1547.
- PETROVSKY, N. 2015. Comparative safety of vaccine adjuvants: a summary of current evidence and future needs. *Drug safety*, 38, 1059-1074.
- PHAYRE, A. N., VANEGAS FARFANO, H. M. & HAYES, M. A. 2002. Effects of pH gradients on liposomal charge states examined by capillary electrophoresis. *Langmuir*, 18, 6499-6503.
- PLANELLES, L., THOMAS, M., MARANON, C., MORELL, M. & LÓPEZ, M. 2003. Differential CD86 and CD40 co-stimulatory molecules and cytokine expression pattern induced by *Trypanosoma cruzi* in APCs from resistant or susceptible mice. *Clinical & Experimental Immunology*, 131, 41-47.
- QU, W., LI, N., YU, R., ZUO, W., FU, T., FEI, W., HOU, Y., LIU, Y. & YANG, J. 2018. Cationic DDA/TDB liposome as a mucosal vaccine adjuvant for uptake by dendritic cells in vitro induces potent humoral immunity. *Artificial cells, nanomedicine, and biotechnology*, 46, 852-860.
- RAMIREZ, J. E. V., SHARPE, L. A. & PEPPAS, N. A. 2017. Current state and challenges in developing oral vaccines. *Advanced drug delivery reviews*, 114, 116-131.
- RANDOLPH, G. J., JAKUBZICK, C. & QU, C. 2008. Antigen presentation by monocytes and monocyte-derived cells. *Current opinion in immunology*, 20, 52-60.
- RASHIDINEJAD, A., BIRCH, E. J., SUN-WATERHOUSE, D. & EVERETT, D. W. 2014. Delivery of green tea catechin and epigallocatechin gallate in liposomes incorporated into low-fat hard cheese. *Food chemistry*, 156, 176-183.
- REED, S. G., ORR, M. T. & FOX, C. B. 2013. Key roles of adjuvants in modern vaccines. *Nature medicine*, 19, 1597-1608.
- RHEE, J. H., LEE, S. E. & KIM, S. Y. 2012. Mucosal vaccine adjuvants update. *Clinical and experimental vaccine research*, 1, 50-63.

- RICHARDSON, E. S., PITT, W. G. & WOODBURY, D. J. 2007. The role of cavitation in liposome formation. *Biophysical journal*, 93, 4100-4107.
- RILEY, T., LYRAS, D. & DOUCE, G. 2019. Status of vaccine research and development for *Clostridium difficile*. *Vaccine*, 37, 7300-7306.
- ROBERTSON, V. K. 2013. *Applications of a Biorelevant In Vitro Dissolution Method Using USP Apparatus 4 in Early Phase Formulation Development*. University of Kansas.
- ROCES, C. B., CHRISTENSEN, D. & PERRIE, Y. 2020. Translating the fabrication of protein-loaded poly (lactic-co-glycolic acid) nanoparticles from bench to scale-independent production using microfluidics. *Drug Delivery and Translational Research*, 1-12.
- ROCES, C. B., KHADKE, S., CHRISTENSEN, D. & PERRIE, Y. 2019. Scale-independent microfluidic production of cationic liposomal adjuvants and development of enhanced lymphatic targeting strategies. *Molecular pharmaceuticals*.
- RODRIGUEZ-FERNANDEZ, S., PUJOL-AUTONELL, I., BRIANSO, F., PERNA-BARRULL, D., CANO-SARABIA, M., GARCIA-JIMENO, S., VILLALBA, A., SANCHEZ, A., AGUILERA, E. & VAZQUEZ, F. 2018. Phosphatidylserine-liposomes promote tolerogenic features on dendritic cells in human type 1 diabetes by apoptotic mimicry. *Frontiers in immunology*, 9, 253.
- ROMÁN, V. R. G., JENSEN, K. J., JENSEN, S. S., LEO-HANSEN, C., JESPERSEN, S., TÉ, D. D. S., RODRIGUES, C. M., JANITZEK, C. M., VINNER, L. & KATZENSTEIN, T. L. 2013. Therapeutic vaccination using cationic liposome-adjuvanted HIV type 1 peptides representing HLA-supertype-restricted subdominant T cell epitopes: safety, immunogenicity, and feasibility in Guinea-Bissau. *AIDS research and human retroviruses*, 29, 1504-1512.
- RUSSELL-JONES, G. 2000. Oral vaccine delivery. *Journal of controlled release*, 65, 49-54.
- RUYSSCHAERT, T., MARQUE, A., DUTEYRAT, J.-L., LESIEUR, S., WINTERHALTER, M. & FOURNIER, D. 2005. Liposome retention in size exclusion chromatography. *BMC biotechnology*, 5, 11.
- RYAN, A., LYNCH, M., SMITH, S. M., AMU, S., NEL, H. J., MCCOY, C. E., DOWLING, J. K., DRAPER, E., O'REILLY, V. & MCCARTHY, C. 2011. A role for TLR4 in *Clostridium difficile* infection and the recognition of surface layer proteins. *PLoS pathogens*, 7.
- SALIM, S. A. Y. & SÖDERHOLM, J. D. 2011. Importance of disrupted intestinal barrier in inflammatory bowel diseases. *Inflammatory bowel diseases*, 17, 362-381.
- SARKER, S. R., HOKAMA, R. & TAKEOKA, S. 2014. Intracellular delivery of universal proteins using a lysine headgroup containing cationic liposomes: deciphering the uptake mechanism. *Molecular pharmaceuticals*, 11, 164-174.
- SATITSUKSANOVA, P., JANSEN, K., GŁOBIŃSKA, A., VAN DE VEEN, W. & AKDIS, M. 2018. Regulatory immune mechanisms in tolerance to food allergy. *Frontiers in immunology*, 9, 2939.
- SAVINA, A. & AMIGORENA, S. 2007. Phagocytosis and antigen presentation in dendritic cells. *Immunological reviews*, 219, 143-156.
- SCHAEFFLER, H. & BREITRUECK, A. 2018. *Clostridium difficile*—From colonization to infection. *Frontiers in microbiology*, 9, 646.
- SCHARNAGL, C., REIF, M. & FRIEDRICH, J. 2005. Stability of proteins: temperature, pressure and the role of the solvent. *Biochimica et Biophysica Acta (BBA)-Proteins and Proteomics*, 1749, 187-213.
- SCHILTZ, E., SCHNACKERZ, K. & GRACY, R. 1977. Comparison of ninhydrin, fluorescamine, and o-phthaldialdehyde for the detection of amino acids and peptides and their effects on the recovery and composition of peptides from thin-layer fingerprints. *Analytical biochemistry*, 79, 33-41.
- SCHMIDT, N., SCHULZE, J., WARWAS, D. P., EHLERT, N., LENARZ, T., WARNECKE, A. & BEHRENS, P. 2018. Long-term delivery of brain-derived neurotrophic factor (BDNF) from nanoporous silica nanoparticles improves the survival of spiral ganglion neurons in vitro. *PloS one*, 13.
- SCHWARTZ, L. & SEELEY, K. 1999. Introduction to tangential flow filtration for laboratory and process development applications. *PALL information brochure PN33213*.

- SCHWENDENER, R. A. 2014. Liposomes as vaccine delivery systems: a review of the recent advances. *Therapeutic advances in vaccines*, 2, 159-182.
- SEDIGHI, M., SIEBER, S., RAHIMI, F., SHAHBAZI, M.-A., REZAYAN, A. H., HUWYLER, J. & WITZIGMANN, D. 2019. Rapid optimization of liposome characteristics using a combined microfluidics and design-of-experiment approach. *Drug delivery and translational research*, 9, 404-413.
- SEELIG, J. 2004. Thermodynamics of lipid-peptide interactions. *Biochimica et Biophysica Acta (BBA)-Biomembranes*, 1666, 40-50.
- SERCOMBE, L., VEERATI, T., MOHEIMANI, F., WU, S. Y., SOOD, A. K. & HUA, S. 2015. Advances and challenges of liposome assisted drug delivery. *Frontiers in pharmacology*, 6, 286.
- SHAH, N. K., GUPTA, S. K., WANG, Z. & MEENACH, S. A. 2019. Enhancement of macrophage uptake via phosphatidylserine-coated acetalated dextran nanoparticles. *Journal of Drug Delivery Science and Technology*, 50, 57-65.
- SHAKYA, A. K., CHOWDHURY, M. Y., TAO, W. & GILL, H. S. 2016. Mucosal vaccine delivery: current state and a pediatric perspective. *Journal of controlled release*, 240, 394-413.
- SHI, Y. & ROCK, K. L. 2002. Cell death releases endogenous adjuvants that selectively enhance immune surveillance of particulate antigens. *European journal of immunology*, 32, 155-162.
- SILVA, A., SOEMA, P., SLÜTTER, B., OSSENDORP, F. & JISKOOT, W. 2016. PLGA particulate delivery systems for subunit vaccines: linking particle properties to immunogenicity. *Human vaccines & immunotherapeutics*, 12, 1056-1069.
- SILVA, R., FERREIRA, H., LITTLE, C. & CAVACO-PAULO, A. 2010. Effect of ultrasound parameters for unilamellar liposome preparation. *Ultrasonics sonochemistry*, 17, 628-632.
- SIMBERG, D., WEISMAN, S., TALMON, Y. & BARENHOLZ, Y. 2004. DOTAP (and other cationic lipids): chemistry, biophysics, and transfection. *Critical Reviews™ in Therapeutic Drug Carrier Systems*, 21.
- SNIPSTAD, S., HAK, S., BAGHIROV, H., SULHEIM, E., MØRCH, Y., LÉLU, S., VON HAARTMAN, E., BÄCK, M., NILSSON, K. P. R. & KLYMCHENKO, A. S. 2017. Labeling nanoparticles: Dye leakage and altered cellular uptake. *Cytometry Part A*, 91, 760-766.
- SOEMA, P. C., WILLEMS, G.-J., JISKOOT, W., AMORIJ, J.-P. & KERSTEN, G. F. 2015. Predicting the influence of liposomal lipid composition on liposome size, zeta potential and liposome-induced dendritic cell maturation using a design of experiments approach. *European Journal of Pharmaceutics and Biopharmaceutics*, 94, 427-435.
- SOLOMON, K. 2013. The host immune response to *Clostridium difficile* infection. *Therapeutic advances in infectious disease*, 1, 19-35.
- SPENCER, J., LEUZZI, R., BUCKLEY, A., IRVINE, J., CANDLISH, D., SCARSELLI, M. & DOUCE, G. R. 2014. Vaccination against *Clostridium difficile* using toxin fragments: Observations and analysis in animal models. *Gut microbes*, 5, 225-232.
- STAVNEZER, J. 1996. Antibody class switching. *Advances in immunology*, 61, 79-146.
- STAVNEZER, J., GUIKEMA, J. E. & SCHRADER, C. E. 2008. Mechanism and regulation of class switch recombination. *Annu. Rev. Immunol.*, 26, 261-292.
- STEBEGG, M., KUMAR, S. D., SILVA-CAYETANO, A., FONSECA, V. R., LINTERMAN, M. A. & GRACA, L. 2018. Regulation of the germinal center response. *Frontiers in immunology*, 9, 2469.
- STEFFEN, U., KOELEMAN, C. A., SOKOLOVA, M. V., BANG, H., KLEYER, A., RECH, J., UNTERWEGER, H., SCHICHT, M., GARREIS, F. & HAHN, J. 2020. IgA subclasses have different effector functions associated with distinct glycosylation profiles. *Nature communications*, 11, 1-12.
- SUN, J. B., CZERKINSKY, C. & HOLMGREN, J. 2010. Mucosally induced immunological tolerance, regulatory T cells and the adjuvant effect by cholera toxin B subunit. *Scandinavian journal of immunology*, 71, 1-11.
- TABOADA, P., BARBOSA, S., CASTRO, E., GUTIÉRREZ-PICHEL, M. & MOSQUERA, V. 2007. Effect of solvation on the structure conformation of human serum albumin in aqueous-alcohol mixed solvents. *Chemical Physics*, 340, 59-68.

- TAIRA, M., CHIARAMONI, N., PECUCH, K. & ALONSO-ROMANOWSKI, S. 2004. Stability of liposomal formulations in physiological conditions for oral drug delivery. *Drug Delivery*, 11, 123-128.
- TANDRUP SCHMIDT, S., FOGED, C., SMITH KORSHOLM, K., RADES, T. & CHRISTENSEN, D. 2016. Liposome-based adjuvants for subunit vaccines: formulation strategies for subunit antigens and immunostimulators. *Pharmaceutics*, 8, 7.
- THERMOFISHER. *SPDP Crosslinkers Instructions* [Online]. Available: http://tools.thermofisher.com/content/sfs/manuals/MAN0011212_SPDP_CrsLnk_UG.pdf [Accessed 09/08/2020].
- TLASKALOVÁ-HOGENOVÁ, H., ŠTĚPÁNKOVÁ, R., KOZÁKOVÁ, H., HUDCOVIC, T., VANNUCCI, L., TUČKOVÁ, L., ROSSMANN, P., HRNČIŘ, T., KVERKA, M. & ZÁKOSTELSKÁ, Z. 2011. The role of gut microbiota (commensal bacteria) and the mucosal barrier in the pathogenesis of inflammatory and autoimmune diseases and cancer: contribution of germ-free and gnotobiotic animal models of human diseases. *Cellular & molecular immunology*, 8, 110.
- TORCHILIN, V. P. 2005a. Fluorescence microscopy to follow the targeting of liposomes and micelles to cells and their intracellular fate. *Advanced drug delivery reviews*, 57, 95-109.
- TORCHILIN, V. P. 2005b. Recent advances with liposomes as pharmaceutical carriers. *Nat Rev Drug Discov*, 4, 145-160.
- TSENG, L. P., CHIOU, C. J., DENG, M. C., LIN, M. H., PAN, R. N., HUANG, Y. Y. & LIU, D. Z. 2009. Evaluation of encapsulated Newcastle disease virus liposomes using various phospholipids administered to improve chicken humoral immunity. *Journal of Biomedical Materials Research Part B: Applied Biomaterials: An Official Journal of The Society for Biomaterials, The Japanese Society for Biomaterials, and The Australian Society for Biomaterials and the Korean Society for Biomaterials*, 91, 621-625.
- TZENG, C.-W., TZENG, W.-S., LIN, L.-T., LEE, C.-W., YEN, F.-L. & LIN, C.-C. 2016. Enhanced autophagic activity of artocarpin in human hepatocellular carcinoma cells through improving its solubility by a nanoparticle system. *Phytomedicine*, 23, 528-540.
- UMRETHIA, M., KETT, V. L., ANDREWS, G. P., MALCOLM, R. K. & WOOLFSON, A. D. 2010. Selection of an analytical method for evaluating bovine serum albumin concentrations in pharmaceutical polymeric formulations. *Journal of pharmaceutical and biomedical analysis*, 51, 1175-1179.
- VAN DISSEL, J. T., JOOSTEN, S. A., HOFF, S. T., SOONAWALA, D., PRINS, C., HOKEY, D. A., O'DEE, D. M., GRAVES, A., THIERRY-CARSTENSEN, B., ANDREASEN, L. V., RUHWALD, M., DE VISSER, A. W., AGGER, E. M., OTTENHOFF, T. H. M., KROMANN, I. & ANDERSEN, P. 2014. A novel liposomal adjuvant system, CAF01, promotes long-lived Mycobacterium tuberculosis-specific T-cell responses in human. *Vaccine*, 32, 7098-7107.
- VANCAMELBEKE, M. & VERMEIRE, S. 2017. The intestinal barrier: a fundamental role in health and disease. *Expert review of gastroenterology & hepatology*, 11, 821-834.
- VANGALA, A., KIRBY, D., ROSENKRANDS, I., AGGER, E. M., ANDERSEN, P. & PERRIE, Y. 2006. A comparative study of cationic liposome and niosome-based adjuvant systems for protein subunit vaccines: characterisation, environmental scanning electron microscopy and immunisation studies in mice. *Journal of pharmacy and pharmacology*, 58, 787-799.
- VARTAK, A. & SUCHECK, S. 2016. Recent advances in subunit vaccine carriers. *Vaccines*, 4, 12.
- VARYPATAKI, E. M., BENNE, N., BOUWSTRA, J., JISKOOT, W. & OSSENDORP, F. 2017. Efficient eradication of established tumors in mice with cationic liposome-based synthetic long-peptide vaccines. *Cancer immunology research*, 5, 222-233.
- VASAVID, P., CHAIWATANARAT, T., PUSUWAN, P., SRITARA, C., ROYSRI, K., NAMWONGPROM, S., KUANRAKCHAROEN, P., PREMPRABHA, T., CHUNLERTRITH, K. & THONGSAWAT, S. 2014. Normal solid gastric emptying values measured by scintigraphy using Asian-style meal: a multicenter study in healthy volunteers. *Journal of neurogastroenterology and motility*, 20, 371.
- VASHIST, S. K. & DIXIT, C. K. 2011. Interference of N-hydroxysuccinimide with biconchonic acid protein assay. *Biochemical and biophysical research communications*, 411, 455-457.

- VEMURI, S. & RHODES, C. 1994. Separation of liposomes by a gel filtration chromatographic technique: a preliminary evaluation. *Pharmaceutica Acta Helvetica*, 69, 107-113.
- VILA-CABALLER, M., CODOLO, G., MUNARI, F., MALFANTI, A., FASSAN, M., RUGGE, M., BALASSO, A., DE BERNARD, M. & SALMASO, S. 2016. A pH-sensitive stearyl-PEG-poly(methacryloyl sulfadimethoxine)-decorated liposome system for protein delivery: An application for bladder cancer treatment. *Journal of Controlled Release*, 238, 31-42.
- VILLANO, S. A., SEIBERLING, M., TATAROWICZ, W., MONNOT-CHASE, E. & GERDING, D. N. 2012. Evaluation of an oral suspension of VP20621, spores of nontoxigenic *Clostridium difficile* strain M3, in healthy subjects. *Antimicrobial agents and chemotherapy*, 56, 5224-5229.
- VOTH, D. E. & BALLARD, J. D. 2005. *Clostridium difficile* toxins: mechanism of action and role in disease. *Clinical microbiology reviews*, 18, 247-263.
- WAGNER, A. & VORAUER-UHL, K. 2010. Liposome technology for industrial purposes. *Journal of drug delivery*, 2011.
- WAGNER, A. & VORAUER-UHL, K. 2011. Liposome technology for industrial purposes. *Journal of drug delivery*, 2011.
- WALKER, J. M. 1996. The Bicinchoninic Acid (BCA) Assay for Protein Quantitation. In: WALKER, J. M. (ed.) *The Protein Protocols Handbook*. Totowa, NJ: Humana Press.
- WANG, N., WANG, T., ZHANG, M., CHEN, R., NIU, R. & DENG, Y. 2014. Mannose derivative and lipid A dually decorated cationic liposomes as an effective cold chain free oral mucosal vaccine adjuvant-delivery system. *European Journal of Pharmaceutics and Biopharmaceutics*, 88, 194-206.
- WATSON, D. S., ENDSLEY, A. N. & HUANG, L. 2012. Design considerations for liposomal vaccines: influence of formulation parameters on antibody and cell-mediated immune responses to liposome associated antigens. *Vaccine*, 30, 2256-2272.
- WEBB, C., FORBES, N., ROCES, C. B., ANDERLUZZI, G., LOU, G., ABRAHAM, S., INGALLS, L., MARSHALL, K., LEAVER, T. J. & WATTS, J. A. 2020. Using microfluidics for scalable manufacturing of nanomedicines from bench to GMP: A case study using protein-loaded liposomes. *International Journal of Pharmaceutics*, 119266.
- WEBB, C., KHADKE, S., TANDRUP SCHMIDT, S., ROCES, C. B., FORBES, N., BERRIE, G. & PERRIE, Y. 2019. The impact of solvent selection: strategies to guide the manufacturing of liposomes using microfluidics. *Pharmaceutics*, 11, 653.
- WEINER, H. L., DA CUNHA, A. P., QUINTANA, F. & WU, H. 2011. Oral tolerance. *Immunological reviews*, 241, 241-259.
- WHITE, K. L., RADES, T., FURNEAUX, R. H., TYLER, P. C. & HOOK, S. 2006. Mannosylated liposomes as antigen delivery vehicles for targeting to dendritic cells. *Journal of pharmacy and pharmacology*, 58, 729-737.
- WILKHU, J. S., MCNEIL, S. E., ANDERSON, D. E. & PERRIE, Y. 2013. Characterization and optimization of bilosomes for oral vaccine delivery. *Journal of Drug Targeting*, 21, 291-299.
- WILKHU, J. S. & PERRIE, Y. 2015. Developing Bilayer-Based Delivery Systems for Oral Delivery of Subunit Vaccines. In: FOGED, C., RADES, T., PERRIE, Y. & HOOK, S. (eds.) *Subunit Vaccine Delivery*. New York, NY: Springer New York.
- WOOF, J. M. & KERR, M. A. 2004. IgA function—variations on a theme. *Immunology*, 113, 175.
- WORSHAM, R. D., THOMAS, V. & FARID, S. S. 2019. Potential of continuous manufacturing for liposomal drug products. *Biotechnology journal*, 14, 1700740.
- WUI, S. R., KIM, K. S., RYU, J. I., KO, A., DO, H. T. T., LEE, Y. J., KIM, H. J., LIM, S. J., PARK, S. A. & CHO, Y. J. 2019. Efficient induction of cell-mediated immunity to varicella-zoster virus glycoprotein E co-lyophilized with a cationic liposome-based adjuvant in mice. *Vaccine*, 37, 2131-2141.
- XU, X., COSTA, A. & BURGESS, D. J. 2012. Protein Encapsulation in Unilamellar Liposomes: High Encapsulation Efficiency and A Novel Technique to Assess Lipid-Protein Interaction. *Pharmaceutical Research*, 29, 1919-1931.

- XU, Y., HUI, S.-W., FREDERIK, P. & SZOKA JR, F. C. 1999. Physicochemical characterization and purification of cationic lipoplexes. *Biophysical journal*, 77, 341-353.
- YAP, Y. A. & MARIÑO, E. 2018. An insight into the intestinal web of mucosal immunity, microbiota, and diet in inflammation. *Frontiers in immunology*, 9, 2617.
- ZAMBONI, W. C., SZEBENI, J., KOZLOV, S. V., LUCAS, A. T., PISCITELLI, J. A. & DOBROVOLSKAIA, M. A. 2018. Animal models for analysis of immunological responses to nanomaterials: challenges and considerations. *Advanced drug delivery reviews*, 136, 82-96.
- ZHANG, C., MARUGGI, G., SHAN, H. & LI, J. 2019. Advances in mRNA vaccines for infectious diseases. *Frontiers in Immunology*, 10, 594.
- ZHANG, S., PALAZUELOS-MUNOZ, S., BALSELLS, E. M., NAIR, H., CHIT, A. & KYAW, M. H. 2016. Cost of hospital management of Clostridium difficile infection in United States—a meta-analysis and modelling study. *BMC infectious diseases*, 16, 447.
- ZHANG, X., GOEL, V. & ROBBIE, G. J. 2020. Pharmacokinetics of Patisiran, the First Approved RNA Interference Therapy in Patients With Hereditary Transthyretin-Mediated Amyloidosis. *The Journal of Clinical Pharmacology*, 60, 573-585.
- ZHOU, F. & NEUTRA, M. R. 2002. Antigen delivery to mucosa-associated lymphoid tissues using liposomes as a carrier. *Bioscience reports*, 22, 355-369.
- ZIZZARI, A., BIANCO, M., CARBONE, L., PERRONE, E., AMATO, F., MARUCCIO, G., RENDINA, F. & ARIMA, V. 2017. Continuous-Flow Production of Injectable Liposomes via a Microfluidic Approach. *Materials*, 10, 1411.